LBNL-40183

ERNEST ORLANDO LAWRENCE
BERKELEY NATIONAL LABORATORY

Ponded Infiltration Test at the Box Canyon Site

Data Report and Preliminary Analysis

Boris Faybishenko, Rohit Salve,
Peter Zawislanski, Christine Doughty,
Ki Ha Lee, Paul Cook, Barry Freifeld,
Janet Jacobsen, Buck Sisson,
Joel Hubbell, and Kirk Dooley

Earth Sciences Division

September 1998

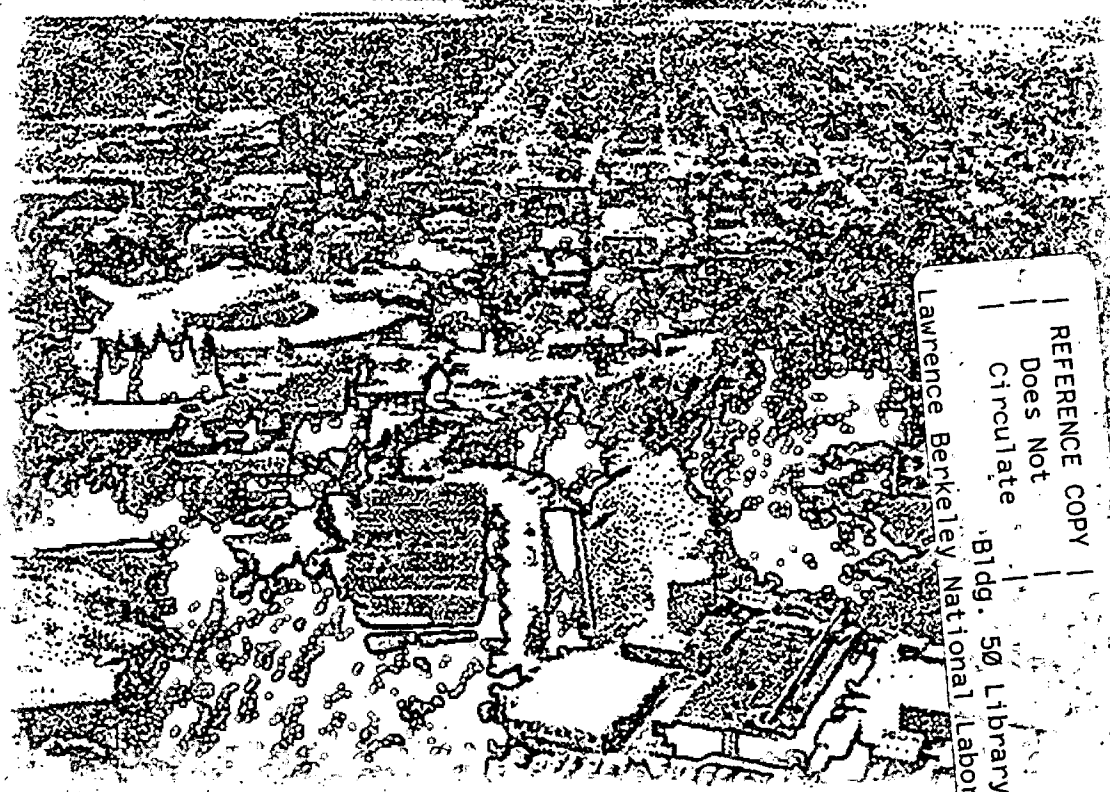

REFERENCE COPY
Does Not
Circulate
Bldg. 50 Library - Ref.
Lawrence Berkeley National Laboratory
Copy 1
LBNL-40183

DISCLAIMER

This document was prepared as an account of work sponsored by the United States Government. While this document is believed to contain correct information, neither the United States Government nor any agency thereof, nor The Regents of the University of California, nor any of their employees, makes any warranty, express or implied, or assumes any legal responsibility for the accuracy, completeness, or usefulness of any information, apparatus, product, or process disclosed, or represents that its use would not infringe privately owned rights. Reference herein to any specific commercial product, process, or service by its trade name, trademark, manufacturer, or otherwise, does not necessarily constitute or imply its endorsement, recommendation, or favoring by the United States Government or any agency thereof, or The Regents of the University of California. The views and opinions of authors expressed herein do not necessarily state or reflect those of the United States Government or any agency thereof, or The Regents of the University of California.

Ernest Orlando Lawrence Berkeley National Laboratory
is an equal opportunity employer.

DISCLAIMER

This document was prepared as an account of work sponsored by the United States Government. While this document is believed to contain correct information, neither the United States Government nor any agency thereof, nor the Regents of the University of California, nor any of their employees, makes any warranty, express or implied, or assumes any legal responsibility for the accuracy, completeness, or usefulness of any information, apparatus, product, or process disclosed, or represents that its use would not infringe privately owned rights. Reference herein to any specific commercial product, process, or service by its trade name, trademark, manufacturer, or otherwise, does not necessarily constitute or imply its endorsement, recommendation, or favoring by the United States Government or any agency thereof, or the Regents of the University of California. The views and opinions of authors expressed herein do not necessarily state or reflect those of the United States Government or any agency thereof or the Regents of the University of California.

LBNL-40183

Ponded Infiltration Test at the Box Canyon Site
Data Report and Preliminary Analysis

Boris Faybishenko, Rohit Salve, Peter Zawislanski, Christine Doughty,
Ki Ha Lee, Paul Cook, Barry Freifeld, and Janet Jacobsen

Earth Sciences Division
Ernest Orlando Lawrence Berkeley National Laboratory
University of California
Berkeley, CA 94720

Buck Sisson, Joel Hubbell, and Kirk Dooley

INEEL

September 1998

This work was supported by the Characterization, Monitoring, and Sensor Technology Crosscutting Program within the Office of Science and Technology, U.S. Department of Energy, Office of Environmental Management, under Contract No. DE-AC03-76SF00098.

ABSTRACT i

ACKNOWLEDGMENTS ii

INTRODUCTION iii

I. TEST DESIGN 1

I.1. GENERAL DESCRIPTION OF LITHOLOGY 1
I.2. SITE LAYOUT 1
I.3. SURFACE TOPOGRAPHY 1
I.4. INSTALLATION OF INSTRUMENTS AND MATERIALS 5
I.5. BOREHOLE SEALING TECHNOLOGY 7
I.6. POND BERM 7
I.7. SUMMARY OF THE INSTRUMENTATION 8
I.7.1. Shallow Tensiometers 8
I.7.2. Deep Tensiometers 10
I.7.3. Shallow Suction Lysimeters 15
I.7.4. Deep Suction Lysimeters 15
I.7.5. Thermistors 15
I.7.6. Electrical Resistivity Probes 15
I.7.7. Water Supply System and Flow Rate Measurements 16
I.7.8. Local Infiltrometers 18
I.7.9. Neutron Logging 22
I.7.10. Rigid Waveguide TDR 23
I.7.11. Flexible Waveguide TDR 26
I.7.12. Groundwater Level Measurements 27
I.8. DATA ACQUISITION SYSTEM 27
I.9. SELECTION OF DEPTHS OF INSTRUMENTATION 31
I.10. TRACER TEST 38

II. TEST RESULTS 38

II. 1. TENSIOMETRY DATA 38
II.1.1. Shallow Tensiometers 38
II.1.2. Deep Tensiometers 51
II.2. RESULTS OF NEUTRON LOGGING 51
II.3. WATER SAMPLING 62
II.4. TRACER TEST RESULTS 78
II.5. TEMPERATURE DATA 90
II.6. FLOWRATE DATA 92
II.7. TDR DATA 106
II.7.1. Shallow TDR Data 106
II.7.2. Deep Borehole TDR Data 112
II.8. GROUNDWATER LEVEL MEASUREMENTS 112

III. SUMMARY 112

IV. REFERENCES 119

ATTACHMENTS 120

A.1. CALIBRATION OF PRESSURE TRANSDUCERS USED IN SHALLOW TENSIOMETERS 120
A.2. TESTING THE DESIGN OF NEUTRON ACCESS HOLES 124
A.2.1. Casing Design 124

A.2.2. Backfill Design 125
A.2.3. Results 127
A.3. CALIBRATION OF THERMISTORS 128
A.3.1. Construction 128
A.3.2. Calibration 128
A.3.3. Field Measurements 128
A.4. IRC FIELD TEST 129
A.4.1. Testing of Borehole Sealing Technology 129
A.4.2. Preliminary Tests and Evaluation of the Deep Tensiometer 131
A.5. SUMMARY OF INSTRUMENT RESPONSES TO INFILTRATION AND TRACER TESTS 133

LIST OF FIGURE CAPTIONS 146

LIST OF TABLES 149

Abstract

In this report, we discuss the design and present the main results of a two-week ponded infiltration test conducted in 1996 at the Box Canyon site near the Idaho National Engineering and Environmental Laboratory. To investigate liquid flow and chemical transport in fractured basalt, the following types of instruments were installed in boreholes: tensiometers, suction lysimeters, thermistors, time domain reflectrometry probes, and electrical resisitivity probes. These probes were installed using an innovative technology of borehole instrumentation and completion using polyurethane foam injection. The probes were attached to plastic packers that were inflated using the polyurethane foam, and then the space between packers was back-filled with the foam in order to ensure the isolation of the instruments at different depths. Polyurethane foam showed great promise in enabling rapid, cost-effective installation of sensors and probes in fractured rock. A ponded infiltration test was conducted from 8/27/96 to 9/9/96, by maintaining water to an average depth of 23 cm in a rectangular infiltration pond. Within the 7 x 8 m pond, nine local infiltrometers (0.25 m diameter) were installed to determine local values of the water flux. A slug of conservative tracer (KBr) was added to the pond on 9/2/96, yielding a tracer concentration in the pond of approximately 3 g/L. The water supply to the pond was halted for two days so that the tracer concentration in the pond water would remain essentially constant. Thereafter, the water supply was re-established to maintain a constant water level. Installation procedures and measurement results for each type of probe are presented, along with a description of the data acquisition system. The attachments include a description of the calibration and testing of instrumentation. The data files can be found at the FTP site zenith/inel/ or the Web site http://www-esd.lbl.gov/ERT/inel/inel.html.

Acknowledgments

We appreciate very much Jane Long's contributions to the project. Marque Mesa and Ryan Nelson participated in field work and preliminary data analysis. April James and Phil Rizzo of LBNL and Brian Higgs and Tony Orme of INEEL participated in field work. Sherry Seybold and Michael Steiger helped in the report preparation. Don Lippert, Ray Solbau and Phil Rizzo participated in instrument design and fabrication. Scott Mountford conducted analytical analysis of water samples. McCabe Bros. Drilling, Inc. conducted bench testing of the polyurethane foam injection and provided borehole completion in the field. This report was reviewed by George Moridis and Michael Steiger, and their comments and recommendations are very much appreciated.

Introduction

A key issue in environmental remediation of contaminated sites is the development of monitoring techniques to characterize fluid flow and contaminant transport. DOE faces the remediation of several sites in unsaturated fractured basalt where chemical and radioactive wastes released from shallow ponds and deep wells have migrated downward through narrow fracture pathways that are difficult, if not impossible, to detect. Perched water zones also create a system of hydraulic baffles that are poorly understood. The behavior of contaminants at these sites has been very difficult to predict.

Twenty years of well drilling and instrumentation in fractured basalt at the Idaho National Environmental and Engineering Laboratory (INEEL), intense instrumentation of boreholes for the Large Scale Infiltration Test (LSIT), and joint Lawrence Berkeley National Laboratory (LBNL) and INEEL research at Box Canyon has shown that there are two critical problems related to the use of monitoring wells in fractured rock: installation of borehole instrumentation in such a way that the probes are placed in contact with the rock and sealing of the borehole. This is particularly true in slanted wells where granular materials tend to collect on the lower side of the borehole and reduce the effectiveness of the seal on the upper side. Conventional well completion materials, including bentonite and sand tend to plug small diameter pipes used in well completion. The LSIT performed by the INEEL in 1994 showed that the technology needed to monitor water flow under ponded infiltration conditions required further development.

The objectives of the investigations at the Box Canyon site were:

(1) To develop a suite of reliable tools and methodologies that can be used together to characterize fluid flow and chemical transport in fractured rocks, and

(2) To develop a conceptual model of fluid flow and chemical transport in unsaturated fractured basalt.

To address these objectives, a ponded infiltration test was conducted at the Box Canyon site using a combination of monitoring techniques specifically designed to study fluid flow and chemical transport in fractured basalt. This report describes the design of tensiometers, suction lysimeters, thermistors, time domain reflectrometry (TDR) probes, miniature electrical resistivity (ER) probes, and the data acquisition system (DAS), and presents the data obtained before, during, and after the infiltration test. Instructions to access the data using the FTP site are also given. Ground-penetrating radar data collected during 1996 are not included here, but are the subject of the report by Peterson, J.E., Jr. and K.H. Williams, 1997.

I. Test Design

I.1. General Description of Lithology

The surface of the site consists of exposed weathered basalt and soils (clays and silts), which infill the near-surface fractures and basalt column joints. Along the cliff face, about 30 m from the pond, two distinct basalt flow fingers and a rubble zone between them can be seen. The basalt flow is divided into an upper and lower zone of distinctly different fracturing, which is probably due to different cooling rates and temperature gradients in the upper and lower portions of the basalt flow. Site characterization, including cliff face mapping, borehole logging, and gas-phase interference tests, revealed that the fractured basalt vadose zone is comprised of the following geological components:

- Topsoil layer, including flow-top rubble
- Upper vesicular zones with numerous near-surface, soil-infilled fractures
- Massive basalt
- Vertical and sub-vertical column-bounding fractures
- Horizontal and sub-horizontal fractures
- Central fracture zone
- Lower vesicular zone
- Underlying rubble zone

The characteristic joint spacing exhibits an increase in spacing with depth in the upper ~2/3 of the flow thickness. The base of each basalt flow also shows an inverted pattern, in which the lower basalt contact contains smaller fracture spacing than the center of the flow. In some basalt flows, there is a region of highly fractured rock in the lower center of the basalt flow that does not display the columnar style of fracturing. This information was used in designing the instrumentation and the infiltration test as described below.

I.2. Site Layout

The location of boreholes drilled at the site is shown in Figure I.2-1. The length, coordinates, and inclination of the boreholes are summarized in Table I.2-1. The lithology and site layout are described in detail in other reports (Faybishenko et al., 1998; Long et al., 1995).

I.3. Surface Topography

Figure I.3-1 shows a map of basalt columns exposed at the surface, and soils within the pond. This figure also shows the locations of several boreholes within and around the pond.

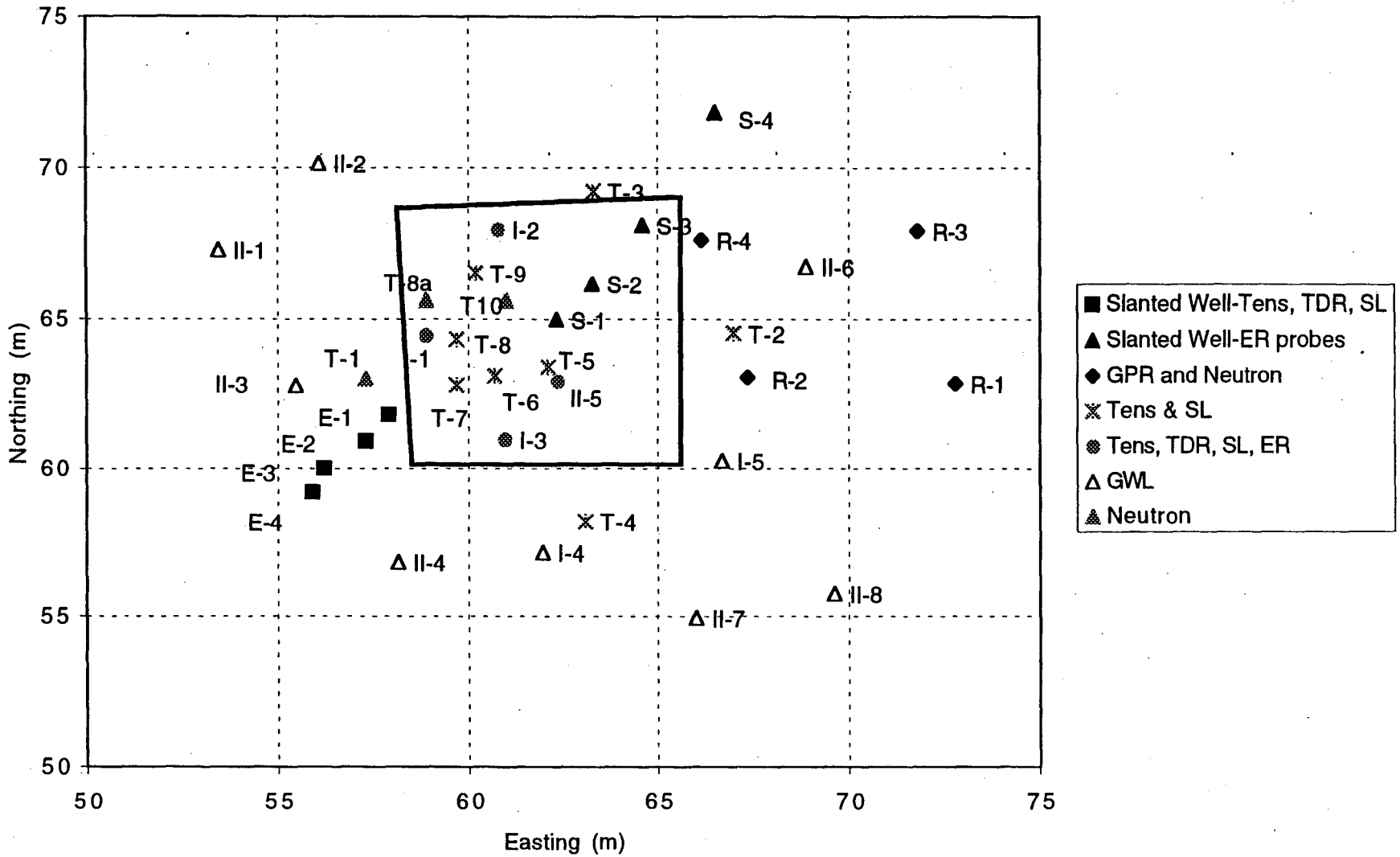

Figure I.2-1. Well layout

Table I.2-1. Well Information for Box Canyon Site

well id	vertical/ slant	angle from vertical	length (ft)	length (m)	xtop (m) (east)	ytop (m) (north)	ztop (m) (elev.)	xbot (m) (east)	ybot (m) (north)	zbot (m) (elev.)
E-1	slant	45.0	60.0	18.29	57.90	61.80	1599.67	68.50	72.04	1586.74
E-2	slant	40.0	60.0	18.29	57.30	60.90	1599.69	64.43	70.25	1585.68
E-3	slant	35.0	60.0	18.29	56.20	60.00	1599.64	62.75	68.19	1584.66
E-4	slant	28.0	60.0	18.29	55.90	59.20	1599.63	61.14	66.00	1583.48
I-1	vertical	0.0	40.0	12.19	58.90	64.40	1599.64	58.90	64.40	1587.45
I-2	vertical	0.0	40.0	12.19	60.80	67.90	1599.70	60.80	67.90	1587.50
I-3	vertical	0.0	40.0	12.19	60.90	61.00	1599.65	60.90	61.00	1587.46
I-4	vertical	0.0	40.0	12.19	61.90	57.20	1599.57	61.90	57.20	1587.38
I-5	vertical	0.0	20.0	6.10	66.70	60.30	1599.46	66.70	60.30	1593.36
II-1	vertical	0.0	63.2	18.29	53.50	67.30	1599.82	53.50	67.30	1581.53
II-2	vertical	0.0	60.0	19.26	56.10	70.10	1599.68	56.10	70.10	1580.42
II-3	vertical	0.0	60.0	18.29	55.50	62.80	1599.65	55.50	62.80	1581.36
II-4	vertical	0.0	60.1	18.32	58.10	56.80	1599.57	58.10	56.80	1581.25
II-5	vertical	0.0	73.7	22.46	62.40	62.90	1599.70	62.40	62.90	1577.23
II-6	vertical	0.0	60.0	18.29	68.90	66.70	1599.34	68.90	66.70	1581.05
II-7	vertical	0.0	60.0	18.29	65.80	54.90	1599.50	65.80	54.90	1581.21
II-8	vertical	0.0	60.0	18.29	69.60	55.70	1599.35	69.60	55.70	1581.06
R-1	slant	27.5	65.0	19.81	72.79	62.84	1599.28	63.65	62.80	1581.71
R-2	slant	41.1	65.0	19.81	67.36	63.04	1599.57	54.38	63.00	1584.64
R-3	slant	27.3	65.0	19.81	71.80	67.89	1599.25	62.71	67.90	1581.65
R-4	slant	29.2	75.0	22.86	66.16	67.60	1599.53	55.05	67.60	1579.58
S-1	slant	30.0	16.0	4.88	62.30	64.90	1599.60	61.04	62.81	1595.37
S-2	slant	30.0	20.1	6.13	63.30	66.10	1599.53	61.44	63.67	1594.22
S-3	slant	30.0	44.4	13.53	64.60	68.10	1599.58	60.71	62.56	1587.86
S-4	slant	30.0	69.4	21.15	66.50	71.80	1599.50	61.01	62.76	1581.18
T-1	vertical	0.0	20.0	6.10	57.30	63.00	1599.65	57.30	63.00	1593.56
T-2	vertical	0.0	20.0	6.10	67.00	64.50	1599.50	67.00	64.50	1593.41
T-3	vertical	0.0	20.0	6.10	63.30	69.20	1599.75	63.30	69.20	1593.65
T-4	vertical	0.0	20.0	6.10	63.10	58.20	1599.56	63.10	58.20	1593.46
T-5	vertical	0.0	10.0	3.05	62.10	63.40	1599.75	62.10	63.40	1596.70
T-6	vertical	0.0	22.0	6.71	60.70	63.10	1599.83	60.70	63.10	1593.13
T-7	vertical	0.0	20.0	6.10	59.70	62.80	1599.64	59.70	62.80	1593.54
T-8	vertical	0.0	10.0	3.05	59.70	64.30	1599.75	59.70	64.30	1596.70
T-8A	vertical	0.0	20.0	6.10	58.90	65.60	1599.60	58.90	65.60	1593.50
T-9	vertical	0.0	10.0	3.05	60.20	66.50	1599.68	60.20	66.50	1596.63
T-10	vertical	0.0	10.0	3.05	61.67	65.70	1599.67	61.70	65.70	1596.62

Notes: Coordinates of bottoms of slant wells have been calculated.

J. Jacobsen - 7/11/97

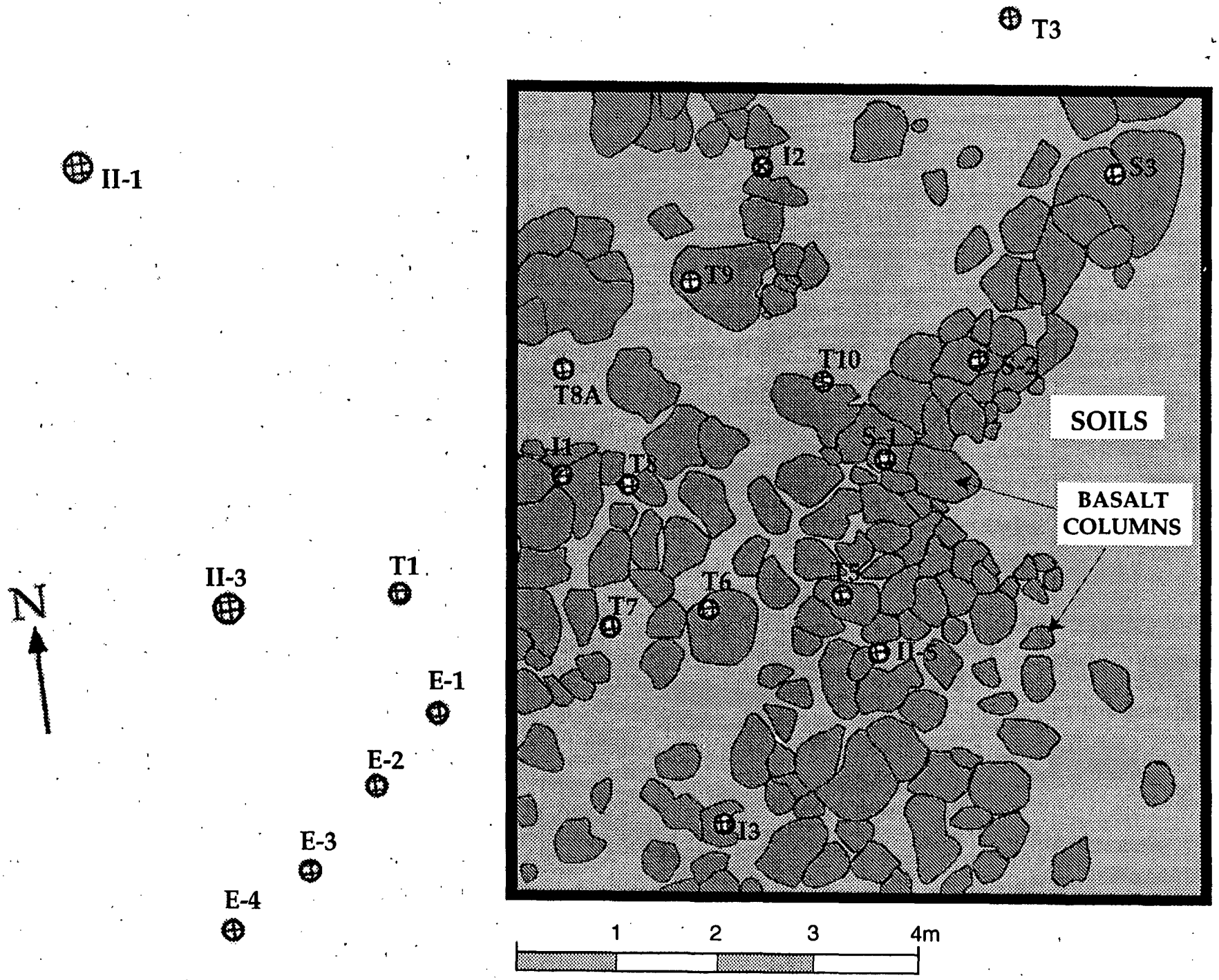

Figure I.3-1. Map of infiltration pond: column tops, soils, and well locations (from Jason Lore, Stanford University)

I.4. Installation of Instruments and Materials

In designing a borehole completion method, we attempted to address three critical problems related to borehole completion in fractured rocks:

(1) Installation of subsurface instrumentation in such a manner that probes can be placed in contact with the main geological components (identified above) that affect fluid flow and chemical transport;

(2) Sealing of the borehole in order to preserve natural pathways of fluid flow in fractured rocks; and

(3) Using a sealing material that will not affect geophysical techniques such as radar and neutron logging.

The conventional installation of instrumentation (tensiometers, TDR probes, etc.) developed for soils, if used for fractured rocks, may lead to the creation of perched water zones within sand layers where the instruments are installed (Figure I.4-1a). INEEL, LBNL and McCabe Bros., Inc. tested several types of a new polyurethane sealant to complete vertical and slanted boreholes at the Box Canyon site and the Idaho Research Center (IRC) field test site in Idaho Falls. Initial testing of the assembly and installation procedures were performed at the IRC field test site (see Attachment A4). A schematic diagram illustrating the installation of the instrumentation and back-filling is shown in Figure I.4-1b.

Shallow and deep tensiometers (DT), TDR probes, piezometers, ER probes, suction lysimeters, thermistors, and soil gas sampling lines were installed in boreholes. The instruments were attached to the outer faces of polyethylene packers mounted onto sections of 3.5 cm (1.5 in) OD PVC manchette pipe, and the sections were glued together to form a continuous string of instruments placed at pre-selected depths.

At the IRC site, only TDR probes and DTs were used in the instrument string. At the Box Canyon site, each type of instrument listed above was installed, although not at all depths or in all boreholes. See Table I.9-1 for the final placement depths in individual boreholes. The instrument string installed at the IRC site was assembled at the borehole, and then a truck crane was used to lower the instrument string to its final position in the borehole. In contrast, the instrument strings installed at Box Canyon were assembled off site and then transported to the site for installation. Instrument strings longer then 12.2 m (40 ft) were assembled in two pieces and then joined on site. Instrument strings shorter than 4.6 m (15 ft) were lowered by hand into the borehole while those longer then 4.6 m (15 ft) were installed with the aid of the truck crane.

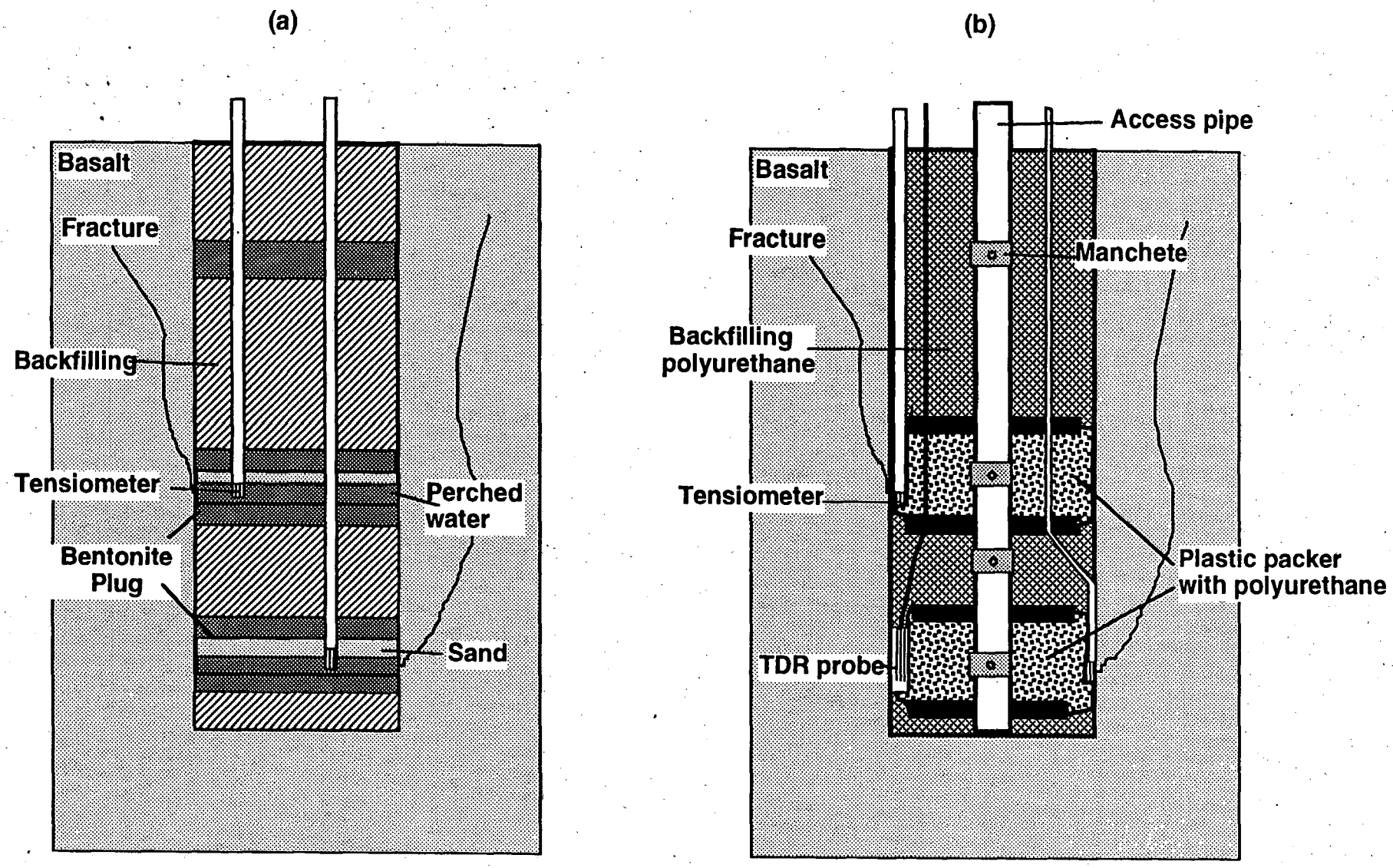

Figure I.4-1. Scheme of installation of instrumentation in boreholes:
(a) conventional in a soil profile, and (b) a new technology for fractured rocks.

I.5. Borehole Sealing Technology

Preliminary testing of a water-activated polyurethane grout (ST-530) for use with Idaho soils and basalts indicated that the material had the following attributes: (1) it adhered well to dry and wet soils and basalts; (2) penetration into fractures was minimal because the set time could be regulated; (3) electrical properties were similar to those of dry sand and had little or no effect on radar and TDR measurements; (4) it could easily be injected through a small diameter tube to infill the annular space in its liquid state; (5) unlike bentonite and cement, it did not affect the moisture content of surrounding soils and basalts; (6) it could be used to back-fill and seal boreholes both below and above the water table; and (7) it had a very low bulk density, which is favorable for neutron logging. This material showed great promise for enabling the rapid, cost-effective installation of sensors and probes in fractured rock.

Once instrument strings were placed in the boreholes at pre-selected depths, a short straddle packer was inserted into the manchette pipe, and the polyurethane grout was pumped into the straddle packer where it exited through the manchette ports to inflate the polyethylene packer. The manchette acted as a check valve and prevented the grout from re-entering the manchette pipe. The deepest packer in each string was inflated first, followed by the next deepest packer, and then the open segment between them was grouted. This alternating pattern of filling packers and segments was repeated moving upward in the borehole.

Estimating the amount of polyurethane foam required to fill a packer or segment was based on the cross sectional area of the borehole, the length of the segment or packer to be filled, and an experimentally determined expansion factor of 20 for the foam. The volume occupied by the manchette pipe, electronic cables, and tensiometer pipe was assumed to be negligible. The resulting estimate was conservative, but the excess foam pressurized the packers and borehole segments, ensuring an adequate borehole seal.

Several boreholes did not have probes installed, but were cased with acrylic pipe. The R boreholes were cased with 5.1 cm (2 in) OD acrylic pipe, and boreholes T1, T8a, and T-10 were cased with 7 cm (3 in) OD acrylic pipe. The pipe was then grouted in place with polyurethane foam to prevent fluid flow in the annular space between the basalt and pipe wall. Two foam injection tubes were placed outside the acrylic casing, and enough foam was injected to fill a 1.8 m (6 ft) length of the annular space. Following a five minute wait, the next interval was grouted, and the pattern was repeated moving upward in the borehole.

I.6. Pond Berm

A 7 x 8 m (23 x 26 ft) artificial pond was created by bounding the area with a 0.5 m (1.6 ft) tall two-layered berm which was intended to be impermeable to water. The outer layer, made of bags filled with crushed basalt and injected with polyurethane, served as a mechanical barrier. The inner layer, made of polyurethane sheltered by a plastic

cover, created a hydraulic barrier to water in the pond. The barrier leaked substantially early in the test, but repairs made during the test resulted in a water-tight pond later in the test. By estimating the surface area and average depth of water that had leaked outside the berm, we determined that about 20-30% of the volume supplied to the pond had leaked through the berm; later leaks were reduced to less than 10%.

I.7. Summary of the Instrumentation

I.7.1. Shallow Tensiometers

The design of the shallow tensiometers for the infiltration experiment had to meet the following criteria: easy installation in the field, ability to obtain automatic measurements, small instrument size to fit in the small diameter boreholes, and a port at the surface to allow for independent measurements with a manually operated Tensimeter™ (manufactured by Soil Measurement Systems). It was also essential that the ceramic tip sense as large an area of the borehole wall as possible.

To allow for convenient field installation, the ceramic and gauge end of the tensiometers were prefabricated in the laboratory, and then transported to the field where the two ends were connected to a pipe of the desired length. Tensiometer measurements were automated by the use of pressure transducers connected to the DAS. To increase the contact area of the ceramic tips, the porous cups were housed in bags of sand.

The design allowed for independent pressure measurements by connecting an acrylic tube with a septum stopper at the surface. The needle of the manually Tensimeter™ was inserted through the septum stopper to measure pressure in the acrylic tube. Figure I.7.1-1 shows the design of the shallow tensiometers used in this test. In Figure I.7.1-2 the dimensions of the porous ceramic tip are summarized.

<u>Materials.</u>

- Schedule 40 gray PVC, 1.40 cm (0.55 in) OD and 0.81 cm (0.32 in) ID.
- Clear acrylic tubing, 1.588 cm (0.625 in) OD and 1.270 (0.500 in) ID.
- Porous cup, round bottom, straight wall ceramic tip (Soil Moisture Equipment Corp., P.O. Box 30025, Santa Barbara, CA 93105).
- Epoxy glue, clear.
- 2.11 cm (0.83 in) ID couples to join plastic tubing.
- Rubber septum stoppers (Soil Measurement Systems, Tucson, AZ).
- Schedule 40 gray PVC 'T' connectors.
- P-155-15-A-B-4 (Kavlico Corporation) pressure transducers.

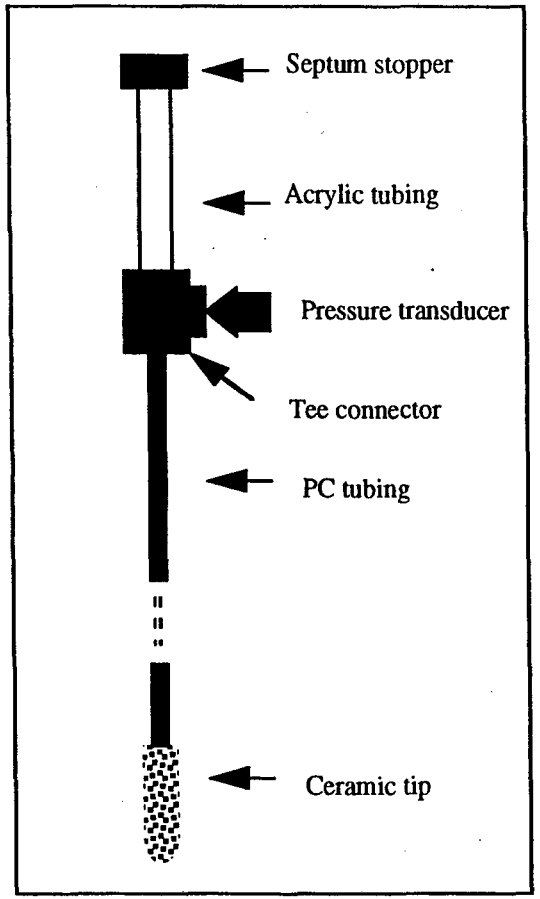

Figure I.7.1-1. Design of shallow tensiometers

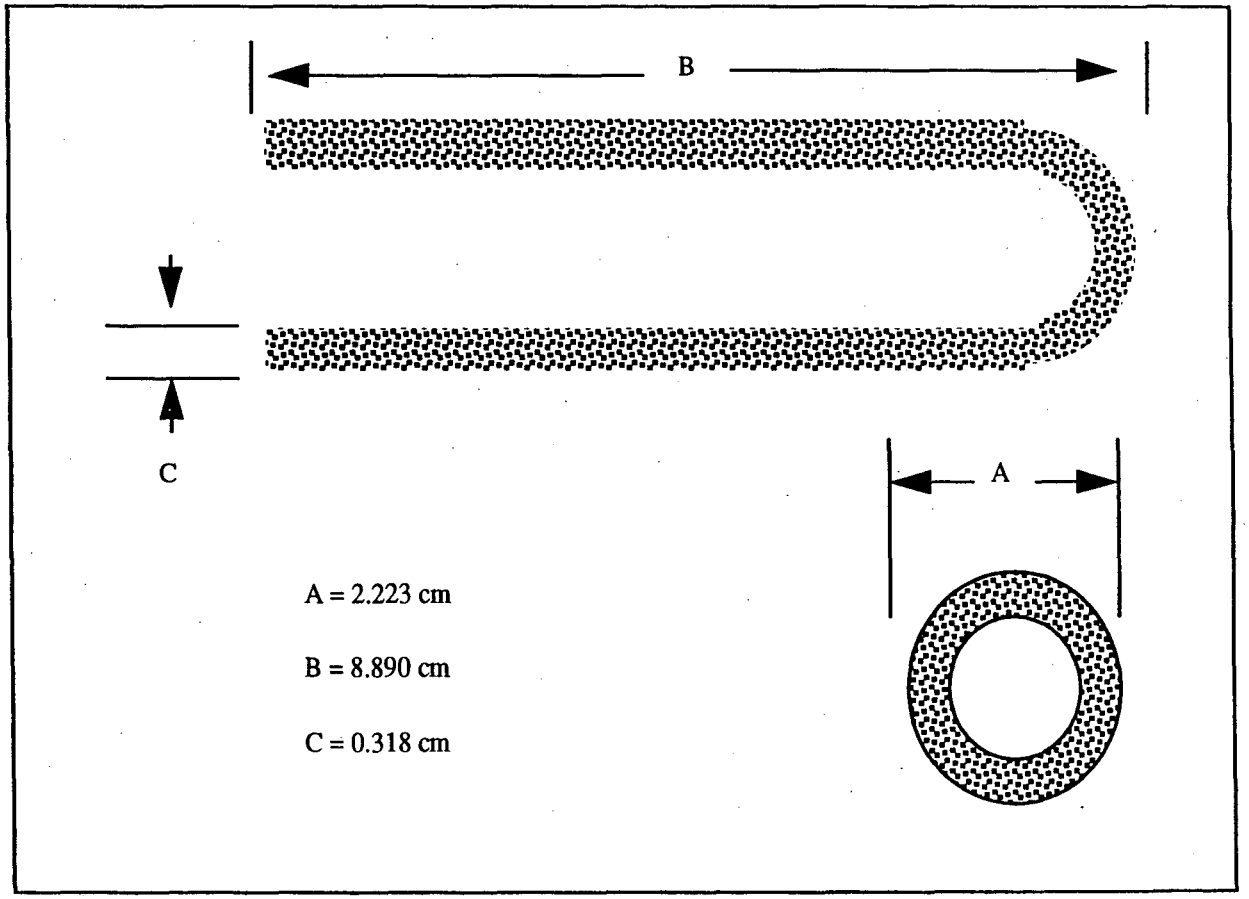

Figure I.7.1-2. Dimensions of ceramic cup used in shallow tensiometers

Construction.

- The acrylic tubing was cut into 7 cm (2.75 in) sections with smooth ends.
- The Schedule 40 tubing was cut to 0.3 m (1 ft) segments used to construct both ends of the tensiometers.
- The OD at one end of the Schedule 40 tubing was reduced to 1.3 cm (0.5 in), so the porous cup, which had an ID of 1.333 cm (0.525 in), could be attached.
- The body of the porous cup was covered with plastic bubble wrap to keep the porous cup clean and free from glue.
- A thin layer of epoxy glue was applied over the shoulder of the porous cup and left to dry for 24 hours.
- At the near-surface end, the tubing was attached to a PVC, schedule 40 T-connector. The sections of acrylic tubing were then connected to the T-connector using epoxy glue.
- The horizontal limb of the T-connector was threaded to the OD of the pressure transducers.

Installation. All tensiometers were installed using the procedure described in Section I.4. In total, shallow tensiometers were installed in eight wells. The location of each tensiometer, and the associated dimensions (i.e. length, depth from surface etc.) are summarized in Table I.7.1-1 and in Figure I.7.1-3. The water level in the tensiometer above the surface is given in Table I.7.1-2.

Measurements. During the infiltration test, pressure measurements were made at regular intervals (6-10 minutes) using the automated DAS. This PC-based system powered the transducers and recorded the signal output, which was then converted to absolute pressure readings from calibration constants. Periodic gauge pressure measurements were made manually using the Tensimeter™.

Due to the varying surface topography and varying length of tensiometers, the total hydraulic head was determined as the sum of pressure at the ceramic tip and the vertical distance from a pre-determined datum - the highest elevation within the site.

I.7.2. Deep Tensiometers

The DT works on the same principle as other tensiometers and is made from the same basic elements: a porous cup that acts as a semi-permeable membrane that is permeable to water but impermeable to air, and a water-filled chamber that transmits pressure from the membrane to a pressure sensor. The DT differs from a shallow tensiometer in that the water filled chamber is relatively short in length, the pressure transducer is mounted very close to the porous cup, and the entire device is installed at the depth of measurements. This configuration was originally designed to allow for tensiometer operation at greater depths below the land surface. An additional feature of the DT was the incorporation of a removable pressure sensor to allow for field

Location	Depth D	Length L	Stick-up S	Surface to z=0 G	z (m) Z
well T-2	-0.61	1.80	1.19		
well T-2	-1.83	2.97	1.14		
well T-2	-3.05	4.14	1.09		
well T-3	-0.61	1.40	0.79		
well T-3	-1.83	2.57	0.74		
well T-3	-3.05	3.89	0.84		
well T-4	-0.53	1.37	0.84		
well T-4	-1.68	2.26	0.58		
well T-4	-2.77	3.51	0.74		
well T-5	-0.30	0.86	0.56	0.13	-0.43
well T-5	-1.52	2.13	0.61	0.13	-1.65
well T-5	-3.05	3.64	0.59	0.13	-3.18
well T-6	-0.69	1.28	0.59	0.03	-0.72
well T-6	-1.80	2.49	0.69	0.03	-1.83
well T-6	-3.00	3.81	0.81	0.03	-3.03
well T-7	-0.61	1.35	0.74	0.28	-0.89
well T-7	-1.83	2.59	0.76	0.28	-2.11
well T-7	-3.05	3.81	0.76	0.28	-3.33
well T-8	-0.30	1.11	0.81	0.12	-0.42
well T-8	-1.52	2.36	0.84	0.12	-1.64
well T-8	-2.74	3.60	0.86	0.12	-2.86
well T-9	-0.30	1.14	0.84	0.18	-0.48
well T-9	-1.52	2.28	0.76	0.18	-1.70
well T-9	-3.05	3.91	0.86	0.18	-3.23

Table I.7.1-1. Shallow Tensiometer Dimensions

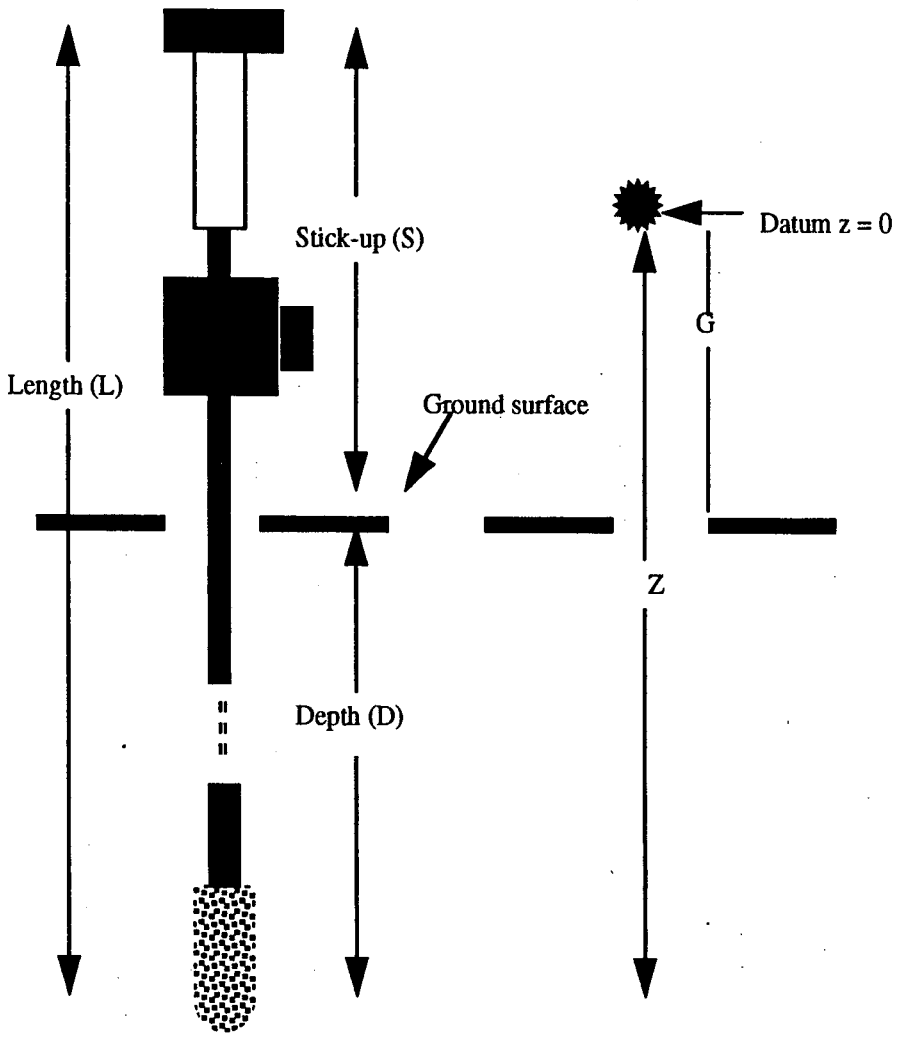

Figure I.7.1-3. Diagram of shallow tensiometer dimensions

Table I.7.1-2. Water Level Height within the Pond

Location	Water Level above the surface (cm)				
					Average
Infiltrometer 1	22.5	22.7	22	22	22.3
Infiltrometer 2	34	34.5	34		34.2
Infiltrometer 3	39	40	39		
Infiltrometer 4	21				21.0
Infiltrometer 5	31	29	28.8	30	29.7
Infiltrometer 6	31.5	32	32		31.8
Infiltrometer 7	39.5	39	31		36.5
Infiltrometer 8	16.5	17.5	17		17.0
Infiltrometer 9	17	15.5	16		16.2
Infiltrometer 10	18.8				
Main water supply pipe	18.5	18.5	21	20	19.5
S-1	21				21.0
T-5	13				13.0
II-5	16.5				16.5
S-2	31.8	29.3	31		30.7
S-3	28.5	31.5	30		30.0
I-2	17.5	14.5	17.7	13.5	15.8
Tensiometer					
T-9	18.5	17	19.5		18.3
T-8	12	11.5	13	13.5	12.5
T-10	17.3				17.3
I-8a	32.5	33			32.8
I-1	25.5	22	20	20	21.9
T-6	4	4.5	4.5		4.3
T-7	24.5	25.5	32.5	27.5	27.5
I-3	25.5	28.5	24.3	24	25.6

Note:
Measurements were taken on August 31, 1996
Water table in pond was1.0 cm above highest basalt exposure within the pond which was located near T-6
Average hight of water 22.4 cm

calibration. The removable sensor also allows the DT to be operated as a vacuum lysimeter, to be converted to operate as a thermocouple psycrometer, or to be used as a gas sampling port. One major benefit of placing the pressure sensor below land surface is the substantial reduction of the effect of diurnal temperature variations on pressure readings.

Materials.

- 5 cm (2 in)-long ceramic cup with fitting to connect with PVC pipe.
- 0.3 m (1 ft) piece of PVC pipe.
- PVC adapter which allows a pressure transducer to be seated as close as possible to the top of the DT.

Construction.

- The ceramic cup was glued to the 0.3 m (1 ft) section of PVC pipe
- An adapter was constructed of 3.18 cm (1.25 in) OD PVC pipe. One end of the pipe was machined so that the PVC pipe with the ceramic cup could be attached. The other machined end was tapered so that a conical rubber stopper affixed to a pressure transducer could be attached and seated with an air tight seal. PVC glue was used to glue all the connections.

The durability of the DTs was a primary concern. The DTs had to be installed at depths of up to 18 m (60 ft) in boreholes with diameters as small as 10 cm (4 in) without breaking the fragile ceramic cup. In order to protect the ceramic cup and to create a better contact with the rocks, nylon socks filled with sand were fitted over the DTs. The sand was compacted so that the DT would not shift inside the nylon sock. The use of the nylon sock did not significantly increase the diameter of the instrument, or increase the difficulty of inserting the instruments into the borehole.

Another concern was that the pressure transducer had to be seated from the surface and form an air tight connection. During preliminary testing, it was observed that a small number of the DTs would not hold an air-tight connection with the conical shaped rubber stopper at the end of the pressure transducer. The machining process left small grooves on the adapter which acted as a conduit for the escaping air. To correct the problem, two steps were taken. First, a longer adapter was constructed in order to allow for a better connection between the pressure transducer and the DT. Second, The inside of the adapter was smoothed with a drummel. All of the instruments were tested and were found to hold air-tight connections after these modifications were made.

I.7.3. Shallow Suction Lysimeters

Shallow suction lysimeters (water samplers) were used to collect water before and during the infiltration test at depths of up to 6 m (20 ft). These lysimeters consisted of a ceramic tip and a chamber covered by a cap. This cap had two ports: (1) a water transfer port, and (2) an air transfer port. The inside part of the water transfer port was connected to a thin 0.3 cm (0.125 in) diameter plastic tube that was extended down to the bottom of the ceramic tip. The outside of this port was connected to the tube running to the water collection vial located outside of the pond. The inside of the air transfer port was cut off just below the cap, and the outside part of this port was connected to a tube running to the outside of the pond.

I.7.4. Deep Suction Lysimeters

Deep suction lysimeters were used to collect water from depths below 6 m (20 ft). The lysimeters consisted of a double-chambered water collector and two tubes running to the surface. The water collector chamber was covered by a cap with two double-side ports. One of these ports was extended downward to the bottom of the upper chamber, and was used to push water up to the surface. Another port was cut off just below the cap inside the upper chamber and connected to the tube used to apply vacuum. Once vacuum was applied, water entered the bottom chamber of the lysimeter and moved upward through the connecting tube between the lower and upper chambers. At the top of this connecting tube, a one-way (upward) valve was installed that did not allow water to go back into the lower chamber.

I.7.5. Thermistors

Temperature was measured before, during, and after the infiltration test using a set of 31 thermistors innstalled in the boreholes. In addition, ambient air and ponded water temperatures were continuously recorded, using 3 sensors above ground level and 3 sensors on the ponded surface.

I.7.6. Electrical Resistivity Probes

A new type of miniature four-electrode array was designed and fabricated at LBNL to monitor real-time changes in the electrical resistivity during the infiltration test. The electrode configuration used is the Wenner array shown in Figure I.7.6-1.

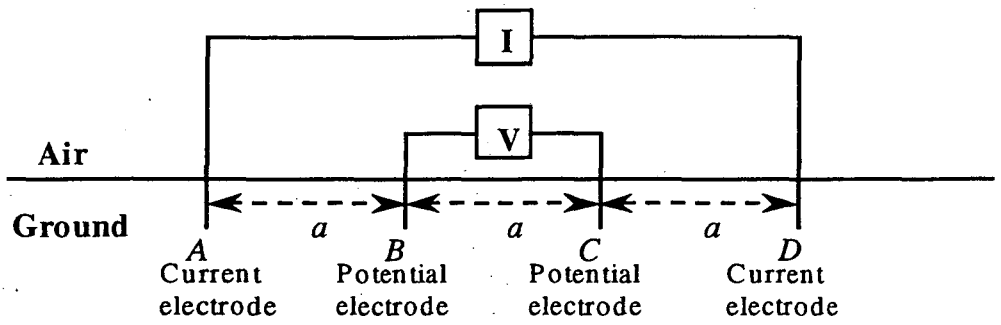

Figure I.7.6-1. The electrode configuration of the miniature ER probe installed in boreholes.

Current electrodes *A* and *D* are used to generate electrical potential in the ground by injecting current (*I*), and potential electrodes are used to measure the potential difference (*V*) between points *B* and *C*. Each potential electrode is separated from the adjacent current electrode by a distance *a* that is one-third the separation of the current electrodes. According to the reciprocity principle, potential and current electrodes may be interchangeable without affecting the apparent resistivity of the half space value given by

$$\rho_a = 2\pi a \frac{V}{I},$$

where ρ_a is the apparent resistivity of a homogeneous medium and is considered a good measure of the average resistivity even when the medium is heterogeneous. If the same array is installed in the whole space, the electrical current density will be exactly halved and result in an apparent resistivity given by

$$\rho_a = 4\pi a \frac{V}{I}.$$

The apparent resistivity is very sensitive to changes in the electrical resistivity of the medium. When the medium in the vicinity of the electrode array is wetted due to infiltration, its electrical resistivity is lowered. The sensitivity of the reduction is proportional to the electrode spacing *a*. The specification of the Wenner array and type of measurements implemented in the miniature ER probe are shown in Figure I.7.6-2.

I.7.7. Water Supply System and Flow Rate Measurements

Water was pumped up to the site using a submerged pump installed at the Big Lost River. The water supply system consisted of a main water tank (1500 gal), which supplied water to the entire pond, a digital total-flow-rate meter, an electronic flow-rate meter, and a float used to maintain a constant water level in the pond. The water supply system also included nine water tanks used to supply water in nine 25.4 cm (10 in)

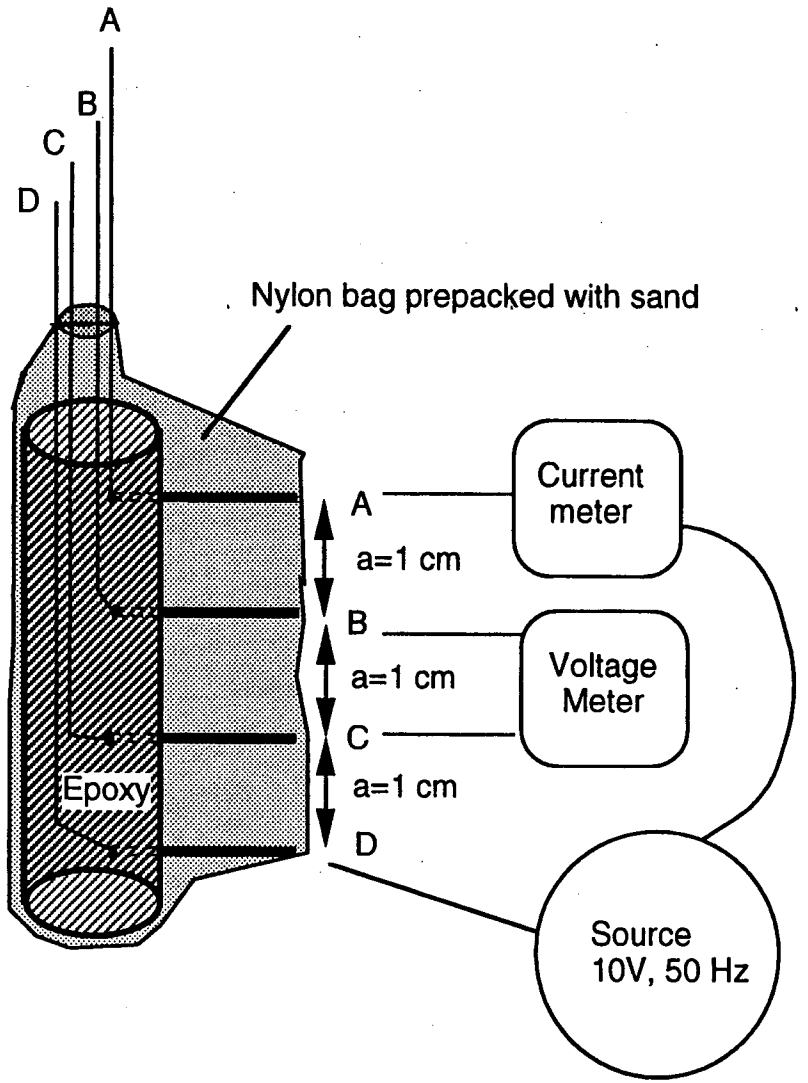

Figure I.7.6-2. Arrangement of the miniature ER probe located in a nylon bag prepacked with sand

diameter infiltrometers installed at the land surface at different locations within the pond. A diagram showing the design of the water supply system is shown in Figure I.7.7-1.

During the test, a practically constant water level was maintained within the entire pond (including infiltrometers) for two weeks, from 8/27/96 to 9/9/96. Because of the varying surface topography within the pond, the height of water differed with location within the pond (Table I.7.1-2.). The average water depth was 22.4 cm.

I.7.8. Local Infiltrometers

A map showing the infiltrometer locations is shown in Figure I.7.8-1. An automated system was developed to determine the spatial and temporal variability in the water flux at the surface during the infiltration experiment. The system specifications included:

1. Continuous measurements of local infiltration rates during the entire experiment. Since the flow rates were expected to range from extremely high in fractures to negligible in the low porosity basalt matrix, it was important that the system have enough flexibility to accommodate these extremes;

2. Maintenance of a constant head boundary above the surface; and

3. No lateral hydrologic communications above the surface between local flux-meters and the ponded water.

Design. Figure I.7.8-2 provides a detailed view of an infiltrometer which was made of 25 cm (10 in) ID PVC pipe. This pipe was approximately 0.6 m (2 ft) tall and was hydraulically isolated at the surface from the pond. During the test, a constant water level was maintained in each infiltrometer, equal to the water level in the entire pond. In order to maintain a constant water level, we used a level switch within each ring, operated using an electrical circuit that remained open at elevations equal to, or greater than, the ponded surface. The level switch was connected to a pump located at the outlet of each tank. The water level in each tank was continuously recorded by pressure transducers sensitive enough to read changes less than 0.001 m in hydraulic head.

To prevent water leaking through the pump during periods of inactivity, the tube supplying water from the tank to the pump was extended vertically to a height above that of the tank. At the high point in the tube pathway, a T-connector with a one-way valve was installed that linked the water supply pump to the pond. When the pump was activated, the valve closed due to the pressure of water, and water was conveyed without head loss to the pump. When pumping stopped, the reduced water pressure caused the valve to disengage, thereby venting the tube to atmosphere and consequently reducing water loss through siphoning effects.

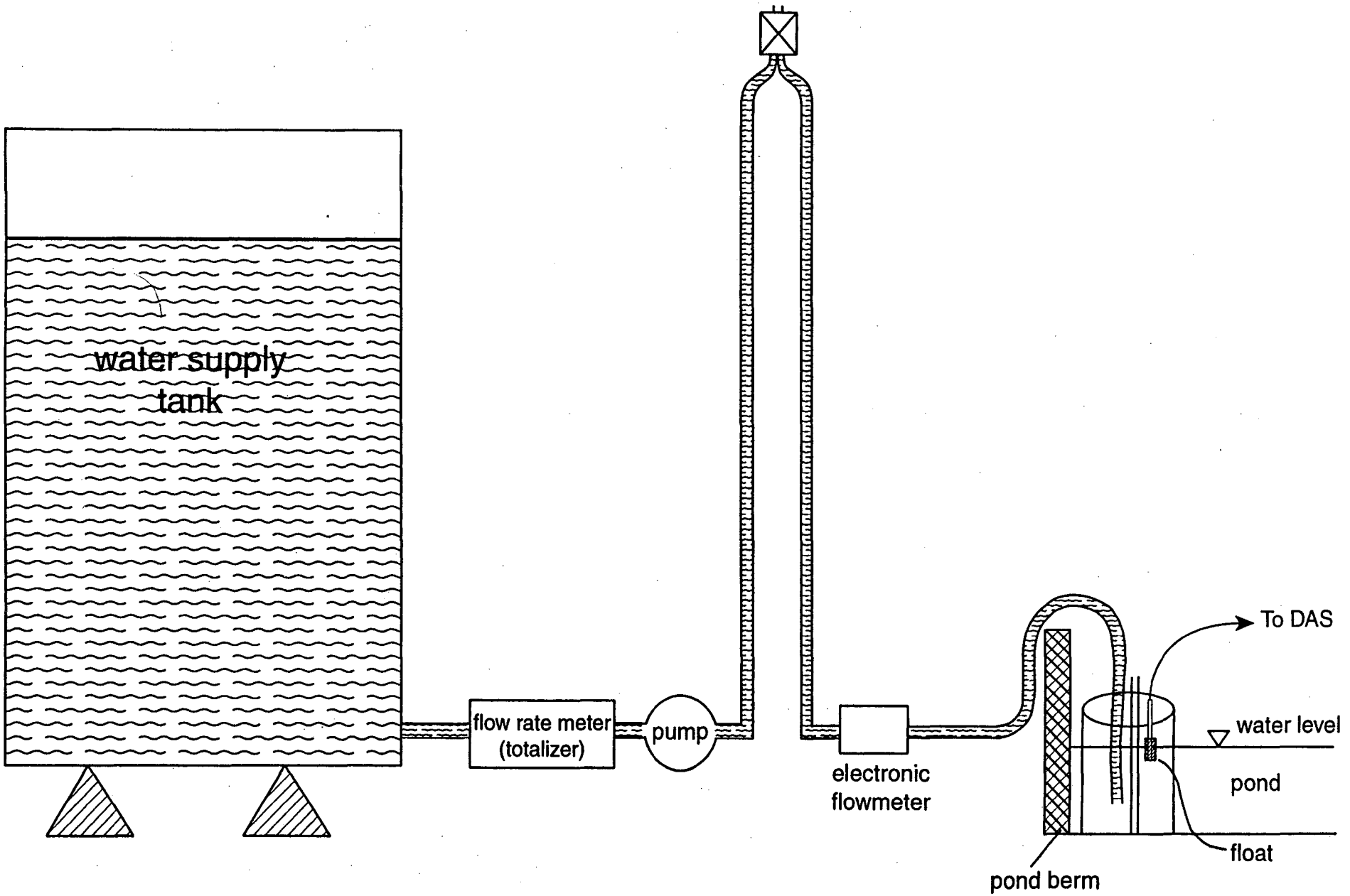

Figure I.7.7-1. Water supply system design

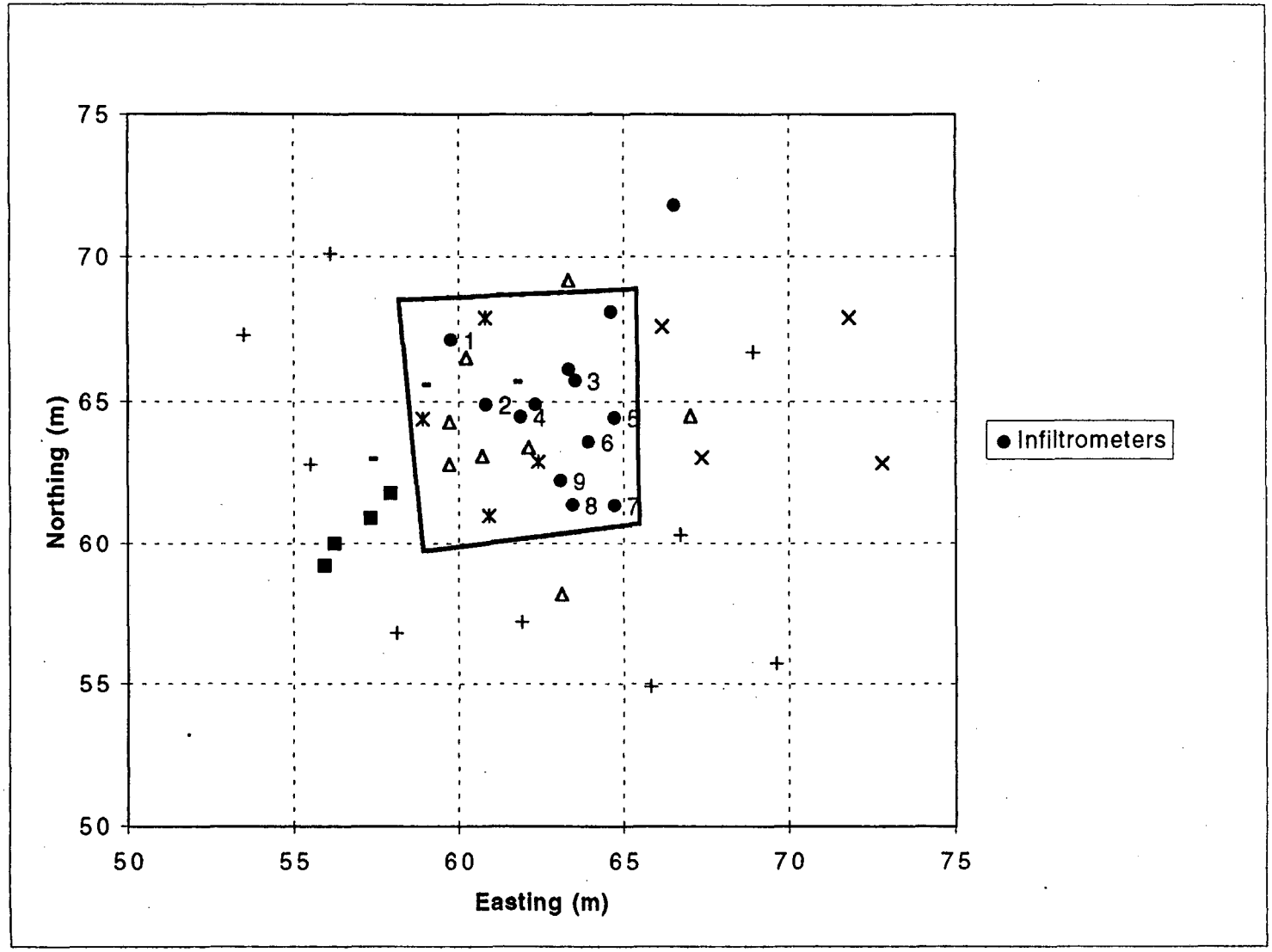

Figure I.7.8-1. Well and infiltrometer layout at the Box Canyon site

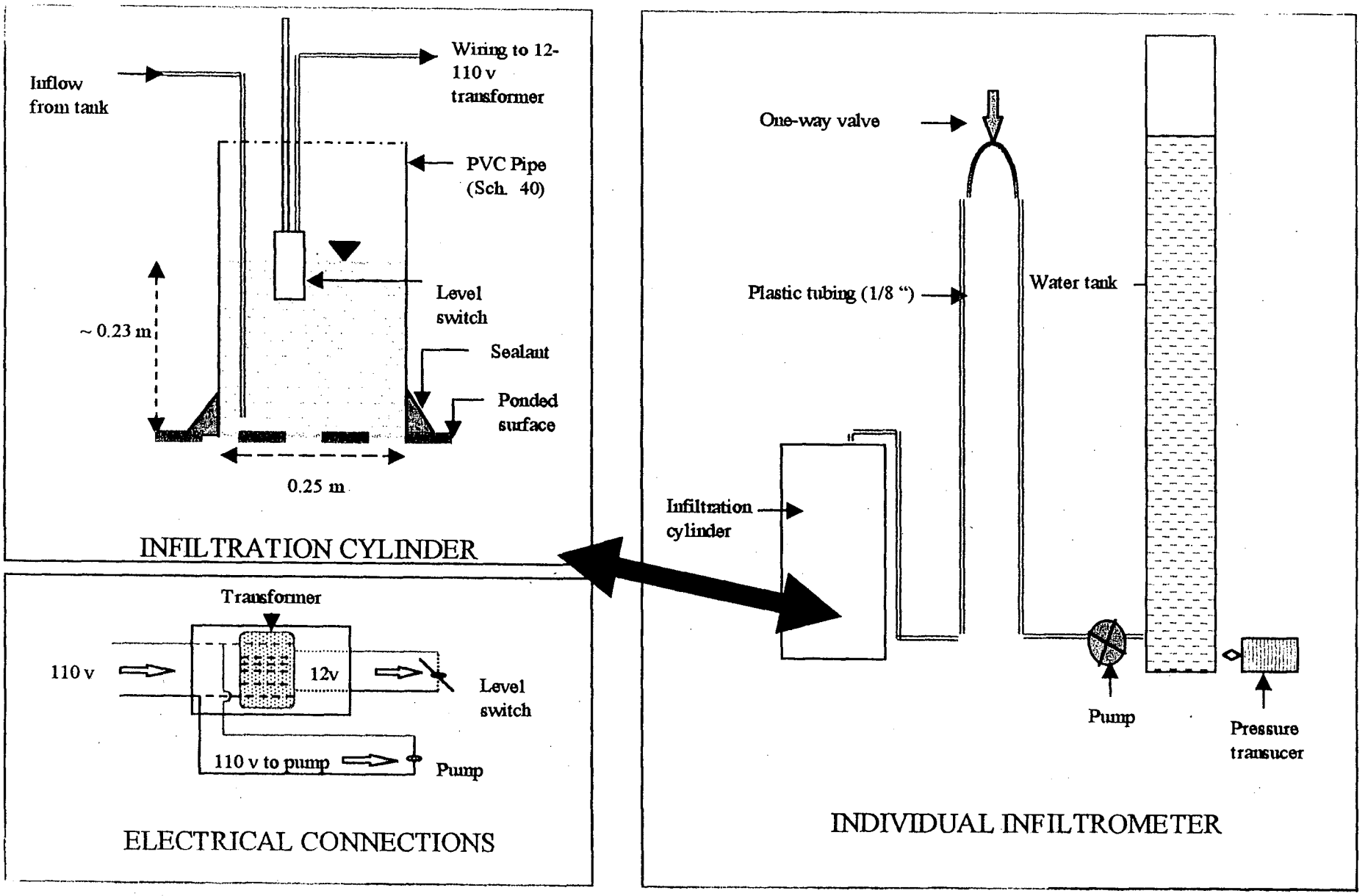

Figure I.7.8-2. Design of the infiltration system used to measure spatial variability in infiltration rate

Materials.

- Schedule 40 PVC pipe, 30 cm (12 in) ID, 1.8 m (6 ft) long, sealed at bottom.
- Schedule 40 PVC pipe, 25 cm (10 in) ID, 0.6 m (2 ft) long.
- Submersible pumps (Teel-1P805, 200 gallons per hour @ 1 foot of head).
- Magnetically actuated polypropylene float switch (model M8000, Madison).
- Polyethylene tubing, 0.318 cm (0.125 in) ID.
- Nalgene tubing reinforced PVC, 1.27 cm (0.50 in) ID.
- Voltage transformer (120<>12 v).
- Pressure transducers (P4100, 0-5 PSI range, Lucas Control Systems).
- Polyurethane sealant
- DAS

I.7.9. Neutron Logging

Theory. Neutron probe measurements are based on the principle of neutron thermalization during collisions with hydrogen atoms. "Fast" neutrons are emitted by the probe into the formation; a detector in the probe counts the "slow" neutrons produced by these collisions. The number of "slow" neutrons is proportional to the moisture content of the surrounding medium. Since water is by far the main source of hydrogen in this setting, the count is proportional to the moisture content. Although many calibrations exist for converting counts to moisture content, conversion is always highly formation- and well-completion-specific. Therefore, the counts, or ratio of counts to some standard count, are most reliably used in the determination of relative moisture content changes. In conjunction with tensiometer data, neutron probe measurements help define movement of water in the subsurface.

Neutron counts are generally unaffected by environmental factors, such as temperature, atmospheric pressure, or humidity, but the electronics of the unit may be. In addition, although the source decays very slowly, there will be decreases in neutron flux with time. To account for both effects, a set of "blank" readings should be taken each day, immediately before the first borehole is logged. These readings should be stable (coefficient of variation <2%) and in the expected range, specific to each unit. Unstable readings suggest electronic problems. Consistently high or low readings could also be due to electronic problems or due to damage to the probe shielding and would need to be further investigated.

Neutron logging has customarily been conducted in metal-cased boreholes. Metal casing interferes with electromagnetic logging and thus was not an option at the Box Canyon site. The disadvantage of the most common non metal casing material, PVC, is its high chlorine content. Chlorine strongly absorbs neutrons and significantly lowers sensitivity.

Installation. Several borehole completion designs were tested in the laboratory in order to find the least attenuative materials. Acrylic was found to be the most viable option because it contains no chlorine, is readily available, and is well suited for other non-seismic geophysical investigations. Laboratory investigations determined that a 2 to 4 mm-thick-walled acrylic pipe is virtually "invisible" to neutrons. Since acrylic pipe has not conventionally been used for well completion, pipe was custom-threaded by McCabe Bros., Inc. Polyurethane was chosen as the back-fill material to fill the annulus, because other back-fill materials, such as bentonite or sand may vary in moisture content. Three vertical (T-1, T-8a, and T-10) and four slanted holes (R-1, R-2, R-3, and R-4) drilled in FY96 were completed in this manner. Relative measurements of soil moisture content were made using a down-hole neutron probe in these wells.

The neutron source required for a measurement with an effective radius of 15 cm is of sufficiently low strength that it poses an insignificant health hazard when properly used. The probe used in this system (CPN 503DR Hydroprobe) consists of a 50 mCi Am-Be neutron source, which emits 1.1×10^5 neutrons per second, and a He detector of thermal neutrons.

During logging, the probe was lowered into an access borehole cased with an acrylic pipe and grouted with polyurethane. Readings were taken at desired depth intervals. Once the entire depth of the borehole was logged, the probe was retracted and placed in its plastic case.

I.7.10. Rigid Waveguide TDR

The most widely used field techniques for repetitive *in situ* measurements of the volumetric water content are the neutron logging and the gamma attenuation techniques. While these methods are only mildly intrusive (i.e. during installation of access tubes) and can provide relatively fast readings, the risks of radiation exposure has greatly limited their use. Additionally, with the neutron logging method, the sampling volume is strongly dependent on the water content itself, and near-surface readings are not accurate because neutrons escape to the surface. When automated, TDR has the potential to obtain accurate measurements of moisture content in porous media. This method is non-destructive (beyond the initial installation of probes) and allows measurements to be taken close to the surface.

Theory. The speed with which a pulse of electricity travels down a parallel transmission line depends on the dielectric value, (Ka), of the material in contact with, and surrounding the transmission line. The higher the dielectric value, the slower the speed. When a microwave pulse travels along a transmission line, it behaves like a light-beam. Discontinuities in the transmission line and in the surrounding material cause some of the energy to be reflected back through the line. When the pulse reaches the end of the transmission line, virtually all the remaining energy in the pulse is reflected back through the line, akin to a light-beam reflected by a mirror at the end of the tube. These

characteristics make it possible to measure the time required for a microwave pulse to travel along a known length of transmission line, referred to as a "waveguide."

The apparent dielectric value, Ka, of soil/rock can be determined by the formula

$$Ka = \left(\frac{tc}{L}\right)^2$$

where L is the length of the waveguide, t is the transit time in nanoseconds (billionths of seconds), and c is the speed of light in centimeters per nanosecond (i.e., 3.1 cm/ns).

The ability to use electromagnetic techniques to measure soil water content is based on the large contrast between the dielectric values of liquid water and of dry soil at microwave. The dielectric value for various materials is as follows:

Air	1
Water	80
Soil minerals	2-4
Basalt rock	11

Because of the extreme differences between the dielectric value of water and that of the other constituents in the soil/rock, the speed of a microwave pulse in a parallel transmission line buried in the soil/rock is greatly influenced by water content. This effect of water on the dielectric value of porous media had been known for some time. However, it was only fairly recently that the applicability of TDR to measuring moisture content was convincingly demonstrated by Topp et al. (1980). By determining the travel time of a step pulse propagating in a transmission line embedded in a dielectric medium, Topp et al., (1980) calculated the apparent dielectric value of the medium. They found that for a wide ranges of soil texture and porosity, the relationship between the moisture content and apparent dielectric value are, to the first order, soil texture and porosity independent.

The TDR instrument used for measuring moisture content was the Trase™ system (Soil Moisture Equip. Corp). This included a cable tester, a 16-channel multiplexer, WinTrase™ PC soft-ware, and 16 waveguides (Figure I.7.10-1). The Trase™ system has a measuring accuracy of +/- 2% when operating within the temperature range of 0 to 45^{0}C. Trase™ launches a series of fast-rise step pulses down the cable. Voltage measurements are taken along the waveguide at precise 10, 20, or 40

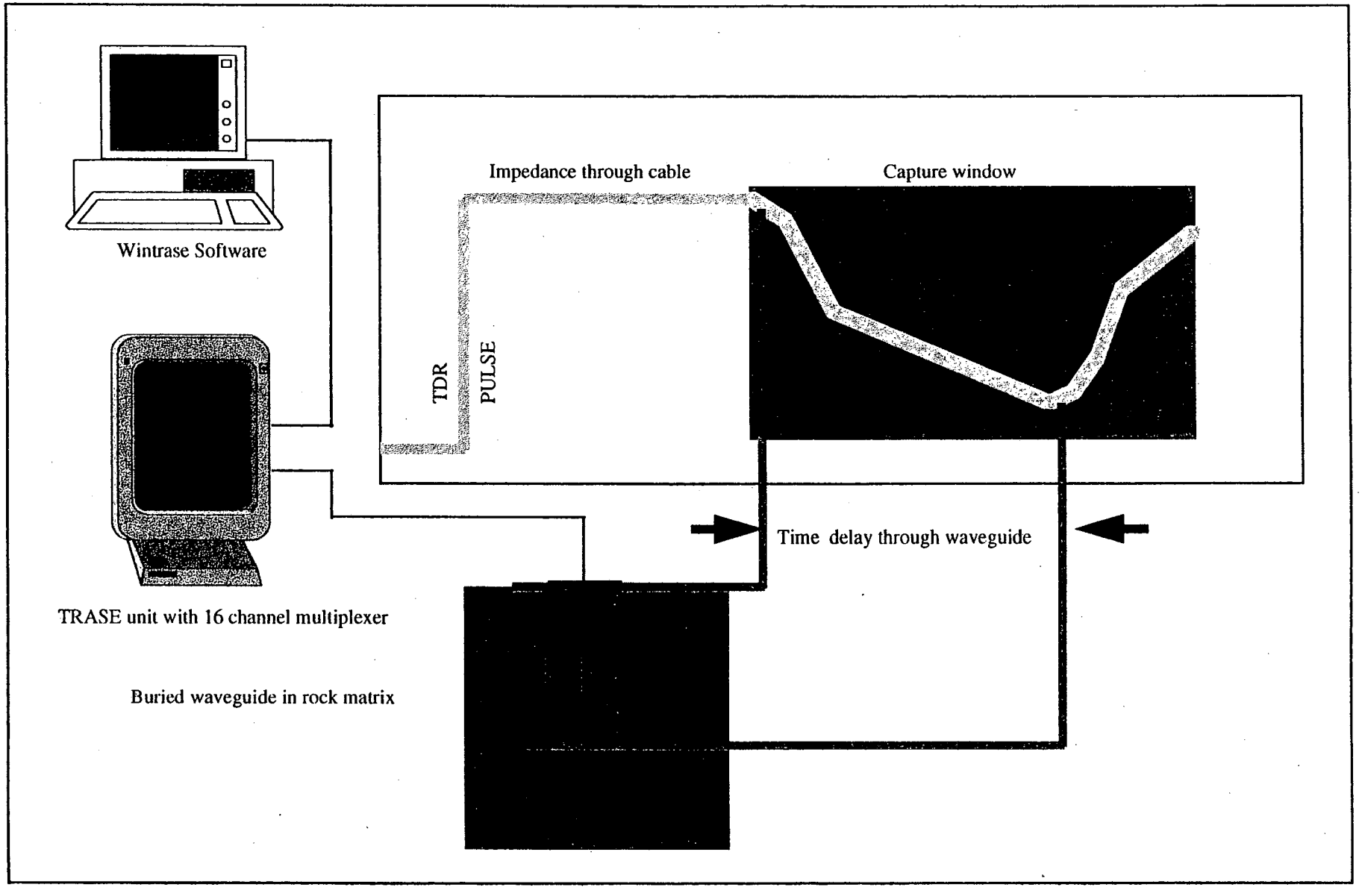

Figure I.7.10-1. Measurement of dielectric value with TDR

picosecond intervals. It takes several nanoseconds for the pulse to complete the journey along a 20 cm long waveguide and through the surrounding material. A TDR waveform for the material is produced by combining over 1,000 averaged sample points, displayed in a 10, 20, or 40-nanosecond-long sampling window. The number of sample point intervals from waveguide start to end are used to determine transit time down the waveguide, and hence the dielectric value of the surrounding material.

The waveguides used had three 0.2 m (0.66 ft) long stainless steel rods. Five waveguides were installed vertically close to the surface, such that the top end of each guide was flush with the ground surface. Of these, two each were installed in the solid basalt matrix and surface exposed fractures, while one was pushed into a layer of soil. To install the probes in the rock matrix, three vertical, 0.2 m (0.66 ft) deep, holes were drilled with a spacing of 2 cm (0.79 in). Cement slurry was then poured into the hole, after which the probes were inserted. This was done to remove any air-cavities around the waveguides. Eleven waveguides were installed in boreholes at depths of up to 0.6 m (2 ft). These waveguides were forced against the borehole wall using the procedure described in Section I.4 of this report. The Trase™ system was programmed to record dielectric values from the sixteen waveguides at intervals of 10 minutes.

I.7.11. Flexible Waveguide TDR

In order to install TDR waveguides in deep boreholes in basalt, a TDR pad was designed and tested. The TDR pad is placed flat on the surface where water contents are to be estimated (Selker et al., 1993), and therefore the flexibility of the TDR pad was critical to its use in fractured basalt. It consisted of a flexible backing material with the waveguides bonded to its surface and then placed in firm contact with the basalt surface where water content is to be monitored. The dielectric values of the basalt κ_B and of the pad κ_P have an additive effect (Maheshwarla et al., 1995) and

$$\kappa_B + \kappa_P = 2\kappa_{Eff}$$

where $2\kappa_{Eff}$ is the measured dielectric value.

This equation can be used to convert the measured dielectric value to that of basalt, provided the dielectric value of the backing material is known and does not change over time. The material selected for the backing material was polyethylene closed-cell foam (PCCF). The dielectric value of the PCCF was estimated by inserting rigid waveguides between sheets of PCCF, recording waveforms, and evaluating the wave traces in the usual manner. The dielectric value of the PCCF was found to be 1 and did not appear to change after soaking it. A TDR pad was constructed and calibrated by placing the pad on soil surfaces of varying water content, measuring κ_{Eff}, and then converted to κ_B using Equation (1) and a value of 1 for κ_P. The Topp equation (Topp et

al., 1980) was used to calculate a moisture content from the estimated κ_B, and good agreement was found with the soil water contents measured by oven drying the soil.

Construction. The first step in the construction of a flexible TDR probe was to attach the coaxial cables to the three stainless steel wires by soldering the stainless steel wire, a connector, and the coaxial cable together. The next step was to glue the three wires to the backing material (PCCF). To improve durability, a portion of the coaxial cable was also glued to the backing material.

It was essential to choose a material for the waveguides that was durable, ductile, economical and conductive. The two materials that performed adequately were stainless steel and copper. Stainless steel was chosen because of its availability and its durability.

There were four important criteria for the selection of the backing material. The material had to be able to mold to the uneven surfaces of fractured media, it could not transmit water through the material, it could not transmit electricity through the material, and it had to be economical. There were several materials considered for the backing material, but the major factors in the selection of PCCF were its flexibility and durability.

The main concern regarding the flexible TDR probe was its durability. The coaxial cable had a tendency to twist during storage and transport, which would cause the stainless steel wire to be torn off of the backing material. By taking the torque out of the cable before the wires were attached to the backing material, a large number of instruments that might have failed were saved. The instruments that were torn during transportation were either repaired immediately before placement in the borehole or eliminated from use. In the future, a better adhesive might solve this problem.

I.7.12. Groundwater Level Measurements

Between 8/30/96 and 9/6/96 the groundwater level was measured daily in open uncased boreholes using a DTW tape measure.

I.8. Data Acquisition System

A DAS was designed to collect data before, during, and after the infiltration test. Data collection began by the middle of August and continued through the end of September. Table I.8-1 summarizes parameters measured and probes used for measurements.

Two automated DASs were used to collect data. The first was designed to record signals emitted the from probes (voltage, current and resistance) and had the capacity of monitoring 440 sensors in real time. The second DAS was comprised of the Trase™ TDR system coupled with a multiplexer to allow for up to 16 successive probes to be

Table I.8-1. Box Canyon Infiltration Experiment 1996, Summary of Parameters Measured

Instruments	Parameter measured	Sensor	Gauge	Data Collection Sytem	Measurement Points (#)	Duration of Data
Neutron Probe	Volumetric moisture content	Neutron source/ counter	CPN Neutron probe	CPN unit	Seven wells	Sporadic
Tensiometers:						08/18-09/24
Shallow (LBNL)	Moisture potentials in wells	Porous ceramic cup	Pressure transducer	Voltmeter-Keithley	24	08/18-09/24
Deep (INEL)	Moisture potentials in wells	Porous ceramic cup	Pressure transducer	Voltmeter-Keithley	51	08/18-9/24
Water samplers	Tracer conc.	Porous cermic cup	Lab Analysis	Manual	56	08/18-09/24
TDR:						08/18-09/24
LBNL	Dielectric	Three-wire wave guides	Trase (automated)	Automated	16	08/18-09/24
INEL	Dielectric	Three-wire wave guides	Tektronix 1502	Manual	100	08/18-09/24
Air pressure	Ambient air pressure	Open tube	Pressure transducer	Voltmeter-Keithley	50	08/18-09/24
Infiltrometers	Infiltration rate		Pressure transducer	Voltmeter-Keithley	10	08/18-09/24
Open wells	Depth to water table		Scale	Manual	8	08/18-09/24
ER	Electrical resistance	ER probes			80	08/18-09/24
Termistors	Temperature	Termistor	Ohmmeter	Ohmmeter-Keithley	38	08/18-09/24

measured at intervals of less than 30 seconds. A general structure of the DAS is given in Figure I.8-1.

Measurements. In the DAS used to make non-TDR readings, pressure changes in fluids (air and water) were measured as voltage changes in transducers that were excited with a known reference voltage (5-12 V). Flow rates were also measured as voltage output. Temperature readings were collected from the DAS as measurements of resistance from thermistors. Electrical resistivity was calculated from measures of voltage and current where the DAS was used to excite a four-prong probe and then measure the voltage and current in alternate pairs of prongs. The pressure transducers and flow meters were continuously connected to a voltage source, and at desired time intervals the output signal from each sensor was recorded in a fixed sequence.

Hardware. The TDR instrument used for measuring moisture content was the Trase™ system (Soil Moisture Equip. Corp.). This included the cable tester, a 16 channel multiplexer, WinTrase PC software, and 16 waveguides.

Pressure transducers and the flow meters were powered with a Hewlett Packard E3611 DC power supply model. The output voltage from the pressure transducers and flow meter were measured by a Keithley 2001 digital multimeter. Resistance measurements from the thermistors was taken with a Keithley 2001 multimeter. The Hewlett Packard 33120A function/waveform generator was used to power the ER probes with a 12-V AC current.

Software. The TDR wave forms were analyzed by the Wintrase™ PC software. The DAS for non-TDR measurements was operated by the LABVIEW software. During a typical data acquisition 'sweep', the LABVIEW program launched from a laptop computer would alert the multiplexer to sequentially connect each of the 440 sensors to the relevant component of the multimeter (voltage, current or resistance). The timing between sweeps could be changed during the period of data collection.

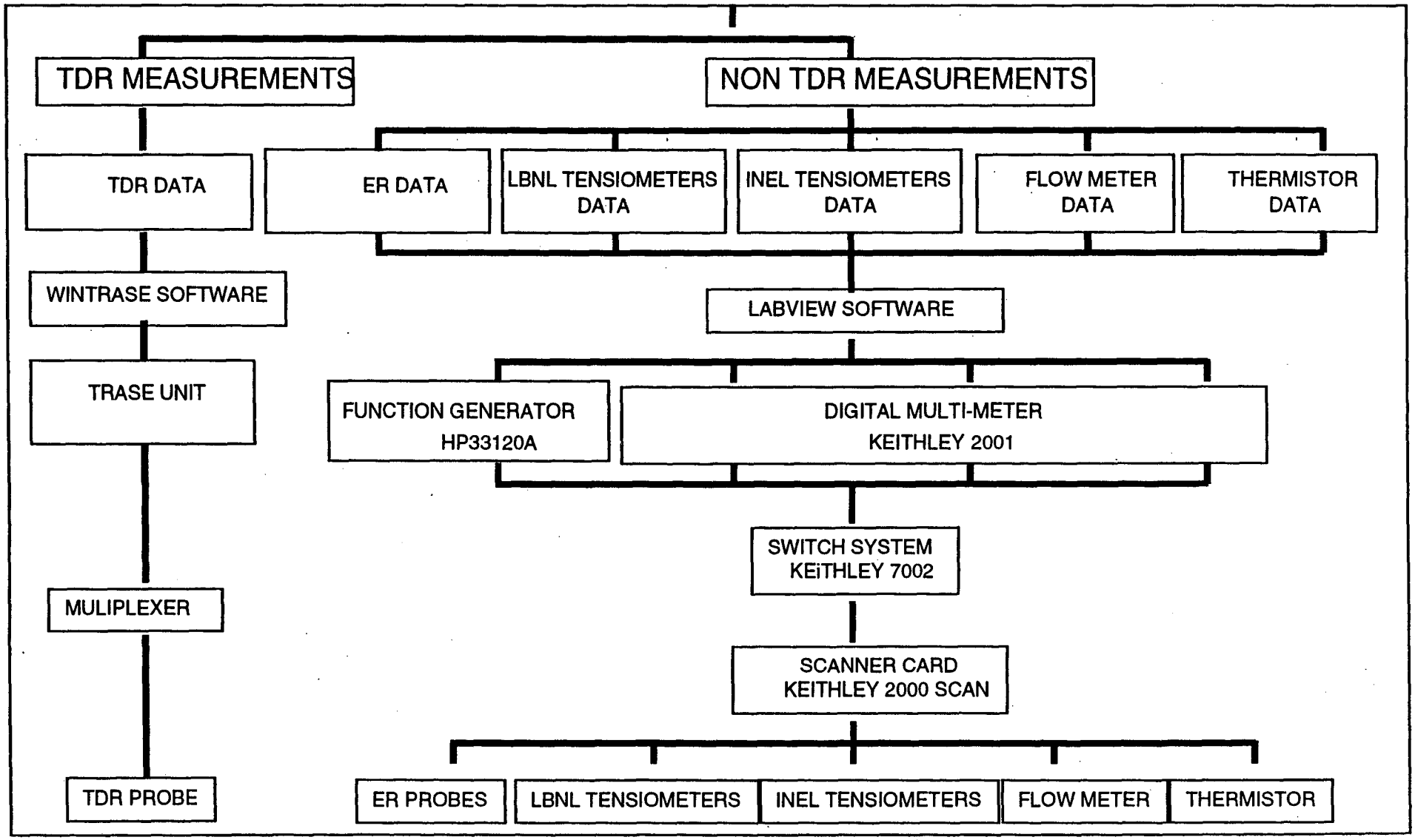

Figure I.8-1. Diagram of DAS used for the infiltration experiment

I.9. Selection of Depths of Instrumentation

We selected instrument installation depths that were near main lithological features such as:

- Soils and flow top breccia and boulders
- Surface soil infilled fractures
- Massive basalt
- Central fracture zone
- Rubble zone
- Fractures

In order to identify these features, we used the results of coring and TV logging. TV logging was completed by the USGS using a video camera with a light attached to it, that was lowered to the bottom of the hole. The camera was slowly lifted up the borehole while recording the features and the depth.

The video logs were first developed into snapshots of the boreholes at 0.3 m (1 ft) intervals, and then arranged on a large board to reflect a cross sectional view of the site. The clarity of the film was too poor to use as a visual representation of the site. Instead, the actual videos of the boreholes were viewed, and each borehole was individually mapped. Two parallel lines were drawn on graph paper, with each square representing a 0.3 m (1 ft) interval of the borehole. The characteristics of the borehole wall within each interval were mapped with important features, such as basalt density, apparent moisture content, rubble zones, horizontal fractures, and vertical fractures. This technique provided a 1-dimensional view of individual boreholes, but not the desired 3-dimensional view.

A 3-D model of the site was constructed using wooden rods to represent the individual boreholes. Red lines were drawn on the rods to represent the fractures seen in the video logs. Blue areas were painted on to the rods to represent moist zones in the bore hole. Purple areas represented rubble zones. The rods were then arranged on a piece of poster board to produce a clear 3-D model.

The instruments were strategically placed at depths near main lithological features, such as fractures in the basalt. Instruments were also placed with increasing density near the surface of the site to increase the accuracy of characterizing the initial infiltration of the water. Table I.9-1 summarizes the types and depths of the instruments installed at the Box Canyon site.

Table I.9-1. Summary of instrumentation at the Box Canyon site

Well E-1

Number	depth (ft)	Tensiometer	Transducer #	Suction Lysimeter	TDR	Thermister	Piezometer
1	7	deep	2	shallow	+	T81	+
2	12	deep	29	shallow	+	T71	+
3	20	deep	45		+	T15	+
4	29	deep	41		+	T73	+
5	36	deep	76		+	T51	+
6	43	deep	48	deep	+	T54	+
7	54	deep	78	deep	+	T55	+
8	57	deep	16	deep	+		+

Well E-2

Number	depth (ft)	Tensiometer	Transducer #	Suction Lysimeter	TDR	Thermister	Piezometer
1	6	deep	38	shallow	+	T50	+
2	12	deep	71		+	T56	+
3	20	deep	23	deep	+	T67	+
4	30' 10"	deep	97	deep	+	T66	+
5	43				+	T74	+
6	50	deep	90	deep	+	T70	+
7	57				+	T72	+

Well E-3

Number	depth (ft)	Tensiometer	Transducer #	Suction Lysimeter	TDR	Thermister	Piezometer
1	7				+		+
2	17			shallow	+	T9	+
3	22	deep	33	deep	+	T69	+
4	29	deep	74	deep	+	T80	+
5	36	deep	12		+	T58	+
6	47	deep	50		+	T61	+
7	56	deep	72	deep	+	T62	+

Table I.9-1. Continued

Well E-4

Number	depth (ft)	Tensiometer	Transducer #	Suction Lysimeter	TDR	Thermister	Piezometer
1	15	deep			+		
2	23	deep	1		+	T64	+
3	28	deep	14	deep	+	T53	+
4	43	deep		deep	+	T48	+
5	50	deep	77	deep	+	T65	+
6	57	deep	93		+		+

Well I-1

Number	depth (ft)	Tensiometer	Transducer #	Suction Lysimeter	TDR	Thermister	Piezometer
1	1	shallow	82	shallow	+		+
2	5	deep	8	shallow	+		+
3	10	deep	9	shallow	+		+
4	15	deep	65	shallow			+
5	20	deep	11	deep			+
6	28	deep	35	deep			+
7	33	deep	44	deep			+
8	38	deep	98				+

Well I-2

Number	depth (ft)	Tensiometer	Transducer #	Suction Lysimeter	TDR	Thermister	Piezometer
1	1' 6"	shallow	60	shallow			+
2	5	deep		shallow			+
3	10	deep		shallow			+
4	14	deep		shallow			+
5	20	deep					+
6	28	deep			+		+
7	35	deep					+
8	40	deep					+

Table I.9-1. Continued

Well I-3

Number	depth (ft)	Tensiometer	Transducer #	Suction Lysimeter	TDR	Thermister	Piezometer
1	1	shallow	88	shallow		T78	+
2	5	deep	15	shallow		T68	+
3	10	deep	28			T60	+
4	15	deep	34			T77	+
5	20	deep	17			T47	+
6	25	deep	79			T52	+
7	30	deep	30		+	T6	+
8	35	deep	75		+	T76	+

Well T-2

Number	depth (ft)	Tensiometer	Transducer #	Suction Lysimeter	TDR	Thermister	Piezometer
1	2	shallow	56	shallow	+		+
2	6	shallow	99	shallow	+		+
3	10	shallow	95	shallow	+		+
4	14' 6"	deep		shallow	+		+
5	19' 6"	deep		shallow	+		+

Well T-3

Number	depth (ft)	Tensiometer	Transducer #	Suction Lysimeter	TDR	Thermister	Piezometer
1	2	shallow	57	shallow	+		+
2	6	shallow	54	shallow			+
3	10	shallow	89	shallow			+
4	15	deep					+
5	20	deep			+		+

Table I.9-1. Continued

Well T-4

Number	depth (ft)	Tensiometer	Transducer #	Suction Lysimeter	TDR	Thermister	Piezometer
1	1' 8"	shallow	27	shallow	+		+
2	5' 6"	shallow	42	shallow	+		+
3	9' 1"	shallow	3	shallow	+		+
4	13' 8"	deep		shallow	+		+
5	19' 3"	deep		shallow	+		+

Well T-5

Number	depth (ft)	Tensiometer	Transducer #	Suction Lysimeter	TDR	Thermister	Piezometer
1	1	shallow	51	shallow			+
2	5	shallow	39	shallow			+
3	10	shallow	52	shallow			+

Well T-6

Number	depth (ft)	Tensiometer	Transducer #	Suction Lysimeter	TDR	Thermister	Piezometer
1	2' 3"	shallow	81	shallow	+		+
2	5' 11"	shallow	100	shallow	+		+
3	9' 10"	shallow	85	shallow	+		+
4	14' 10"	deep		shallow	+		+
5	19' 10"	deep		shallow	+		+

Table I.9-1. Continued

Well T-7

Number	depth (ft)	Tensiometer	Transducer #	Suction Lysimeter	TDR	Thermister	Piezometer
1	2	shallow	22	shallow	+		+
2	6	shallow	84	shallow			+
3	10	shallow	83	shallow			+
4	15		5	shallow			+
5	19		4	shallow			+

Well T-8

Number	depth (ft)	Tensiometer	Transducer #	Suction Lysimeter	TDR	Thermister	Piezometer
1	1	shallow	73	shallow	+		+
2	5	shallow	31	shallow	+		+
3	9	shallow	10	shallow	+		+

Well T-9

Number	depth (ft)	Tensiometer	Transducer #	Suction Lysimeter	TDR	Thermister	Piezometer
1	1	shallow	64	shallow	+		+
2	5	shallow	63	shallow	+		+
3	10	shallow	62	shallow	+		+

Table I.9-1. Continued

Well II-5

Number	depth (ft)	Tensiometer	# ER Probes	Piezometer
1	1		1	+
2	5			+
3	13		1	+
4	19		1	+
5	25	shallow	1	+
6	31		1	+
7	36		2	+
8	42		1	+
9	46' 7"		1	+
10	53' 5"			+
11	59'		1	+

Well S-1

Number	depth (ft)	# ER Probes	Piezometer
1	2	2	+
2	6	2	+
3	10	2	+
4	14	2	+

Well S-2

Number	depth (ft)	# ER Probes	Piezometer
1	3	2	+
2	7.5	2	+
3	10	2	+
4	14	2	+

Well S-3

Number	depth (ft)	# ER Probes	Piezometer
1	2.5	1	+
2	6.5	1	+
3	11	1	+
4	15	1	+
5	19.5	1	+
6	26.3	1	+
7	30	1	+
8	35	1	+

Well S-4

Number	depth (ft)	# ER Probes	Piezometer
1	5	1	+
2	10	1	+
3	15	1	+
4	19	1	+
5	25	1	+
6	33.5	1	+
7	41	1	+
8	44	1	+
9	48	1	+

I.10. Tracer test

A slug of potassium bromide tracer was added to the pond on 9/2/96, between 3:58 p.m. and 4:20 p.m., resulting in a tracer concentration in the pond of approximately 3 g/l. The movement of the tracer was monitored with ER probes and by collecting water samples. At this low concentration, the tracer was not expected to affect radar data. Just before the test, the water supply into the pond was stopped. The water supply was reestablished on 9/4/96 at 4:24 p.m. in order to prevent atmospheric air from entering the soils and to continue the infiltration test.

II. Test Results

II. 1. Tensiometry Data

II.1.1. Shallow Tensiometers

The results of water pressure measurements using the shallow tensiometers are shown in Figures II.1.1-1 through II.1.1-8. Figure II.1.1-9 shows the variations in the barometric pressure throughout the test. Table II.1-1. shows a summary of lithology, water pressure measured using shallow tensiometers, and depths where water samples were collected before and during the infiltration test. The following is a brief discussion of the results obtained.

In general, tensiometers identified the arrival of water at sensor locations by showing an increase in the water potential, or liquid saturation. We observed two types of saturation increases:

(1) Rapid increase in saturation:

(a) of the top soil-rock layer, which was typical for all tensiometers at 0.3 m (1ft) depth.

(b) of the vadose zone profile, which was observed, for example, in Well T-9 at 0.3 m (1 ft), 1.5 m (5 ft), and 2.7 m (9 ft).

(2) Gradual increase in saturation, which was observed in Well T-5 at 3 m (10 ft).

There was evidence of preferential flow when deeper probes saturated earlier than shallow ones. For example, in Wells T-5 and T-8, the initial saturation was observed at 2.7-3 m (9-10 ft), while 1.5 m (5 ft) was still dry.

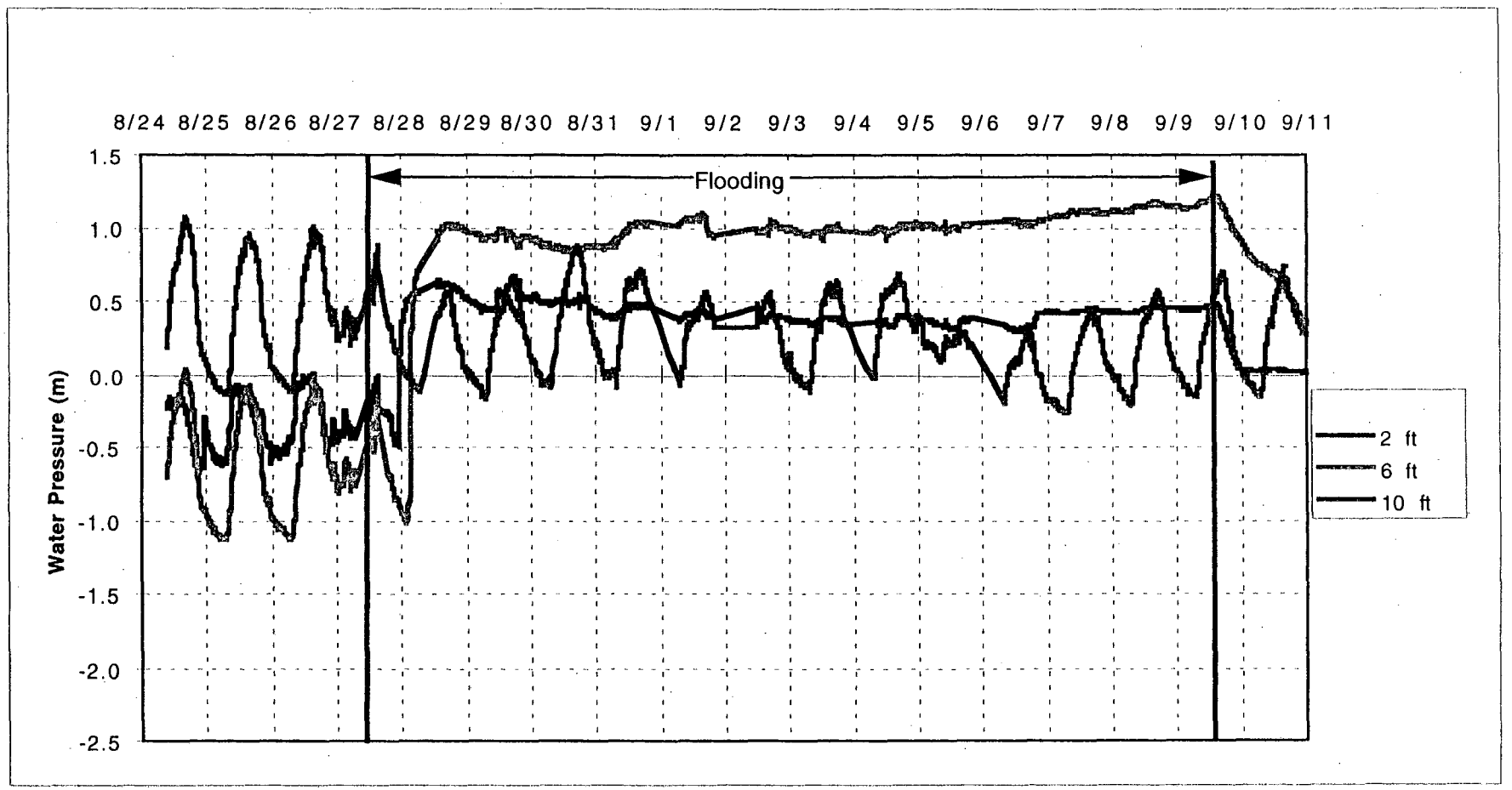

Figure II.1.1-1. Time-trend of water pressure in well T-2

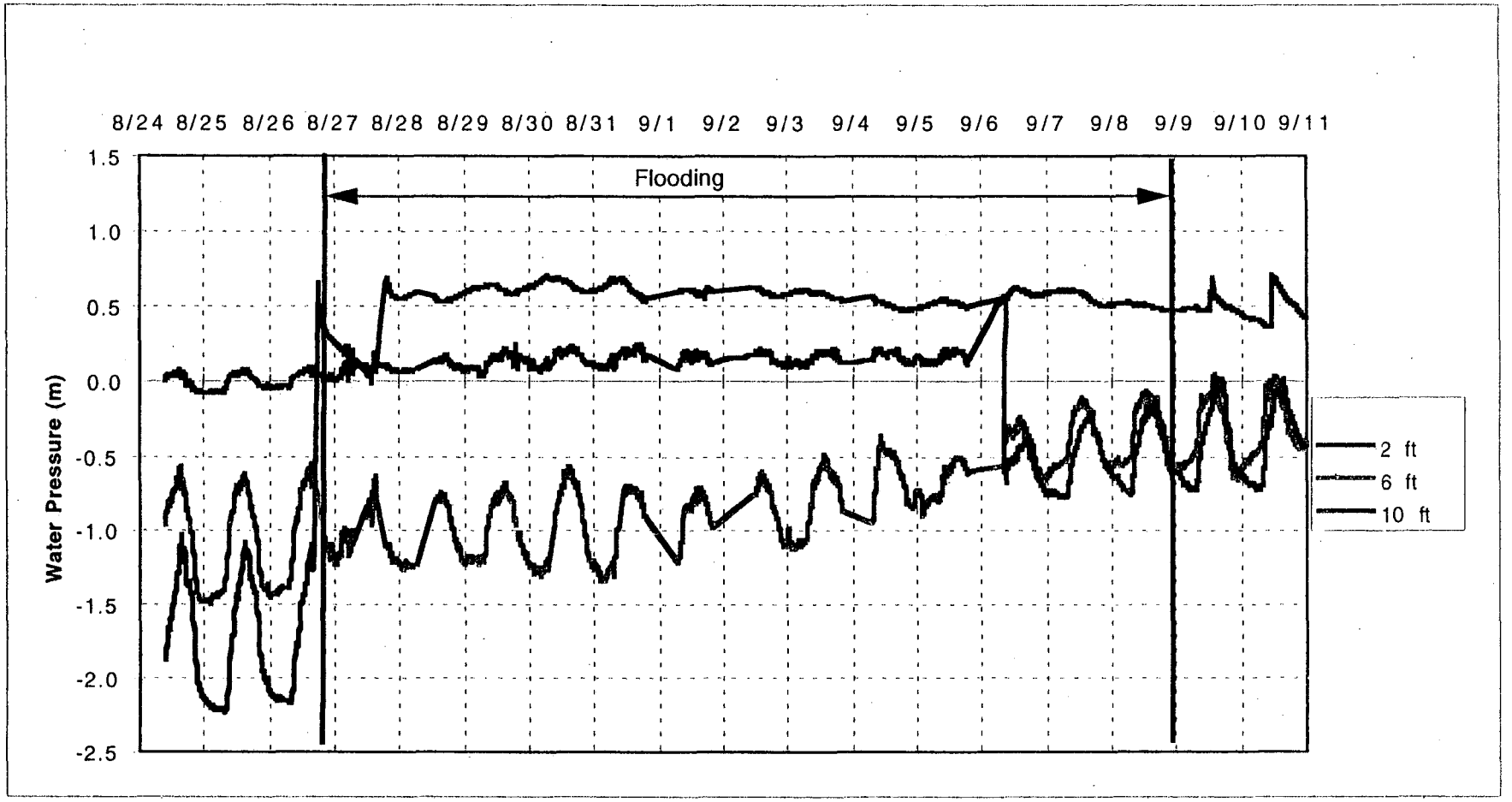

Figure II.1.1-2. TIme trend of water pressure in well T-3

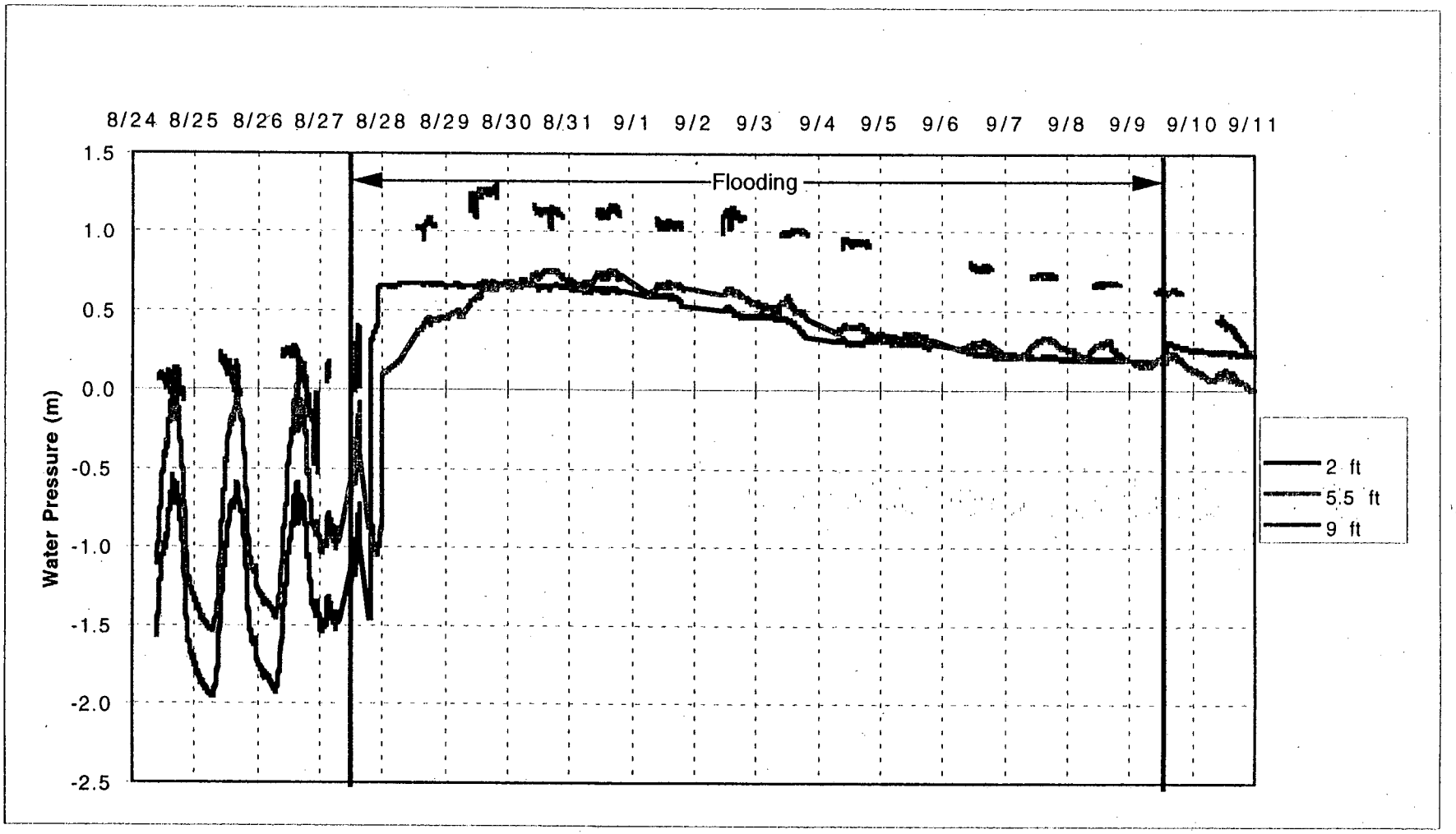

Figure II.1.1-3. Time trend of water pressure in well T-4

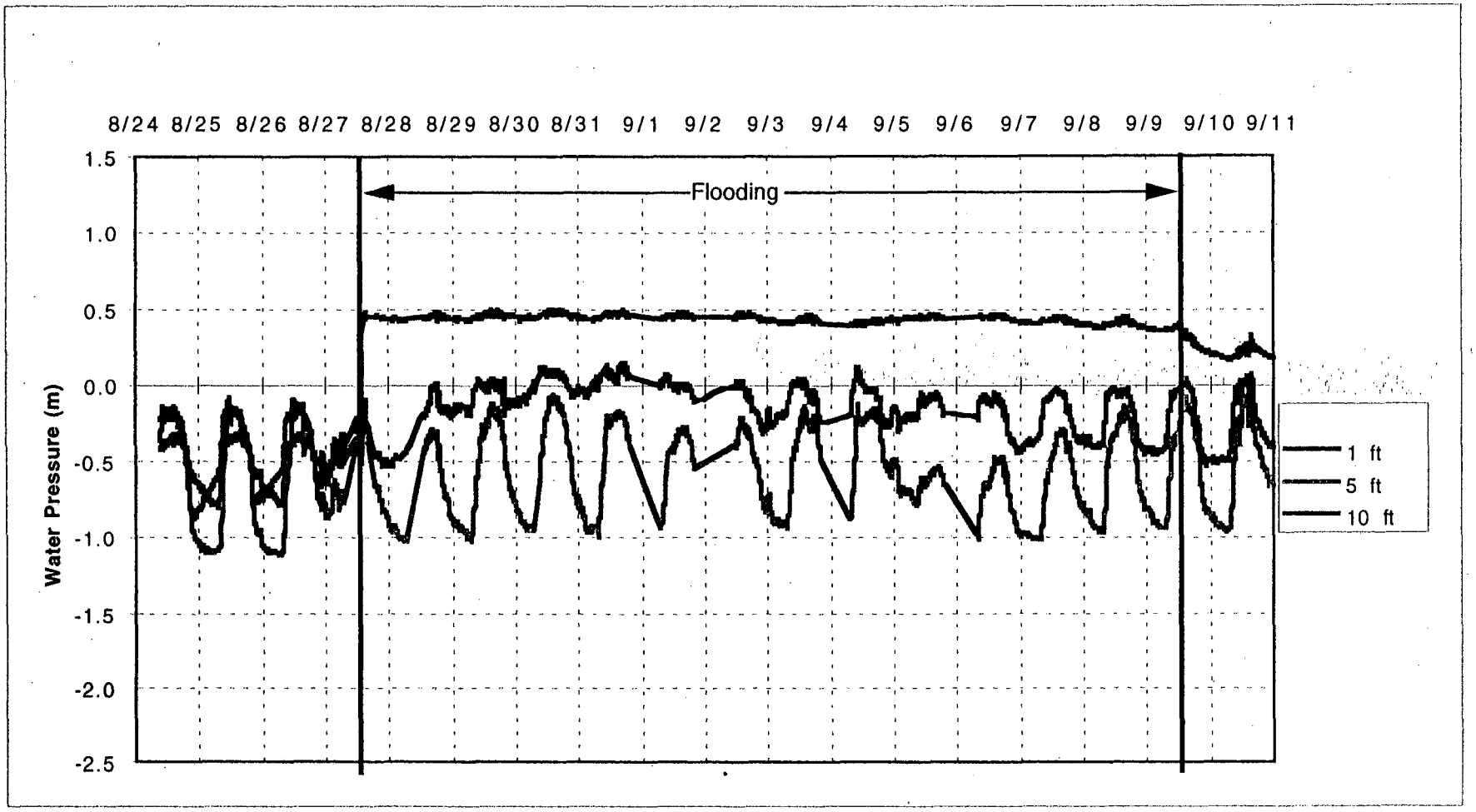

Figure II.1.1-4. Time trend of water pressure in well T-5

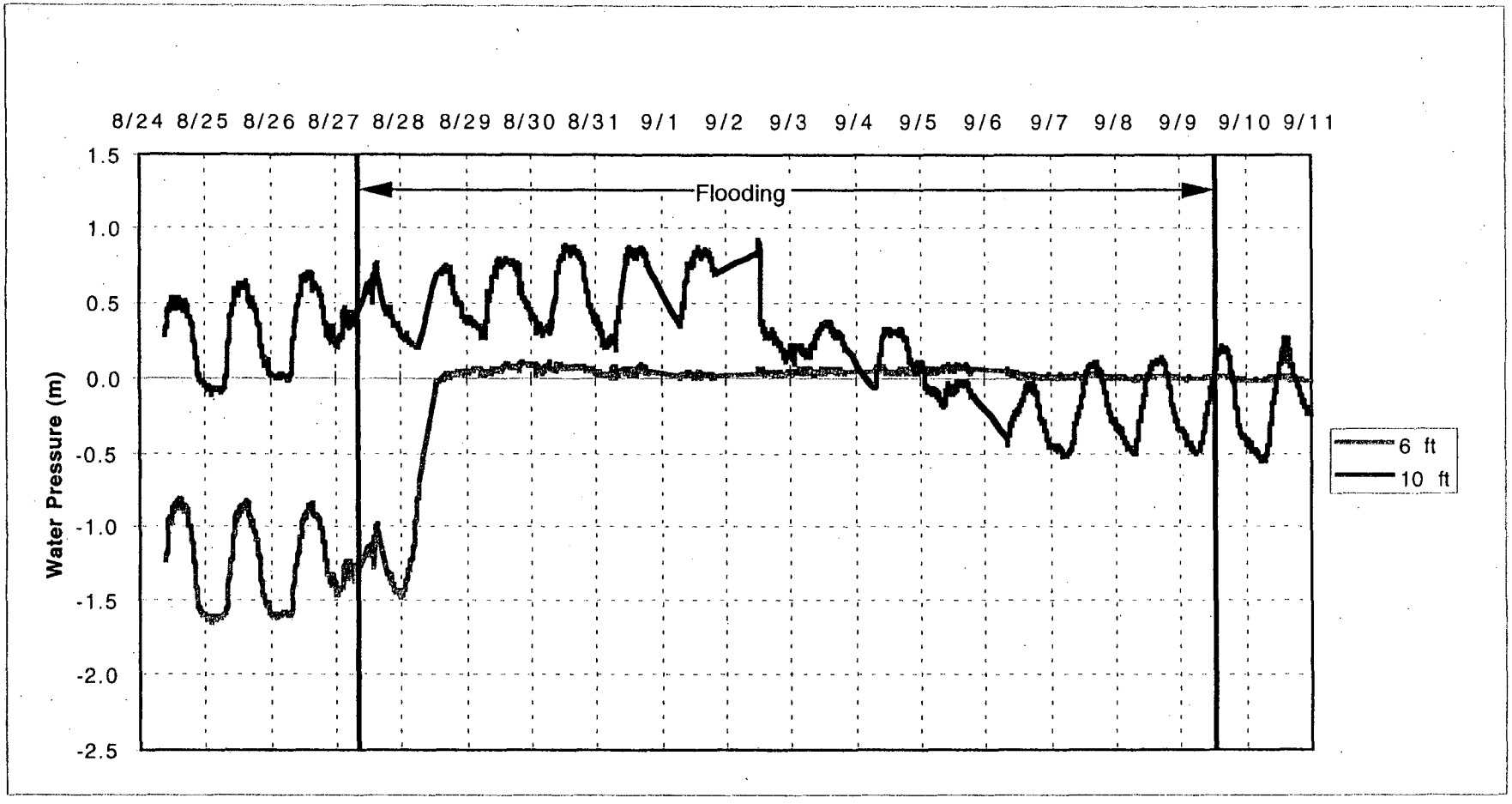

Figure II.1.1-5.Time trend of water pressure in well T-6.

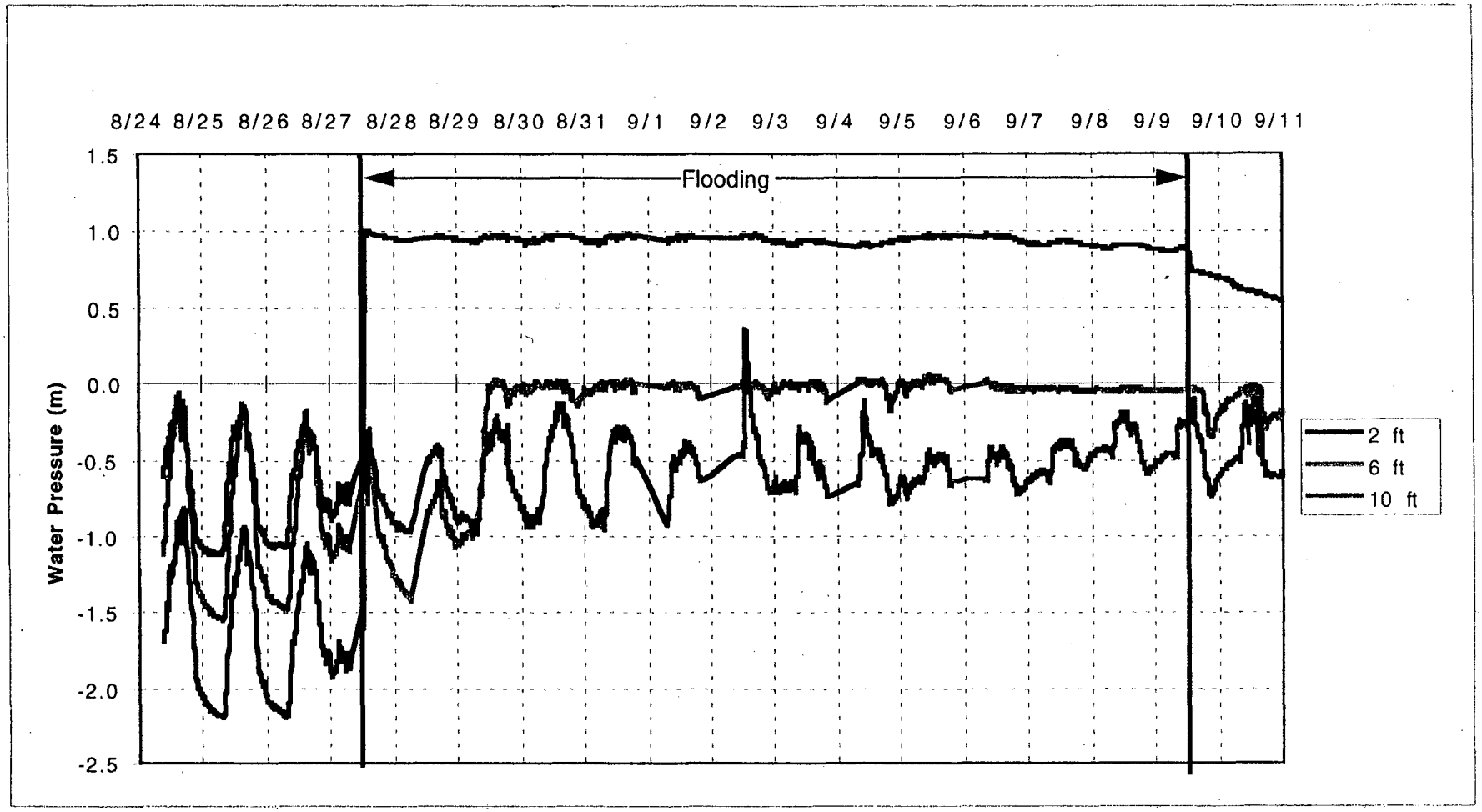

Figure II.1.1-6. Time trend of water pressure in well T-7

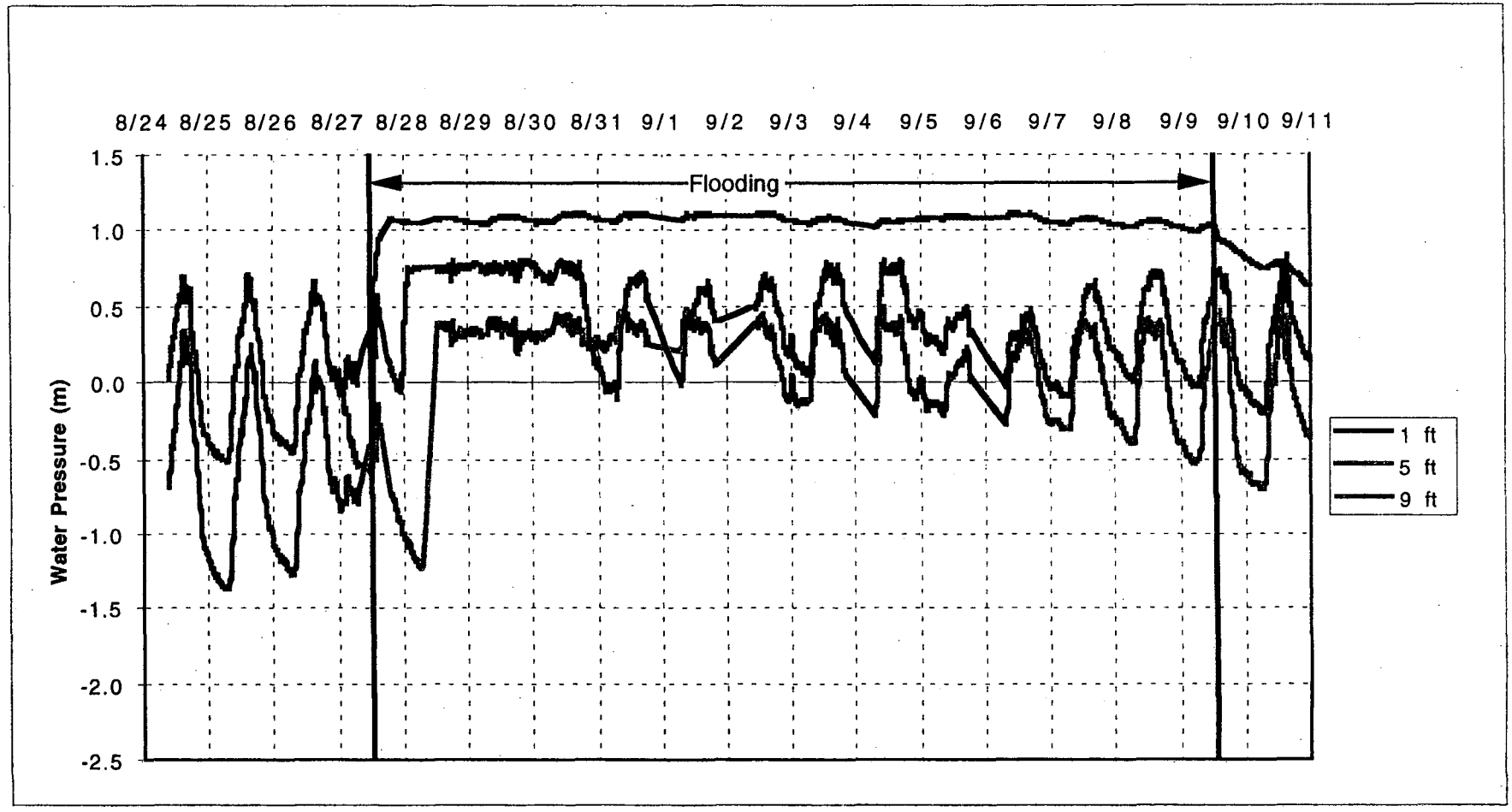

Figure II.1.1-7. Time trend of water pressure in well T-8

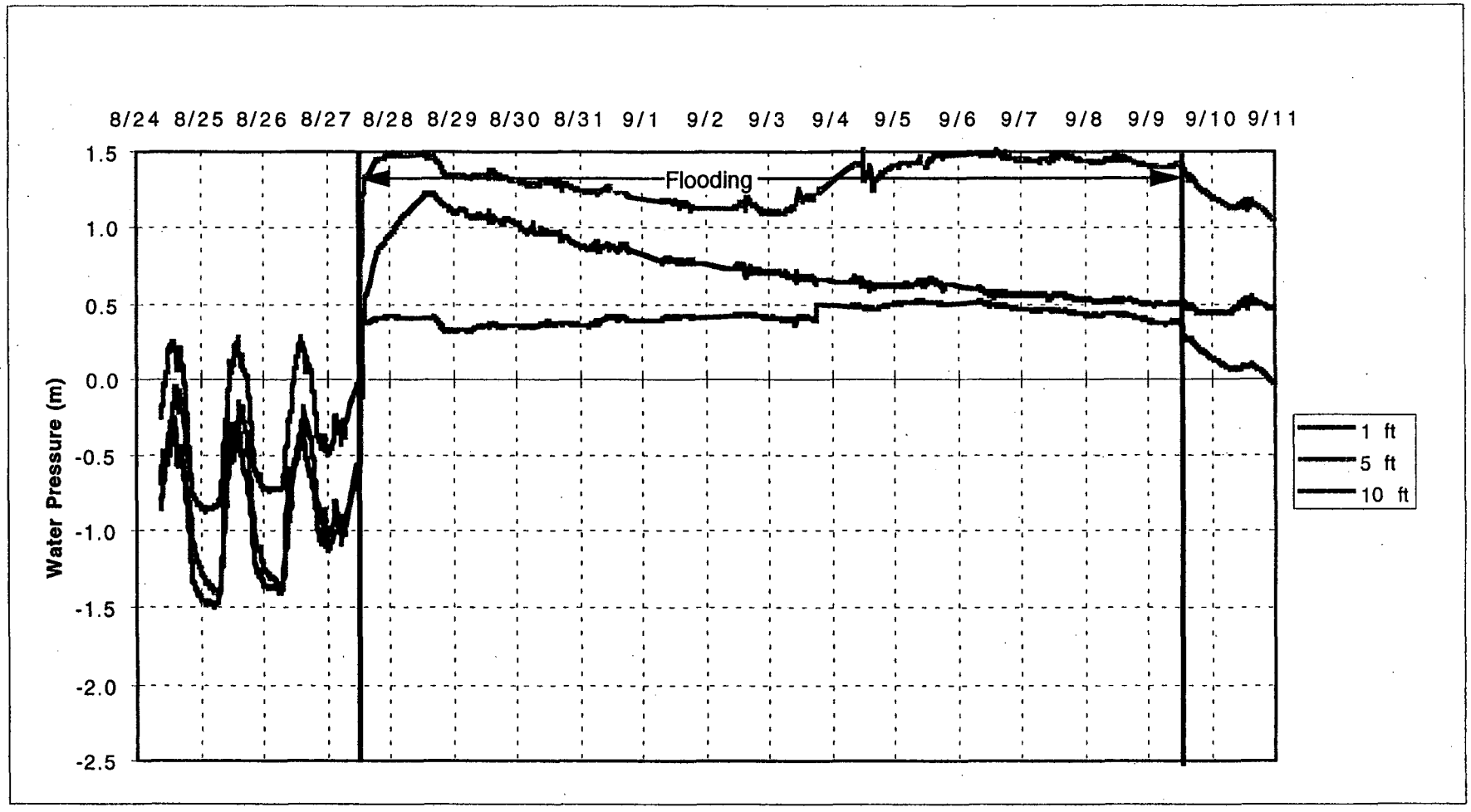

Figure II.1.1-8. Time trend of water pressure in well T-9

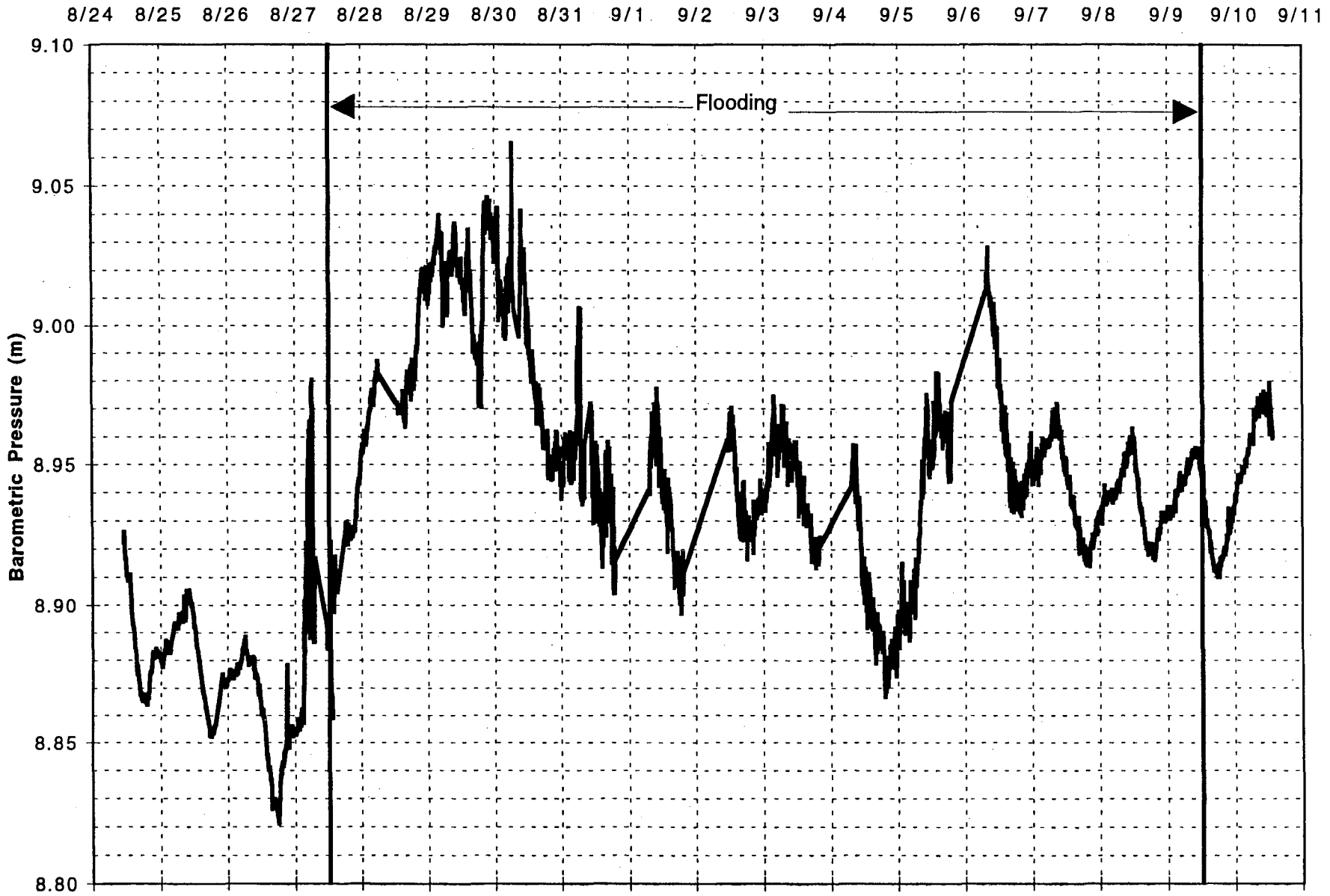

Figure II.1.1-9. Barometric pressure

Table II.1-1. Summary of Tensiometer and Lysimeter Correlations

Summary of Tensiometer and Lysimeter Data					Water Sample		
Well	**depth**	**Location**	**Lithology**	**Affect of Infiltration as shown by Tensiometer Readings**	**Before**	**During**	**Notes**
T-2	2'	Outside of Pond	Vesicular Zone and at 3' low angle fracture	Half-day stagger before being affected by initial infiltration. Immediately affected at end of infiltration. During the infitration amplitude of cyclic fluctuations decrease.	no	yes	Stagger shows that the preferential flow path from the pond to the tensiometer is continuous but takes about a half day for water to migrate. The flow path is saturated during the test as is apparent when the pressure drops at end of test.
T-2	6'	Outside of Pond	One large Vesicle	Half-day stagger before being affected by initial infiltration. Immediately affected at end of infiltration. During the infitration amplitude of cyclic fluctuations decrease.	no	yes	Stagger shows that the preferential flow path from the pond to the tensiometer is continuous but takes about a half day for water to migrate. The flow path is saturated during the test as is apparent when the pressure drops at end of test.
T-2	10'	Outside of Pond	Low angle Fracture	Mostly unaffected by infiltration test.	no	small volume collected at one day during test.	This low angle fracture does not act as a main flow of water from the ponded area at the surface.
T-3	2'	Just outside of Pond Berm	Vesicular Zone and at 3' low angle fracture	Water pressure jumps on 8/26 at night. Pressure jumps after infiltration. During infiltration the amplitude of cyclic fluctuations decreases.	no	no	Water pressure jumps drastically from -1.6 m to 0.4 m on 8/26/1996 at night. Why? Ponded water affects the water pressure, but no water was collected. The collection vial did get moist near the end of the infitration test.
T-3	6'	Just outside of Pond Berm	Vesicular Band	Gradual increase of water pressure during the infiltration test. Amplitude of cyclic fluctuations stays constant before and during the test.	no	no	Water travels very slowly and in small amounts from the pond to this vesicular band.

Table II.1-1. Continued

T-3	10'	Just outside of Pond Berm	Horizontal Fracture	Very gradual increase of water pressure during the infiltration test. Drastic drop in pressure on 9/6/1996 in the afternoon. Amplitude of cyclic fluctuations increases after the drop in pressure.	no	no	
T-4	2'	Outside of Pond	Vesicular Zone	Half-day stagger before being affected by infiltration. During infiltration the pressure maximizes and then decreases. Pressure jump after end of test.	no	yes	Stagger shows the preferential flow path from the pond to the tensiometer is continuous but takes time for water to migrate. Maximize and then drop of pressure could show that the infiltrating water brought with it sediments that decrease permeability.
T-4	5'	Outside of Pond	Horizontal Fracture	Half-day stagger before being affected by infiltration. During infiltration the pressure maximizes and then decreases. Pressure jump after end of test.	n/a	n/a	Stagger shows the preferential flow path from the pond to the tensiometer is continuous but takes time for water to migrate. Maximize and then drop of pressure could show that the infiltrating water brought with it sediments that decrease permeability.
T-5	1'	Inside of Pond	Vesicular Zone	Large jump in water pressure at beginning of infiltration test and stays constant throughout the test. Drops in pressure after infiltration test.	no	no	Almost instantaneous increase in pressure shows that there is a fast flow path for water from the surface of the pond to the vesicular zone at 1'. Maybe through soils or through interconnected vesicles.
T-5	5'	Inside of Pond	Vesicular Zone	Mostly unaffected by test.	no	no	Shows that there is not a main flow path for water from the surface of the pond to the vesicular zone at 5 feet.
T-5	10'	Inside of Pond	Vesicular Zone	Gradual Increase of pressure after the infiltration. Pressure decreases after reaching a maximum value during the infiltration.	no	no	Gradual increase in pressure shows that water increase as time proceeds until a maximum amount of flow is obtained. The resulting decrease after could showthat the infiltrating water brought with it sediments that decrease permeability.
T-6	2'	Inside of Pond	Vesicular Zone	Water pressure increases at the start of the infiltration and then decreases on 9/2/1996. Pressure drops at end of the infiltration test.	no	yes	Almost instantaneous increase in pressure shows that there is a fast flow path for water from the surface of the pond to the vesicular zone at 2'. Drop in pressure at end of test shows that the constant head in the pond quickly affects the water pressure
T-6	6'	Inside of Pond	Basalt	Half day stagger before affected by test. Increase in pressure and amplitude of cyclic fluctuations diminish.	no	no	Tensiometer in an area of basalt and is affected by infiltration test. What is the porosity of this basalt? Flow rate through this massive basalt?
T-6	10'	Inside of Pond	Low angle fracture	Mainly unaffected by test.	no	no	Drop in pressure at 9/2/1996 is simultaneous with the drop in pressure at T-6 2' Vesicular Zone. Could these two areas be interconnected in some way?

Table II.1-1. Continued

T-7	2'	Inside of Pond	Vesicular Zone	Instantly affected by both the beginning and the end of the infiltration test. Cyclic fluctuations diminish during the infiltrationt test.	no	yes	Almost instantaneous increase in pressure shows that there is a fast flow path for water from the surface of the pond to the vesicular zone at 2'. Drop in pressure at end of test shows that the constant head in the pond quickly affects the water pressure
T-7	6'	Inside of Pond	Low angle and horizontal fracture zone	Staggered and gradual increase of pressure after test starts and then reaches a constant pressure. Pressure immediately drops at the end of the test.	no	yes	Slow response the infiltration test shows that there is a gradual pathway for water to reach the low angle and horizontal fracture zone. Once the pathway is saturated any changes in pressure at the surface affect the tesiometer.
T-7	10'	Inside of Pond	Massive Basalt	No affect.	no	no	Shows that there is a good seal in the grouting. Assume that massive basalt is quite impermeable to water.
T-8	1'	Inside of Pond	Low and high angle fracture zone	During the test the pressure is constant. Before and after the test the pressure drops.	no	no	Why is there a huge drop in the pressure before the test?
T-8	5'	Inside of Pond	High Angle Fracture	Half-day stagger before affected. Cyclic fluctuations increase as test proceeds.	no	no	Why do the cyclic fluctuations increase during the test?
T-8	9'	Inside of Pond	Low Angle Fracture	Half-day stagger before affected. Cyclic fluctuations increase as test proceeds.	no	no	Why do the cyclic fluctuations increase during the test?
T-9	1'	Inside of Pond	Vesicular Zone	Instantaneously affected at beginning and end of the infiltration test. Amplitude of cyclic fluctuations decrease during the test.	no	yes	During the test there are smooth fluctuations of pressure. Instananeous affect of infiltration test shows that there is a fast flow path for water from the surface of the pond to the vesicular zone at 1'.
T-9	5'	Inside of Pond	Low Angle Fracture	Instantaneous increase of pressure at the start of the infiltration test. Pressure maximizes and then decreases during the test.	yes	yes	Instananeous affect of infiltration test shows that there is a fast flow path for water from the surface of the pond to the low angle fracture at 5 feet. Maximizing of pressure and then drop could show that sediments are washed into the fracture.
T-9	10'	Inside of Pond	Two Low Angle Fractures	Instantaneous increase of pressure at the start of the infiltration test. Pressure maximizes and then decreases during the test.	no	yes	During the test there are smooth fluctuations of pressure. Instananeous affect of infiltration test shows that there is a fast flow path for water from the surface of the pond to the 2 low angle fractures at 10'.

Two types of desaturation were observed:

(1) Rapid desaturation like that in Well T-8 at 2.7 m (9 ft).

(2) Progressive desaturation like that in Well T-8 at 1.5 m (5 ft).

One notable feature of is the oscillations of pressure that were observed in all tensiometers before the infiltration test, and in some of them during the infiltration test. Before the test, when the basalt was relatively dry and the relative permeability low, the gauge pressure oscillations were the largest. During the infiltration test, when the basalt was wet and the relative permeability increased, the gauge pressure oscillations reduced or disappeared. It is interesting to note that after a period of stable water pressure during infiltration, the oscillations in gauge pressure appeared again.

II.1.2. Deep Tensiometers

A total of 48 DTs were installed in 10 wells at the Box Canyon site. A list of wells and depths of installation is presented in Table I.9-1. Data collected from the DTs are presented in Figures II.1.2-1 through II.1.2-10.

Many of the DTs equilibrated at tensions between 1.5 and 2.5 m and remained unchanged throughout the infiltration experiment, indicating that the DTs were functioning properly but were unaffected by the infiltrating water. In one instance, the difference from this trend at 4.6 m (15 ft) in well I-1 (Figure II.1.2-1) has been attributed to transducer problems and incomplete calibration. Other DTs showed an apparent response to ponding (Figures II.1.2-2, II.1.2-9), but these changes have been attributed to other causes, such as leaky ceramic tips. While the trends could be indications of the arrival of a wetting front, the same behavior has been observed in tensiometers that develop small leaks. Therefore, it cannot be said with certainty that wetting took place.

The low percentage of DTs responding to the infiltration test was not unexpected. The number of fractures conducting water (especially at deep locations) is very small, and thus the chances of intersecting one of these fractures with a tensiometer is small. The responses confirm the funneling of flow to a few major fractures with depth.

II.2. Results of Neutron Logging

Raw neutron count readings were converted to "relative counts" by the following equation:

$$CNT_{relative} = (CNT_{raw,z,t}/CNT_{blank,t}) / (CNT_{raw,z,0}/CNT_{blank,0})$$

where

$CNT_{raw,z,t}$ = slow neutron count at depth z, at time t

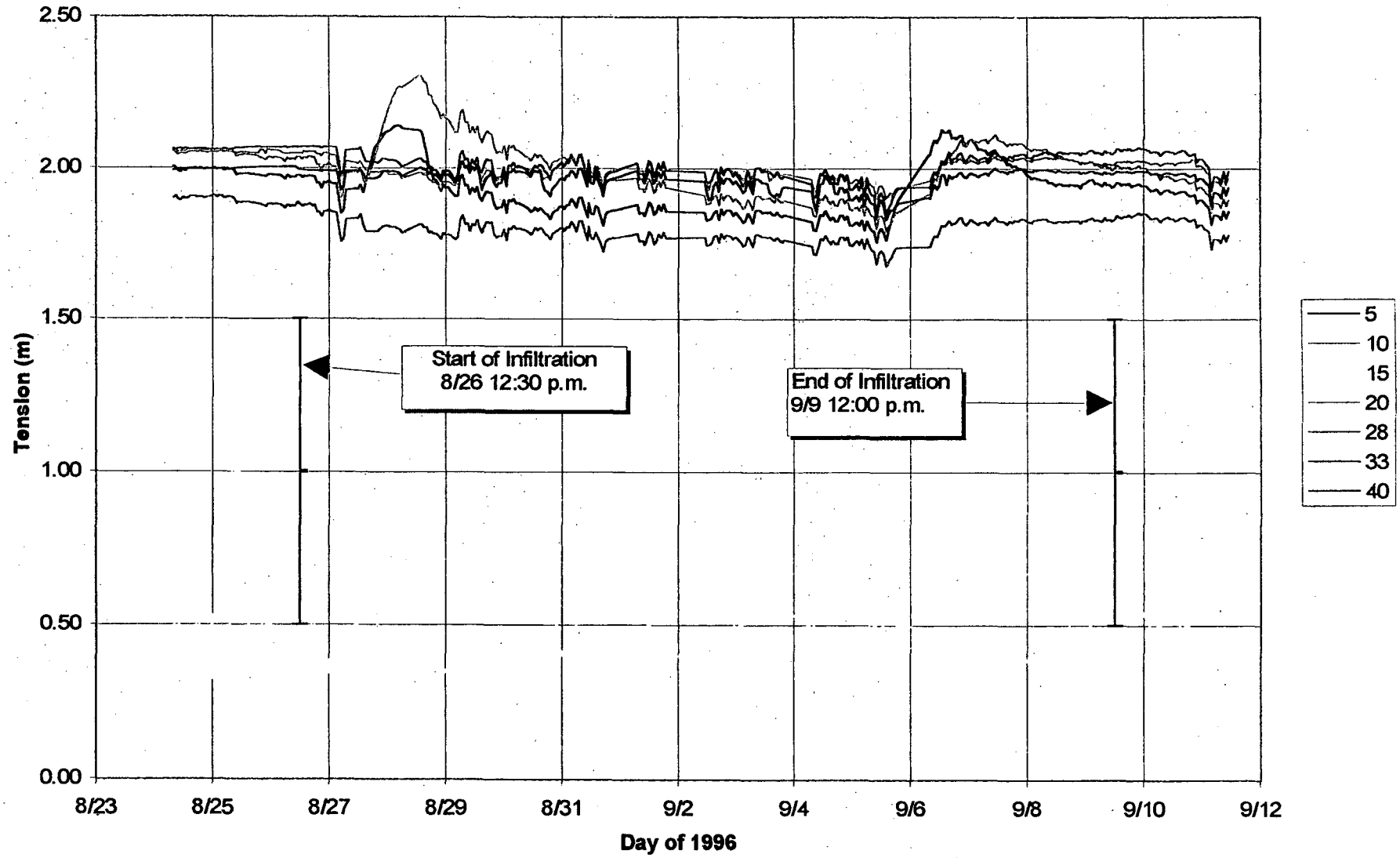

Figure II.1.2-1. Time trend of water pressure measurements using DTs in well I-1

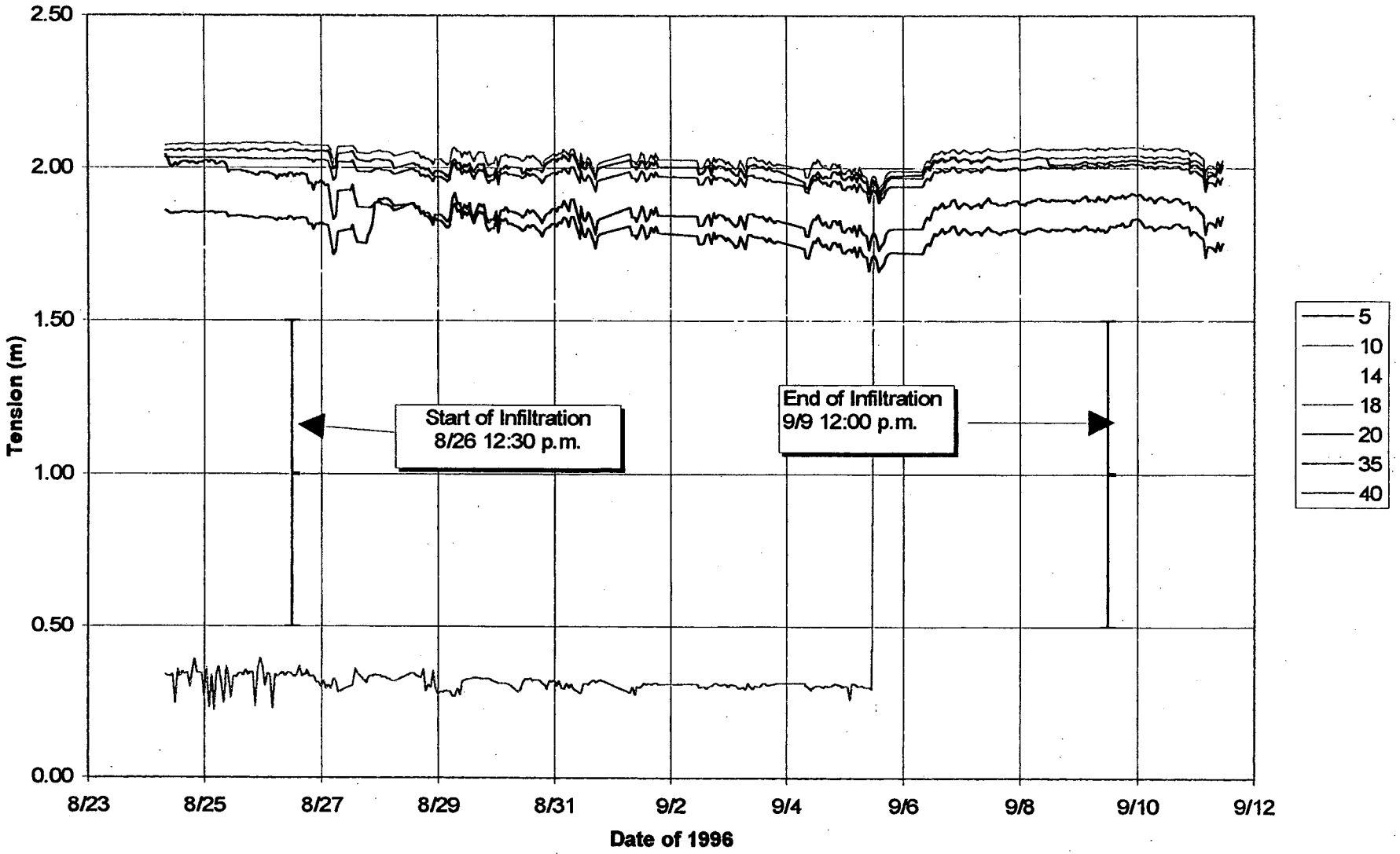

Figure II.1.2-2. Time trend of water pressure measurements using DTs in well I-2

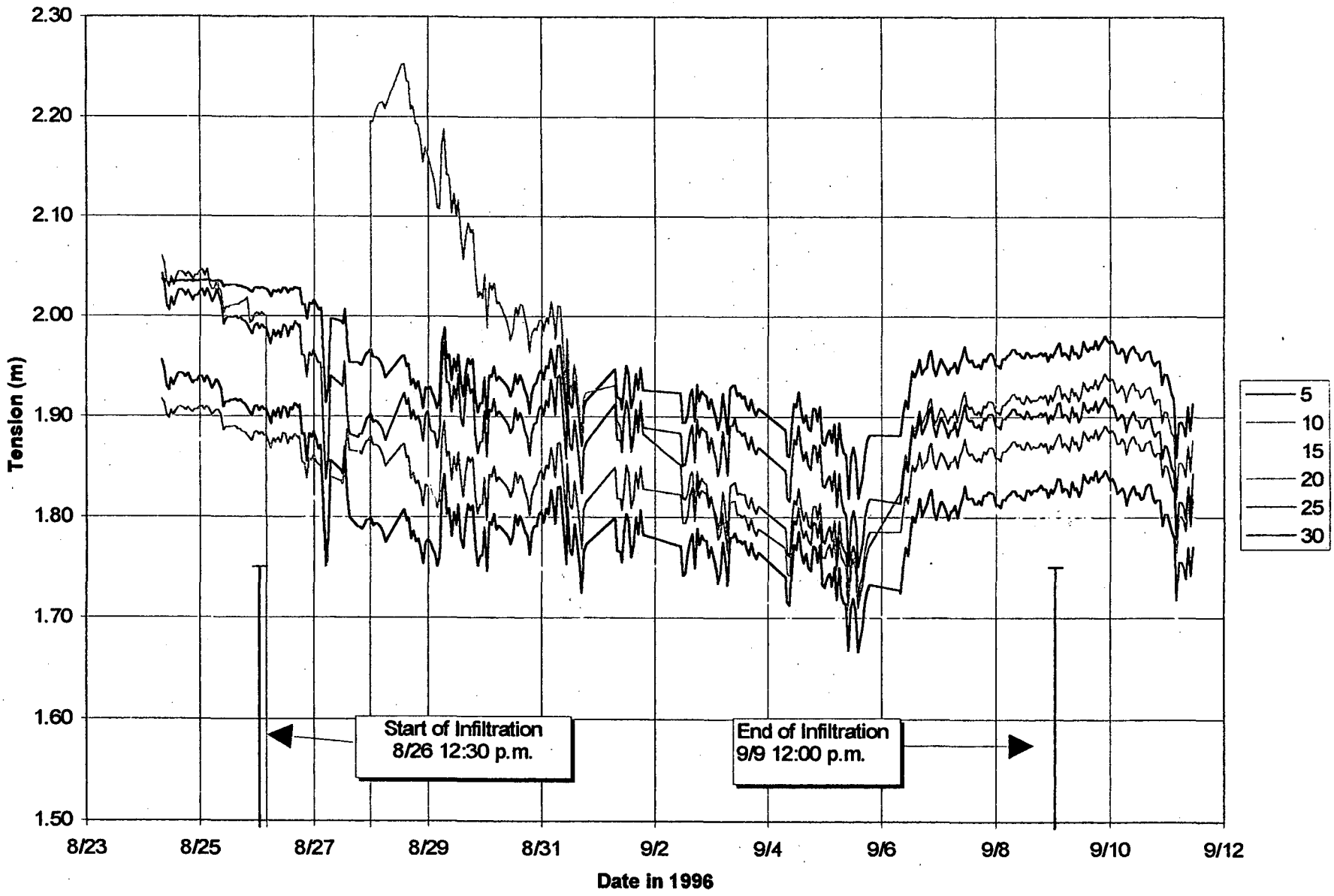

Figure II.1.2-3. Time trend of water pressure measurements using DTs in well I-3

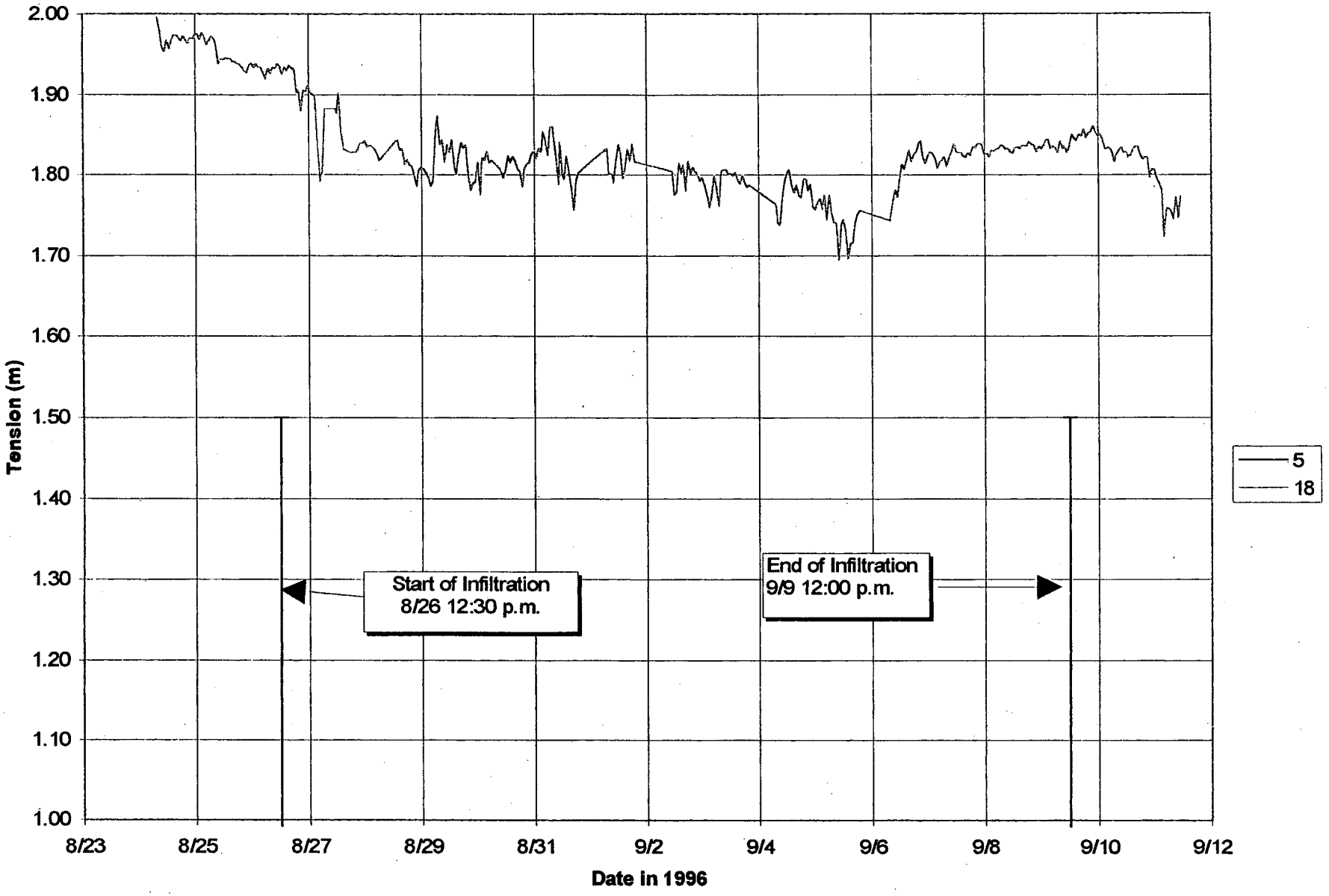

Figure II.1.2-4. Time trend of pressure measured using DTs in well T-2

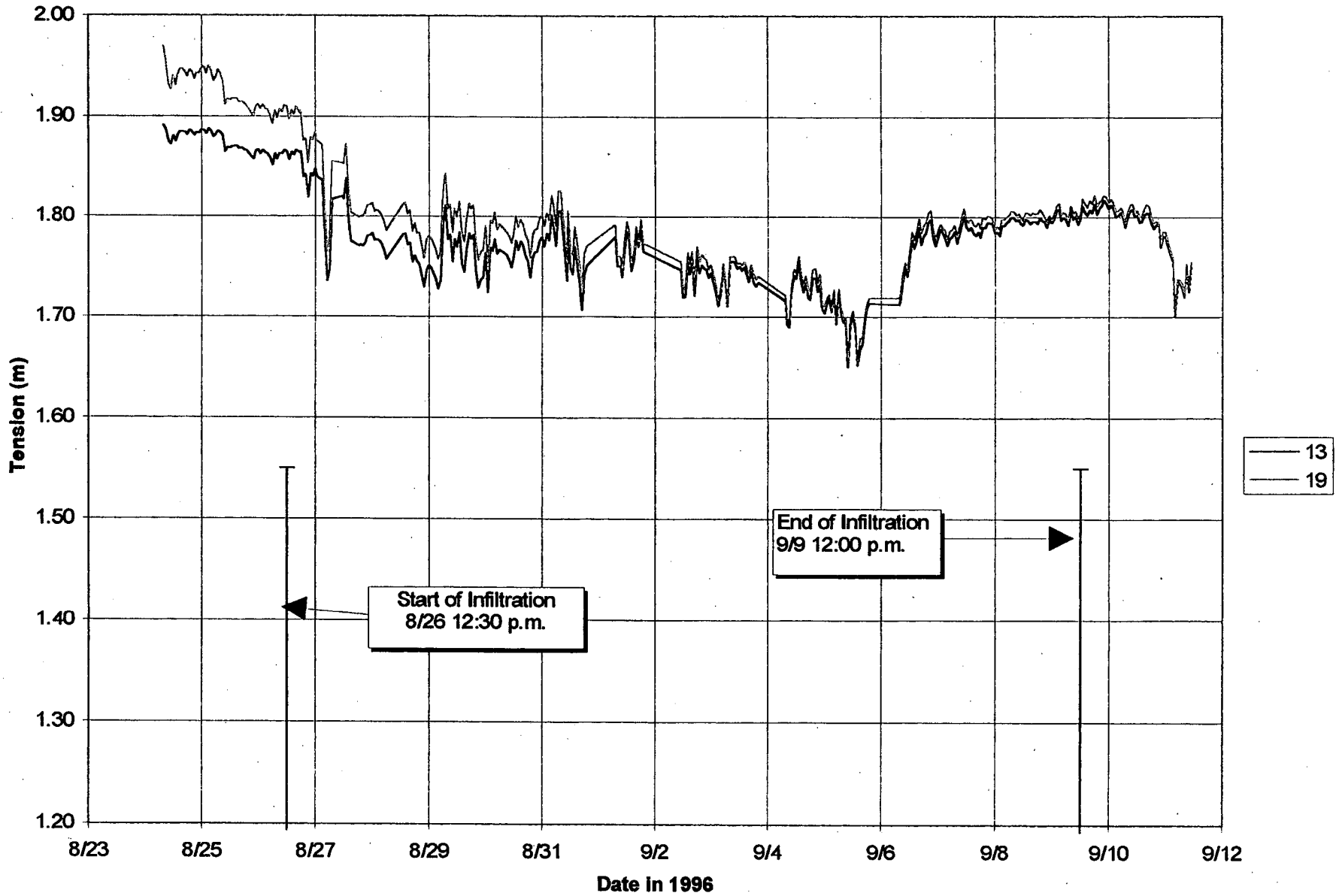

Figure II.1.2-5. Time trend of water pressure measurements using DTs in well T-3

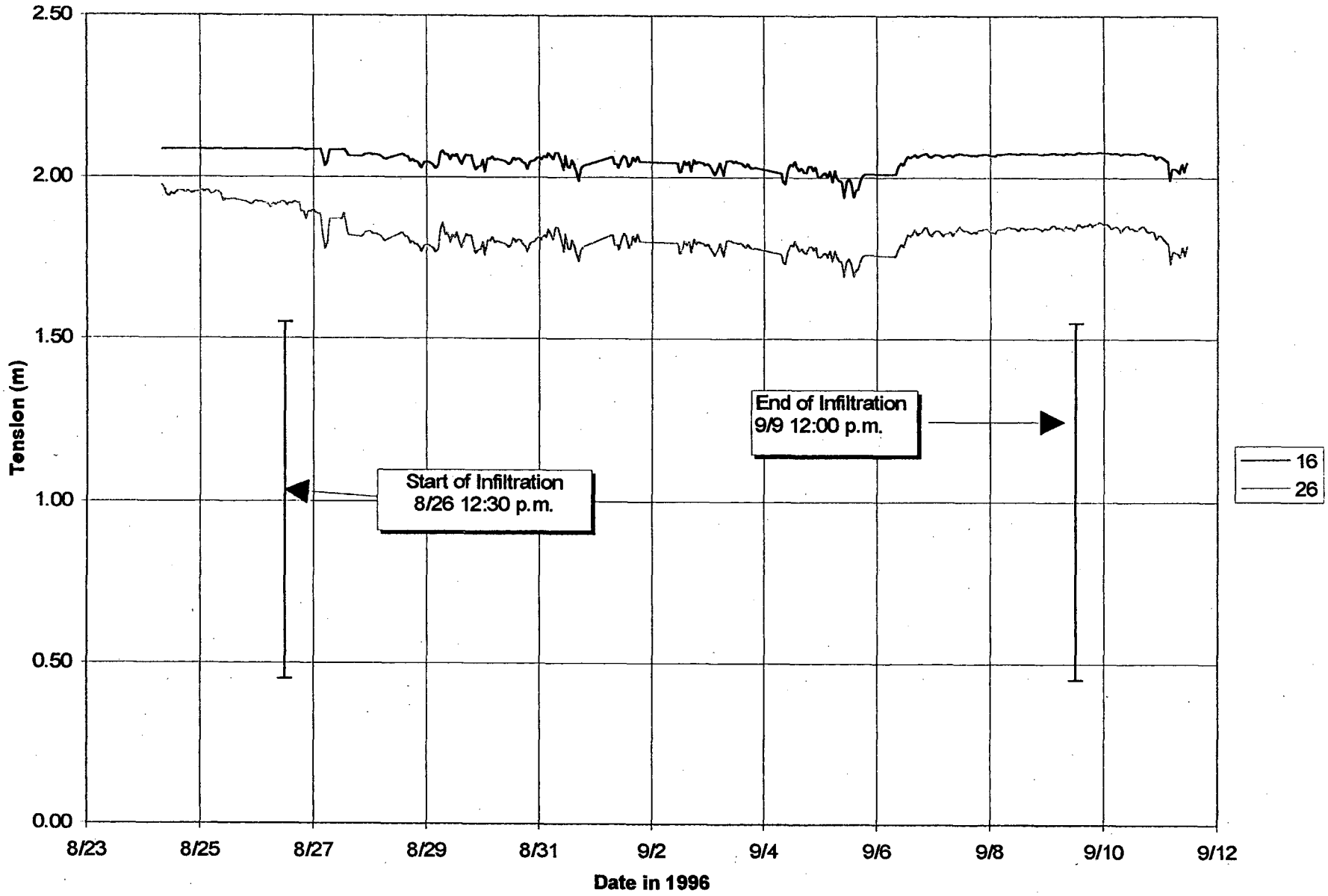

Figure II.1.2-6. Time trend of water pressure measurements using DTs in well T-6

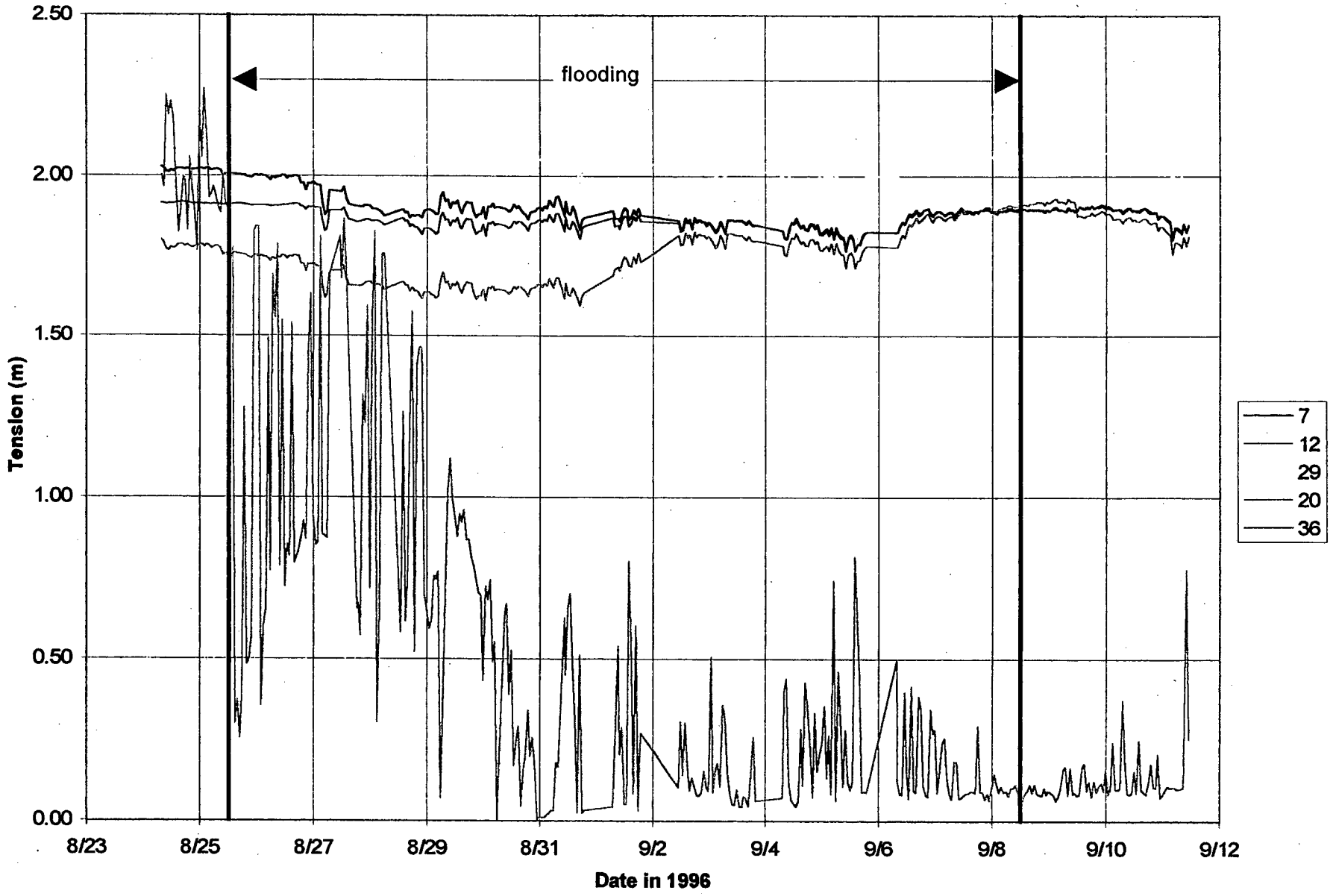

Figure II.1.2-7. Time trend of water pressure measurements using DTs in well E-1

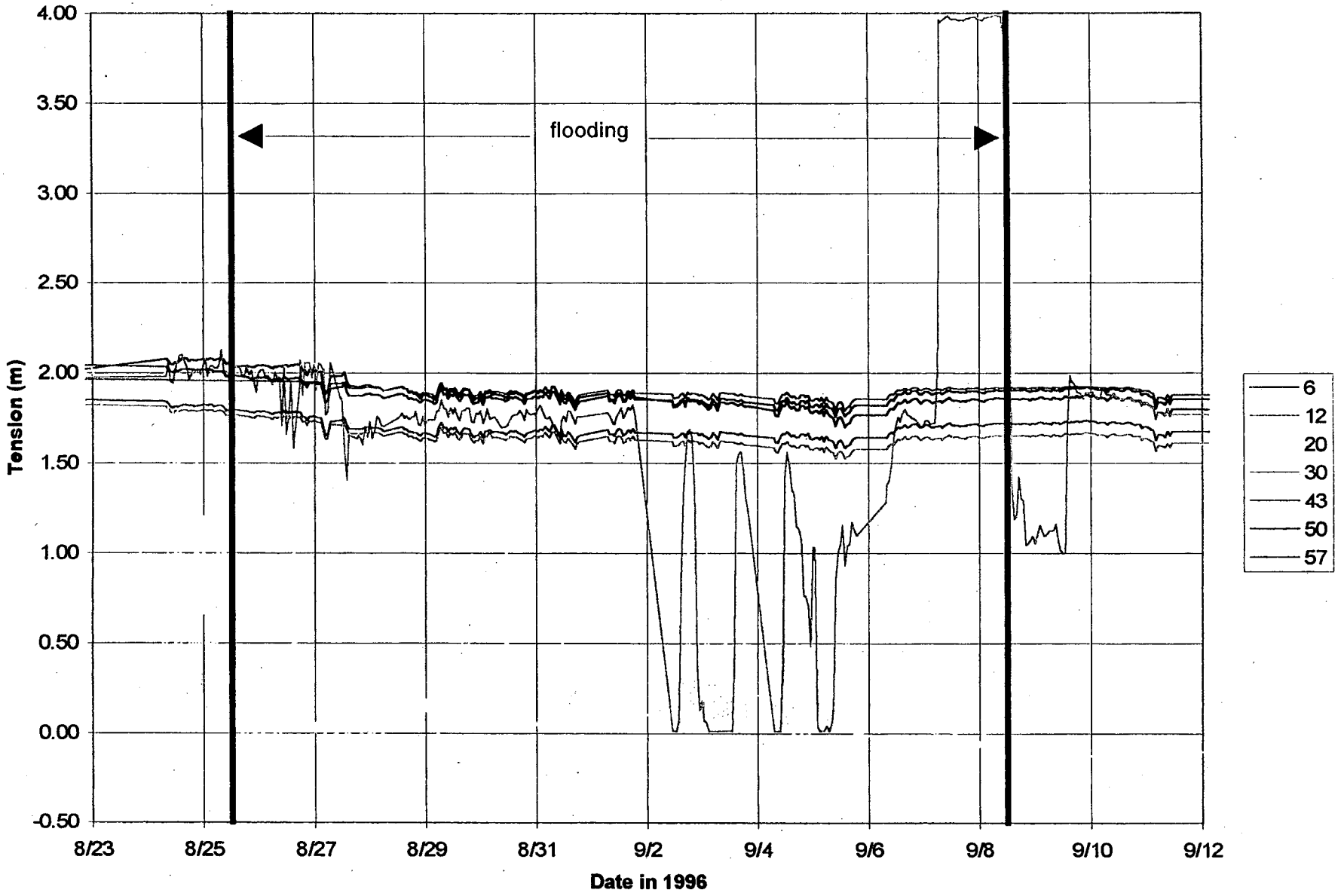

Figure II.1.2-8. Time trend of water pressure measurements with DTs in well E-2

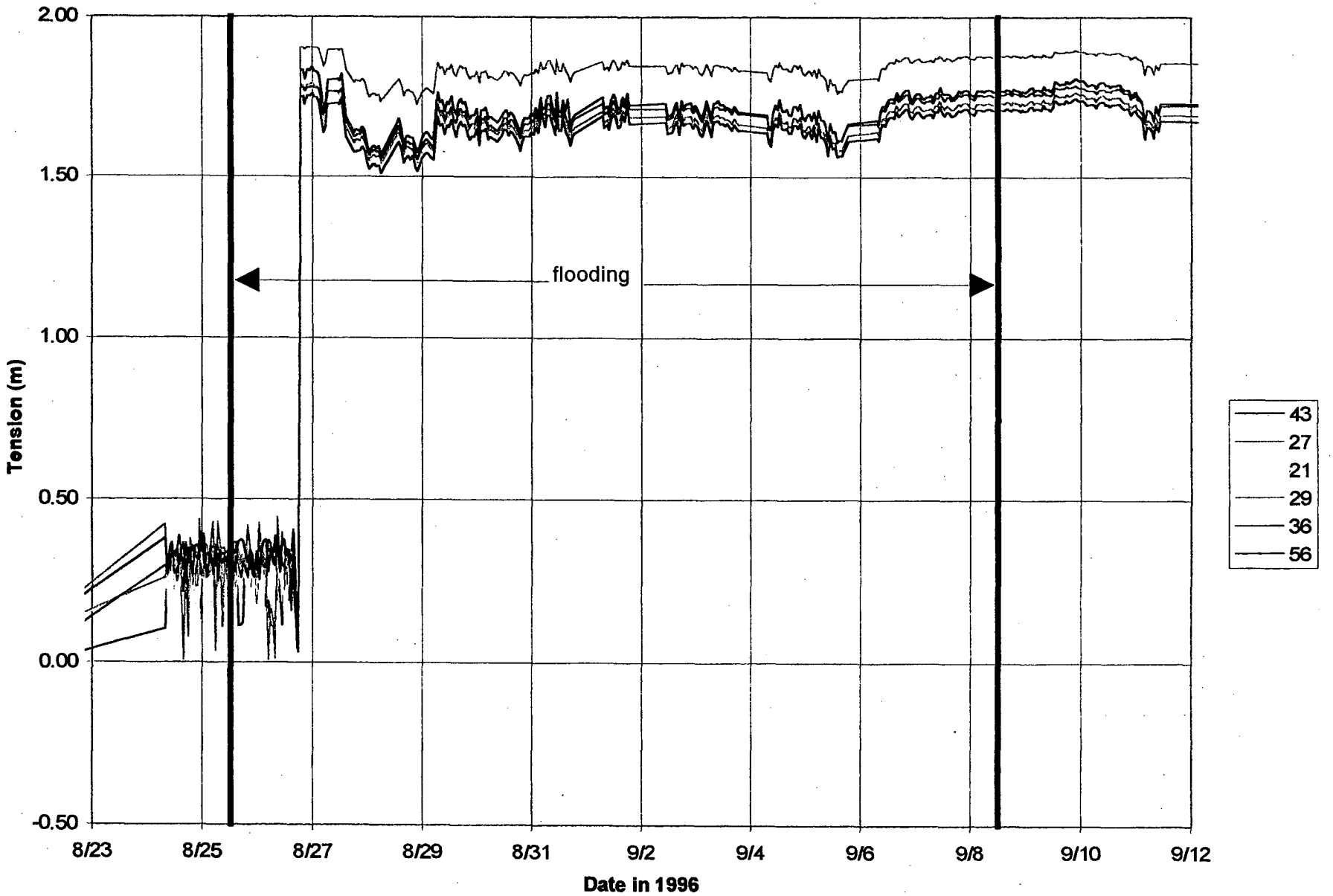

Figure II.1.2-9. Time trend of water pressure measurements using DTs in well E-3

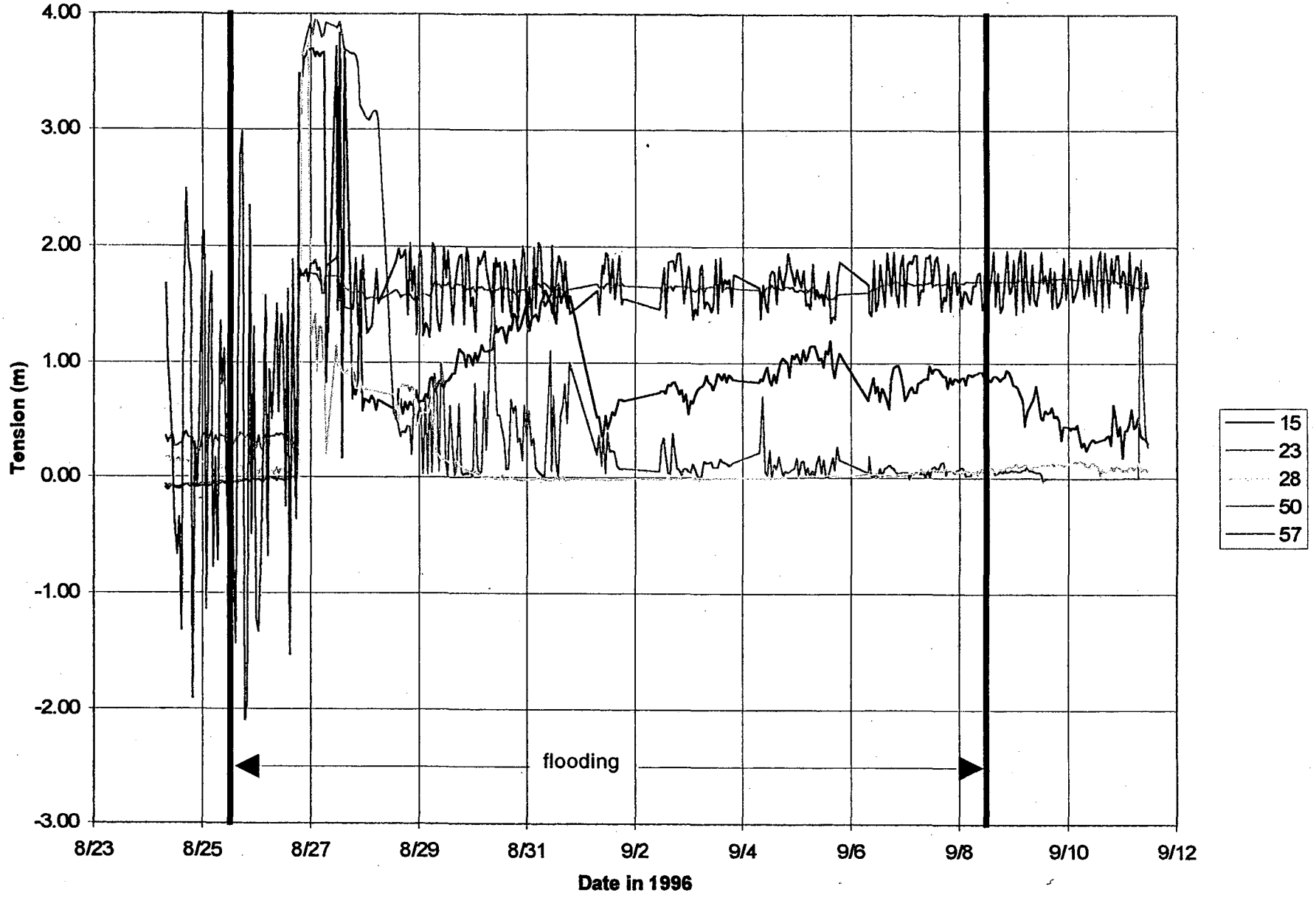

Figure II.1.2-10. Time trend of water pressure measurements using DTs in well E-4

$CNT_{blank,t}$ = mean slow neutron blank count, at time t
$CNT_{raw,z,0}$ = slow neutron count at depth z, at time "t=0" or pre-test
$CNT_{blank,0}$ = mean slow neutron blank count, at time "t=0" or pre-test

Such a conversion permits easier analysis of relative changes at all depths. Of special interest is the identification of locations and times where changes in moisture content are minor, yet statistically significant. This interpretation of the results is shown in Figures II.2-1 through II.2-7. An error band equivalent to ±2 standard deviations around the pre-test neutron count (which, by definition is equal to 1 at all points) is plotted to discern between noise and signal. The choice of 2 standard deviations is somewhat arbitrary, but reasonable given the observed fluctuations within this band. Furthermore, the interpretation as to whether the signal is beyond noise is also based on whether increases in moisture are mirrored by roughly equal decreases at the same depth but at different times. If the fluctuations are roughly equal and fall within 5% of the initial reading of 1, they are not considered to be significant. Note that the pre-test blank count for well R-4 was not used as it was extremely high; instead, an average of other blank counts taken that day was used. Well T-10 was not completely sealed at the bottom, and water entered the casing on the second day of the infiltration test. A column of water was present in the casing for all subsequent readings, at a depth of approximately 2.5 m (8.2 ft). Therefore, these data need to be carefully interpreted. The continued presence of water in the casing suggests that the surrounding rock was saturated and potentially affords the opportunity to study entrapped air dissipation.

Data shown in Figures II.2-1 through II.2-7 are generally in agreement with the model for fracture-dominated flow. There is a wetting of the top 1 m (3.3 ft) of rock in most cases, commonly an absence of moisture increase immediately below that depth, and numerous isolated areas where moisture content increases by 25% to 300%. The final data for each well (except for T-10) is presented in Figure II.2-8. This comparison shows the range of observed responses and qualitative similarities amongst some of the wells, most notably increases in moisture content at depths of 4 to 5 m (13 to 16 ft) and 6.5 to 8 m (21 to 26 ft).

II.3. Water Sampling

Tables II.3-1 and II.3-2 show the locations and time of water sampling of suction lysimeters. As can be seen from Table II.3-2, before the infiltration test, we were able to collect water samples from several suction lysimeters located within wetted zones. Since the rocks were relatively wet in background conditions, we were able to collect water samples from 24% of suction lysimeters before the infiltration test.

During the test, water samples were taken from some other suction lysimeters once the rock saturation increased. Table II.3-3 summarizes the arrival time of water in different suction lysimeters. During the infiltration test, 62% of suction lysimeters produced water that was collected for analytical analysis.

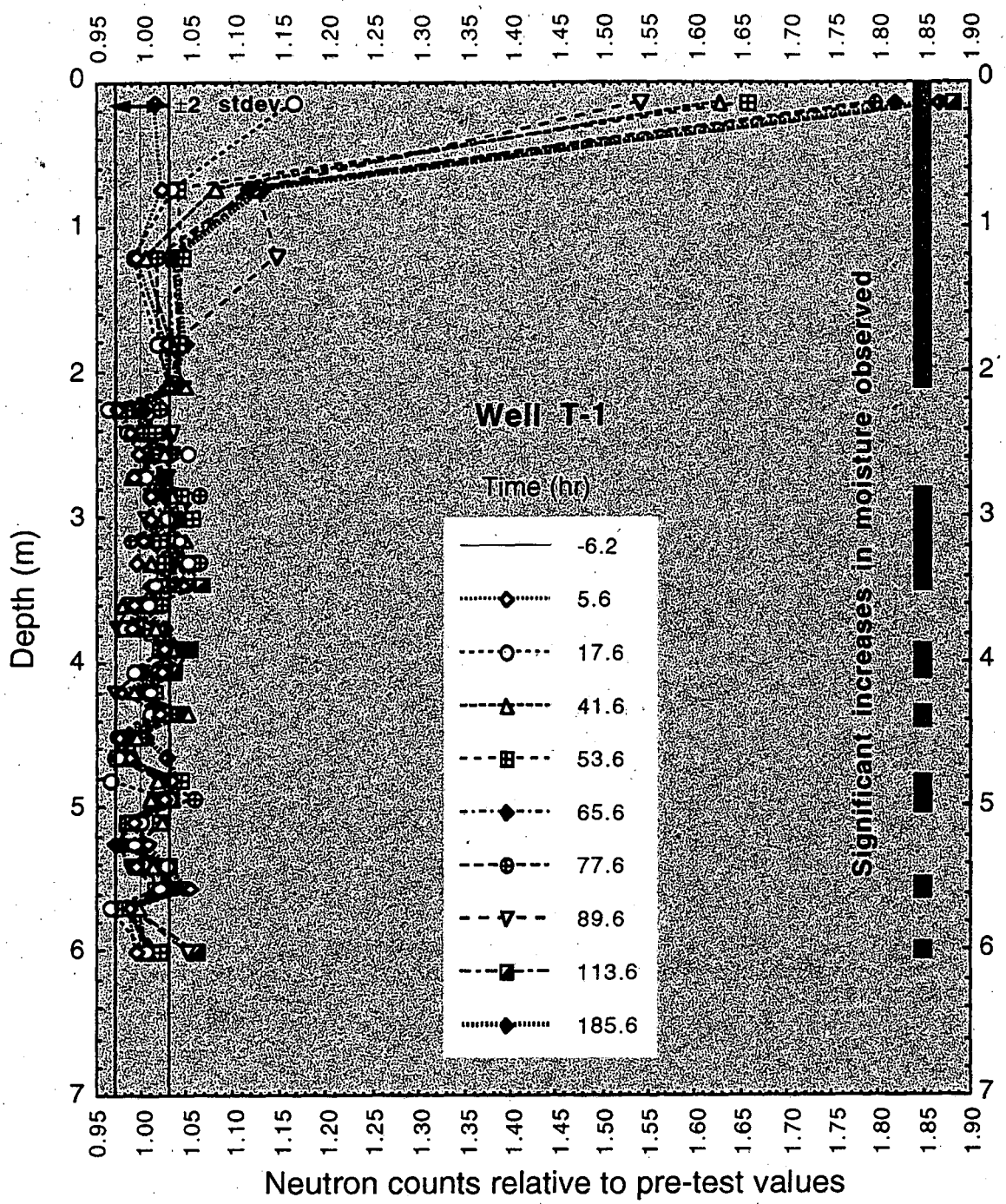

Figure II.2-1. Relative neutron counts over during the first 185 hours of the infiltration test in well T-1.

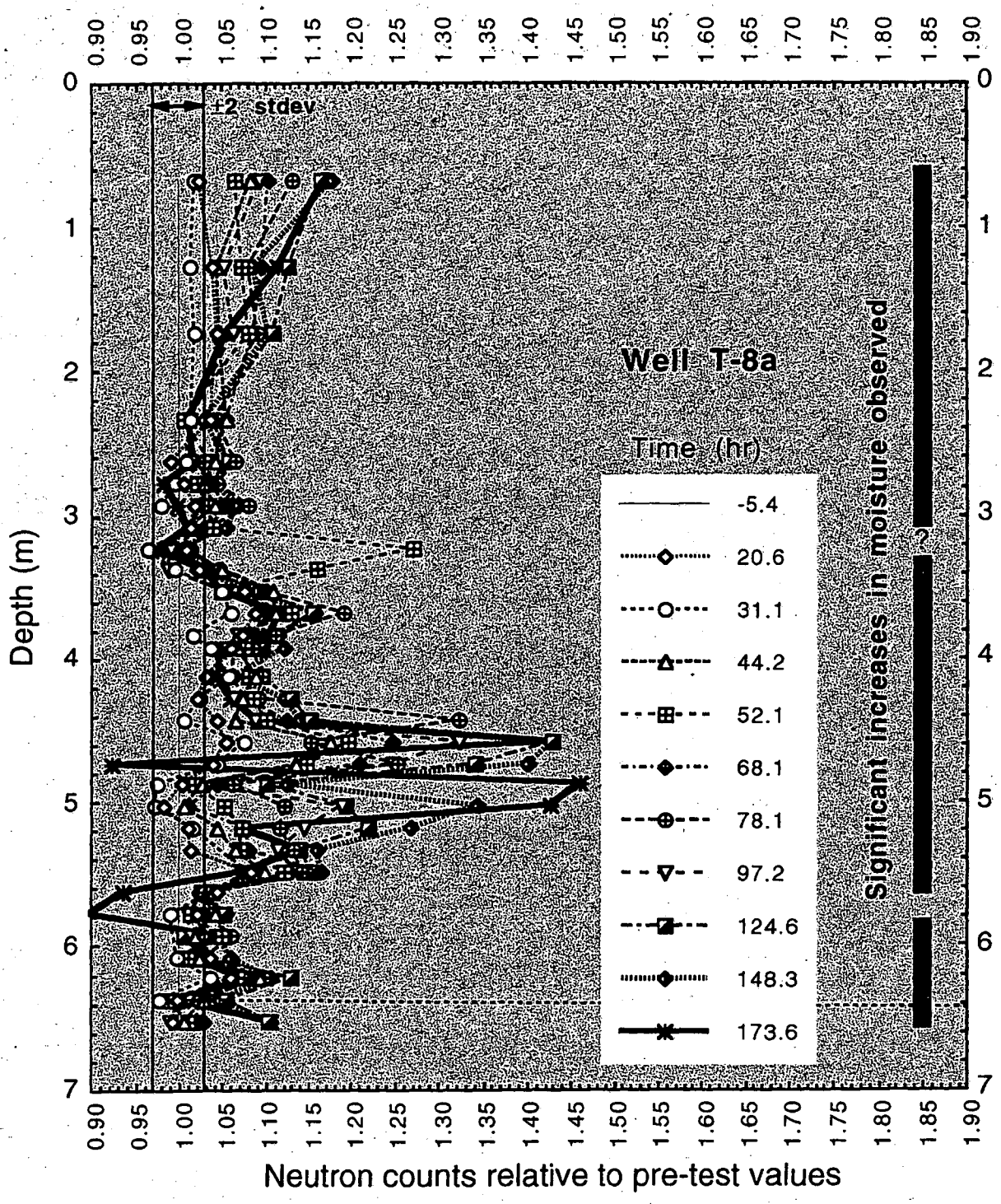

Figure II.2-2. Relative neutron counts over during the first 174 hours of the infiltration test in well T-8a.

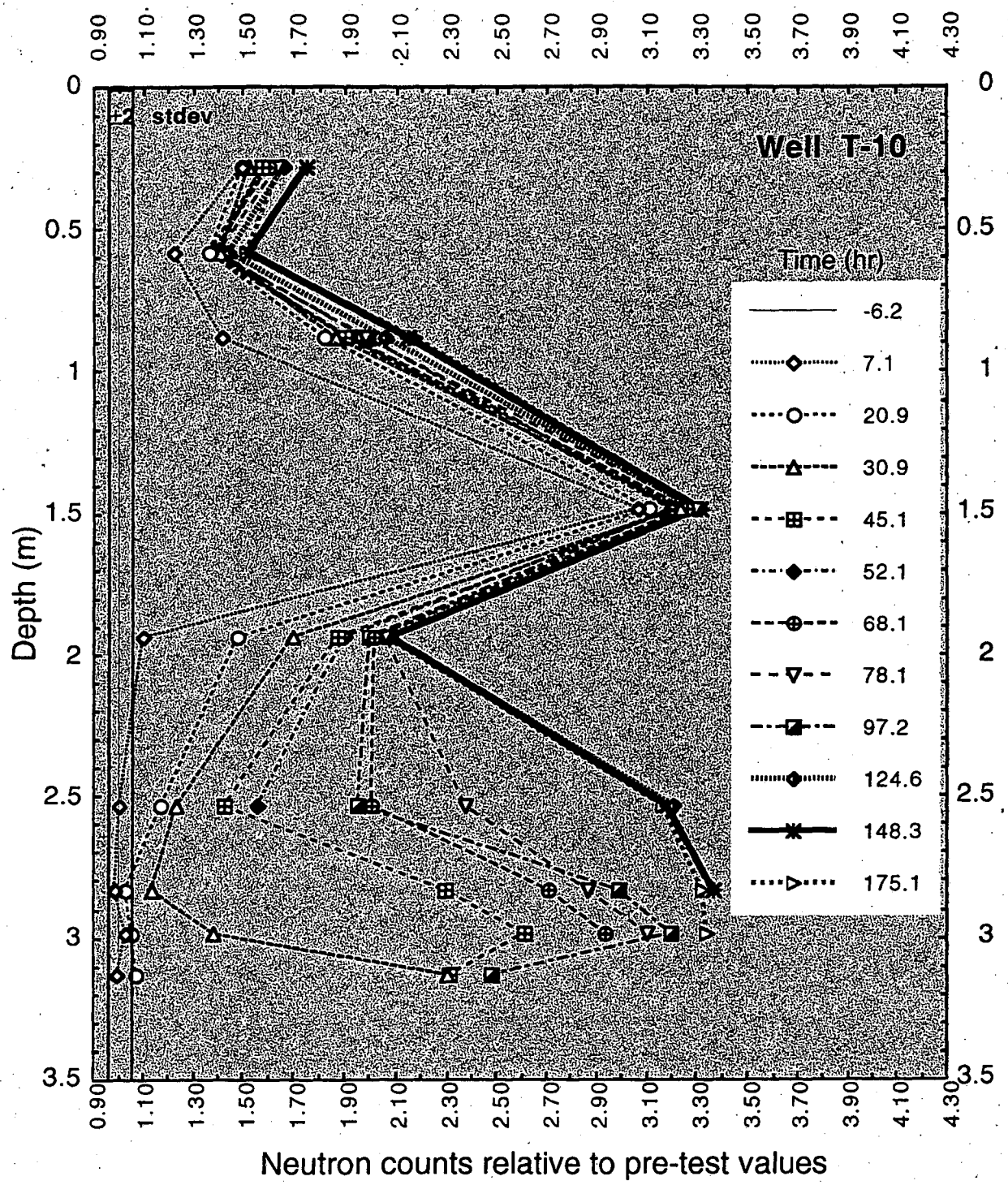

Figure II.2-3. Relative neutron counts over during the first 175 hours of the infiltration test in well T-10. Significant increases were observed at all depths.

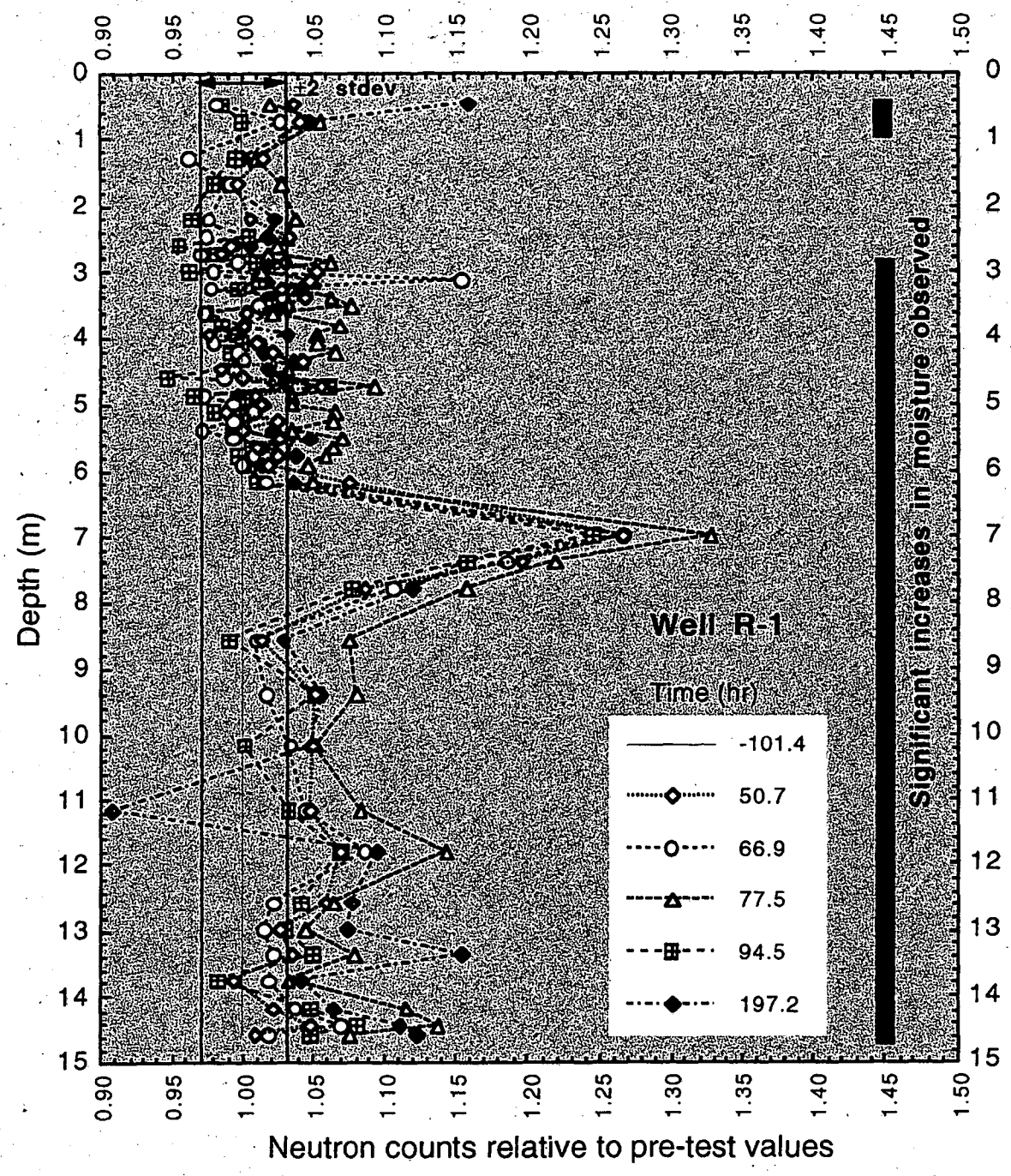

Figure II.2-4. Relative neutron counts over during the first 197 hours of the infiltration test in well R-1.

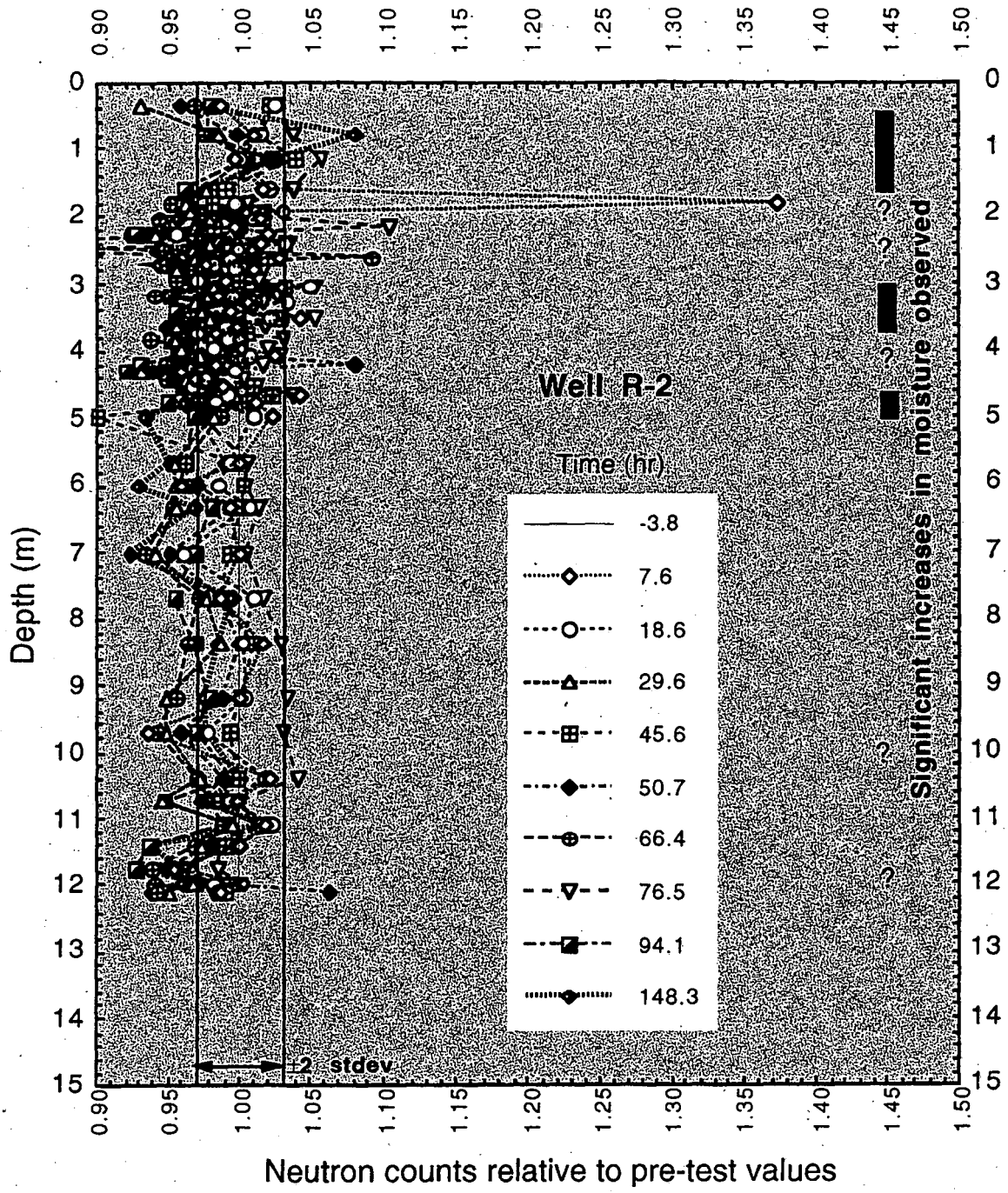

Figure II.2-5. Relative neutron counts over during the first 148 hours of the infiltration test in well R-2.

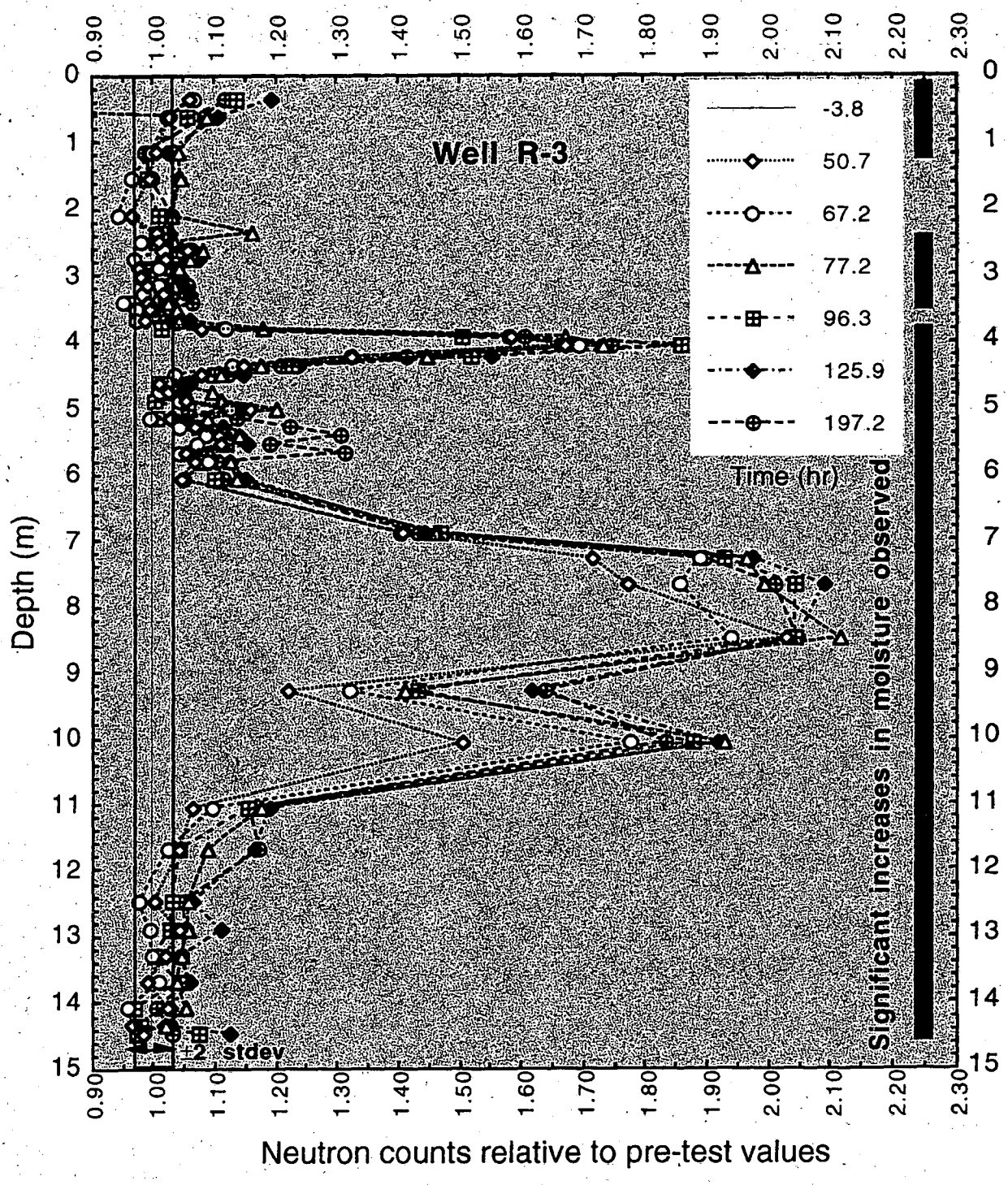

Figure II.2-6. Relative neutron counts over during the first 197 hours of the infiltration test in well R-3.

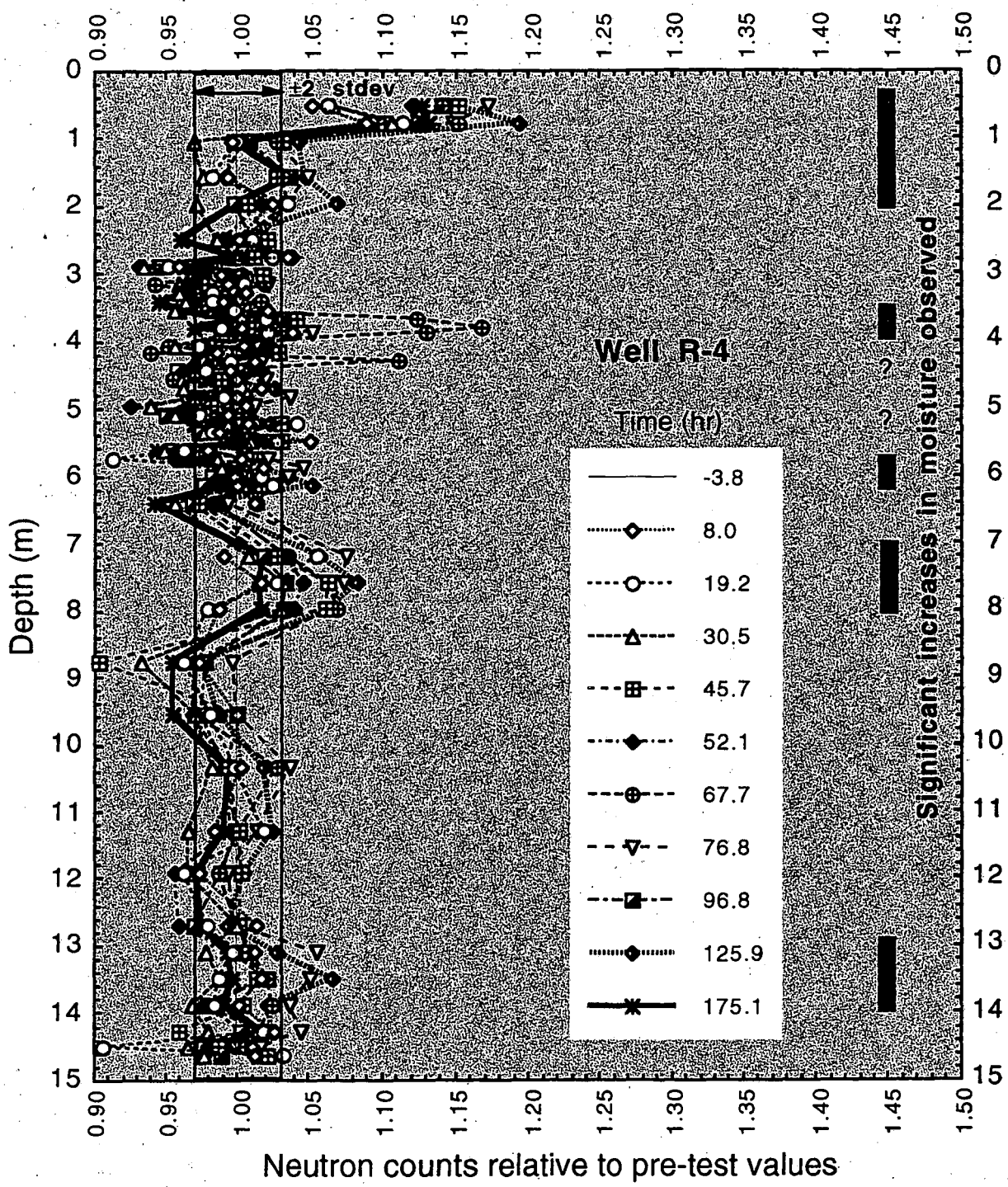

Figure II.2-7. Relative neutron counts over during the first 175 hours of the infiltration test in well R-4.

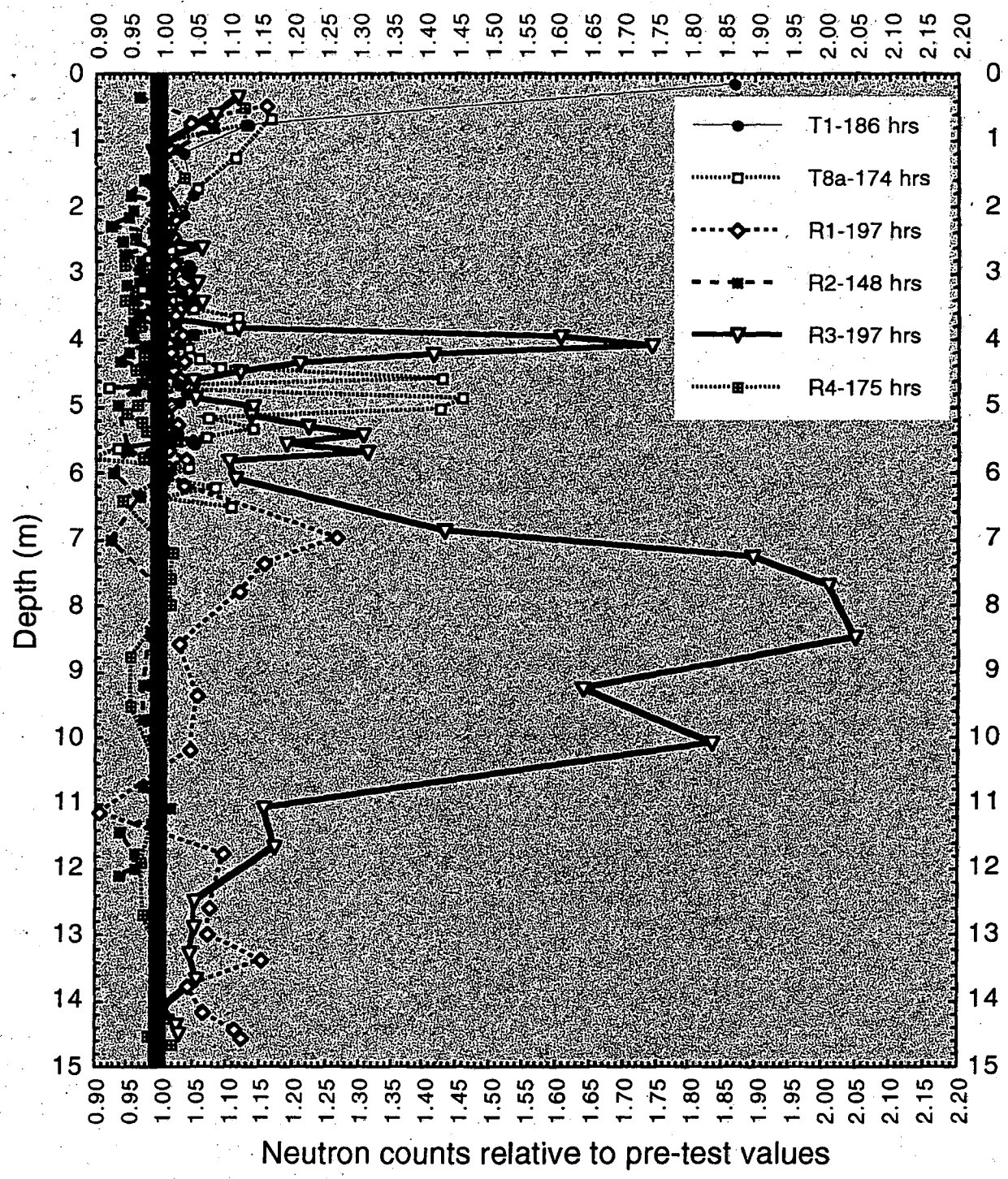

Figure II.2-8. Final relative neutron counts for wells T-1, T-8a, R-1, R-2, R-3, and R-4.

Table II.3-1. Water Samples Collected at the Box Canyon Site

note: All samples before 08/27/96 12:26 pm are taken before the infiltration test.

i.d. date-number	well	depth feet	volume 60 ml	time	notes
0820-01	I1	20'	0.2	9:00	
0821-01	I1	20'	0.6	16:10	
0821-02	I1	28'	0.1	16:10	
0821-03	I3	5'	0.2	10:40	
0821-04	E3	17'	0.2	10:25	*Debris.*
0821-05	E1	7'	0.3	10:30	
0821-06	T4	9'	0.1	10:32	
0821-07	T9	5'	0.1	10:45	
0822-01	I1	28'	0.3	9:00	
0823-01	E1	7'	0.2	9:15	
0823-02	E3	17'	0.2	9:10	*Slightly yellowish.*
0823-03	I1	20'	0.1	19:15	
0826-01	I2	14'	0.7	10:36	*Precipitate and yellowish.*
0826-02	T2	6'	0.7	11:06	*Precipitate.*
0827-01	T4	2'	0.7	21:05	*Precipitate.*
0827-02	I3	5'	0.7	19:52	
0827-03	T7	15'	0.5	21:00	*Precipitate.*
0828-01	T4	2'	full	15:30	*Slightly yellowish.*
0828-02	T4	9'	full	15:25	*Slightly yellowish.*
0828-03	T4	14'	0.8	15:45	*Slightly yellowish.*
0828-04	T9	5'	0.7	10:45	
0828-05	T9	10'	0.4	10:54	
0828-06	I1	1'	full	15:35	
0828-07	I1	5'	full	15:40	
0828-08	I3	5'	full	12:20	
0829-1	I1	5'	full	9:30	
0829-2	I1	15'	full	9:35	
0829-3	E1	7'	full	11:30	
0829-4	T4	2'	full	11:55	
0829-5	T4	9'	0.6	12:00	
0829-6	T4	14'	full	11:57	
0829-7					*From the Water supply tank.*
0829-8	I2	14'	full	13:40	
0829-9	T9	5'	full	13:45	
0829-10	T9	10'	full	13:48	
0829-11	I2	10'	0.3	13:55	
0829-12	T2	2'	full	13:59	
0829-13	T2	6'	full	14:45	
0829-14	E3	22'	0.2	18:20	

Table II.3-1. Continued

0829-15	E2	50'	0.4	18:25	
0829-16	E1	7'	0.3		
0830-1	E1	7'	full	15:40	*Slightly yellowish color.*
0830-2	T4	2'	full	16:15	
0830-3	T4	14'	full	16:30	
0830-4	T4	9'	0.3	16:43	
0830-5	I1	10'	0.4	16:50	*Since 08/29/96*
0830-6	I1	5'	full	16:55	
0830-7	I1	15'	0.6	17:00	
0830-8	I1	1'	0.7	17:05	
0830-9	I2	14'	full	17:20	
0830-10	T9	10'	0.9	17:25	
0830-11	T9	5'	0.9	17:30	
0830-12	T2	6'	full	17:37	
0830-13	T2	2'	full	17:38	
0830-14			full	17:45	*Water Supply sample.*
0830-15	I1	28'	0.2	18:05	
0830-16	I1	33'	0.4	18:05	
0831-1	T7	6'			
0831-2	E1	7'	full		
0901-1	E2	30'10"	0.5	15:15	
0901-2	E2	50'	0.4	15:15	
0901-3	E3	22'	0.2	15:20	
0901-4	E4	29'	0.5	15:20	
0901-5	I1	20'	full	15:35	
0901-6	I1	28'	0.2	15:40	
0902-1	T4	2'	full	13:00	
0902-2	T4	14'	full	13:00	
0902-3	T4	9'	0.2	13:00	
0902-4	I3	1'	0.1	13:15	
0902-5	I3	5'	0.3	13:15	
0902-6	E1	7'	full	13:15	
0902-7	E3	29'	0.3	13:45	
0902-8	I1	33'	0.5	13:50	
0902-9	I1	20'	full	13:50	
0902-10	I1	5'	0.9	14:00	
0902-11	I1	1'	0.5	14:30	
0902-12	I1	15'	0.1	14:45	
0902-13	I1	10'	0.3	14:45	
0902-14	T9	1'	0.1	15:15	
0902-15	I2	10'	full	15:20	
0902-16	I2	14'	full	15:20	*Yellow color.*
0902-17	T2	6'	full	15:20	
0902-18	T2	2'	full	15:20	
0902-19				15:25	*Water Supply*
0902-20				15:25	*Pond Water (from inside pond).*
0902-21	T9	5'	0.4	15:30	
0902-22	I2	10'	0.1	15:30	

Table II.3-1. Continued

0902-23				16:00	*tracer*
0902-24				16:00	*tracer*
0903-1	T9	10'	full	10:10	
0903-2	I2	14'	full	10:45	*Pale yellow color.*
0903-3	I2	10'	0.8	10:17	
0903-4	T9	1'	0.2	10:25	
0903-5	T9	5'	0.5	10:28	*Residual water by negative pressure.*
0903-6	T9	1'	0.8	10:35	*Withdrawn by positive pressure.*
0903-7	I2	5'	0.1	11:00	*Vacuum: positive pressure.*
0903-8	T2	2'	0.5	11:30	
0903-8A	T3	2'	0.2	11:45	
0903-9	T2	6'	0.6	11:30	*Vacuum: positive pressure.*
0903-10	I1	1'	0.6	13:50	
0903-11	I1	5'	0.3	13:54	
0903-12	I1	15'	0.2	13:56	
0903-13	S3	2'6"	full	15:45	*Pale yellow upon extraction. Black after storage.*
0903-14	I2	10'	0.4	18:05	
0903-15	I2	14'	full	18:09	*Red yellow color and precipitate.*
0903-16	T9	10'	0.8	18:13	
0903-17	T9	1'	0.3	18:18	
0903-18	T9	5'	0.7	18:15	
0903-19	I1	20'	full	18:50	
0903-20	I1	1'	0.5	19:50	
0904-1	T4	2'	full	10:02	
0904-2	T4	14'	0.6	10:12	
0904-3	E1	7'	0.3	10:30	
0904-4	E1	12'	0.2	10:35	
0904-5	T9	5'	0.6	11:48	
0904-6	T9	10'	0.4	11:50	
0904-7	I2	14'	0.2	11:50	*Slight yellow color.*
0904-8	T9	1'	0.3	11:55	
0904-9	T2	9'9"	0.1	12:02	
0904-10	T2	6'	0.6	12:08	
0904-11	T2	2'	0.5	12:06	
0904-12	T3	2'	0.2	14:45	
0904-13	T9	5'	0.8	14:55	
0904-14	T9	10'	0.4	15:10	
0904-15	I2	14'	0.6	15:12	*Yellow color. Red preciptate.*
0904-16	T9	1'	0.3	15:15	
0904-17			full	15:20	*Pond Water. From near S3*
0904-18	T2	2'	0.4	15:28	
0904-19	T2	6'	0.6	15:30	
0904-20	E4	23'	0.3	14:45	
0904-21	E4	28'	0.2	15:47	
0904-22	E3	29'	0.4	15:50	
0904-23	E3	22'	0.1	15:51	
0904-24	E2	50'	0.4	15:52	
0904-25	E2	30'10'	0.2	15:53	
0904-26	I1	1'	0.3	18:10	
0904-27	I1	5'	0.1	18:10	

Table II.3-1. Continued

0904-28	I2	14'	0.3	18:10	
0905-1	T2	2'	0.1	10:15	
0905-2	T2	6'	0.2	10:20	
0905-3	T3	2'	0.3	10:27	
0905-4	T9	5'	0.7	10:34	
0905-5	I2	14'	0.1	10:35	
0905-6	T9	1'	0.3	10:45	
0905-7	I2	10'	0.1	10:50	
0905-8	I2	14'	full	11:26	*Yellow Color. Reddish residue.*
0905-9	I3	1'	0.4	15:13	
0905-10	I1	10'	0.2	15:23	
0905-11	T4	2'	0.6	15:35	
0905-12	T4	14'	0.5	15:45	
0905-13	T4	2'	0.4	15:46	
0905-14	T4	9'	0.5	15:48	
0905-15	T4	19'	<0.1	15:52	
0905-16	I1	1'	0.5	16:15	
0905-17	I1	5'	full	16:22	
0905-18	I1	15'	0.1	16:27	
0905-19	I1	20'	0.6	16:40	
0905-20	E1	7'	0.2	19:00	
0905-21	E1	12'	<<0.1	19:00	
0906-1	I3	1'	0.6	9:53	*Yellowish*
0906-2	I3	5'	<0.1	9:54	
0906-3	I1	1'	0.5	11:28	
0906-4	E3	29'	0.2	12:50	
0906-5	I3	5'	0.4	13:00	
0906-6	I3	1'	0.5	13:02	*Yellowish*
0906-7	T3	2'	0.3	13:15	
0906-8	T9	1'	0.2	13:40	
0906-9	I2	10'	0.6	13:55	
0906-10	I2	14'	0.6	13:58	*Yellowish*
0906-11	T9	10'	0.6	14:08	
0906-12	T7	2'	0.4	14:14	
0906-13	T9	1'	0.2	14:20	
0906-14	I1	20'	0.6	15:13	
0906-15	I1	28'	0.1	15:25	
0906-16	I1	33'	0.2	15:32	
0907-1	I2	14'	0.6	10:35	*Yellowish.*
0907-2	I2	10'	0.4	10:34	
0907-3	I2	1'	<0.1	10:33	
0907-4	I1	5'	0.4	10:22	
0907-5	I1	1'	0.6	10:33	
0907-6	T9	5'	0.5	10:37	
0907-7	T9	10'	0.3	10:36	

Table II.3.2. Continued

Table II.3-2. Water Sample Data

Well I.D.	Depth	20-Aug	21-Aug	22-Aug	23-Aug	25-Aug	27-Aug	28-Aug	29-Aug	30-Aug	31-Aug	1-Sep	2-Sep	3-Sep	4-Sep	5-Sep	6-Sep	7-Sep
T2	2'	S/D	S/D	S/D	S/D	S/D	NS	S/D	W	W	NS	NS	W	W	W	W	S/D	NS
	6'	S/D	S/D	S/D	S/D	S/D	NS	W	W	W	NS	NS	W	W	W	W	S/D	NS
	9'9"	S/D	S/D	S/D	S/D	S/D	NS	S/D	S/D	S/D	NS	NS	S/D	S/D	W	S/D	S/D	NS
	14'5"	S/D	S/D	S/D	S/D	S/D	NS	S/D	S/D	S/D	NS	NS	S/D	S/D	S/D	S/D	S/D	NS
T3	2'	S/D	S/D	S/D	S/D	S/D	NS	S/D	S/D	S/D	NS	NS	S/D	W	W	W	W	NS
	6'	S/D	S/D	S/D	S/D	S/D	NS	S/D	S/D	S/D	NS	NS	S/D	S/D	S/D	S/D	S/D	NS
	10'	S/D	S/D	S/D	S/D	S/D	NS	S/D	S/D	S/D	NS	NS	S/D	S/D	S/D	S/D	S/D	NS
	15'	S/D	S/D	S/D	S/D	S/D	NS	S/D	S/D	S/D	NS	NS	S/D	S/D	S/D	S/D	S/D	NS
	20'	S/D	S/D	S/D	M	M	S/D	S/D	S/D	S/D	NS	NS	S/D	S/D	S/D	S/D	S/D	NS
T4	2'	S/D	S/D	S/D	S/D	S/D	W	W	W	W	NS	NS	W	S/D	W	W	S/D	NS
	9'	S/D	W	S/D	S/D	M	W	W	W	W	NS	NS	W	S/D	S/D	W	S/D	NS
	14'	S/D	W	S/D	S/D	M	S/D	W	W	W	NS	NS	W	S/D	W	W	S/D	NS
	19'	S/D	S/D	S/D	S/D	S/D	NS	M	S/D	M	NS	NS	S/D	S/D	S/D	W	S/D	NS
T5	1'	S/D	S/D	S/D	S/D	S/D	S/D	S/D	S/D	S/D	NS	NS	S/D	S/D	S/D	S/D	S/D	S/D
	5'	S/D	S/D	S/D	S/D	S/D	S/D	S/D	S/D	S/D	NS	NS	S/D	S/D	S/D	S/D	S/D	S/D
	10'	S/D	S/D	S/D	S/D	S/D	S/D	S/D	S/D	S/D	NS	NS	S/D	S/D	S/D	S/D	S/D	S/D
T6	2'	S/D	S/D	S/D	S/D	S/D	S/D	S/D	S/D	S/D	NS	NS	S/D	S/D	S/D	S/D	S/D	S/D
	10'	S/D	S/D	S/D	S/D	S/D	S/D	S/D	S/D	S/D	NS	NS	S/D	S/D	S/D	S/D	S/D	S/D
	15'	S/D	S/D	S/D	S/D	S/D	S/D	S/D	S/D	S/D	NS	NS	S/D	S/D	S/D	S/D	S/D	S/D
	21'	S/D	S/D	S/D	S/D	S/D	S/D	S/D	S/D	S/D	NS	NS	S/D	S/D	S/D	S/D	S/D	S/D
T7	2'	NS	NS	NS	NS	NS	NS	NS	NS	NS	NS	NS	NS	NS	NS	NS	W	S/D?
	6'	S/D	S/D	S/D	S/D	S/D	S/D	S/D	W	S/D	W	NS	S/D	S/D	S/D	S/D	S/D	S/D
	15'	S/D	S/D	S/D	S/D	S/D	W	S/D	S/D	S/D	S/D	NS	S/D	S/D	S/D	S/D	S/D	S/D
	19'	S/D	S/D	S/D	S/D	S/D	S/D	S/D	S/D	S/D	S/D	NS	S/D	S/D	S/D	S/D	S/D	S/D
T9	1'	NS	NS	NS	NS	NS	NS	NS	NS	NS	NS	NS	W	W	W	W	W	S/D
	5'	W	W	S/D	M	M	NS	W	W	W	NS	NS	W	W	W	W	S/D	W
	10'	S/D	S/D	S/D	S/D	S/D	NS	W	W	W	NS	NS	S/D	W	W	S/D	W	W

M - moisture observed
NS - not sampled
S/D - location sampled, but was dry
W - wet
? - log unclear

J. Jacobsen - 2/14/97

Table II.3.2. Continued

Well I.D.	Depth	20-Aug	21-Aug	22-Aug	23-Aug	25-Aug	27-Aug	28-Aug	29-Aug	30-Aug	31-Aug	1-Sep	2-Sep	3-Sep	4-Sep	5-Sep	6-Sep	7-Sep
E1	7'	W	W	S/D	W	M	S/D	W	W	W	W	S/D	W	S/D	W	W	S/D	NS
	12'	S/D	S/D	S/D	S/D	S/D	S/D	S/D	S/D	S/D	S/D	S/D	S/D	S/D	W	W	S/D	NS
	43'	S/D	S/D	S/D	S/D	S/D	S/D	S/D	S/D	S/D	S/D	S/D	S/D	S/D	M	S/D	S/D	NS
	54'	S/D	S/D	S/D	S/D	S/D	S/D	S/D	S/D	S/D	S/D	S/D	S/D	S/D	M	S/D	S/D	NS
	57	S/D	S/D	S/D	S/D	S/D	S/D	S/D	S/D	S/D	S/D	S/D	S/D	S/D	S/D	S/D	S/D	NS
E2	6'	S/D	S/D	S/D	S/D	S/D	S/D	S/D	S/D	S/D	S/D	S/D	S/D	S/D	S/D	S/D	S/D	NS
	20'	S/D	S/D	S/D	S/D	S/D	S/D	S/D	S/D	S/D	S/D	S/D	S/D	S/D	S/D	S/D	S/D	NS
	30'10"	S/D	S/D	S/D	S/D	S/D	S/D	S/D	S/D	S/D	S/D	W	S/D	S/D	W	S/D	S/D	NS
	50'	S/D	S/D	S/D	S/D	S/D	S/D	S/D	W	S/D	S/D	W	S/D	S/D	W	S/D	S/D	NS
E3	17'	W	W	S/D	W	M	S/D	S/D	S/D	S/D	S/D	S/D	S/D	S/D	S/D	S/D	S/D	NS
	22'	S/D	S/D	S/D	S/D	S/D	S/D	S/D	W	S/D	S/D	W	S/D	S/D	W	S/D	S/D	NS
	29'	S/D	W	S/D	S/D	S/D	S/D	S/D	S/D	S/D	S/D	S/D	W	S/D	W	W	W	NS
E4	23'	S/D	S/D	S/D	S/D	S/D	S/D	S/D	S/D	S/D	S/D	S/D	S/D	S/D	W	S/D	S/D	NS
	28'	S/D	W	S/D	S/D	S/D	S/D	S/D	S/D	S/D	S/D	W	S/D	S/D	W	S/D	S/D	NS
	50'	S/D	S/D	S/D	S/D	S/D	S/D	S/D	S/D	S/D	S/D	S/D	S/D	S/D	S/D	S/D	S/D	NS
I1	1'	S/D	S/D	S/D	S/D	S/D	S/D	W	S/D	W	S/D	NS	W	W	W	W	W	W
	5'	S/D	S/D	S/D	S/D	M	S/D	W	W	W	S/D	NS	W	W	W	W	S/D	W
	10'	S/D	S/D	S/D	S/D	S/D	S/D	W	W	W	S/D	NS	W	W	S/D	W	S/D	S/D
	15'	S/D	S/D	S/D	S/D	S/D	S/D	W	W	W	S/D	NS	W	W	W	W	S/D	S/D
	20'	W	W	W	W	S/D	S/D	S/D	S/D	S/D	S/D	W	W	W	S/D	W	W	S/D
	28'	S/D	W	W	M	S/D	S/D	S/D	S/D	W	S/D	W	S/D	S/D	S/D	S/D	W	S/D
	33'	S/D	S/D	S/D	S/D	S/D	S/D	S/D	S/D	W	S/D	S/D	W	S/D	S/D	S/D	W	S/D
I2	1'	W	S/D	S/D	S/D	S/D	S/D	S/D	S/D	S/D	NS	NS	S/D	S/D	S/D	S/D	S/D	W
	5'	S/D	S/D	S/D	S/D	S/D	S/D	S/D	S/D	S/D	NS	NS	S/D	W	S/D	S/D	S/D	S/D
	10'	S/D	S/D	S/D	S/D	S/D	S/D	S/D	W	W	NS	NS	W	W	S/D	W	W	W
	14'	S/D	S/D	S/D	S/D	S/D	W	S/D	W	W	NS	NS	W	W	W	W	W	W
I3	1'	NS	NS	NS	NS	NS	NS	NS	NS	NS	NS	NS	W	S/D	S/D	W	W	S/D
	5'	S/D	W	S/D	S/D	M	W	W	S/D	S/D	NS	NS	W	S/D	S/D	S/D	W	S/D
S3	2'6"	NS	NS	NS	NS	NS	NS	NS	NS	NS	NS	NS	NS	W	NS	NS	NS	NS

M - moisture observed
NS - not sampled
S/D - location sampled, but was dry
W - wet
? - log unclear

J. Jacobsen - 2/14/97

Table II.3-3. Summary of Water Sample Data

Well I.D.	Depth	Before	After	Detection		Well I.D.	Depth	Before	After	Detection
E1	7'	C	C	early		T2	2'		C	early
	12'		S	late			6'		C	early
	43'		S	late			9'9"		S	late
	54'		S	late			14'5"			
	57									
						T3	2'		C	late
E2	6'						6'			
	20'						10'			
	30'10"		S	mid			15'			
	50'		S	early			20'	s		
E3	17'	C				T4	2'		C	early
	22'		S	early			9'	S	C	early
	29'	S	C	late			14'	S	C	early
							19'		s	early
E4	23'		S	late						
	28'	S	S	mid		T5	1'			
	50'						5'			
							10'			
I1	1'		C	early						
	5'	s	C	early		T6	2'			
	10'		C	early			10'			
	15'		C	early			15'			
	20'	C	C	mid			21'			
	28'	C	S	early						
	33'		S	early		T7	2'		S	?
							6'		S	early
I2	1'	S	S	late			15'		S	early
	5'		S	late			19'			
	10'		C	early						
	14'		C	early		T9	1'		C	?
							5'	C	C	early
I3	1'	*NS*	C?	late			10'		C	early
	5'	S	C?	early						

C - consistently wet
NS - not sampled
S - sporadically wet
s - sporadically moist
? - uncertain

detection before 9/1 - early,
on 9/1 - mid, after 9/1 - late

II.4. Tracer Test Results

During the tracer test, the tracer movement was monitored, using water sampling with suction lysimeters and measurements of the voltage and current with a new design of miniature ER probes. Measurements of the electrical resistivity using ER probes were obtained in vertical well II-5, and slanted wells S-1, S-2, S-3, and S-4. In wells S-1 and S-2, there were multiple probes installed at a single depth. The results of the ER measurements are presented in Figures II.4-1 through II.4-5. The ER probes showed that the following depths were affected by the tracer during the infiltration test:

Well II-5: depths 0.3, 11.0, and 18.0 m (1, 36, and 59 ft),
Well S-1: depths 0.6 and 1.8 m (2 and 6 ft),
Well S-2: none of the probes was affected by the tracer,
Well S-3: 0.8, 3.4, and 8.1 m (2.5, 11, and 26.5 ft), and
Well S-4: 14.6 m (48 ft).

The tracer data confirmed that there was a delay in the tracer moving downward with the infiltrating water in the top soil-rock layer at 0.3-0.6 m (1-2 ft), when compared to the rapid initial saturation of the top soil layer at the beginning of the test.

The test showed the ER probes are a robust field technique for continuous monitoring of the tracer distribution. ER probe measurements of the voltage and current, along with the calculation of the electrical resistance confirmed that the tracer appeared in the fracture zones and rubble zones, but not in low-permeability basalt and single non-conductive fractures. The main difference in the performance of ER probes from the other probes is that the ER probes only respond when the electrolyte concentration changes in the immediate vicinity of the probe. Therefore, local lithology in the immediate vicinity of the probe has a strong affect on the response.

Water samples were collected before and after the tracer was added, from 8/28/96 through 9/6/96. Not all wells or depths were sampled every day, however. The number of sampling locations totaled 56. Of these, 19 never produced water samples. After the tracer was added, sample collection varied from 16 to 27 samples per day. At some locations, samples were collected two to three times a day. Tables II.3-1 and II.3-2 show the results from the sample collection.

Samples were analyzed using a Dionex high-performance liquid chromatograph with a conductivity detector. Anions in solution were separated using an AS5A resin. The bromide concentration was determined using a four-point calibration curve of bromide retention time. The calibration curve was obtained from a standard solution. Samples collected from 9/2/96 through 9/6/96 were analyzed twice. For samples with a bromide concentration over 100 mg/l, the two analyses differed from their average value by less than 20% for 70% of the samples.

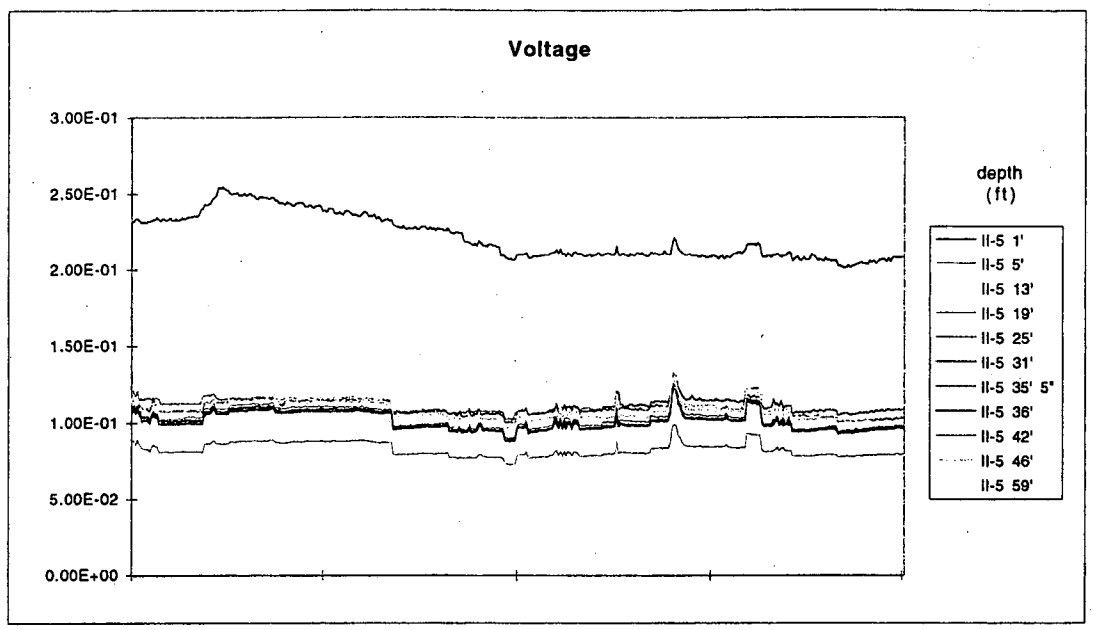

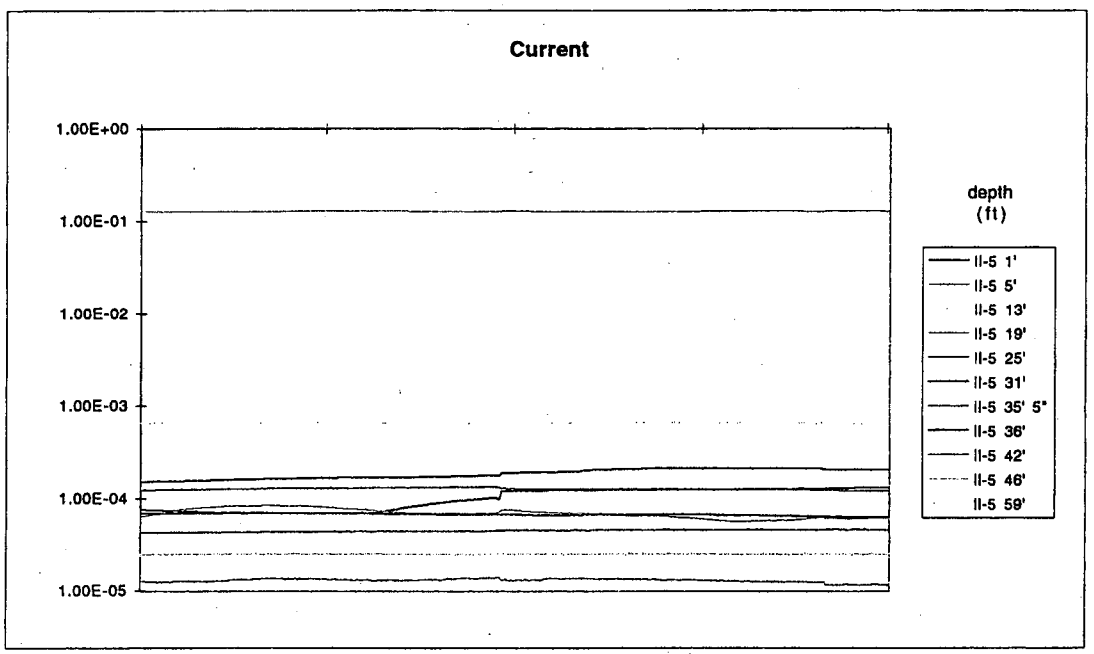

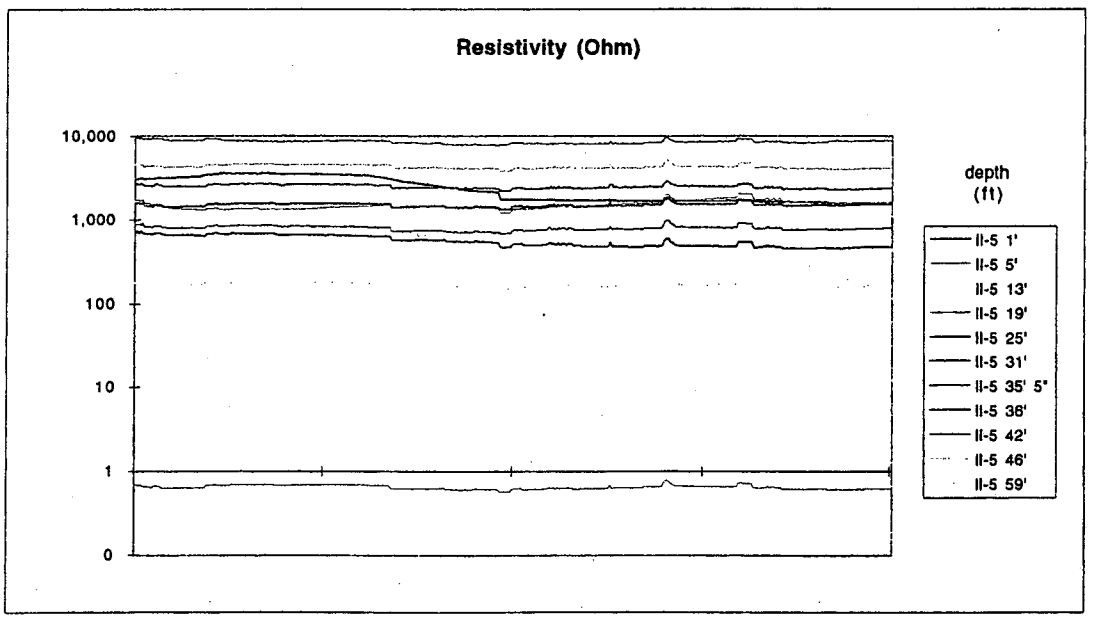

Figure II.4-1. Electrical Resistivity Measurements on Well II-5

Figure II.4-2. Electrical Resistivity Measurements on Well S-1

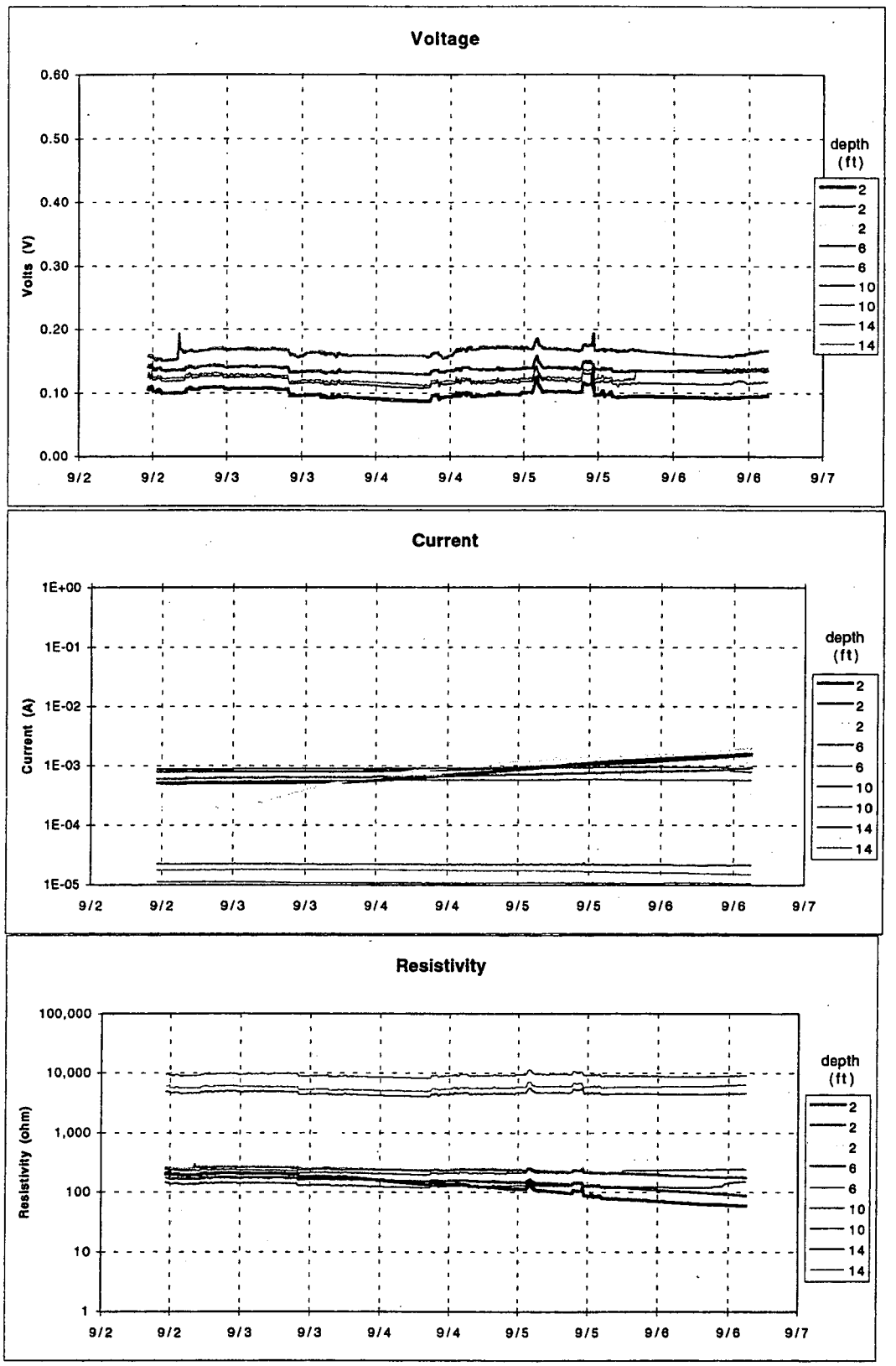

Figure II.4-3. Electrical Resistivity Measurements on Well S-2.

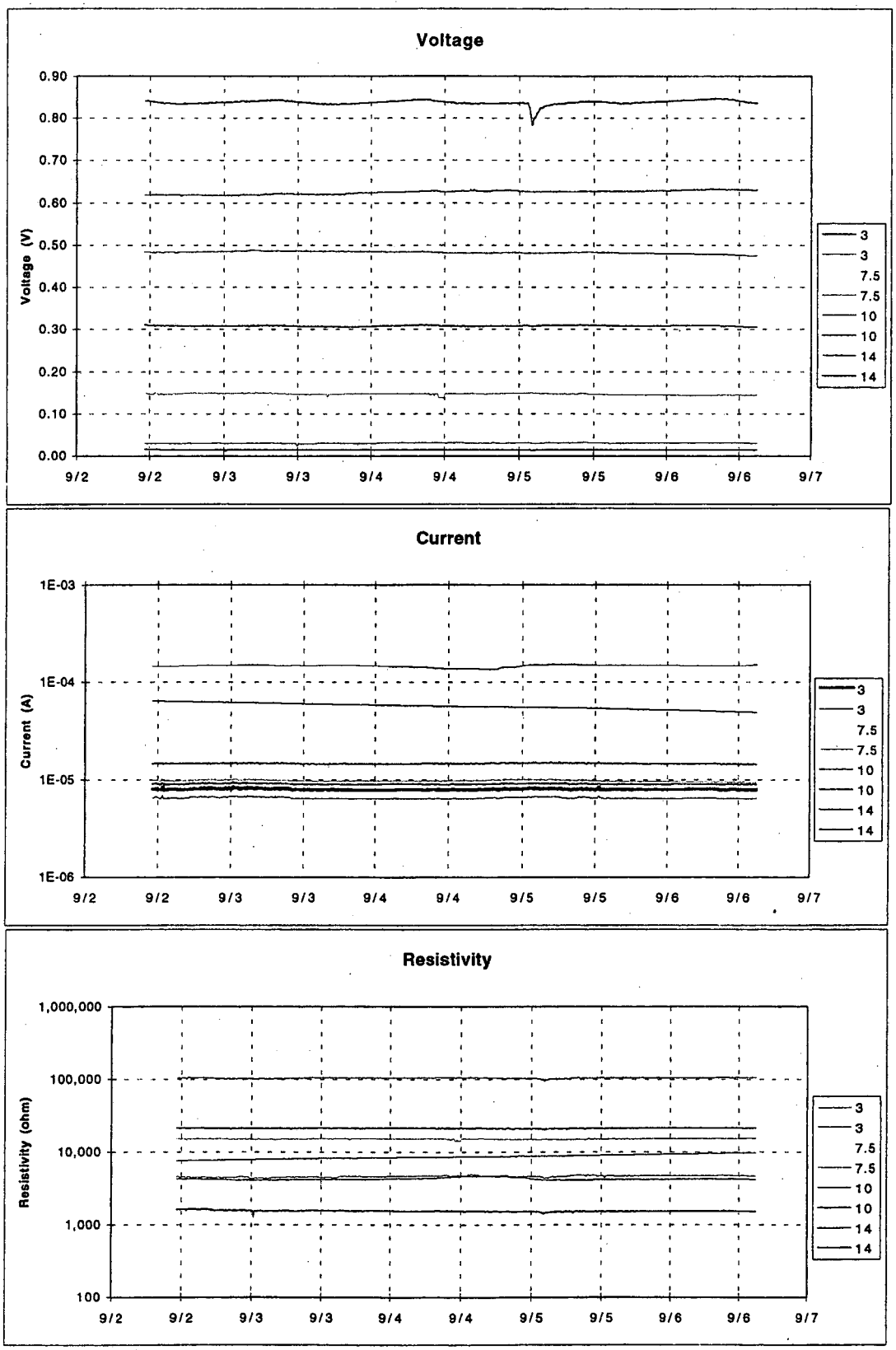

Figure II.4-4. Electrical Resistivity Measurements on Well S-3

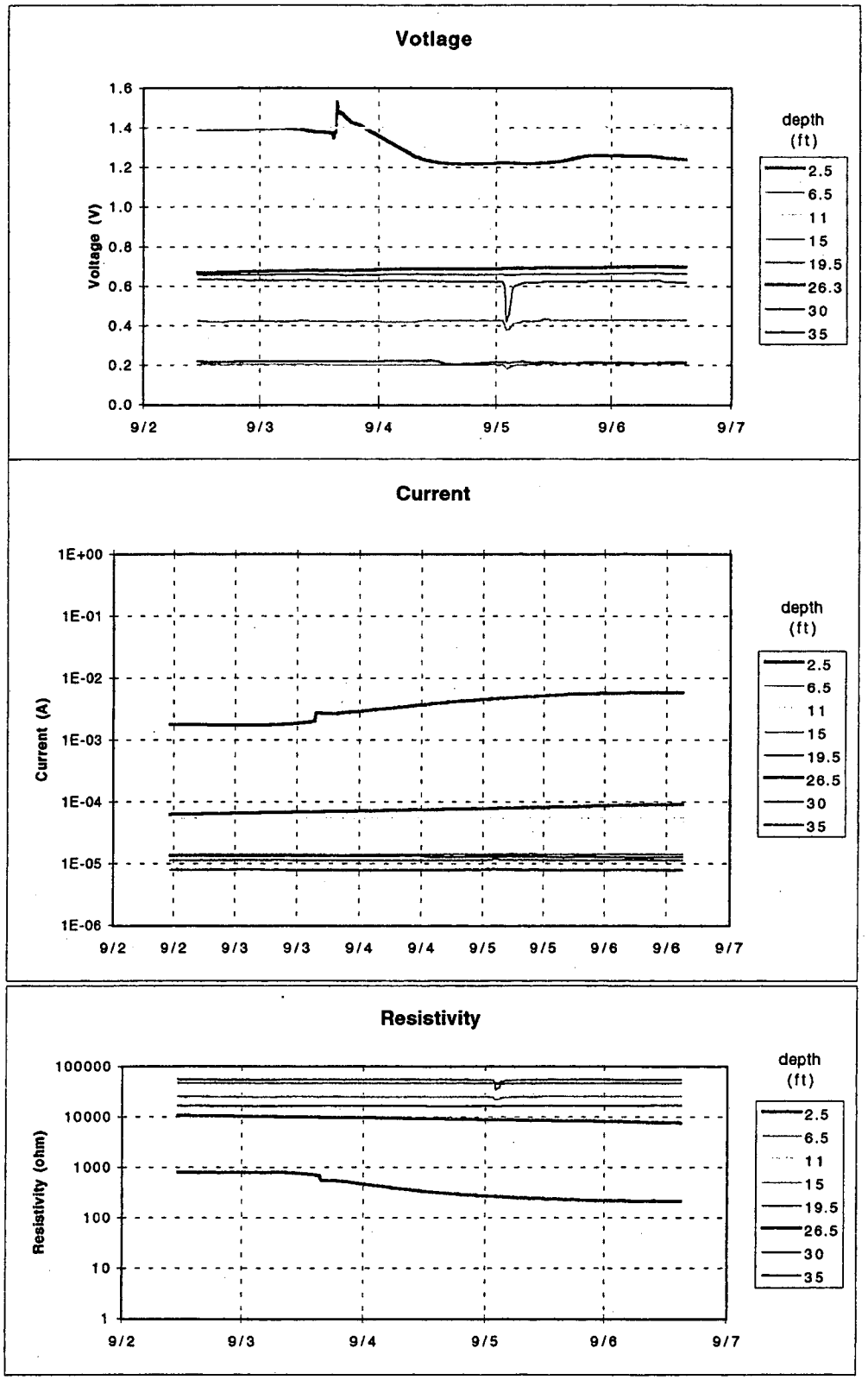

Figure II.4-5. Electrical Resistivity Measurements on Well S-4

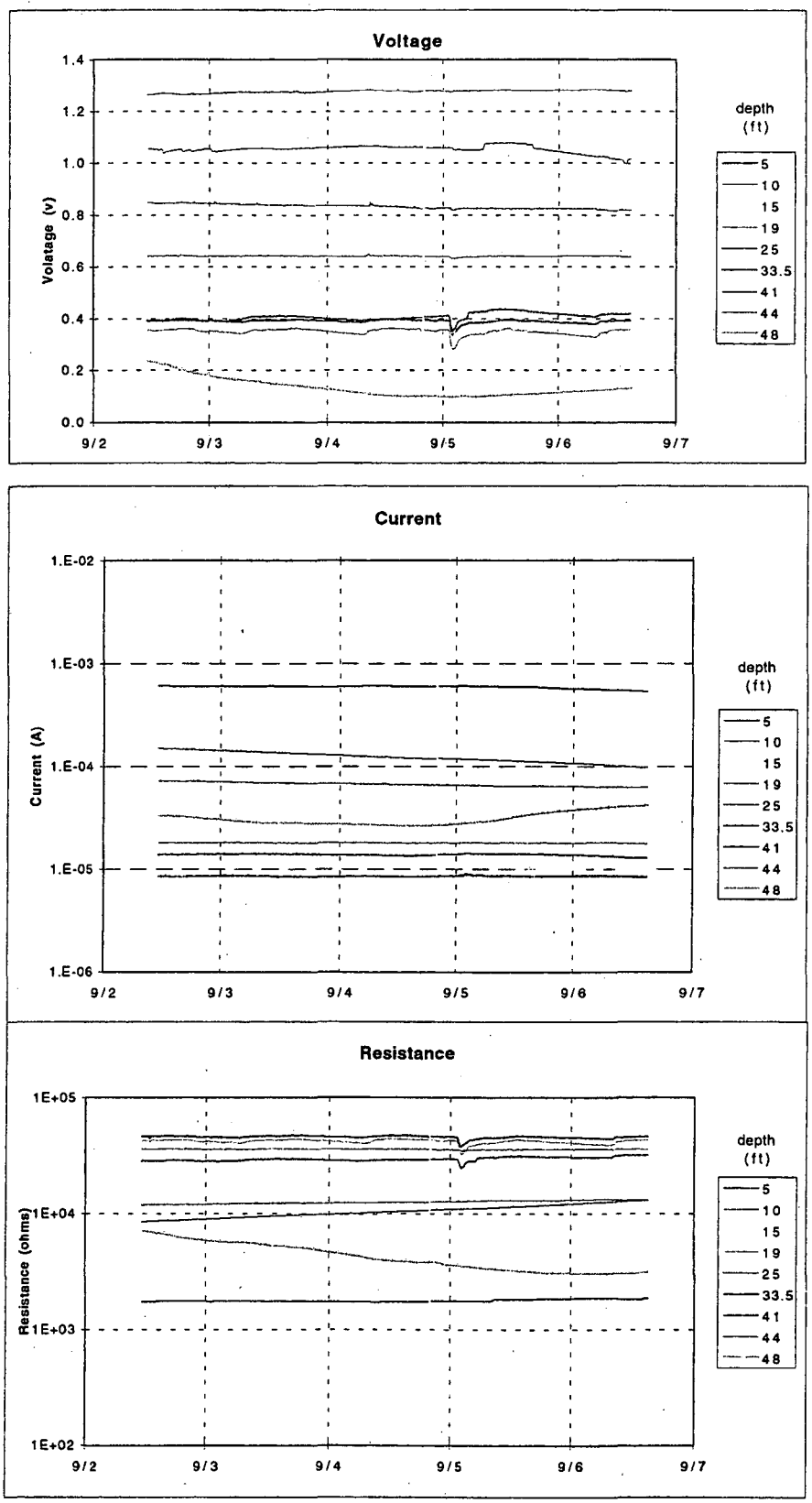

Table II.4-1 gives the results of the bromide sample analysis during the collection period of 8/28/96 through 9/7/96. Note that bromide was detected in samples collected before tracer was added to the infiltration pond, but concentrations were less than 10 mg/l (with one exception). After the tracer was added to the pond, bromide concentrations in excess of 100 mg/l were observed at 16 of the 34 sample locations* where enough water could be collected to analyze. Of these, tracer was observed at

- 75% of the sampling locations 0-1 m (0-3.3 ft)
- 80% of the sampling locations 1-2 m (3.3-6.6 ft)
- 33% of the sampling locations 2-3 m (6.6-9.8 ft)
- 57% of the sampling locations 3-5 m (9.8-16.4 ft)
- 14% of the sampling locations 5-9 m (16.4-29.5 ft)
- 0% of the sampling locations deeper than 9 m (29.5 ft)

Considering, however, that sampling collection ended on 9/7/96, it is likely that the percentages cited above would have changed had sample collection continued past that date.

Sampling of the E wells and wells S-3, T-3 and T-7 was relatively infrequent. Wells T-5 and T-6 were dry. None of the samples collected from T-3 or the E wells shows bromide concentrations larger than 38 mg/l. Though the bromide concentrations were large in the samples collected at S3 and T-7, only one sample was collected at each well. For these reasons, the discussion in this section will focus on wells I-1, I-2, and T-2. Note that I-1 and I-2 are located in the northwest quadrant of the infiltration pond, and T-2 is just outside of the eastern edge. (See Figure I.2-1 for a plan view of the site.)

Figures II.4-6 through II.4-8 show breakthrough curves for six locations in wells I-1, I-2, and T-2. These locations were chosen because there are five or more samples per location. The error bars in the figures show the spread of the two analyses about their average value.

One of the most interesting features of the breakthrough curves is that the time of arrival of the tracer does not correlate with depth. For example, tracer arrives at the two shallow locations (0.3 m and 1.5 m) in well I-1 two days after arriving at deeper locations in I-2 (4.3 m). Also notable is that the breakthrough curve for a the 4.3 m depth in well I-2 (Fig. II.4-7) shows an unequivocal downturn, whereas all of the other curves show a continuing increase in concentration with time, or a leveling off in concentration. The curves for depths of 0.3 m and 1.5 m in I-1 (Figure II.4-6) are similar to each other in

* Three locations produced water samples before tracer was added to the infiltration pond, but not after, thus the apparent discrepancy between the expected number of locations that produced water samples after tracer was added (37) and the actual number of locations that produced samples after tracer was added (34).

Table II.4.1
Bromide Concentrations (mg/l) - 1996 Tracer Test

NOTE: Concentrations for 2-Sep - 6-Sep are averages of two sample analyses.

Well I.D.	Depth (m)	28-Aug	29-Aug	30-Aug	31-Aug	1-Sep	2-Sep	3-Sep	4-Sep	5-Sep	6-Sep
E1	2.1		ND, ND	ND			ND		ND	19.30	
	3.7								0.66	1.18	
	13.1										
	16.5										
	17.4										
E2	1.8										
	6.1										
	9.4					2.44			3.01		
	15.2		6.45			4.29			3.79		
E3	5.2										
	6.7		2.67			1.50			1.89		
	8.8						5.14		4.23		4.68
E4	7.0								1.49		
	8.5					5.38			0.89		
	15.2										
I1	0.3	ND		1.11			1.18	2.17, 5.43	5.89	470	726
	1.5	0.33	ND	ND			ND	0.21	0.52	532	
	3.0			3.35			0.68			0.84	
	4.6		ND	1.05			1.70	0.92	0.82	10.31	
	6.1					1.71	0.61	0.53		0.55	0.94
	8.5			2.16		1.81					5.89
	10.1			3.28			4.04				3.92
I2	0.3										
	1.5							0.48			
	3.0		2.40				0.47,2.32	4.13, 101		435	1029
	4.3		ND	ND			ND		5365	3685, 2170	975
I3	0.3						0.55			487	1077
	1.5	1.30					0.87				4.13
S3	0.8							661			

Notes:
1. Br added 9/2; pond conc. approx. 3 g/l.
2. ND - not detected.
3. Some locations sampled more than once a day.

J. Jacobsen - 8/13/97 (tratoz2dr.xls)

Table II.4.1
Bromide Concentrations (mg/l) - 1996 Tracer Test

NOTE: Concentrations for 2-Sep - 6-Sep are averages of two sample analyses.

Well I.D.	Depth (m)	28-Aug	29-Aug	30-Aug	31-Aug	1-Sep	2-Sep	3-Sep	4-Sep	5-Sep	6-Sep
T2	0.6		0.65	0.36			ND	0.97	277, 1795	3205	
	1.8		1.04	0.51			ND	ND	474	4070	
	3.0								4.76		
	4.4										
T3	0.6								2.47	3.99	37.75
	1.8										
	3.0										
	4.6										
	6.1										
T4	0.6	ND	ND	261			ND		0.45	5.63, 41.6	
	2.7	1.22	ND	ND			ND			653	
	4.3	0.82	36.30	ND			ND		0.18	339	
	5.8									247	
T5	0.3										
	1.5										
	3.0										
T6	0.6										
	3.0										
	4.6										
	6.4										
T7	0.6										1825
	1.8										
	4.6										
	5.8										
T9	0.3						0.86	89.65, 936, 735	940, 856		756
	1.5	ND	ND	ND			ND	6.19, 394	911, 706	815	
	3.0	1.68	0.67	0.38				63.55, 239	277, 340		660

Notes:
1. Br added 9/2; pond conc. approx. 3 g/l.
2. ND - not detected.
3. Some locations sampled more than once a day.

J. Jacobsen - 8/13/97 (trato2dr.xls)

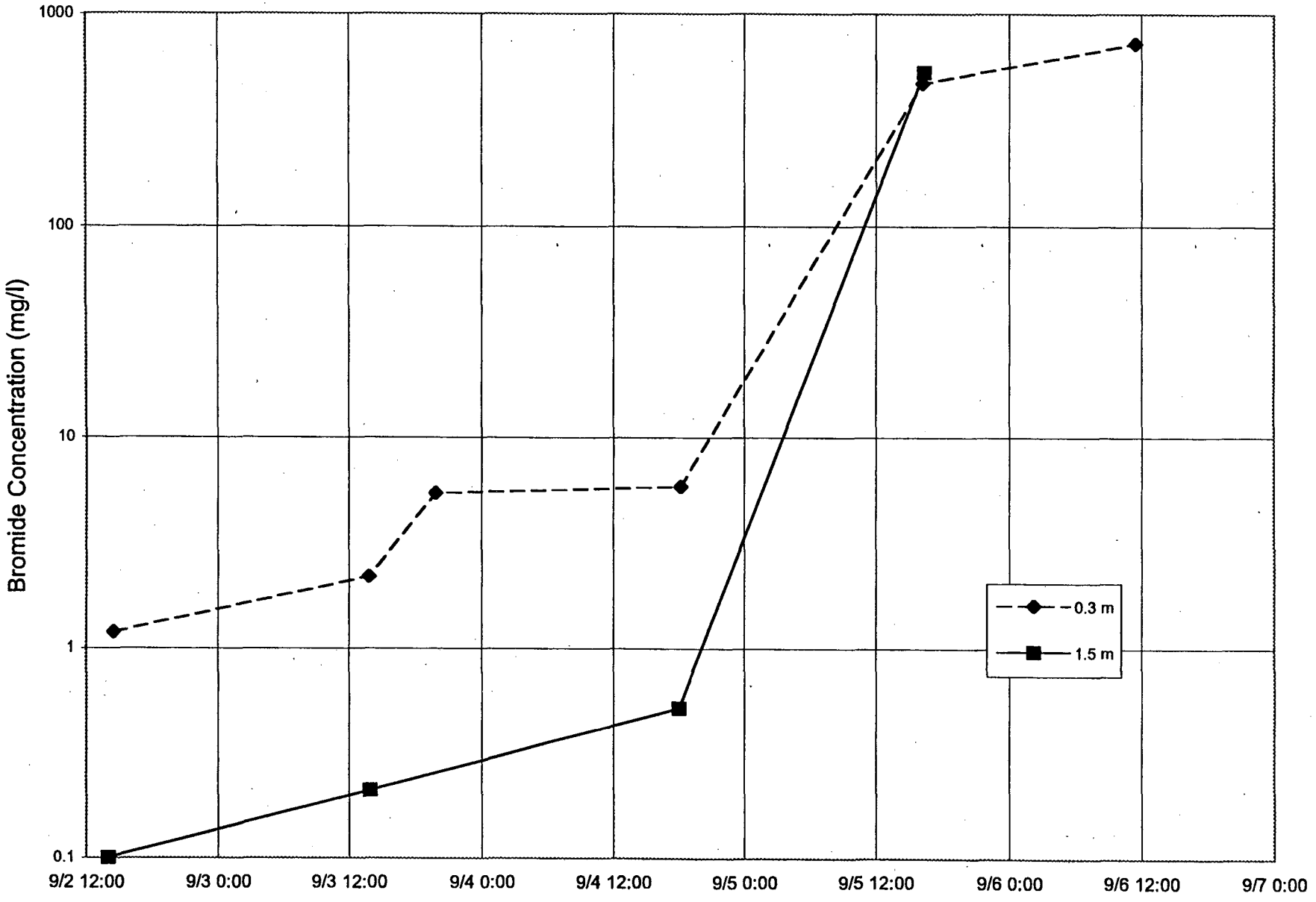

Figure II.4-6. Tracer breakthrough curves at two sampling locations in well I-1.

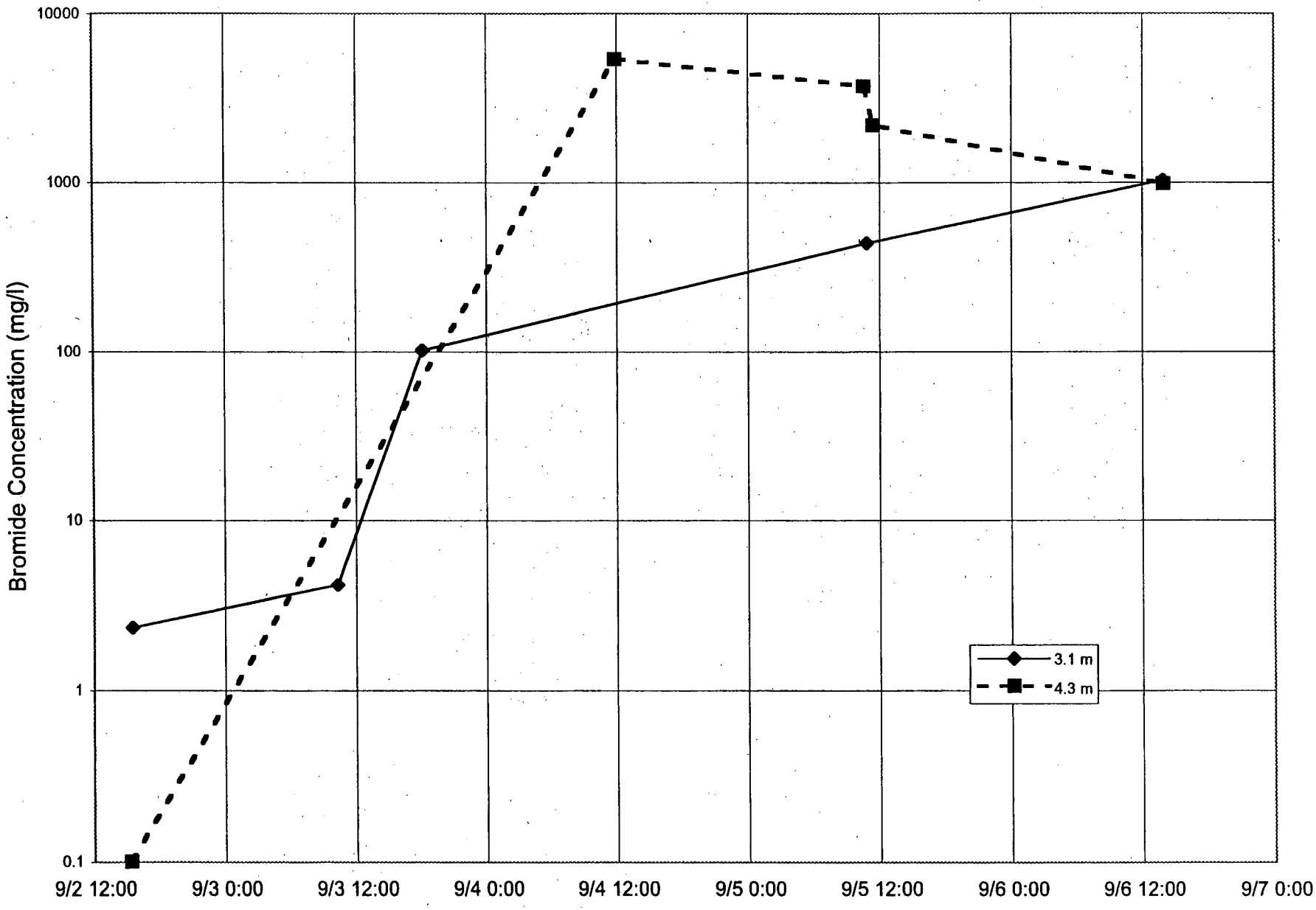

Figure II.4-7. Tracer breakthrough curves at two sampling locations in well I-2.

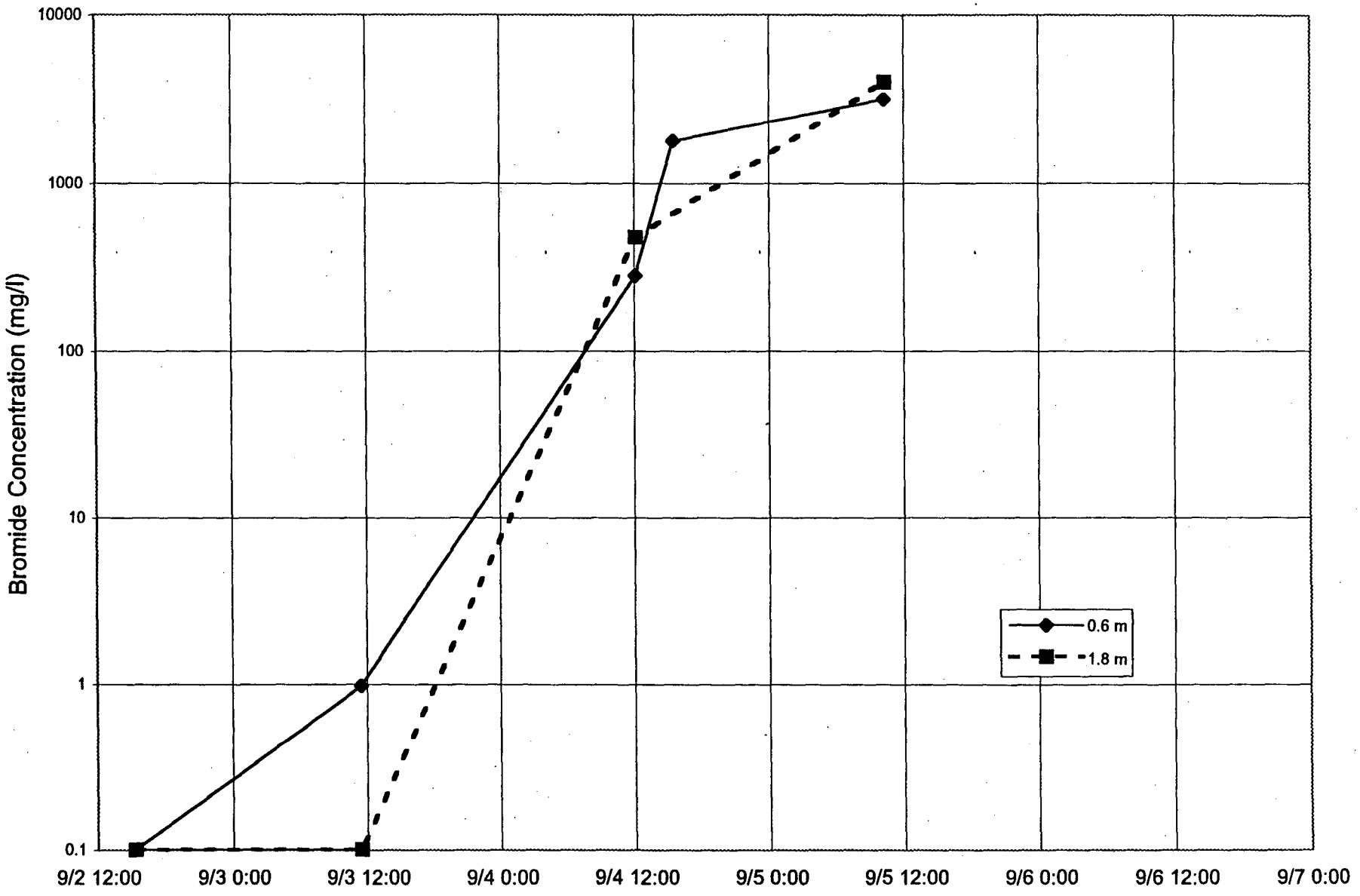

Figure II.4-8. Tracer breakthrough curves at two sampling locations in well T-2

shape and in magnitude of concentration. The same comment can be made about the curves for depths of 0.6 m and 1.8 m in T2 (Figure II.4-8).

Table II.4-2 provides a classification of the breakthrough curves for wells I-1, I-2 and T-2 and also includes information about two additional locations in I-1 (4.6 m and 6.1 m), one location in I-3 (0.3 m), one location in T3 (0.6 m), and three locations in T-9.

The column "Characterization of Arrival" in Table II.4-2 attempts to classify how quickly the concentration of bromide increased over background conditions in the basalt below the infiltration pond after the tracer was added. A concentration of 100 mg/l was chosen as a measure of the tracer arrival at the sampling location. No classification is given for the depth of 0.3 m at I-3 because of lack of samples between 9/2/96 and 9/5/96.

For most of the sampling locations listed in Table II.3-2, the maximum concentration was reached on the day of the last sample collection, when concentrations were still rising at almost every location. The notable exception is at the depth of 4.3 m in well I-2. The tracer concentration peaks on 9/4/96 and decreases by nearly an order of magnitude by 9/6/96.

The tracer data discussed above support the conclusion that fluid is conducted downward through vertical or near-vertical fractures, and that the "connectedness" of some fractures results in fast flow paths. Specifically, we note the following.

- It is likely that there are well connected flow paths intersecting at least the first 1.5 m of I-1, the first 1.8 m of T-2, and the first 3.1 m of T-9. For all of these wells, the breakthrough at various depths in a well are similar to each other in time of arrival, shape, and magnitude of concentration.

- There must be a non-vertical fast path between the surface and well I-2 at a depth of 4.3 m. This depth has the largest concentrations of any sampling location, shows a rapid increase in concentration, and is one of the few depths that shows both an increase and decrease in concentration. Moreover, the behavior of tracer breakthrough at depths of 3.1 m and 4.3 m in I-2 is dissimilar, suggesting that the lithology of these two depths is dissimilar and/or that the two depths are not connected to the same flow path. Also, although the two shallower locations in I-2 (at depths of 0.3 m and 1.5 m) were sampled daily after tracer was added to the pond, it was possible only to collect a sample at 1.5 m on 9/3/96, and that sample did not contain a detectable amount of tracer.

II.5. Temperature Data

The temperature at different depths was measured using thermistors installed in wells I-3 (8 thermistors), E-1 (7 thermistors), E-2 (6 thermistors), E3 (6 thermistors), and E-4 (4 thermistors). Also, the ambient temperature and temperature of water in the pond

Table II.4-2. Characteristics of Arrival of Bromide Tracer at Selected Wells - 1996 Tracer Test

Well ID	Depth (m)	Characterization of Arrival	Approx. Date Br Conc. Reaches 100 mg/l	Maximum Br Conc. (mg/l)	% diff. from av. value
I1	0.3	slow	Sept. 5	726 +/- 103	14%
	1.5	slow	Sept. 5	532 +/- 2	0%
	4.6	little change	doesn't (before end of exp.)	10 +/- 1	9%
	6.1	no change	doesn't (before end of exp.)	1 +/- 0	8%
I2	3.1	rapid	Sept. 3	1,029 +/- 152	15%
	4.3	very rapid	Sept. 3	5,365 +/- 625	12%
I3	0.3	uncertain	unknown	1,077 +/- 84	8%
T2	0.6	gradual	Sept. 4	3,205 +/- 265	8%
	1.8	gradual	Sept. 4	4,070 +/- 920	23%
T3	0.6	little change	doesn't (before end of exp.)	38 +/- 0	0%
T9	0.3	very rapid	Sept. 3	940 +/- 42	4%
	1.5	rapid	Sept. 3	911 +/- 121	13%
	3.1	rapid	Sept. 3	660 +/- 145	22%

J. Jacobsen - 9/9/97

were monitored. The data obtained are shown in Figures II.5-1 through II.5-10. Surface temperature measurements (Figure II.5-1) made before and during the ponded infiltration test show large daily fluctuations, as well as a trend of gradual decrease in the average daily temperature, which is probably due to seasonal cooling. Subsurface temperature measurements taken during the test were for the most part consistent with purely conductive heat flow: temperature changes generally decrease with depth, and no thermistor deeper than 7 m showed any temperature change during the infiltration test.

II.6. Flowrate Data

To calculate the water flux into the subsurface, we first determined the total cumulative flow into the pond using the flux meter (totalizer) installed at the exit from the water supply tank. The cumulative infiltration into the subsurface was calculated by subtracting the evaporation measured in a 1.5 m diameter evaporation pan from the total flow into the pond. The evaporation data, shown in Table II.6-1, varied between 1 and 2 cm/day. The data denoted in Figure II.6-1 by squares is the calculated cimulative infiltration into the subsurface. Figure II.6-1 also includes Horton's infiltration equation, which describes an exponential decrease of the water flux with time. This exponential decrease is typical for many infiltration tests in soils. When the water supply was terminated during the tracer test (9/2/96 through 9/4/96) we used measurements of the water level in the pond.

In order to calculate the flow rates in the local infiltrometers, we used the infiltrometer water level data measured while the water supply was terminated during the tracer test on 9/2/96 through 9/4/96 (Figure II.6-2). For this period of time, Table II.6-1 summarizes the flow rate calculated for individual infiltrometers within the pond and the value of the total flow rate within the entire pond. As can be seen from this table, seven out of nine infiltrometers showed a local infiltration rate less than that in the entire pond. One possible explanation of this observation is that the flow rate is influenced by edge effects, such as increased evaporation close to the pond berm and backward water flow, which are typical for ponded infiltration tests.

It should be noted that the data on the flow rate obtained from individual water supply tanks were, most likely, affected by drift in the pressure transducer measurements, therefore, these data can not be used in analyzing the flow rate in the pond.

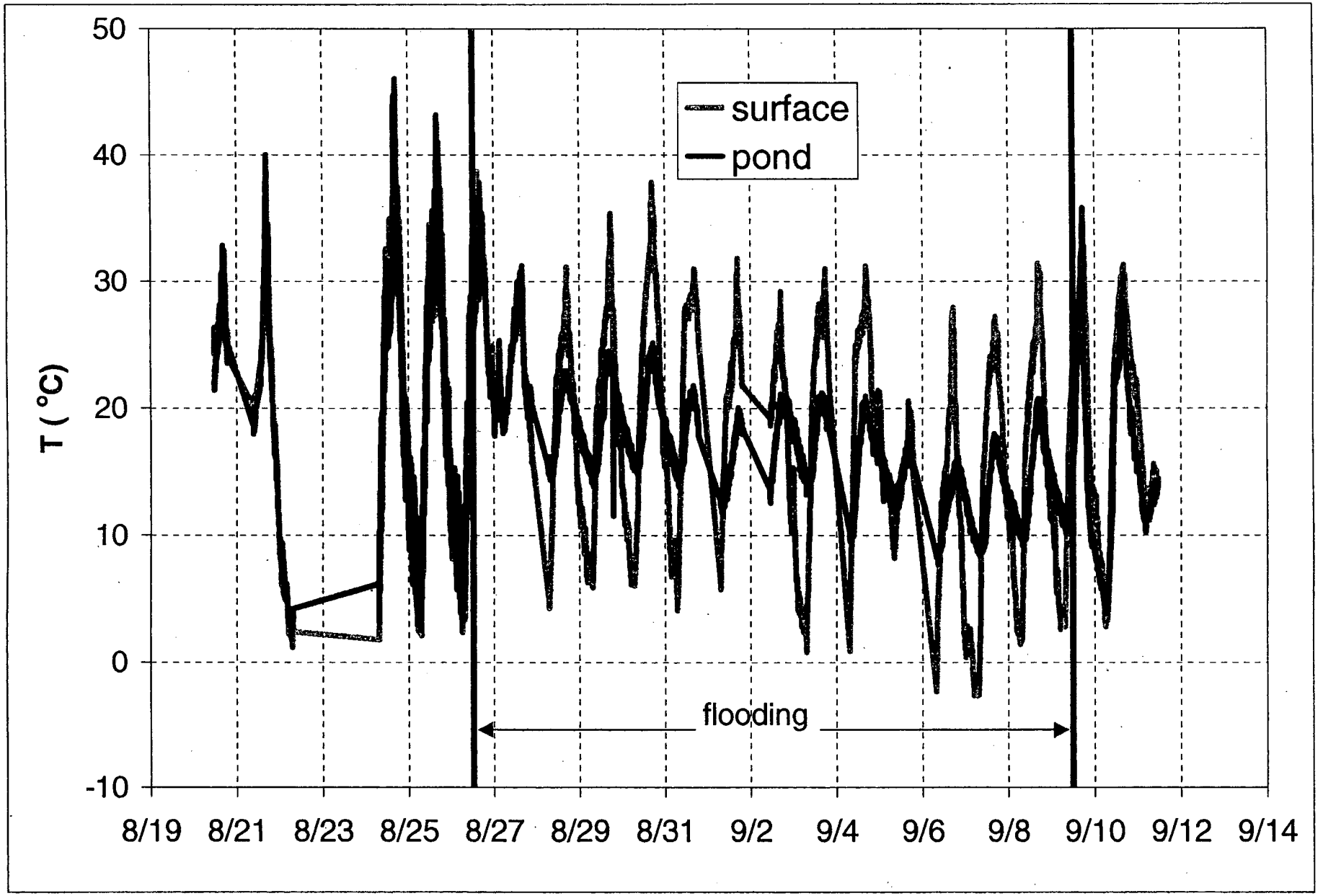

Figure II.5-1. Temperature within the pond and ambient air

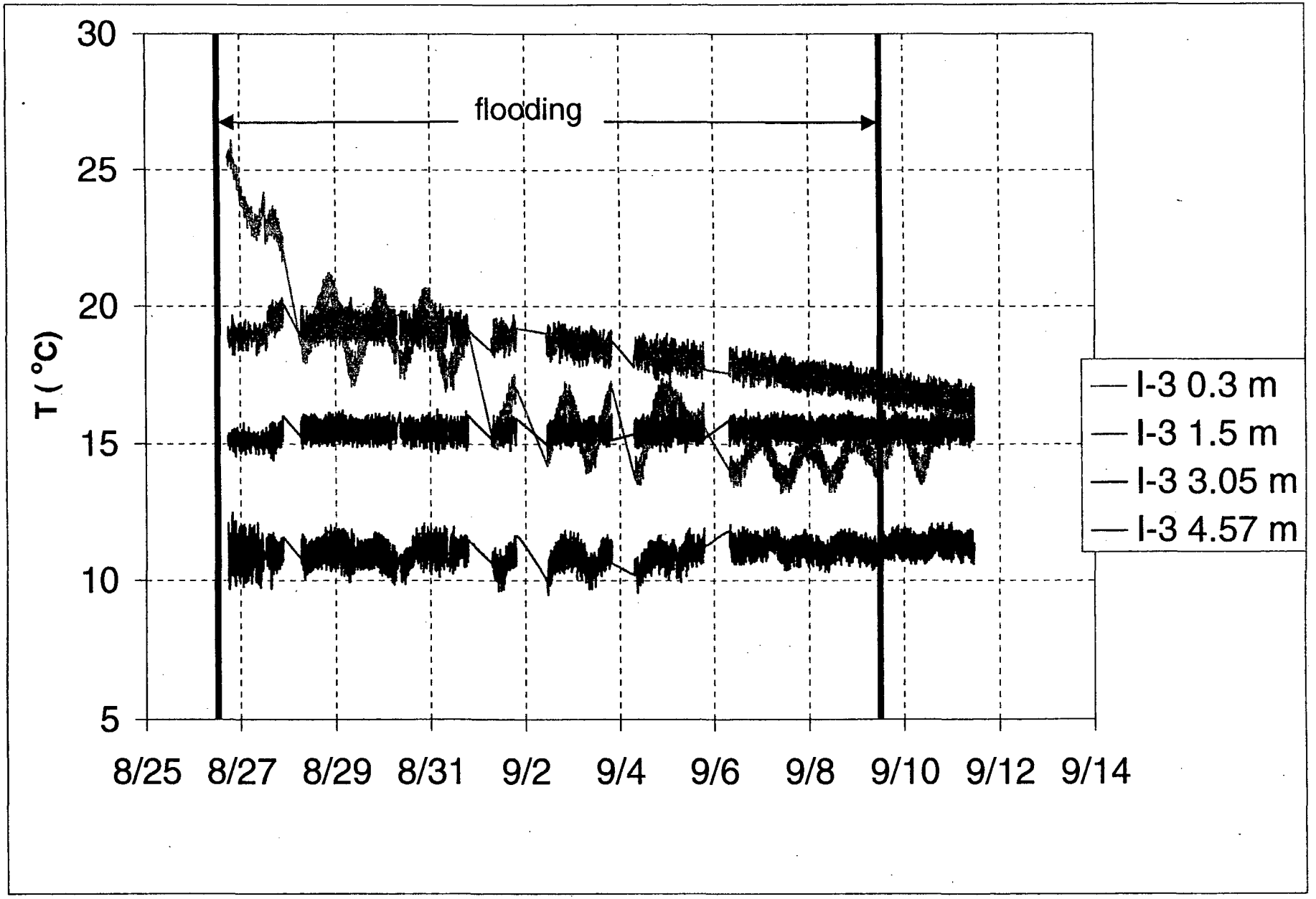

Figure II.5-2. Time trend of temperature in well I-3

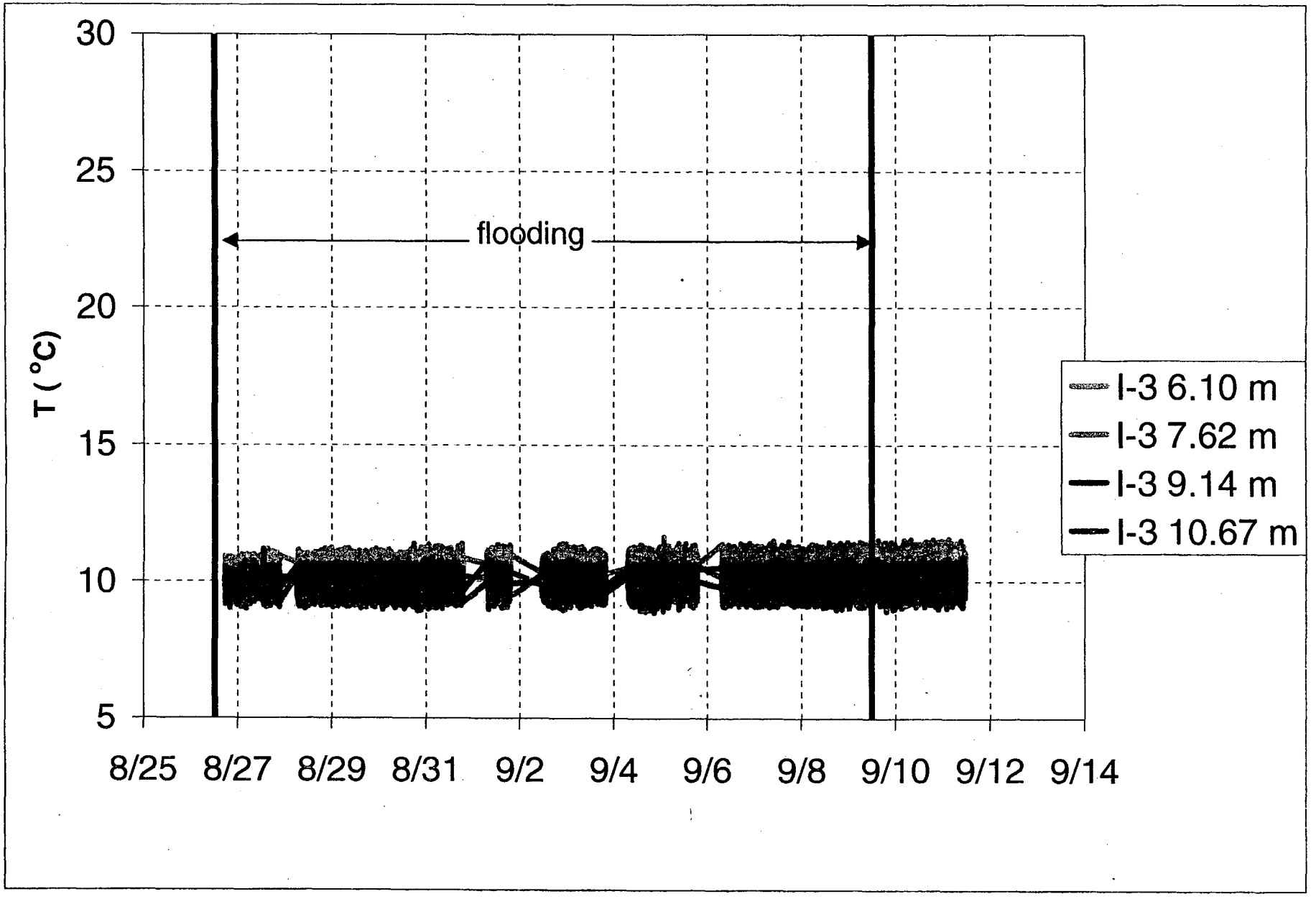

Figure II.5-3. Time trend of temperature in well I-3

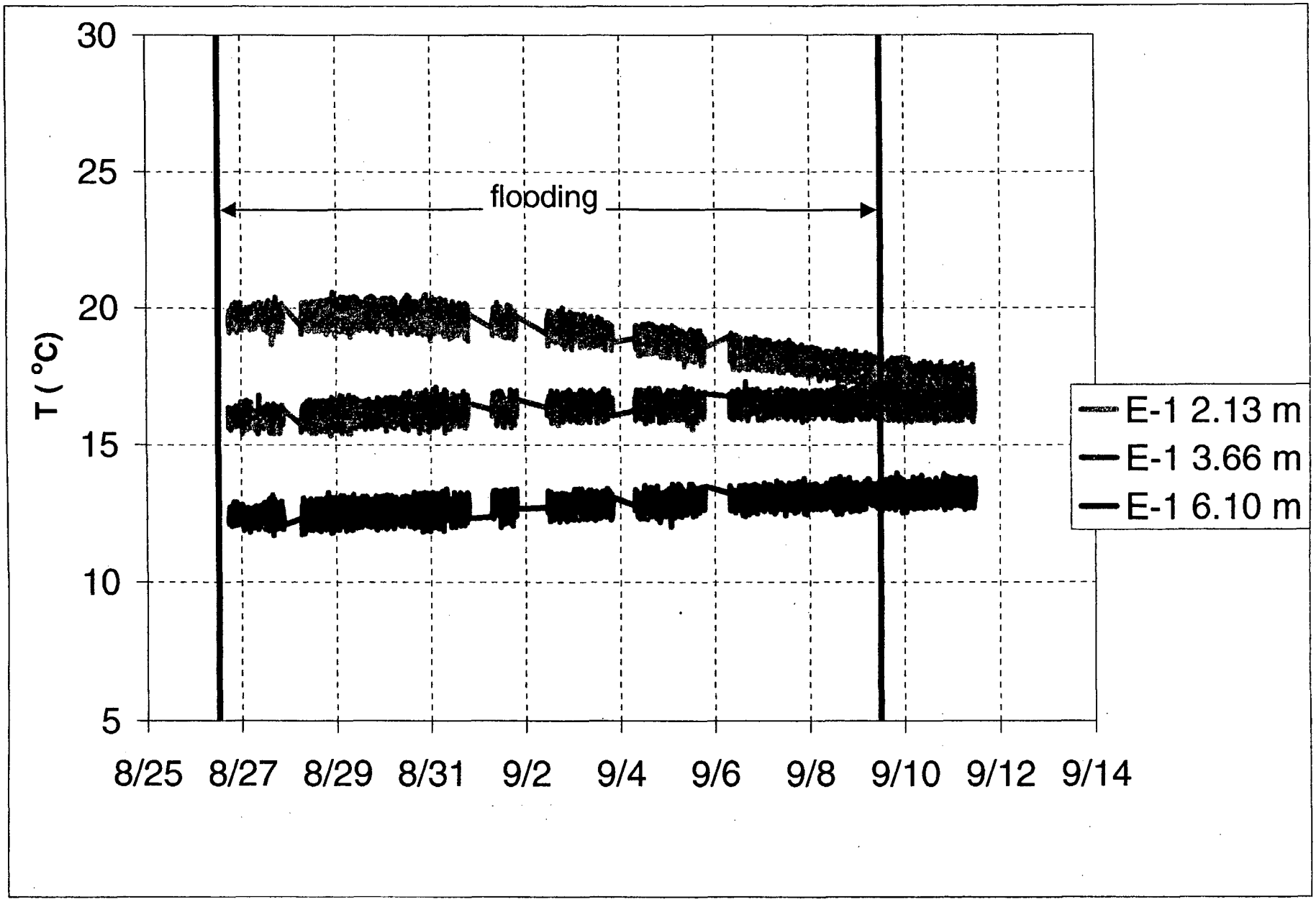

Figure II.5-4. Time trend of temperature in well E-1

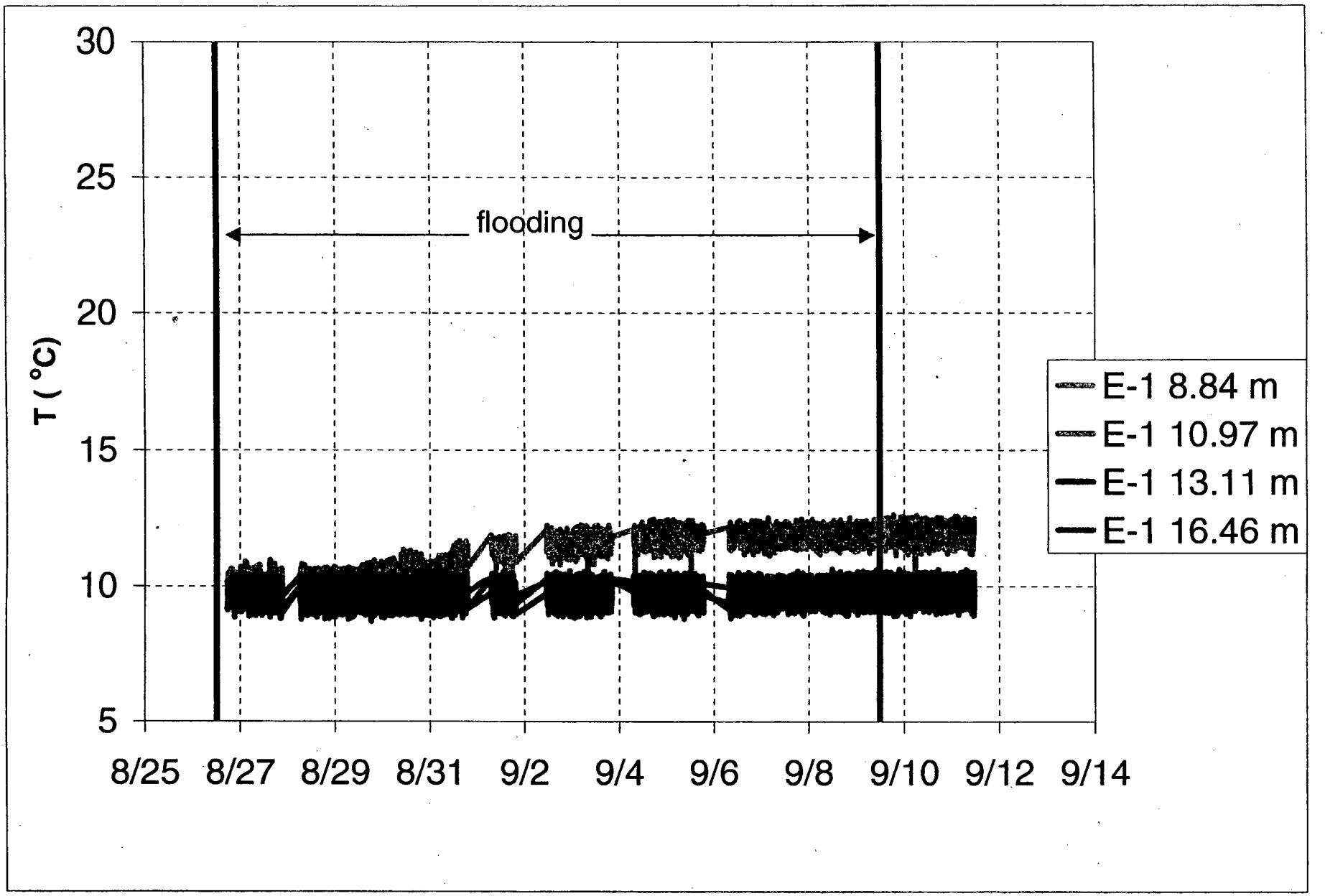

Figure II.5-5. Time trend of temperature in well E-1

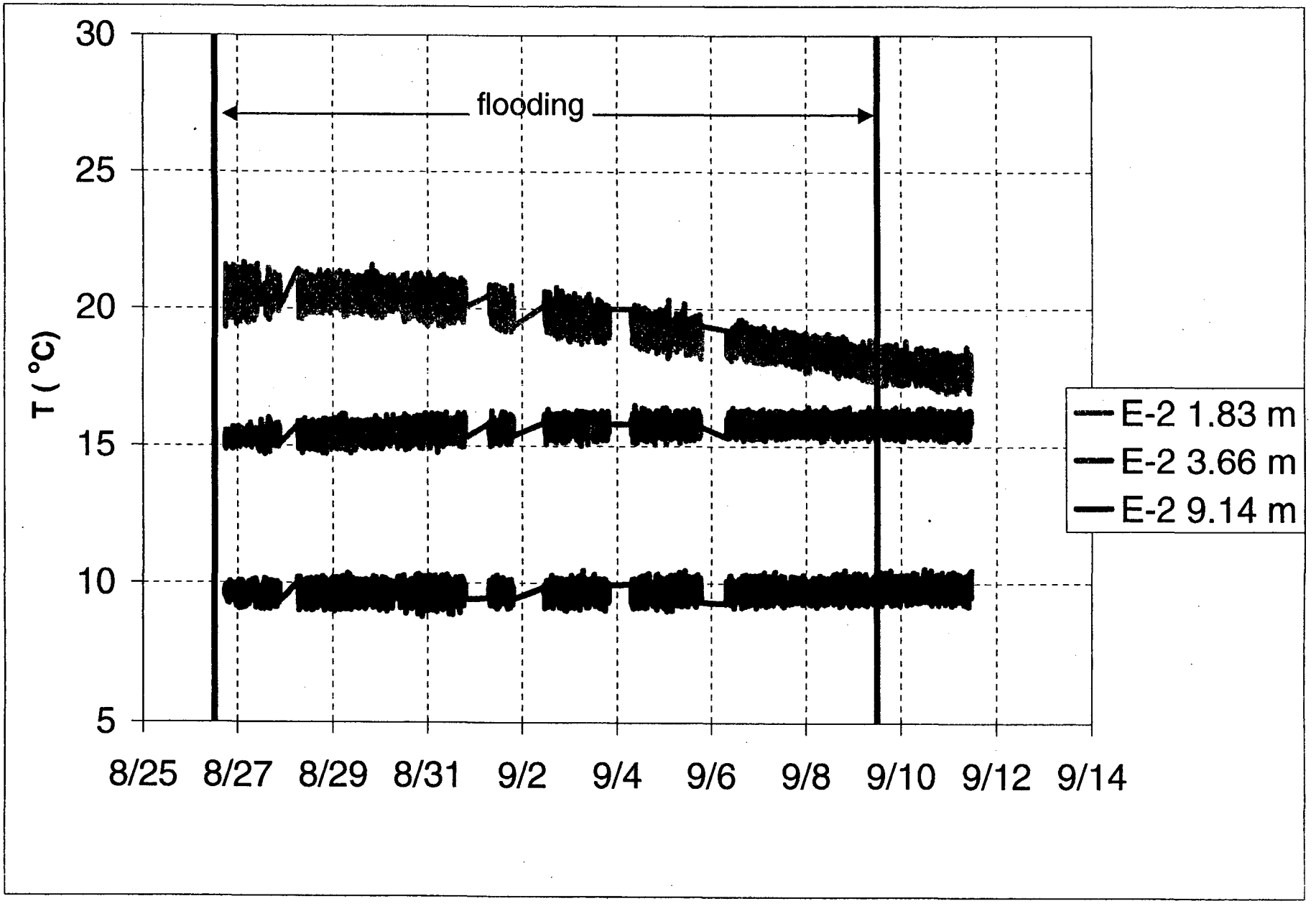

Figure II.5-6. Time trend of temperature in well E-2

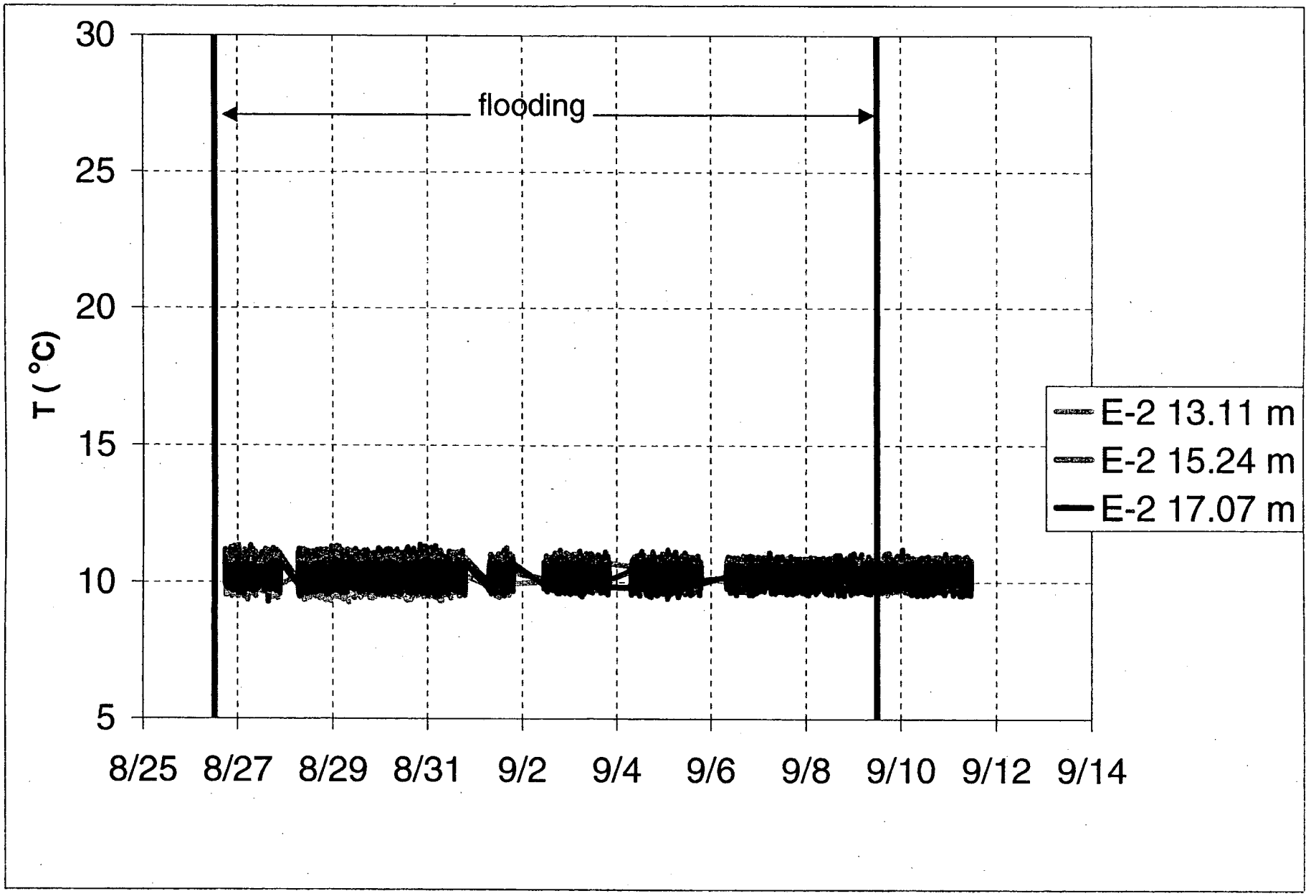

Figure II.5-7. Time trend of temperature in well E-2

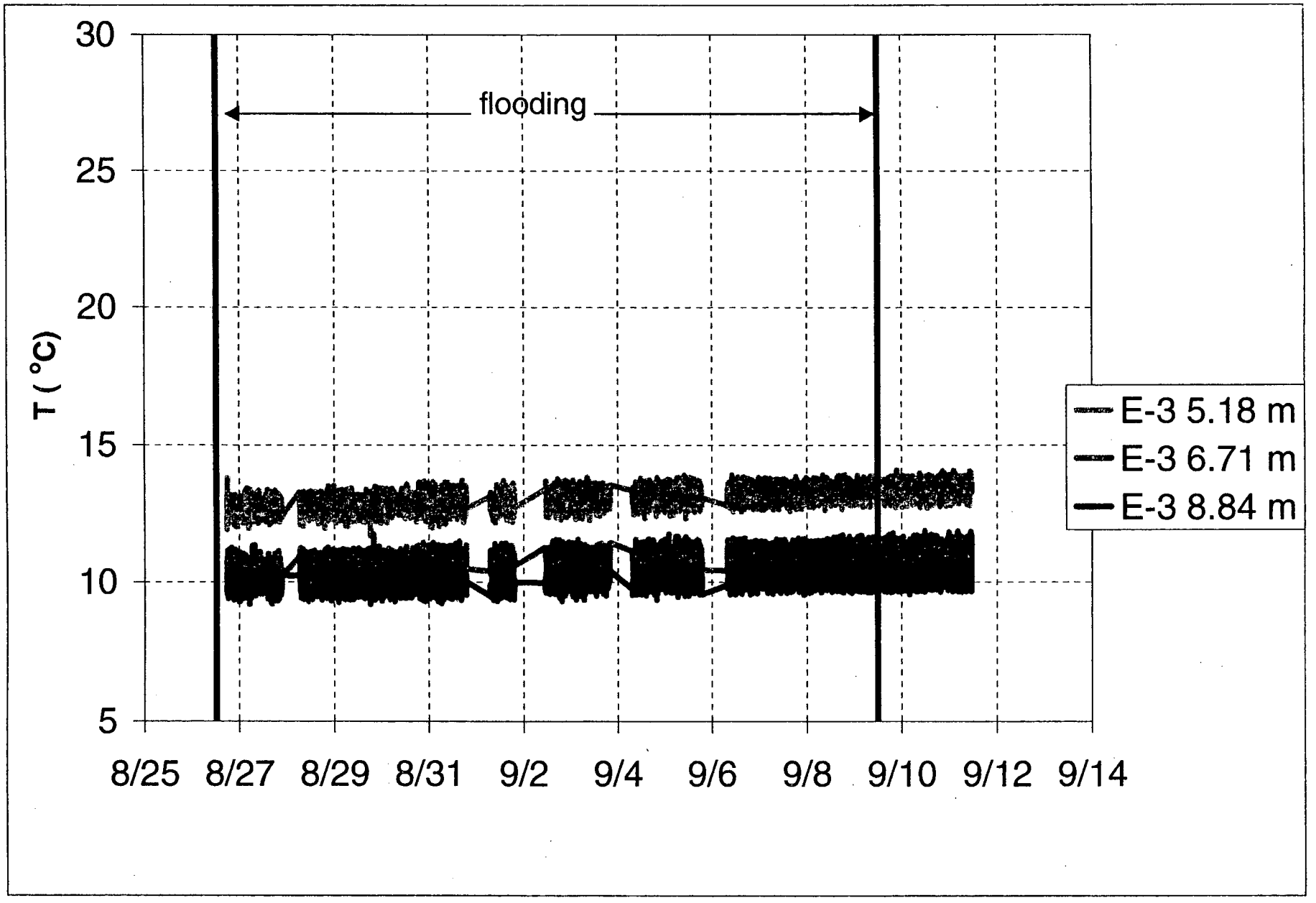

Figure II.5-8. Time trend of temperature in well E-3

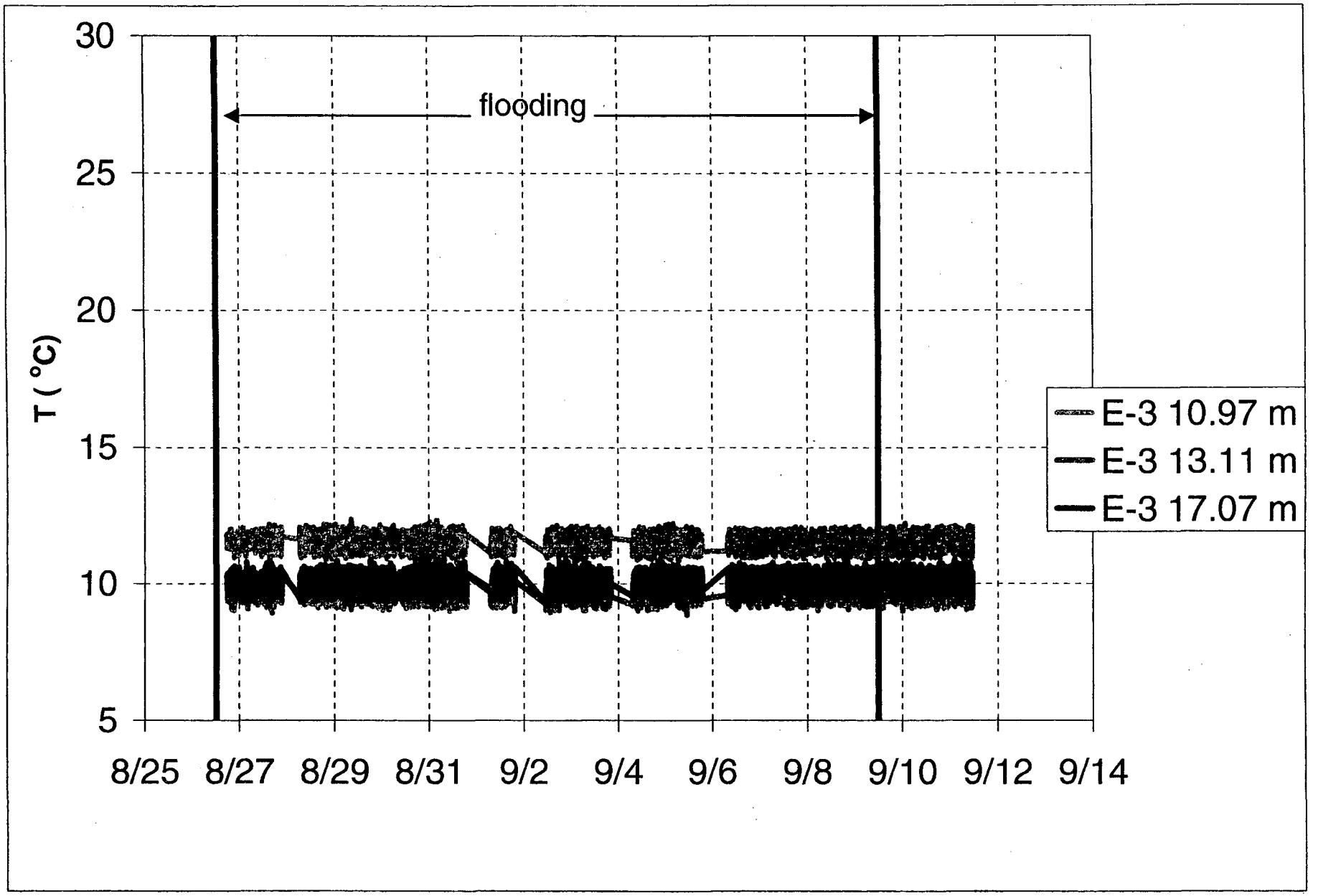

Figure II.5-9. Time trend of temperature in well E-3

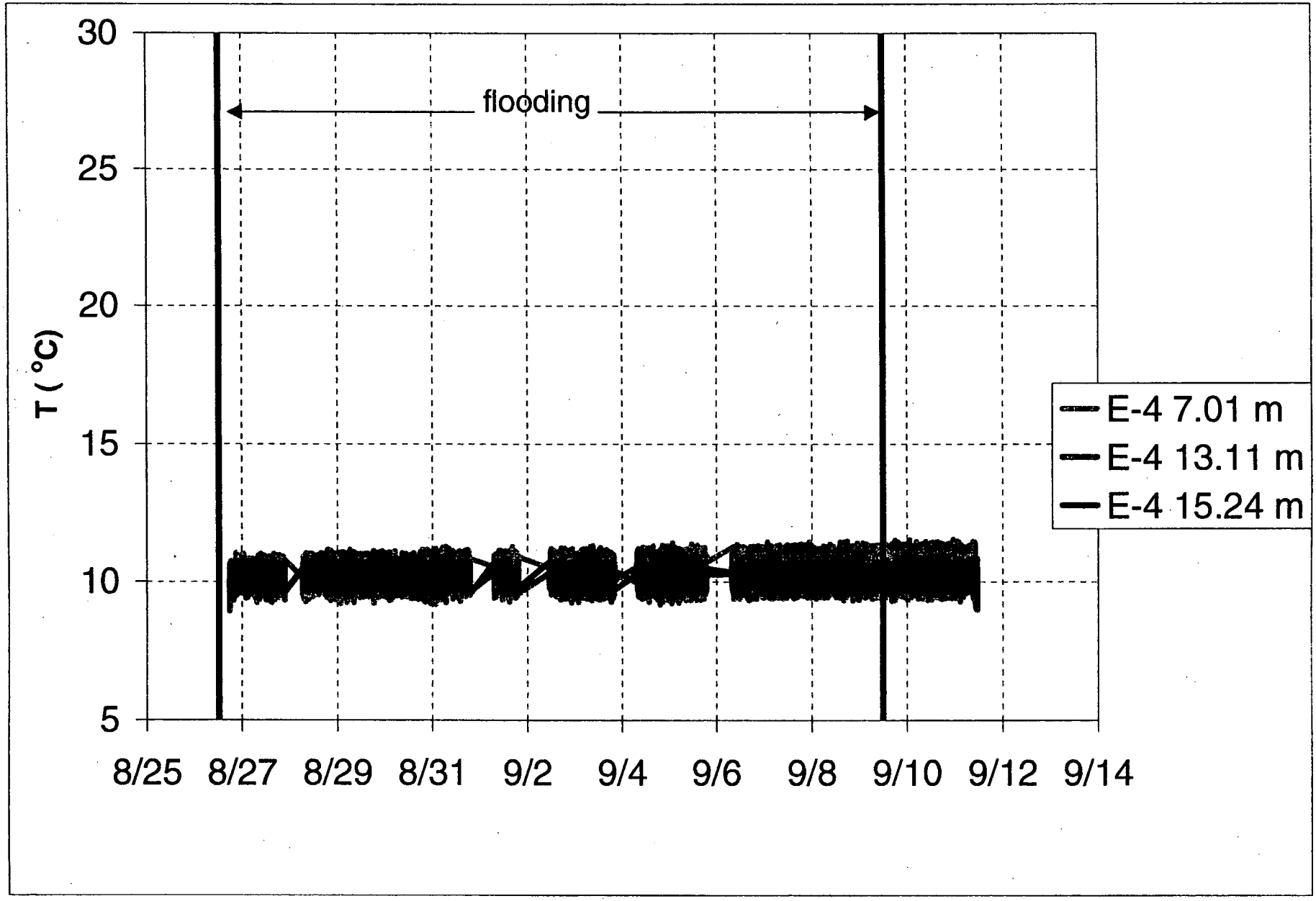

Figure II.5-10. Time trend of temperature in well E-4

Table II.6-1. Flow Rate Calculated for Individual Infiltrometers and the Entire Pond on September 2nd-4th.
(see Figure 1.7.8.1 for Infiltrometer Locations.)

Infiltrometer Number	Average Flow Rate (m/day)
1	0.033
2	0.036
3	0.032
4	0.004
5	0.017
6	0.024
7	0.033
8	0.024
9	0.018
Pond	0.031

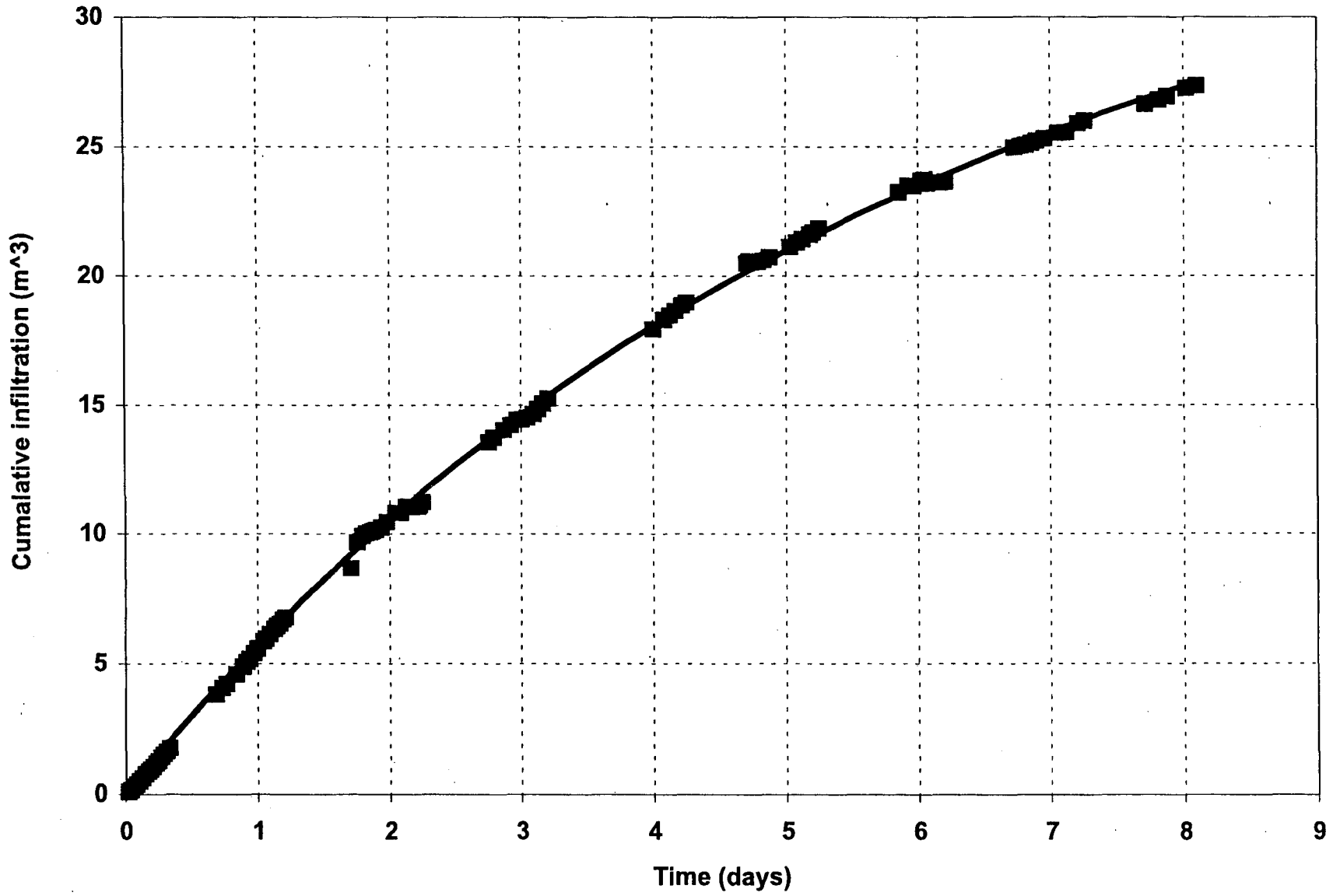

Figure II.6-1. Time trend of cumulative water flux during the infiltration test in the pond

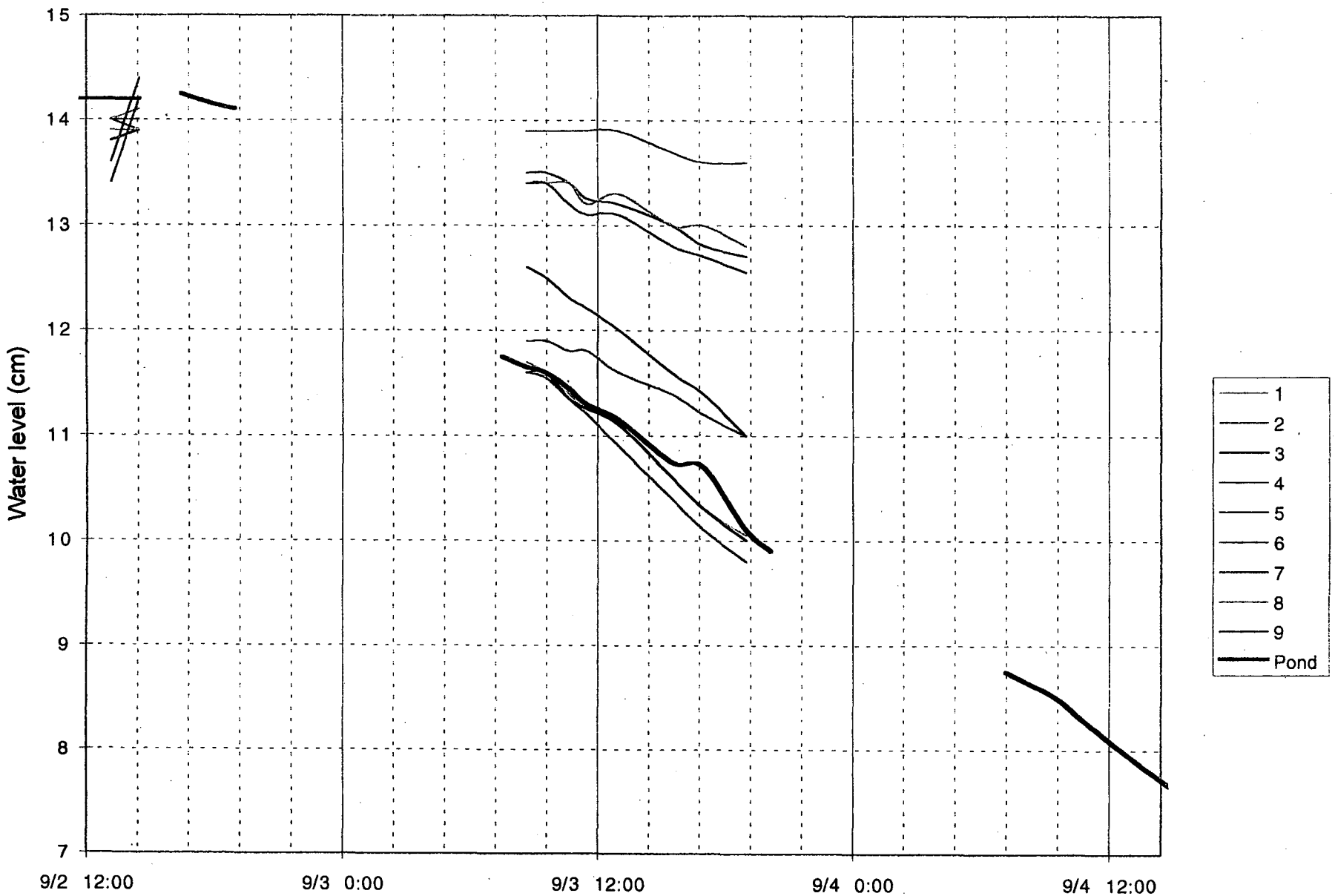

Figure II.6-2. Water level in infiltrometers within the pond when the water supply was terminated

II.7. TDR Data

II.7.1. Shallow TDR Data

Dielectric values were measured near the surface using the TDR technique outlined in Section I.7.10. Table II.7.1-1 shows the response times of the various probes to wetting. Figures II.7.1-1 through II.7.1-3 summarize the dielectric values measured before, during, and after the ponding event.

Pre-ponding dielectric values ranged between 1.3 and 9.1. Dielectric values between 1-5 suggest that probes installed in boreholes are most likely in the immediate vicinity of the polyurethane back fill material (polyurethane, $K_a \sim 2.5$), or partially or fully exposed to air ($K_a \sim 1.2$-2.0). Probes with pre-ponding dielectric values between 5 and 9 are most likely in direct connection with porous basalt. Probes A and G, located in surface fractures, are most likely in the vicinity of dense basalt rock (i.e. narrow fractures with dense basalt walls), as suggested by $K_a \sim 6.9$-9.1.

There were four distinct patterns of response to the ponding event:

1. Abrupt rise in K_a followed by constant values, (probe A)
2. Abrupt rise in K_a followed by a slight continuous rise, (probes B and C)
3. Steady continuous rise in K_a, (probes D, E and F)
4. Abrupt rise in K_a followed by continuous drop, (probe G)

Eight of the eleven probes in the pond responded within minutes to ponding, with the remaining three showing changes in the dielectric value in a little over one hour. The four probes outside the ponded area responded between 1.5 to 11 hours later. Relatively small increases in dielectric value (i.e., <10) were observed at three locations outside the pond, and four within the pond. In the remaining locations, most increases in dielectric value were between 10-20, with two locations recording increases greater than 30. The time to reach maximum saturation ranged from 3-245 hours, with only three probes reaching maximum values in less than 200 hours. Two probes (E and G) began to record decreasing dielectric values before the pond was drained.

There were three distinct patterns of response to drainage of the pond:

1. Steady decrease in Ka towards pre-ponding values, (probe F)
2. Abrupt decrease in Ka towards pre-ponding values, (probes B and C)
3. Continuous steady increase in Ka, (probe D).

The first response (i.e., drop in dielectric value) to the removal of ponded water was seen only after 6 hours, mostly in locations close to the surface. Generally, probes in the boreholes began to respond 24-112 hours later. All locations in which drying was

Table II.7.1-1. Time to Wetting and Drying Determined from TDR Probes

			Dielectric value	Dielectric value	Dielectric value	% Change in dielectric	PROBE RESPONSE TO WETTING[2]		PROBE RESPONSE TO DRYING[3]	
Probe	Location	Depth (m)	pre-ponding	ponding	post-ponding	POST-PRE PONDING	Time to first response[4]	Time to max. wetting	Time to first response	Time to max. drying
A	Fracture[1]	0.00	6.9	26.0	7.4	10	1:27	244:22	6:34	150:34
B	Bore-hole (T-9)	0.61	2.3	17.3	5.1	130	0:08	235:34	72:34	69:34
C	Bore-hole (T-6)	0.30	1.9	17.9	3.2	74	1:10	236:36	24:36	30:36
D	Bore-hole (T-5)	0.61	2.0	4.9	4.8	158	0:30	234:36	No drying	
E	Bore-hole (T-4)[1]	0.36	2.1	6.5	4.0	96	5:31	159:39	Before t_0	144:37
F	Bore-hole (T-2)[1]	0.41	2.3	7.7	5.1	130	11:11	233:57	6:37	147:37
G	Fracture	0.00	9.1	27.0	21.9	155	0:01	2:51	Before t_0	150:37
H	Rock matrix	0.00	5.7	35.9	5.4	2	Measurement error	-	6:34	144:33
I	Rock matrix	0.00	6.0	12.8	8.5	46	0:17	238:23	9:34	27:34
J	Fracture	0.00	7.8	15.9	12.3	63	0:18	236:53	No drying	
K	Bore-hole (T-9)	0.61	2.6	20.2	6.1	142	0:08	234:44	72:34	69:34
L	Bore-hole (T-8)	0.61	1.6	6.8	4.6	213	1:38	242:34	11:30	318:35
M	Bore-hole (T-3)[1]	0.61	3.6	13.9	6.1	91	2:39	240:55	78:35	126:35
N	Bore-hole (T-5)	0.61	2.4	4.4	4.3	79	0:29	186:00	No drying	
O	Bore-hole (T-8)	0.61	2.9	15.3	7.7	178	1:19	235:15	111:36	117:36
P	Bore-hole (T-7)	0.43	1.3	59.2	7.0	447	0:10	235:26	27:36	162:36

[1] Located outside pond
[2] Here t_0 is time at which pond was filled (8/27/96 12:50 pm)
[3] Here t_0 is time at which pond was completely drained(9/9/96 1:00 pm)
[4] All times are in hours and minutes

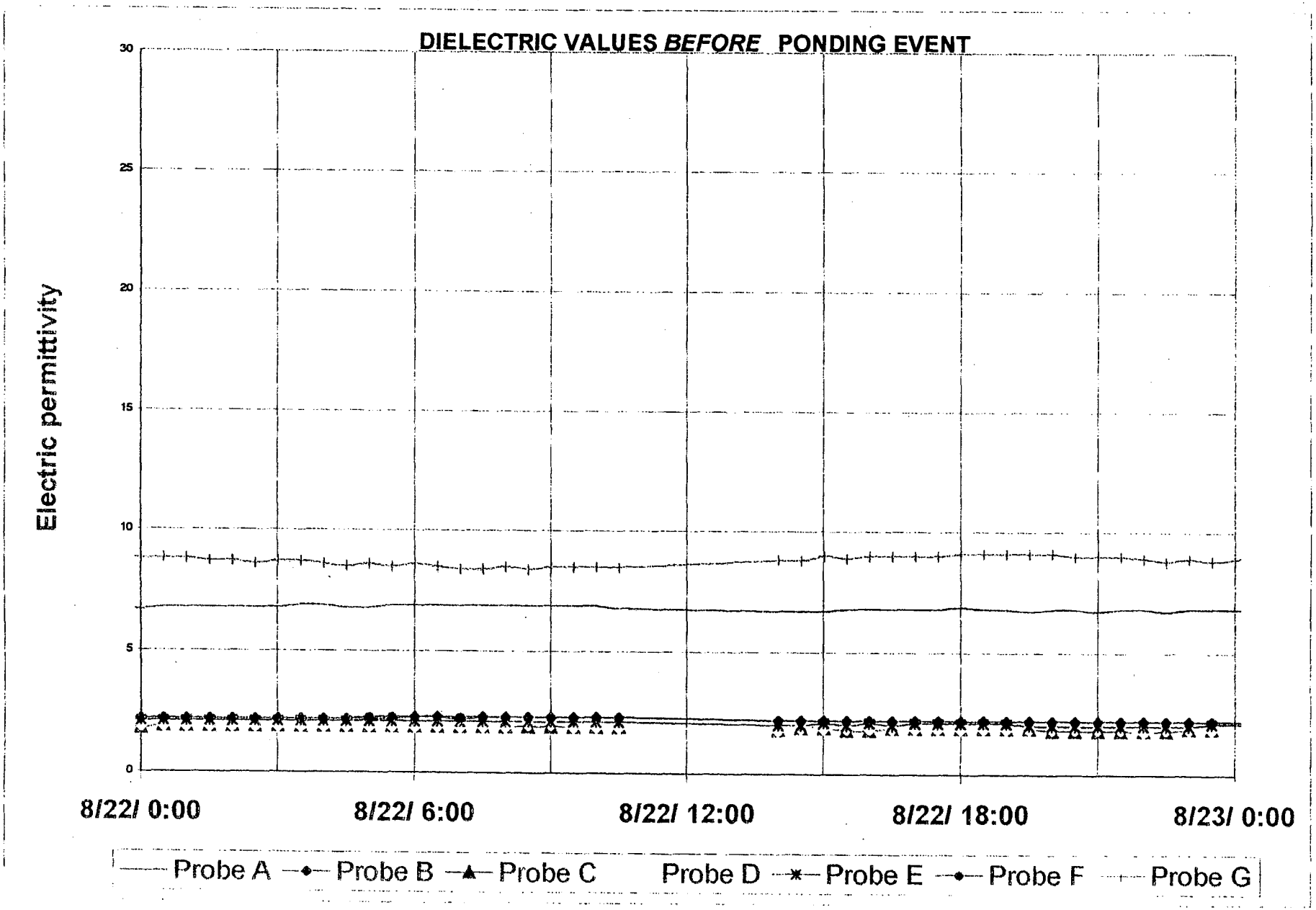

Figure II.7.1-1. Dielectric values before the ponding event

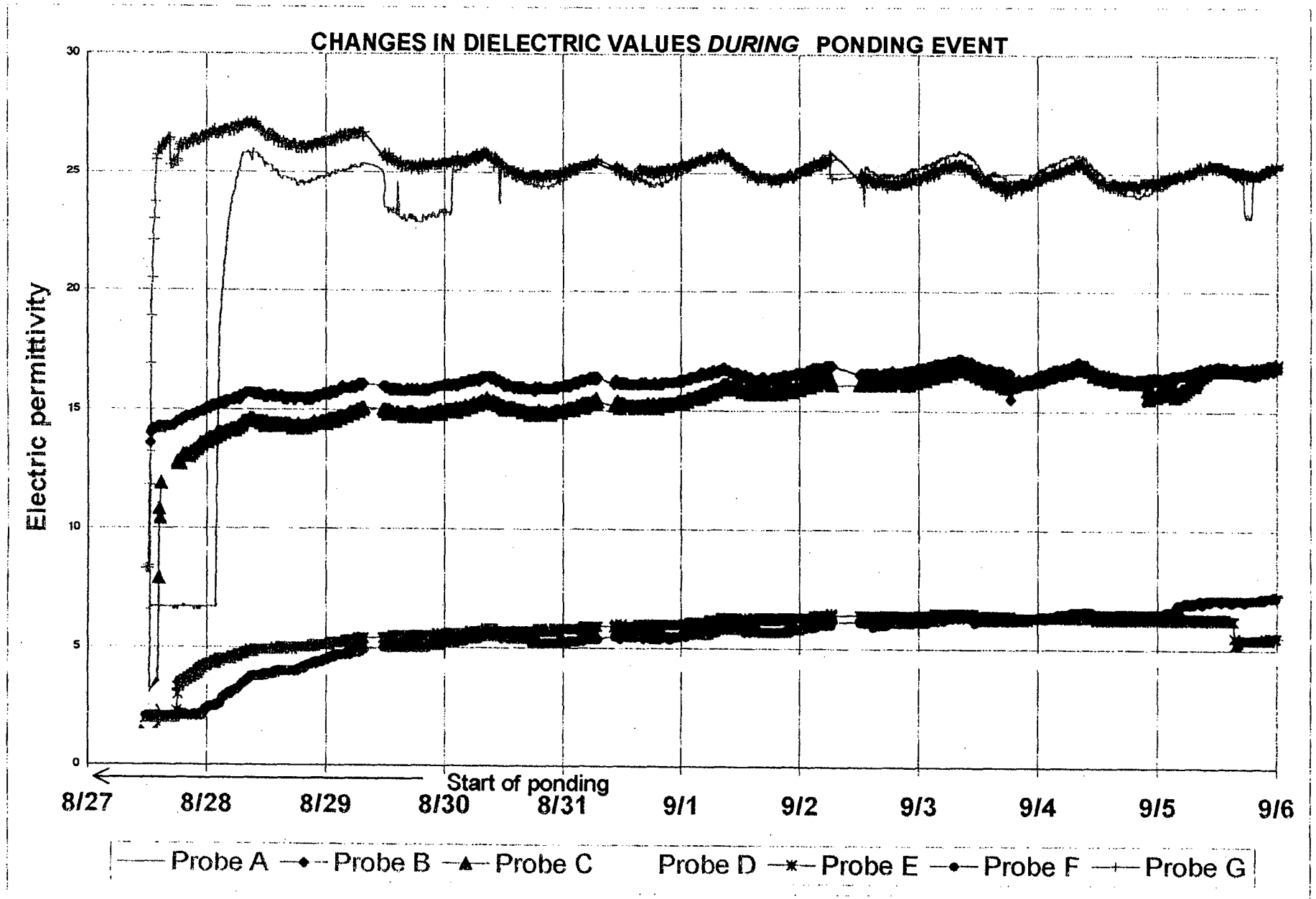

Figure II.7.1-2. Dielectric values during the ponding event

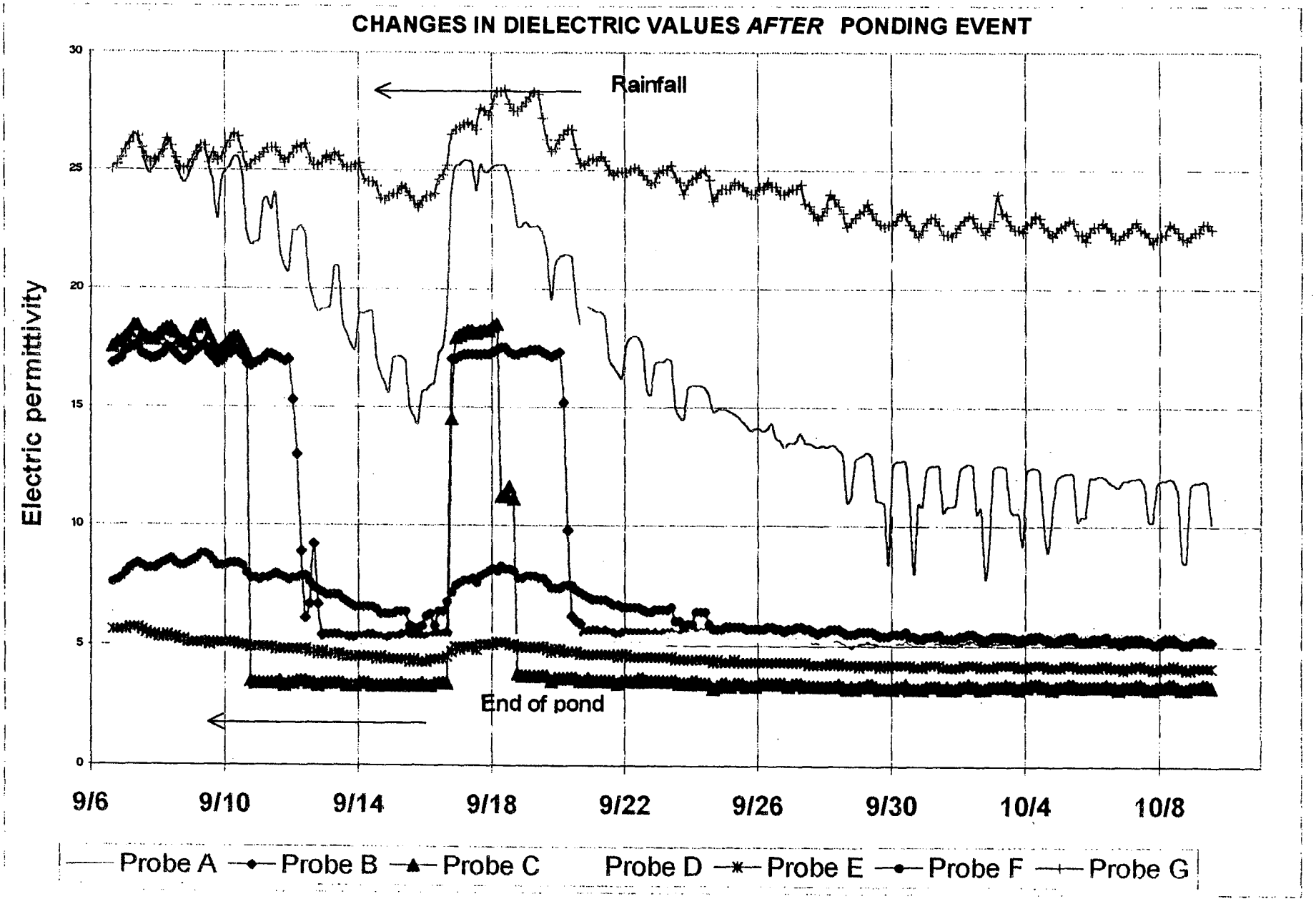

Figure II.7.1-3. Dielectric values after the ponding event

evident, reached constant dielectric values which were 2-447% greater than the pre-ponding levels. The time taken to reach these near constant values ranged between 30-318 hours.

A rainfall event (between 9/12/96 and 9/14/96), was detected in most locations where the pattern of changes in the dielectric value mimicked the response observed at the start of ponding. One location (probe J) that did not show a drying trend following the end of ponding had further increases in dielectric values after the rains. In another (probe N) the dielectric value continued to increase steadily with no visible response to the rainfall event.

All TDR measurements showed diurnal fluctuations in dielectric values coinciding with temperature changes. Diurnal changes of the dielectric value can be described using the equation for pure water (Handbook of Chemistry and Physics, 1974):

$$K_{water} = 78.14[1-4.579*10^{-3}(t_0-25) + 1.19*10^{-5}(t_0-25)^2 - 2.8*10^{-8}(t_0-25)^3]$$

When this equation is applied to determine dielectric changes for measured temperature changes at the pond surface and at a depth of 0.30 m, the fluctuations are observed to be similar to those observed during the ponding experiment.

- The pattern of changes in dielectric values in response to ponding suggests that wetting and drying of the near-surface is extremely variable in the vicinity of the pond.

- The variability in the time to first change in dielectric value immediately following ponding in locations within the pond indicates that migration of the wetting front is not uniform.

- Changes in dielectric values in locations outside the pond suggest that there is a lateral component to flow in the subsurface.

- A nearly similar time to maximum wetting (i.e. ~ 240 minutes) in 12 of the 16 locations suggests that most of the near surface profile reaches a maximum level of wetness. However, levels of saturation vary significantly within the profile (as suggested by the range of K_a values). Thus, for a given boundary condition, there appears to be a "system saturation level", with various components of the formation showing different degrees of maximum wetting.

- The variability in the time to first detection of drying was much larger than that observed for the time to first wetting (i.e., between 6-112 hours). However, locations that began to dry first did not dry out the fastest.

- 25 days after the last precipitation event, portions of the profile were still significantly wetter than at the start of ponding.

II.7.2. Deep Borehole TDR Data

The results of TDR measurements are shown in Figure II.7.2-1 for well I-1 where it appears that TDR probes at 0.3, 1.5 and 3 m (1, 5, 10 ft) depths responded to the infiltration event. Based on the TDR data, it appears that 17 borehole TDR probes responded to the infiltration event. The well names and depths where a response appeared to have taken place are presented in Table II.7.2-1.

The borehole TDR produced a substantial number of negative water contents, which is physically impossible. One explanation is that the use of round wires to form the wave guides allowed the geometry of the waveguides to change over time. When they were pressed in contact with rock surfaces, stresses would relax. These changes in geometry could create a moving calibration curve. The presence of fractures, large void spaces, or incomplete contact along the waveguide could also serve to underestimate the dielectric value of moist basalt and lead to underestimation of water content. But the major problem was in interpreting the waveforms echoed back from the waveguides. The waveform changed with water content, and field technicians noted that the points used to estimate the start of the waveguide changed and were difficult to locate consistently. This problem resulted in the water contents of basalt appearing to jump from low to high values and from high to low values. The data were smoothed using a 3 point moving average because they too noisy to allow consistent interpretation.

II.8. Groundwater Level Measurements

The results of the groundwater level measurements are summarized in Figure II.8-1. It should be noted that before the test, all wells, except well R-3, were dry. The saturation of well I-5 most likely happened due to the leakage through the berm of the pond. In well II-7, it was noted that there was seepage at the depth of 11 m (36 ft) where the rubble zone was located.

III. Summary

In FY96, INEEL and LBNL (jointly with McCabe Bros., Inc.) tested several types of new polyurethane sealants to complete vertical and slanted boreholes at the Box Canyon site and Idaho Research Center (IRC) in Idaho Falls. This material was be used to inflate packers to which probes were attached, and to back-fill the rest of the borehole between packers. Testing of the polyurethane resin on Idaho soils and basalts indicated that the material had the following attributes: (1) it adhered well to dry and wet soils and basalts; (2) penetration into fractures was minimal because the set time could be regulated; (3) electrical properties were similar to those of dry sand and had little or no effect on radar and TDR measurements; (4) it could easily be injected through a small diameter tube to infill the annular space in its liquid state; (5) unlike bentonite and cement, it did not

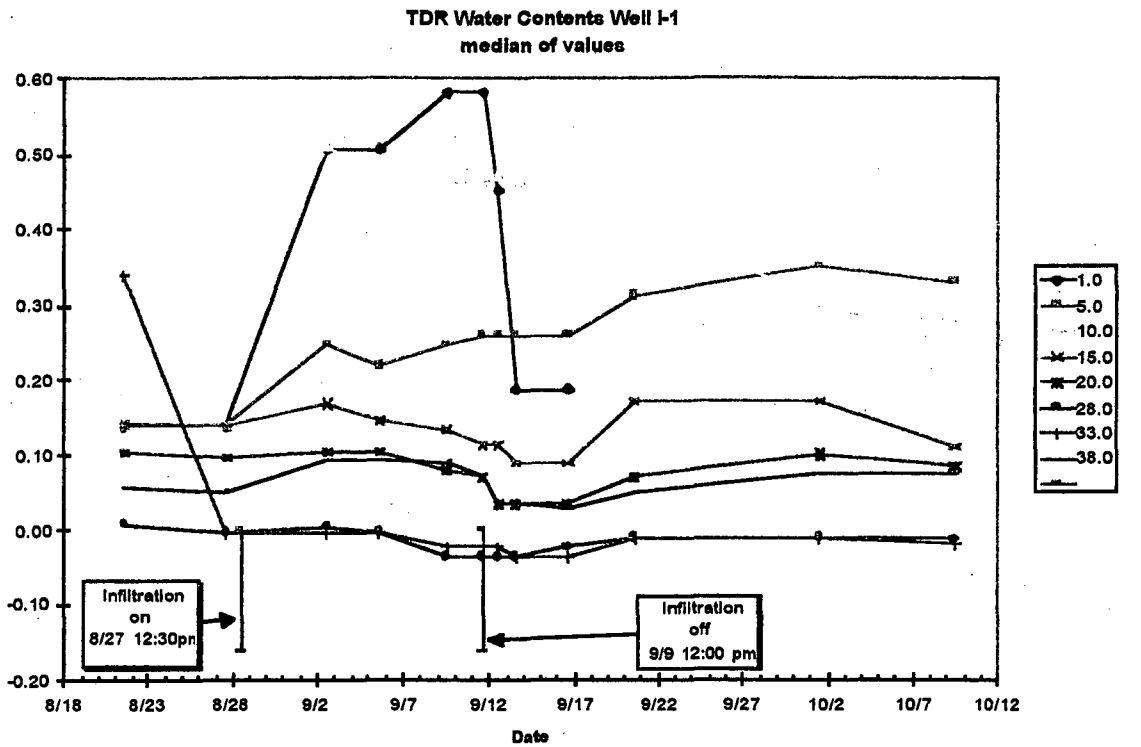

Figure II.7.2 - 1. Water contents in well I-1 estimated using borehole TDR probes.

Table II.7.2-1. Depths where TDR Probes Responded to the Infiltration Test

Well	Depths in feet.
I-1	1, 5, and 10
I-2	28
I-3	none
T-2	1.7, and 5
T-3	1.5
T-4	5.3, 13.3, and 18.8
T-5	none
T-6	5.6
T-7	1.5
T-8	1
T-9	1, 5, and 10
E-1	none
E-2	none
E-3	29
E-4	none
TOTAL NUMBER RESPONDING	***17***

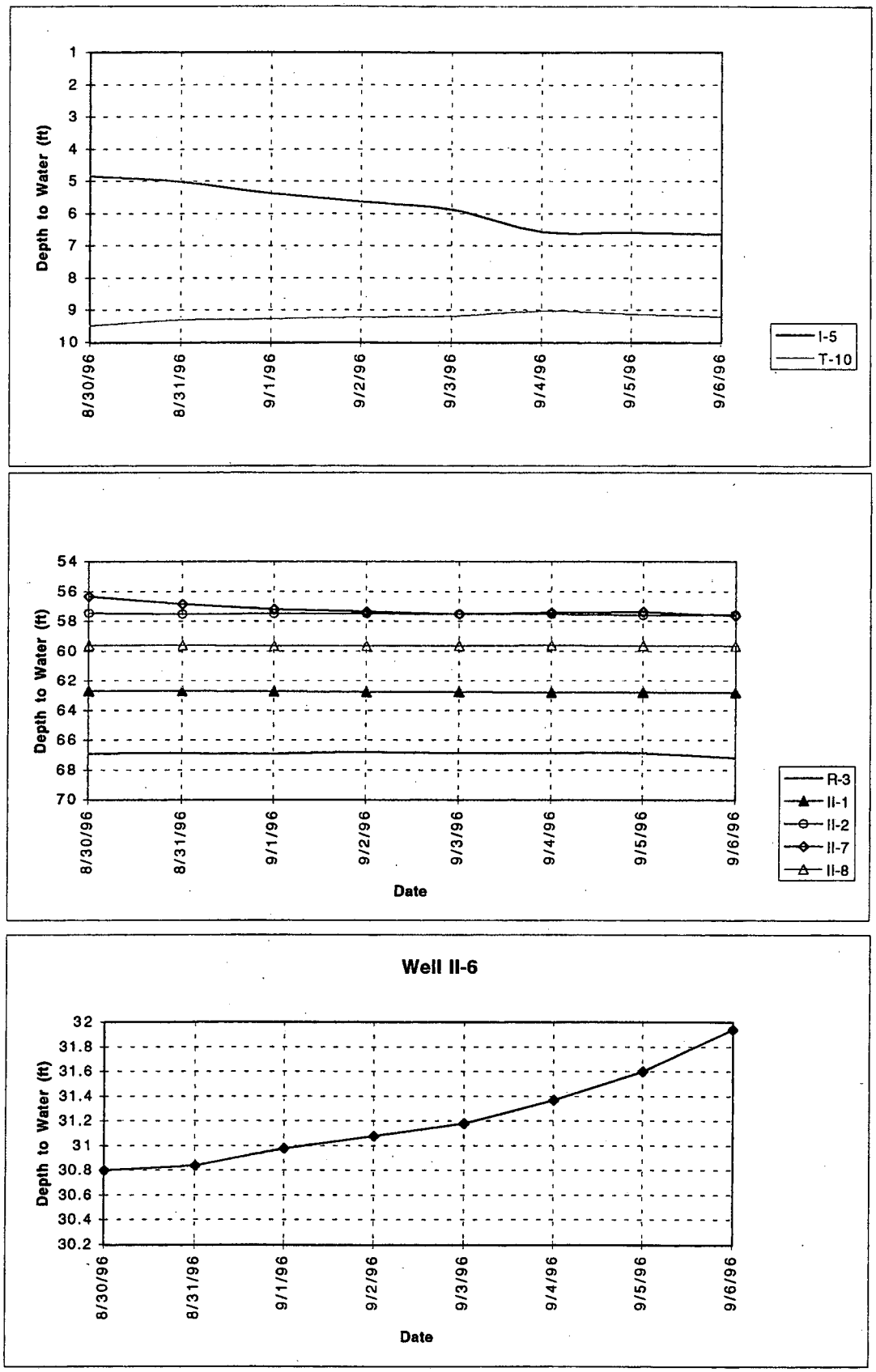

Figure II.8-1. Groundwater levels in the monitoring wells during the infiltration test

affect the moisture content of surrounding soils and basalts; (6) it could be used to back-fill and seal boreholes both below and above the water table; and (7) it had a very low bulk density, which is favorable for neutron logging. This material showed great promise for enabling the rapid, cost-effective installation of sensors and probes in fractured rock. This material showed great promise for enabling the rapid, cost-effective installation of sensors and probes in fractured rock.

A 7 x 8 m (23 x 26 ft) artificial pond was created by bounding the area with a 0.5 m (1.6 ft) tall two-layered berm which was intended to be impermeable to water. The outer layer, made of bags filled with crushed basalt and injected with polyurethane, served as a mechanical barrier. The inner layer, made of polyurethane sheltered by a plastic cover, created a hydraulic barrier to water in the pond. The barrier leaked substantially early in the test, but repairs made during the test resulted in a water-tight pond later in the test.

Eight 3-6 m (10-20 ft) deep vertical wells and four 18.3-21.3 m (60-70 ft) long slanted wells drilled in 1996, and four slanted wells and four vertical wells drilled in 1995, were instrumented with the following:

- Tensiometers - to measure moisture potential
- Air-pressure tubes - to measure air pressure
- Thermistors - to measure temperature
- ER probes - to determine the appearance of water and electrolyte during the tracer test
- Flow meters - to determine water flux
- TDR probes - to determine moisture content
- Suction lysimeters - to collect water samples from rocks

The water supply system consisted of a main water tank (1500 gal), which supplied water to the entire pond, a digital total-flow-rate meter, an electronic flow-rate meter, and a float used to maintain a constant water level in the pond. The water supply system also included nine water tanks used to supply water in nine 25.4 cm (10 in) diameter infiltrometers installed at the land surface at different locations within the pond. During the test, a practically constant water level was maintained within the entire pond (including infiltrometers) for two weeks, from 8/27/96 to 9/9/96. Because of the varying surface topography within the pond, the water depth varied with location within the pond , but the average water depth was 22.4 cm.

The DAS consisted of two units. The first unit was operated by a LABVIEW program, and it was designed to record signals (voltage, current, and resistance) and had the capacity to monitor 440 sensors in real time. Tensiometers and piezometers were connected to the DAS through pressure transducers in which pressure changes were measured every 6 minutes as voltage changes. Flow rates were also measured as voltage

output at this time interval. Temperature readings were collected as measurements of resistance of thermistors. ER probes operated by a separate program allowed us to measure both the voltage and current every 12 minutes.

The second unit of the DAS was comprised of a TRACE TDR system that was coupled with a multiplexer to allow up to 16 separate TDR probes to be measured every 10 minutes. The rigid-waveguide probes (manufactured by Soil Moisture, Inc., Santa Barbara, CA) were used to determine the moisture content of soils and rocks.

In addition to the instruments connected to the DAS, we also used a neutron logging probe (CPN) with a 50 mCi source to determine moisture content, which weused in three vertical and four slanted boreholes. These boreholes were cased using acrylic pipes, and the annular space was sealed with polyurethane. This design was pre-tested under laboratory conditions.

A slug of potassium bromide tracer was added to the pond on 9/2/96, yielding a tracer concentration in the pond of approximately 3 g/l. The movement of the tracer was monitored with ER probes and by collecting water samples. At this low concentration, the tracer was not expected to affect radar data.

In order to evaluate drain-out conditions, monitoring continued for three weeks after the test.

In analysis of the data obtained using single probes (tensiometers, suction lysimeters, etc.), we realized that all probes used give volume averaging data that may change over time. We observed two types of initial saturation with tensiometers: (1) Rapid saturation, which occurred in: (a) the top soil-rock layer down to 0.3-0.6 m (1-2 ft) at the beginning of the infiltration test as measured in all tensiometers installed throughout the site, and (b) in well T-9 at 0.3, 1.5 and 2.7 m (1, 5, and 9 ft); and (2) gradual saturation, which was observed at different locations. We have obtained evidence of preferential flow when deeper probes saturated earlier than upper ones. For example, in wells T-5 and T-8, the initial saturation was observed at 2.7-3 m (9-10 ft), while probes at 1.5 m (5 ft) remained dry.

Note that in some tensiometers, after a period of stable water pressure during infiltration, the desaturation of some fractures was observed despite that the infiltration was still occurring. Most likely, the water supply to these depths decreased over time. Two types of desaturation during the test were observed: (1) rapid desaturation like that in well T-8 at 2.7 m (9 ft) depth, and (2) progressive desaturation like that in well T-8 at 1.5 m (5 ft) depth.

One of the main points of interest in the data analysis was the fundamental issue of measurements of water pressure in fractured rocks using tensiometers. We analyzed

the time and depth variations of the water pressure before and during the infiltration test. It was determined that diurnal fluctuations of the water pressure measured with air-pocket tensiometers were affected primarily by ambient temperature fluctuations, and the magnitude and pattern of these fluctuations depend upon the saturation and permeability of rocks. It became apparent that the pattern of the diurnal changes in the water pressure is particularly useful in the characterization of saturation and relative permeability of rocks, as well as the water arrival time at different depths.

Sampling of water from rocks began before the infiltration test. Since the rocks were relatively wet in background conditions, we were able to collect water samples from 24% of suction lysimeters before the infiltration test. During the infiltration test, 62% of suction lysimeters produced water that was collected for analytical analysis. The ER probes showed that in general the electrical resistivity of pore solution is decreased with depth. During the tracer test, the tracer movement was monitored using water sampling with suction lysimeters and measurements of the voltage and current with a new design of miniature ER probes. The tracer data confirmed that it was a delay in the downward tracer movement along with infiltrating water in the top soil-rock layer in comparison with a rapid initial saturation of the top soil layer at the beginning of the test. The test showed the ER probes are a robust field technique for continuous monitoring of the tracer distribution. ER probe measurements of the voltage and current along with the calculations of the electrical resistance confirmed that the tracer appeared in the fracture zones and rubble zones, while it was not detected by ER probes located in contact with low permeable basalt and single non-conductive fractures. In addition, a comparison of the ER probe data with the lithological data showed that the decrease in the electrical resistance of the pore solution is most likely to be associated with liquid movement along conductive fractures and fracture zones saturated with electrolyte. The main difference in the performance of the suction lysimeters and ER probes is that the suction lysimeters are able to withdraw water from surrounding rocks and fractures (a volume affected is, indeed, unknown in fracture rocks) around a porous tip of the lysimeter, while the ER probes are able to respond when the electrolyte concentration was changed in the near vicinity of the probe.

IV. References

Faybishenko, B., P. Holland, M. Mesa, D. Burgess, C. Knutson, and B. Sisson, Lithological conditions at Box Canyon site: results of drilling, coring, and open borehole measurements, 1995-1997 data report, Lawrence Berkeley National Laboratory, LBNL-40182, September, 1998.

Long, J.C.S., C. Doughty, B. Faybishenko, A. Aydin, B. Freifeld, K. Grossenbacher, P. Holland, J. Horsman, J. Jacobsen, T. Johnson, K. Lee, J. Lore, K. Nihei, J. Peterson, R. Salve, J. Sisson, B. Thapa, D. Vasco, K. Williams, T. Wood, and P. Zawislanski, Analog site for fractured rock characterization: annual report FY 1995, Lawrence Berkeley National Laboratory, LBNL-38095, October, 1995.

Maheshwarla, S.V., R. Venkatasubramanian, and R.F. Boehm, Comparison of time domain reflectrometry performance factors for several dielectric geometries: Theory and experiments, Water Resour. Res., 31(8) ,1927-1933, 1995.

Peterson, J.E. Jr. and K.H. Williams, Ground penetrating radar results at the Box Canyon site: 1996 survey as part of infiltration test, Lawrence Berkeley National Laboratory, LBNL-40915, August, 1997.

Selker, J.S., L. Graff, and T. Steenhuis, Noninvasive time domain reflectrometry moisture measurement probe, SSSAJ, 57:934-936, 1993.

Topp, G.C., J.L. Davis, and A.P. Annan, Electromagnetic determination of soil water content: Measurements in coaxial transmission lines, Water Resour. Res., 16, 1573-1584, 1980.

Attachments

A.1. Calibration of Pressure Transducers Used in Shallow Tensiometers

There were 120 pressure transducers initially identified for use in the Idaho Project. Each transducer was calibrated against a previously calibrated transducer over a range of pressures anticipated in the field. Further, a temperature check was done on the transducers to test the manufacturers claim that these transducers were temperature compensated.

Pressure transducers were calibrated in batches of ten. The transducers were connected to a manifold, along with a reference pre-calibrated transducer. The manifold was connected to an air-tank fitted with a vacuum pump (Figure A.1-1).

The voltage output associated with pressures ranging from 1-14.5 psi was documented for each of the transducers. A linear regression was used to determine the calibration constants (slope and intercept).

To test for temperature effects, transducers attached to the manifold were subjected to a fixed pressure, and then the temperature around the transducers was increased, while the voltage output was recorded at intervals of a few minutes.

The calibration coefficients determined for the transducers are summarized in Table A.1-1. Included in this table is the voltage output corresponding to the applied absolute pressure. For all 120 transducers, the slope describing the relationship between voltage output and the corresponding absolute pressure was found have an R^2 value of 1.0. The transducers did not appear to show any responses which could be linked to changes in temperature.

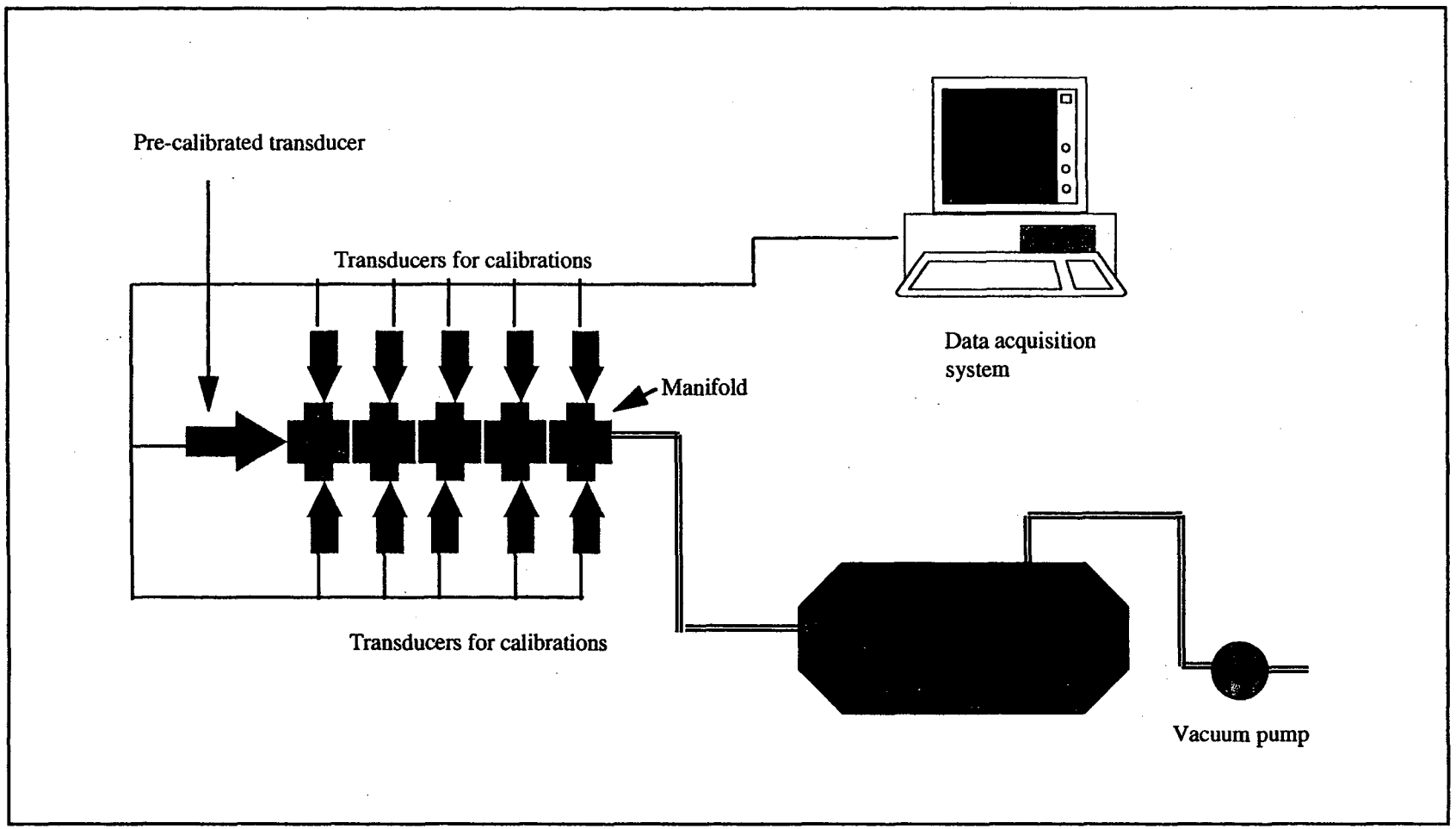

Figure A.1.1-1. Calibration layout fro pressure transducers

Table A.1-1. Calibration Data for Transducers

	PRESSURE (m)	VOLTAGE OUTPUT IN TRANSDUCERS BEING CALIBRATED									
Transducer ID	Reference Transducer	PT-1	PT-2	PT-3	PT-4	PT-11	PT-6	PT-7	PT-8	PT-9	PT-10
	1.11	0.96	0.94	0.96	0.96	0.95	0.95	0.97	0.95	0.95	0.97
	3.10	1.71	1.70	1.71	1.72	1.71	1.71	1.72	1.70	1.71	1.73
	5.15	2.50	2.49	2.49	2.51	2.50	2.50	2.50	2.48	2.49	2.51
	6.16	2.88	2.87	2.88	2.89	2.88	2.88	2.88	2.87	2.88	2.89
	8.17	3.64	3.63	3.64	3.65	3.64	3.65	3.64	3.64	3.64	3.65
	9.97	4.33	4.32	4.32	4.33	4.33	4.34	4.33	4.33	4.33	4.33
Slope		2.63	2.63	2.63	2.63	2.62	2.61	2.64	2.62	2.62	2.64
Intercept		-1.40	-1.38	-1.42	-1.44	-1.39	-1.38	-1.43	-1.37	-1.38	-1.46
R-Squared		1.00	1.00	1.00	1.00	1.00	1.00	1.00	1.00	1.00	1.00
Transducer ID	Reference Transducer	PT-5	PT-12	PT-13	PT-14	PT-15	PT-16	PT-17	PT-18	PT-19	PT-20
	1.44	1.08	1.10	1.08	1.09	1.09	1.08	1.10	1.09	1.08	1.11
	2.90	1.64	1.65	1.63	1.64	1.65	1.64	1.66	1.64	1.64	1.65
	4.64	2.31	2.32	2.29	2.30	2.31	2.31	2.31	2.30	2.31	2.31
	6.25	2.92	2.93	2.90	2.91	2.92	2.93	2.92	2.92	2.93	2.92
	8.01	3.59	3.59	3.57	3.58	3.59	3.59	3.59	3.59	3.60	3.59
	9.82	4.28	4.28	4.25	4.28	4.29	4.28	4.27	4.28	4.28	4.29
Slope		2.63	2.63	2.64	2.63	2.62	2.62	2.64	2.62	2.61	2.63
Intercept		-1.41	-1.45	-1.40	-1.43	-1.42	-1.39	-1.48	-1.40	-1.38	-1.45
R-Squared		1.00	1.00	1.00	1.00	1.00	1.00	1.00	1.00	1.00	1.00
Transducer ID	Reference Transducer	PT-21	PT-22	PT-23	PT-24	PT-25	PT-26	PT-27	PT-28	PT-29	PT-30
	1.24	1.01	1.01	1.01	1.01	0.99	1.00	1.00	1.01	1.02	1.01
	2.88	1.63	1.64	1.64	1.64	1.62	1.62	1.63	1.64	1.64	1.64
	4.54	2.27	2.27	2.27	2.27	2.25	2.25	2.27	2.27	2.27	2.27
	6.34	2.95	2.96	2.96	2.95	2.94	2.93	2.95	2.96	2.95	2.95
	8.14	3.64	3.65	3.65	3.63	3.63	3.62	3.64	3.65	3.63	3.64
	9.99	4.35	4.35	4.36	4.33	4.34	4.33	4.34	4.36	4.34	4.34
Slope		2.61	2.62	2.62	2.63	2.61	2.63	2.63	2.62	2.64	2.63
Intercept		-1.39	-1.42	-1.42	-1.43	-1.34	-1.38	-1.41	-1.41	-1.44	-1.42
R-Squared		1.00	1.00	1.00	1.00	1.00	1.00	1.00	1.00	1.00	1.00
Transducer ID	Reference Transducer	PT-31	PT-32	PT-33	PT-34	PT-35	PT-36	PT-37	PT-38	PT-39	PT-40
	1.20	0.99	0.99	1.00	0.99	0.99	1.00	0.97	0.99	0.99	1.00
	3.09	1.70	1.72	1.72	1.71	1.72	1.72	1.69	1.72	1.72	1.72
	4.66	2.30	2.32	2.32	2.31	2.33	2.33	2.30	2.32	2.32	2.31
	6.35	2.94	2.96	2.96	2.96	2.98	2.97	2.95	2.97	2.97	2.95
	8.00	3.58	3.59	3.59	3.60	3.60	3.60	3.58	3.60	3.60	3.58
	9.99	4.34	4.34	4.35	4.36	4.35	4.36	4.34	4.35	4.35	4.34
Slope		2.62	2.63	2.62	2.61	2.61	2.62	2.61	2.62	2.62	2.63
Intercept		-1.37	-1.43	-1.42	-1.39	-1.41	-1.43	-1.33	-1.40	-1.42	-1.43
R-Squared		1.00	1.00	1.00	1.00	1.00	1.00	1.00	1.00	1.00	1.00
Transducer ID	Reference Transducer	PT-41	PT-42	PT-43	PT-44	PT-45	PT-46	PT-47	PT-48	PT-49	PT-50
	1.00	0.91	0.91	0.92	0.91	0.90	0.92	0.89	0.91	0.91	0.92
	3.02	1.67	1.69	1.69	1.68	1.69	1.70	1.66	1.69	1.69	1.69
	4.57	2.26	2.29	2.28	2.28	2.29	2.29	2.26	2.29	2.29	2.28
	6.59	3.03	3.05	3.05	3.05	3.07	3.06	3.03	3.06	3.06	3.04
	8.03	3.58	3.60	3.60	3.60	3.61	3.61	3.59	3.61	3.61	3.59
	9.99	4.34	4.34	4.35	4.36	4.35	4.36	4.34	4.35	4.35	4.34
Slope		2.62	2.63	2.62	2.61	2.61	2.62	2.60	2.61	2.62	2.63
Intercept		-1.37	-1.42	-1.41	-1.38	-1.39	-1.42	-1.31	-1.39	-1.41	-1.43
R-Squared		1.00	1.00	1.00	1.00	1.00	1.00	1.00	1.00	1.00	1.00
Transducer ID	Reference Transducer	PT-51	PT-52	PT-53	PT-54	PT-55	PT-56	PT-57	PT-58	PT-59	PT-60
	1.13	0.98	0.95	0.99	1.02	0.97	0.93	0.96	0.98	0.98	0.94
	3.03	1.70	1.67	1.70	1.75	1.69	1.67	1.68	1.71	1.69	1.67
	4.61	2.29	2.28	2.30	2.35	2.30	2.28	2.28	2.32	2.29	2.28
	6.29	2.93	2.92	2.93	2.99	2.94	2.92	2.92	2.96	2.93	2.93
	8.06	3.60	3.59	3.61	3.66	3.61	3.60	3.59	3.63	3.61	3.60
	9.98	4.34	4.33	4.34	4.39	4.34	4.33	4.33	4.36	4.35	4.33
Slope		2.63	2.62	2.64	2.63	2.63	2.60	2.63	2.62	2.63	2.61
Intercept		-1.44	-1.35	-1.45	-1.57	-1.41	-1.30	-1.39	-1.45	-1.42	-1.33
R-Squared		1.00	1.00	1.00	1.00	1.00	1.00	1.00	1.00	1.00	1.00
Transducer ID	Reference Transducer	PT-61	PT-62	PT-63	PT-64	PT-65	PT-66	PT-67	PT-68	PT-69	PT-70
	1.45	1.10	1.08	1.08	1.10	1.09	1.09	1.08	1.08	1.09	1.10
	2.99	1.69	1.67	1.67	1.68	1.68	1.68	1.67	1.67	1.67	1.68
	4.66	2.33	2.32	2.31	2.32	2.32	2.32	2.31	2.31	2.31	2.32
	6.36	2.97	2.96	2.96	2.96	2.96	2.97	2.96	2.96	2.95	2.97
	8.05	3.61	3.61	3.60	3.61	3.60	3.61	3.61	3.61	3.60	3.62
	10.00	4.34	4.35	4.34	4.36	4.34	4.35	4.36	4.35	4.34	4.36
Slope		2.64	2.61	2.62	2.63	2.64	2.62	2.60	2.61	2.63	2.62
Intercept		-1.46	-1.38	-1.40	-1.44	-1.44	-1.42	-1.36	-1.38	-1.41	-1.43
R-Squared		1.00	1.00	1.00	1.00	1.00	1.00	1.00	1.00	1.00	1.00

Table A.1-1. Calibration Data for Transducers

	PRESSURE (m)	VOLTAGE OUTPUT IN TRANSDUCERS BEING CALIBRATED									
Transducer ID	Reference Transducer	PT-71	PT-72	PT-73	PT-74	PT-75	PT-76	PT-77	PT-78	PT-79	PT-80
	1.23	1.01	1.00	1.00	0.98	0.98	1.02	1.00	1.01	1.01	1.01
	3.10	1.72	1.71	1.72	1.70	1.70	1.72	1.71	1.72	1.72	1.72
	4.63	2.31	2.30	2.31	2.29	2.29	2.30	2.29	2.31	2.30	2.30
	6.31	2.94	2.94	2.95	2.93	2.93	2.94	2.93	2.95	2.94	2.94
	8.04	3.60	3.59	3.60	3.58	3.59	3.60	3.59	3.61	3.60	3.60
	9.99	4.33	4.33	4.33	4.32	4.33	4.35	4.34	4.35	4.35	4.35
Slope		2.64	2.63	2.63	2.62	2.62	2.63	2.62	2.62	2.62	2.63
Intercept		-1.44	-1.40	-1.43	-1.35	-1.35	-1.44	-1.39	-1.43	-1.41	-1.42
R-Squared		1.00	1.00	1.00	1.00	1.00	1.00	1.00	1.00	1.00	1.00
Transducer ID	Reference Transducer	PT-81	PT-82	PT-83	PT-84	PT-85	PT-86	PT-87	PT-88	PT-89	PT-90
	1.28	1.03	1.02	1.01	1.03	1.02	1.03	1.00	1.01	1.02	1.02
	3.00	1.67	1.67	1.67	1.68	1.68	1.68	1.65	1.67	1.68	1.67
	4.62	2.29	2.29	2.29	2.29	2.30	2.29	2.27	2.29	2.30	2.28
	6.50	3.00	3.00	3.01	3.00	3.01	3.01	2.98	3.01	3.01	3.00
	8.12	3.62	3.62	3.62	3.63	3.63	3.63	3.61	3.63	3.63	3.63
	10.00	4.34	4.34	4.34	4.34	4.34	4.35	4.33	4.34	4.35	4.35
Slope		2.63	2.62	2.62	2.63	2.63	2.63	2.62	2.62	2.62	2.62
Intercept		-1.41	-1.39	-1.37	-1.41	-1.41	-1.42	-1.32	-1.38	-1.41	-1.37
R-Squared		1.00	1.00	1.00	1.00	1.00	1.00	1.00	1.00	1.00	1.00
Transducer ID	Reference Transducer	PT-91	PT-92	PT-93	PT-94	PT-95	PT-96	PT-97	PT-98	PT-99	PT-100
	1.10	0.94	0.97	0.95	0.94	0.96	4.99	0.97	0.96	0.95	0.96
	3.02	1.68	1.69	1.68	1.68	1.69	4.99	1.69	1.70	1.69	1.69
	4.56	2.27	2.28	2.27	2.27	2.28	4.99	2.27	2.28	2.28	2.27
	6.41	2.97	2.97	2.97	2.98	2.98	4.99	2.97	2.99	2.99	2.97
	7.95	3.56	3.56	3.55	3.57	3.57	4.99	3.56	3.57	3.57	3.55
	10.00	4.34	4.34	4.33	4.35	4.34	4.99	4.35	4.36	4.34	4.34
Slope		2.62	2.64	2.63	2.61	2.63	4431.01	2.63	2.62	2.62	2.64
Intercept		-1.37	-1.45	-1.40	-1.36	-1.43	########	-1.43	-1.42	-1.41	-1.43
R-Squared		1.00	1.00	1.00	1.00	1.00	0.07	1.00	1.00	1.00	1.00
Transducer ID	Reference Transducer	PT-101	PT-102	PT-103	PT-104	PT-105	PT-106	PT-107	PT-108	PT-109	PT-110
	1.35	1.06	1.06	1.05	1.05	1.03	1.06	1.01	1.05	1.04	1.04
	3.01	1.68	1.69	1.68	1.68	1.67	1.70	1.66	1.68	1.68	1.67
	4.51	2.24	2.26	2.24	2.25	2.24	2.26	2.23	2.25	2.25	2.24
	6.41	2.96	2.98	2.96	2.97	2.97	2.99	2.96	2.97	2.98	2.97
	8.27	3.68	3.71	3.70	3.71	3.72	3.74	3.72	3.74	3.76	3.76
	10.00	4.34	4.35	4.34	4.34	4.36	4.36	4.32	4.33	4.35	4.35
Slope		2.63	2.62	2.62	2.62	2.59	2.61	2.59	2.61	2.59	2.59
Intercept		-1.41	-1.41	-1.39	-1.41	-1.31	-1.41	-1.29	-1.38	-1.33	-1.32
R-Squared		1.00	1.00	1.00	1.00	1.00	1.00	1.00	1.00	1.00	1.00
Transducer ID	Reference Transducer	PT-111	PT-112	PT-113	PT-114	PT-115	PT-116	PT-117	PT-118	PT-119	PT-120
	1.21	0.99	1.00	1.00	0.99	0.98	0.99	0.99	0.97	0.99	1.00
	2.99	1.67	1.69	1.68	1.67	1.67	1.67	1.67	1.65	1.67	1.67
	4.81	2.36	2.38	2.37	2.36	2.37	2.37	2.36	2.34	2.37	2.36
	6.55	3.01	3.04	3.04	3.02	3.03	3.04	3.02	3.01	3.03	3.02
	8.13	3.61	3.64	3.64	3.63	3.63	3.64	3.62	3.62	3.63	3.62
	9.99	4.32	4.34	4.36	4.34	4.33	4.35	4.32	4.33	4.34	4.34
Slope		2.64	2.63	2.62	2.62	2.62	2.61	2.64	2.61	2.62	2.63
Intercept		-1.41	-1.44	-1.40	-1.37	-1.39	-1.37	-1.42	-1.32	-1.39	-1.41
R-Squared		1.00	1.00	1.00	1.00	1.00	1.00	1.00	1.00	1.00	1.00
Transducer ID	Reference Transducer	PT-121	PT-122	PT-123	PT-124	PT-125	PT-116	PT-117	PT-118	PT-119	PT-120
	1.23	1.00	1.01	1.01	1.00	1.01	0.98	1.00	0.98	1.00	1.01
	3.14	1.73	1.73	1.73	1.72	1.73	1.72	1.73	1.71	1.73	1.73
	4.71	2.33	2.32	2.33	2.31	2.33	2.33	2.33	2.31	2.33	2.32
	6.27	2.92	2.92	2.93	2.91	2.92	2.93	2.92	2.91	2.92	2.91
	8.07	3.60	3.61	3.62	3.59	3.60	3.62	3.60	3.60	3.61	3.60
	9.99	4.33	4.34	4.35	4.32	4.33	4.35	4.32	4.33	4.34	4.33
Slope		2.64	2.63	2.62	2.64	2.64	2.60	2.64	2.61	2.62	2.63
Intercept		-1.42	-1.42	-1.41	-1.40	-1.45	-1.33	-1.43	-1.32	-1.40	-1.41
R-Squared		1.00	1.00	1.00	1.00	1.00	1.00	1.00	1.00	1.00	1.00

A.2. Testing the Design of Neutron Access Holes

Neutron logging requires an access hole through which the logging tool is lowered into the formation. There are several common designs for such access holes, depending on the application and nature of the formation. When using high neutron flux sources, such as the 1 to 2 Ci sources used in the oil-well logging industry, a large diameter borehole can be used. Neutron penetration distance is greater, and the tool need not be in close contact with the formation. Casing and borehole effects can be partly compensated for by using near and far detectors, or by using a gamma detector in addition to slow neutron detectors. In general, steel casing is used in the oil-well industry, and has little or no effect on neutron and gamma logging.

In environmental applications, wells are generally cased using PVC and occasionally steel. PVC is problematic for neutron logging because it has a very high chlorine content, which yields a very large capture cross section for neutrons. This greatly reduces the number of neutrons that arrive back at the detector. Steel was problematic in this field study because of the use of geophysical methods sensitive to metal (radar imaging). Therefore, an alternative casing material was needed.

The grouting of access boreholes is also of concern. Backfill material can significantly affect neutron counts, even if the annular thickness is small, because the effective radius for the 50 mCi source used in this study is around 15 cm. Therefore, alternative grouting materials were investigated. The goal was to find a material inert to water, which will not be affected by saturation changes in the surrounding formation, and will only minimally affect neutrons.

A.2.1. Casing Design

The ideal material for this application is one which contains no chlorine, is fairly inexpensive, easy to work with, and compatible with both neutron and radar investigations. Acrylic meets these requirements to variable degrees. It contains no chlorine, and is not very expensive, but it is much more brittle than PVC, has less strength than fiberglass, and is not commercially available in flush-threaded pipe form. Fiberglass pipe is often reinforced with PVC, which contains chlorine. Pure fiberglass pipe is difficult to work with, difficult to thread, and more expensive. All three materials were compared with respect to their neutron moderation properties.

A laboratory experiment was performed in which a 50 mCi source probe (described in I.7.9) was used to collect data in various casings under wet and dry conditions. The probe was placed, with and without casings, vertically in air and water-filled glass containers of different diameters. Table A.2.1-1 shows the results in counts per second.

The advantage of acrylic casing (lucite) over PVC and fiberglass-reinforced PVC is apparent. The 45 mm-thick PVC block was used to illustrate the effect of PVC on neutron thermalization and capture. The counts from the acrylic pipe were virtually the same as when no casing was used, which shows the negligible effect of acrylic on both high and low energy neutrons.

Table A.2.1-1. Slow Neutron Counts Under Various Conditions and through Casings of Variable Composition or Thickness (50 mCi source).

Water annulus (cm)	no casing	Lucite (4mm)	PVC (4mm)	PVC (5mm)	PVC (45mm)	Fiberglass (2mm)
0	255	267	212	199	2063	194
4.5	15210	13488	6317	6389		6697
12	23452	23235	12416	11933	2986	12116

Based on these findings, and the fact that acrylic has negligible effects on radar, acrylic pipe was chosen for the completion of the neutron probe/radar access boreholes.

A.2.2. Backfill Design

The ideal backfill for this application is one that is inert to water, fairly inexpensive, easy to work with, and compatible with both neutron and radar investigations. Porous earth materials such as benotite clay, sand, or gravel are undesirable because their moisture content changes as the formation moisture content changes, and their saturation curves are often significantly different from the formation. In this case, the neutron measurements will be, for the most part, of the backfill moisture content. Cement grout has also been used because it does not absorb water from the formation. However, it does contain a large mass fraction of structural water which will affect neutron readings. Cement also tends to settle unevenly over the length of the borehole. In this experiment several materials, primarily polyurethane resins, were tested for their potential applicability as backfill for neutron logging.

A series of laboratory experiments was performed to test the relative effects of backfill material on neutron count. Most of the tests were in acrylic pipe, and one in PVC. The various backfill materials are summarized in Table A.2.2-1.

Table A.2.2-1. Summary of Materials Tested for Backfill Design.

Material name	Activation*	Properties of final product	Main advantages	Main disadvantages
ST 504, polyurethane resin	A water-activated injection resin	Highly-elastic, fairly dense, rubbery solid	fills cracks well, inexpensive	shrinks significantly when dry
ST 530, polyurethane resin	A water-activated injection resin, accelerated chemically	Very low density† solid foam, hydrophobic, insoluble	inexpensive, low density, easy to handle, maintains shape and texture	high porosity, though largely unconnected
ST 540, polyurethane resin	A chemically-activated injection resin	High bulk density solid, impermeable	highly impermeable, stable	expensive due to chemical activation, strongly exothermic
ST 545, polyurethane resin	A chemically-activated injection resin	High bulk density solid, impermeable	highly impermeable, stable	shrinks slightly, expensive due to chemical activation, strongly exothermic
Colloidal-silica	$CaCl_2$-activated Nyacol	Soft, impermeable gel	self-annealing, low H concentration	cracks significantly when dried, not biologically inert

* *The activation time is dependent on the ratio of resin to activator and can be controlled to within a minute.*

† *The density of ST 530 is dependent on the activation time. Since the foam expands with time, the faster the activation, the lower the final bulk density. For this experiment, the final bulk density was 76 kg m^{-3}.*

Each material was tested by placing it in a lab-scale "borehole" around a "well." The "air" case represents a setup where the system was dry, or theoretically, 100% porosity, 0% saturation. The "wet" case represents a system with 100% porosity, 100% saturation.

The ideal material would have a response similar to the no-backfill scenario. In fact, such a response is observed when ST 530 is used. There is only a very slight depression of the signal in water. The other polyurethane resins produce elevated readings, meaning that fast neutrons are being adsorbed in the backfill, before reaching the water (or air). The PVC-cased well produced an elevated count in air and a depressed count in water. Overall, it had the smallest slope. These observations agree with the prediction that chlorine in PVC captures slow neutrons, but at the same time, in air, hydrogen in the PVC slows down a significant fraction of fast neutrons. Because of the small slope, precision is reduced. The high slope and elevated readings in the colloidal-Si sample are difficult to explain. Suffice it to say that colloidal-Si was eliminated from the list of potential backfill materials for reasons explained in Table A.2.2-2. However, the

large slope is not necessarily unfavorable for neutron logging if only relative differences are being measured.

A.2.3. Results

As a result of these experiments, acrylic pipe and ST 530 polyurethane resin were chosen for the completion of boreholes for neutron logging. Further testing in the laboratory of porous and fractured rocks would serve to quantify readings from the field test.

A.3. Calibration of Thermistors

Thermistors were used during the infiltration tests to measure temperature. The model of thermistor used was the NTC-DC95 (Thermometrics, New Jersey). This type of thermistor is a ceramic semiconductor with a negative temperature coefficient of resistance (NTC), (i.e., it gives decreasing resistance readings with increasing temperatures). This bead-shaped thermistor has platinum alloy leadwires that are directly sintered into a ceramic body. The DC95 thermistors are designed for use over a range of temperatures (0°C to 70°C) with an accuracy of ± 0.1°C.

A.3.1. Construction

Each thermistor was soldered onto a 38.1 m long electric cable. To protect the thermistor from mechanical stresses in the field, each bead was housed in a stainless steel shield. To prevent moisture from seeping into the leadwires, each wire was wrapped in shrink tubing and then insulated in the steel shield with epoxy.

A.3.2. Calibration

Calibration of each thermistor was done in the laboratory. The procedure used was that recommended by the manufacturer (Thermometrics).

A.3.3. Field Measurements

The temperature at each of the 34 locations was measured at intervals of 6-110 minutes during the entire infiltration experiment. These measurements were made with an Keithly digital multi-meter connected to a multiplexer. A typical measurement 'sweep' of 34 thermistors took less than 5 seconds.

A.4. IRC Field Test

A.4.1. Testing of Borehole Sealing Technology

After the instrumentation package design was finalized and the polyurethane foam decided upon, a field test was conducted. The location chosen for the field test was a borehole behind the Idaho National Engineering Laboratory Research Center (IRC). There were several reasons for choosing this location. The location was close and accessible to scientists and engineers working on the project. The approximate soil water tension and water content profiles at the site were known, and there was an available bore hole already in existence at the site.

The materials for the field test were similar to the materials used in the shop test. The only exception was the use of two different polyurethane foams. Polyurethane foam #530 was used to fill the polyethylene bags in order to push the instruments out against the bore hole wall. Polyurethane foam #530 was also used to fill most of the void space. Above each polyethylene bag there was planned to be a 2 inch layer of Polyurethane #540 foam.

The first step in the testing procedure was to assemble the instrument packages on to the manchet pipe. To accomplish this, 16.8 m (55 ft) of manchet pipe in 2 m (6.6 ft) sections was laid on the ground beside the hole. The manchet pipe sections were glued together with PVC glue. The joints on the pipe were reinforced with PVC sleeves that were affixed with epoxy.

The next step was to slide the polyethylene foam collars on to the manchet pipe and glue them in place. These collars had holes drilled in them so that there was a snug fit to the manchet pipe. There were also holes drilled to allow for the PVC pipe that would connect the DTs to the land surface to be threaded through the collars.

After placing the collars on the manchet pipe, 6.1 m (20 ft) sections of schedule 40, PVC pipe were threaded through the collars at appropriate locations. The sections of PVC pipe were then glued together. There was a continuous length of PVC pipe extending from each DT: this would cause the majority of the weight of the package to be near the top of the hole.

Next, the polyethylene bags were glued and taped to the foam collars. The bags were double the thickness of the bags used in the shop test to insure that the bags could be placed in the bore hole without being punctured during the installation process.

The final step was to glue the DTs onto the lengths of PVC pipe. This was accomplished with the use of ordinary PVC glue. The TDR probes were also glued to the outside of the polyethylene bags. The coaxial cable that connect the TDR probe to the

data collection system at the surface were taped to the manchet pipe in order to keep them in place.

After the completed instrumentation package was put together, the assembly had to be lowered down the hole. It was thought that the 15.2 m (50 ft) long assembly could be lowered down the hole by hand, but this proved to be an incorrect assumption. The arc in the manchet pipe proved to cause too much stress to the manchet pipe and the manchet pipe failed due to the bending of the pipe. The broken sections were taken out and replaced with new manchet pipe.

The second attempt to lower the assembly down the hole was more successful. This attempt utilized a boom truck with a 12.2 m (40 ft) extending arm. The assembly was raised up and lowered down the hole by the boom truck. This method of installation greatly improved the reliability of the installation process.

The next step in the field test was to inject polyurethane foam #530 into the polyethylene bags. A chart was prepared that detailed the depth of installation and the volume of foam to be injected into each bag. Beginning with the bag at the greatest depth, foam was injected into each bag. The only observable problems with the injection of the Polyurethane foam #530 into the polyethylene bags seemed to be that the foam would begin to harden in the injection pipe itself. When this occurred the pipe had to be taken out of the hole and flushed with water to clean it. In some instances the injection nozzle was replaced. After the polyethylene bags were filled, the foam was allowed to fully harden.

Next, the Polyurethane foam #540 was to be injected in small volumes to completely seal the bore hole. There were several attempts at injecting the #540 foam. The first attempt to pump the Polyurethane #540 foam into the borehole failed. The foam set up in the tubing that was intended to carry the foam to the proper depth. The second attempt involved a pressure chamber. The intent was to apply pressure to the foam to accelerate the injection process. Due to unknown factors this attempt also failed. The velocity at which the foam could be pumped was considerably too slow. It was thought that the high viscosity of the foam was a contributing factor.

The final step was to fill the void space in the hole with Polyurethane foam #530. The injection process was relatively uneventful, with three exceptions. The first exception was that the manchet pipe was partially filled with foam from the first injection of the 530 foam. A device was constructed to clean out the manchet pipe. The second problem was that one of the rubber collars at one depth would not open to allow the injection of the foam. It is thought that the next manchet opening one foot below the inoperable opening could have been used. The third problem was encountered after all of the annular space have been filled and the injection pipe was being removed. The injection pipe became stuck in the manchet pipe at a depth of 0.3 m (1 ft) below land

surface. The problem was that the Polyurethane foam #530 had expanded and hardened between the rubber packers in the injection pipe. Once this happened, it was virtually impossible to retrieve the injection pipe. This problem would prove to be a recurring one.

A.4.2. Preliminary Tests and Evaluation of the Deep Tensiometer

Knowing the status of soil moisture beneath landfills and buried hazardous waste sites is important to the management of these sites. One of the variables determining the status of soil moisture is the water potential (actually the energy required to remove a small quantity of water). While tensiometers are one instrument used for estimating soil water potential, their design limits their use to shallow depths. The DT was designed to allow operation to any depth and was therfore selected for deployment at the Box Canyon site. Prior to deploying the DTs at Box Canyon, a field test was conducted at the IRC 5-Well site in Idaho Falls, Idaho. This appendix describes the tests carried out at the 5-Well Site and provides an evaluation of their performance in fractured basalt.

At the 5-Well site, five boreholes were drilled with a 7-7/8 inch diameter bit using tricone drilling technology, and 1 borehole was cored leaving a 4 inch bit. In one of the 7-7/8 inch boreholes, 5 DTs were installed, one each at the depths of 9, 20, 28, 40, and 50 feet below land surface. The method for installing the tensiometers consisted of lowering each tensiometer to depth, pouring enough dry soil to fill the borehole to about one foot below the tensiometer, and adding enough dry bentonite to form a one foot plug. Dry soil was added to fill the borehole to the depth of the next tensiometer while tamping. The next tensiometer was placed and backfilled using the same method. The four tensiometers installed in basalt were equipped with pressure sensors connected to a data logger and their outputs monitored.

The first notable result of these pressure measurements is that all depths were found to be in the range of pressures that the tensiometer could measure. Initial indications were that the basalts would be too dry and the water potentials would be less then the lower tensiometer range of -1000 cm. The second feature is the relatively long time periods possible between tensiometer purges. Conventionally installed tensiometers, with the pressure sensor above land surface, require weekly or bi-weekly purging to remove entrapped air to reduce the tendency of the instruments to act as gas thermometers. Data obtained at other sites indicate that DTs can operate for more then 100 days without purging. Another feature is the positive pressures shown at the 50 ft depth, indicating perched water at that depth. The 5-Well Site is on a grass covered area that has not received supplemental irrigation for more then 20 years. The last feature to be noticed is the rippled nature of the pressure time trend. These ripples have been found to be strongly correlated with barometric pressure changes and are a new phenomena in soil water potential data. It remains to be established whether barometric changes effect soil water potential or if they are an artifact of the pressure measurement system.

DTs appear to be viable instruments for monitoring water potentials in fractured basalt when installed in soil and bentonite backfilled boreholes. Measurements indicate that barometric pressure changes will introduce noise into the water potential measurements, causing the measured potentials to fluctuate ±10 cm, about the moving average.

In order to instrument densely spaced fractures, the Box Canyon effort required a close vertical spacing between instruments in each borehole. Conventional backfilling procedures, such as those used to install the tensiometers in well 3 at the 5-Well Site, limit the vertical spacing of instruments in boreholes to intervals greater than 5 feet. Results of lab and shop tests indicated that by using the polyethylene packers and polyurethane grouting procedures (See Section I.5) the vertical spacing could be reduced to less than 3 feet. Well 4 at the 5-Well site was instrumented with 9 DTs, one tensiometer each at the depths of 7, 11.7, 15, 22, 27, 37, 42, and 47.5 ft. Polyethylene packers and polyurethane grouting procedures were further developed during the installation of these DTs.

The prime concern following the grout emplacement was that excess grout could coat and seal the tensiometers, rendering them useless. Thus, during the first 10 days following the grouting operation, the results were interpreted as positive because the tensiometers were responding as they normally would do. The surface casing that was placed from ground surface to the top of the basalt to prevent soil from sloughing into the borehole was left uncapped and open to the atmosphere. Late in August, rainfall occurred and water ponded on the grout, apparently moving down to the tensiometer at the 28 ft depth. Further rainfall events occurring during September appear to have wetted to at least the 38 ft depth. The deep and rapid penetration of precipitation in the borehole indicates that the grout seal failed. The failure was attributed to inadequate volumes of grout being injected into the borehole.

During the grout emplacement, several problems were encountered and solved. The first problem was the short period of time required by the grout to form foam and expand. The quantity of accelerator added to the grout was adjusted and the reaction time extended. The second problem was that the grout would expand in the straddle packer and wedge it in the manchet pipe. This problem was only partially overcome by removing the straddle packer from the manchet pipe if excessive force was required to move it from point to point. Once removed, the straddle packer was cleaned and reused. Although these precautions were applied, a straddle packer was wedged and became immovable while grouting well 4. The wedged packer prevented the injection of enough grout to complete well 4, creating the failed seal. Failure of the seal appears to have been a singular event in that the tensiometers installed at Box Canyon have not shown a similar behavior. Overall the tests at well 4 have contributed to the program by providing methods for installing a large number of instruments in a single borehole and providing criteria for evaluating the seal between the instruments.

A.5. Summary of Instrument Responses to Infiltration and Tracer Tests

The following tables (Tables A.5.1 through A.5.6) summarize the responses of seven kinds of instruments (ER probes, neutron probes, shallow tensiometers and DTs, suction lysimeters, TDR sensors, and thermistors) to the infiltration and tracer tests conducted at the Box Canyon site in August and September, 1996. Also included in the tables are the coordinates of the instruments, whether the instruments are located inside of or outside of the infiltration pond, and the type of rock and fracture at the instrument locations.

For the most part, the instrument responses have been simplified to indicate whether there was a response to the infiltration and tracer tests. In some cases, the magnitude of the response is indicated. For some types of data, specifically neutron data and pressure data, actual data values are given.

Rock types have been categorized as 'basalt', 'vesicular', or 'rubble'. For some locations, the degree of vesicularity has been noted. Fractures are characterized by angle ('high' or 'low") and by whether there is a single fracture or fracture zone. Except where noted, a blank indicates that no measurement of the type indicated by the column heading was made at that location.

Each column heading contains a reference to the section in this report that gives more details about data collected (except for rock type and fracture data, which are described in more detail in a separate data report on lithology).

Table A.5-1. Summary of Instrument Responses to Infiltration and Tracer Tests for Wells E-1 to E-4

Well ID	Distance Down Borehole (m)	Vertical Depth from Top of Borehole (m)	Reference Depth (m) *highest pt. (1599.5) - elevation*	Elevation (m)	Easting (m)	Northing (m)	Inside or Outside of Infiltration Pond?	Rock Type
								Lithological Data Rpt. - Feb. 1998
E-1	2.1	1.5	1.3	1598.2	58.8	63.0	inside	basalt
E-1	3.7	2.6	2.4	1597.1	59.5	63.8	inside	basalt
E-1	6.1	4.3	4.1	1595.4	60.5	65.2	inside	basalt
E-1	8.8	6.3	6.1	1593.4	61.7	66.7	inside	vesicular
E-1	11.0	7.8	7.6	1591.9	62.6	67.9	inside	basalt
E-1	13.1	9.3	9.1	1590.4	63.6	69.1	outside	basalt
E-1	16.5	11.6	11.5	1588.0	65.0	71.0	outside	rubble
E-1	17.4	12.3	12.1	1587.4	65.4	71.5	outside	vesicular
E-2	1.8	1.4	1.2	1598.3	58.0	61.8	outside	vesicular
E-2	3.7	2.8	2.6	1596.9	58.7	62.8	inside	basalt
E-2	6.1	4.7	4.5	1595.0	59.7	64.0	inside	basalt
E-2	9.1	7.0	6.8	1592.7	60.9	65.6	inside	basalt
E-2	9.4	7.2	7.0	1592.5	61.0	65.7	inside	basalt
E-2	13.1	10.0	9.8	1589.7	62.4	67.6	inside	rubble
E-2	15.2	11.7	11.5	1588.0	63.2	68.7	inside	rubble
E-2	17.1	13.1	12.9	1586.6	64.0	69.6	outside	
E-2	17.4	13.3	13.1	1586.4	64.1	69.8	outside	
E-3	?	?	?	?	?	?	outside	?
E-3	2.1	1.7	1.6	1597.9	57.0	61.0	outside	basalt
E-3	5.2	4.2	4.1	1595.4	58.1	62.3	outside	basalt
E-3	6.4	5.2	5.1	1594.4	58.5	62.9	outside	basalt
E-3	6.7	5.5	5.3	1594.2	58.6	63.0	outside (edge)	basalt
E-3	8.2	6.7	6.6	1592.9	59.1	63.7	inside	basalt
E-3	8.8	7.2	7.1	1592.4	59.4	64.0	inside	basalt
E-3	11.0	9.0	8.8	1590.7	60.1	64.9	inside	basalt
E-3	13.1	10.7	10.6	1588.9	60.9	65.9	inside	rubble
E-3	14.3	11.7	11.6	1587.9	61.3	66.4	inside	
E-3	17.1	14.0	13.8	1585.7	62.3	67.6	inside	
E-4	4.6	4.0	3.9	1595.6	57.2	60.9	outside	basalt
E-4	7.0	6.2	6.1	1593.4	57.9	61.8	outside	basalt
E-4	8.5	7.5	7.4	1592.1	58.3	62.4	outside	vesicular
E-4	13.1	11.6	11.4	1588.1	59.7	64.1	inside	
E-4	15.2	13.5	13.3	1586.2	60.3	64.9	inside	
E-4	17.4	15.3	15.2	1584.3	60.9	65.7	inside	

Table A.5-1. Summary of Instrument Responses to Infiltration and Tracer Tests for Wells E-1 to E-4

	Before Infiltration	After Infiltration				
Fracture Type	Water Sample Collected?	Water Sample Collected?	Bromide (>100 mg/l) Detected?	Response at Deep Tensio-meters?	Response from Thermistors?	Response from Deep TDR Sensors?
			[1] sampled, but dry			
		wet before infil. test	after tracer added			
		dry before infil. test				
Lithological Data Rpt. - Feb. 1998	*Data Report Section II.3*	*Data Report Section II.3*	*Data Report Section II.4*	*Data Report Section II.1.2*	*Data Report Section II.5*	*Data Report Section II.7.2*
high angle zone	yes	yes	*no*	no effect	yes	no
low angle	*sampled, but dry*	yes	*no*	no effect	no	no
high angle				*uncertain*	no	no
				no effect	yes	no
				no effect	no	no
	sampled, but dry	*sampled, but dry*	*sampled, but dry*		no	no
	sampled, but dry	*sampled, but dry*	*sampled, but dry*		no	no
low angle zone	*sampled, but dry*	*sampled, but dry*	*sampled, but dry*			no
	sampled, but dry	*sampled, but dry*	*sampled, but dry*	no effect	yes	no
				no effect	no	no
	sampled, but dry	*sampled, but dry*	*sampled, but dry*	*perched water?*		no
low angle				elec. problem	no	
low angle	*sampled, but dry*	yes	*no*			no
				no effect	no	no
	sampled, but dry	yes	*no*	no effect	no	no
					no	
				no effect		no
					no	
						no
	yes	*sampled, but dry*	*sampled, but dry*			no
low angle zone				no effect		
low angle zone	*sampled, but dry*	yes	*no*		no	no
				no effect		
	yes	yes	*no*	no effect	no	yes
				no effect	no	no
				no effect	no	
						no
				no effect	no	no
				uncertain		no
	sampled, but dry	yes	*no*	leak	no	no
low angle zone	yes	yes	*no*	*wetting front?*	yes	no
					no	no
	sampled, but dry	*sampled, but dry*	*sampled, but dry*	no effect	no	no
				elec. problem		no

Table A.5-2. Summary of Instrument Responses to Infiltration and Tracer Tests for Wells I-1 to I-3

Well ID	Distance Down Borehole (m)	Vertical Depth from Top of Borehole (m)	Reference Depth (m) *highest pt. (1599.5) - elevation*	Elevation (m)	Easting (m)	Northing (m)	Inside or Outside of Infiltration Pond?	Rock Type
								Lithological Data Rpt. - Feb. 1998
I-1	0.3	0.3	0.2	1599.3	58.9	64.4	inside	vesicular
I-1	1.5	1.5	1.4	1598.1	58.9	64.4	inside	vesicular
I-1	3.0	3.0	2.9	1596.6	58.9	64.4	inside	basalt
I-1	4.6	4.6	4.4	1595.1	58.9	64.4	inside	vesicular
I-1	6.1	6.1	6.0	1593.5	58.9	64.4	inside	basalt
I-1	8.5	8.5	8.4	1591.1	58.9	64.4	inside	basalt
I-1	10.1	10.1	9.9	1589.6	58.9	64.4	inside	basalt
I-1	11.6	11.6	11.4	1588.1	58.9	64.4	inside	rubble
I-1	12.2	12.2	12.1	1587.4	58.9	64.4	inside	rubble
I-2	0.3	0.3	0.1	1599.4	60.8	67.9	inside	basalt
I-2	1.5	1.5	1.3	1598.2	60.8	67.9	inside	basalt
I-2	3.0	3.0	2.8	1596.7	60.8	67.9	inside	basalt
I-2	4.3	4.3	4.1	1595.4	60.8	67.9	inside	vesicular
I-2	5.5	5.5	5.3	1594.2	60.8	67.9	inside	vesicular
I-2	6.1	6.1	5.9	1593.6	60.8	67.9	inside	basalt
I-2	8.5	8.5	8.3	1591.2	60.8	67.9	inside	basalt
I-2	10.7	10.7	10.5	1589.0	60.8	67.9	inside	basalt
I-2	12.2	12.2	12.0	1587.5	60.8	67.9	inside	rubble
I-3	0.3	0.3	0.2	1599.3	60.9	61.0	inside	vesicular
I-3	1.5	1.5	1.4	1598.1	60.9	61.0	inside	vesicular
I-3	3.0	3.0	2.9	1596.6	60.9	61.0	inside	vesicular
I-3	4.6	4.6	4.4	1595.1	60.9	61.0	inside	basalt
I-3	6.1	6.1	5.9	1593.6	60.9	61.0	inside	vesicular
I-3	7.6	7.6	7.5	1592.0	60.9	61.0	inside	basalt
I-3	9.1	9.1	9.0	1590.5	60.9	61.0	inside	basalt
I-3	10.7	10.7	10.5	1589.0	60.9	61.0	inside	rubble

Table A.5-2. Summary of Instrument Responses to Infiltration and Tracer Tests for Wells I-1 to I-3

	Before Infiltration	After Infiltration				
Fracture Type	Water Sample Collected?	Water Sample Collected?	Bromide (>100 mg/l) Detected?	Response at Deep Tensio-meters?	Response from Thermistors?	Response from Deep TDR Sensors?
		[illegible]	[1] sampled, but dry			
		wet before infil. test	after tracer added			
		dry before infil. test				
Lithological Data Rpt. - Feb. 1998	*Data Report Section II.3*	*Data Report Section II.3*	*Data Report Section II.4*	*Data Rpt. Sect. II.1.2*	*Data Report Section II.5*	*Data Report Section II.7.2*
	sampled, but dry	yes	yes			yes
	sampled, but dry	yes	yes	no effect		yes
low angle	*sampled, but dry*	yes	*no*	no effect		yes
	sampled, but dry	yes	*no*	no effect		no
	yes	yes	*no*	no effect		no
high angle zone	yes	yes	*no*	no effect		no
high angle zone	*sampled, but dry*	yes	*no*	no effect		no
						no
				no effect		
	yes	yes	yes			
	sampled, but dry	yes	*no*	no effect		
	sampled, but dry	yes	yes	no effect		
	sampled, but dry	yes	yes	no effect		
				no effect		
				no effect		
low angle zone						yes
low angle				no effect		
				no effect		
	not sampled	yes	yes		no	
	yes	yes	*no*	no effect	yes	
				no effect	yes	
				no effect	yes	
low angle				*uncertain*	no	
high angle zone				no effect	no	
				no effect	no	no
					no	no

Table A.5-3. Summary of Instrument Responses to Infiltration and Tracer Tests for Wells R-1 to R-4

Well ID	Distance Down Borehole (m)	Vertical Depth from Top of Borehole (m)	Reference Depth (m) *highest pt. (1599.5) - elevation*	Elevation (m)	Easting (m)	Northing (m)	Inside or Outside of Infiltration Pond?
R-1	0.5	0.5	0.7	1598.8	72.5	62.8	outside
R-1	0.8	0.7	1.0	1598.5	72.4	62.8	outside
R-1	1.4	1.3	1.5	1598.0	72.1	62.8	outside
R-1	1.9	1.7	1.9	1597.6	71.9	62.8	outside
R-1	3.1	2.7	3.0	1596.5	71.4	62.8	outside
R-1	3.4	3.0	3.2	1596.3	71.2	62.8	outside
R-1	4.9	4.3	4.6	1594.9	70.5	62.8	outside
R-1	5.2	4.6	4.8	1594.7	70.4	62.8	outside
R-1	6.5	5.8	6.0	1593.5	69.8	62.8	outside
R-1	7.0	6.2	6.4	1593.1	69.6	62.8	outside
R-1	7.9	7.0	7.2	1592.3	69.2	62.8	outside
R-1	11.5	10.2	10.4	1589.1	67.5	62.8	outside
R-1	16.4	14.6	14.8	1584.7	65.2	62.8	inside
R-2	0.5	0.4	0.3	1599.2	67.1	63.0	outside
R-2	1.1	0.8	0.7	1598.8	66.7	63.0	outside
R-2	2.1	1.6	1.5	1598.0	66.0	63.0	outside
R-2	2.4	1.8	1.7	1597.8	65.8	63.0	outside
R-2	3.6	2.7	2.7	1596.8	65.0	63.0	inside
R-2	4.1	3.1	3.0	1596.5	64.7	63.0	inside
R-2	5.7	4.3	4.2	1595.3	63.6	63.0	inside
R-2	6.2	4.7	4.6	1594.9	63.3	63.0	inside
R-2	7.5	5.7	5.6	1593.9	62.4	63.0	inside
R-2	8.0	6.0	5.9	1593.6	62.1	63.0	inside
R-2	8.4	6.4	6.3	1593.2	61.8	62.9	inside
R-2	12.9	9.7	9.7	1589.8	58.9	62.9	inside
R-2	16.1	12.1	12.0	1587.5	56.8	62.9	outside
R-3	0.4	0.4	0.6	1598.9	71.6	67.9	outside
R-3	0.7	0.6	0.9	1598.6	71.5	67.9	outside
R-3	1.8	1.6	1.8	1597.7	71.0	67.9	outside
R-3	3.1	2.8	3.0	1596.5	70.4	67.9	outside
R-3	3.4	3.0	3.3	1596.2	70.2	67.9	outside
R-3	4.9	4.4	4.6	1594.9	69.5	67.9	outside
R-3	5.2	4.6	4.9	1594.6	69.4	67.9	outside
R-3	6.5	5.8	6.1	1593.4	68.8	67.9	outside
R-3	6.9	6.1	6.3	1593.2	68.7	67.9	outside
R-3	7.8	6.9	7.1	1592.4	68.2	67.9	outside
R-3	11.4	10.1	10.3	1589.2	66.6	67.9	outside
R-3	16.3	14.5	14.7	1584.8	64.3	67.9	inside
R-4	0.6	0.5	0.5	1599.0	65.9	67.6	outside
R-4	1.8	1.6	1.5	1598.0	65.3	67.6	inside
R-4	2.2	2.0	1.9	1597.6	65.1	67.6	inside
R-4	3.2	2.8	2.7	1596.8	64.6	67.6	inside
R-4	3.4	3.0	3.0	1596.5	64.5	67.6	inside
R-4	4.9	4.3	4.3	1595.2	63.7	67.6	inside
R-4	5.2	4.6	4.6	1594.9	63.6	67.6	inside
R-4	6.6	5.8	5.7	1593.8	62.9	67.6	inside
R-4	7.0	6.2	6.1	1593.4	62.7	67.6	inside
R-4	7.3	6.4	6.4	1593.1	62.6	67.6	inside
R-4	11.8	10.3	10.3	1589.2	60.4	67.6	inside
R-4	16.8	14.7	14.6	1584.9	58.0	67.6	outside

Table A.5-3. Summary of Instrument Responses to Infiltration and Tracer Tests for Wells R-1 to R-4

		Before Infiltration	After Infiltration	
Rock Type	Fracture Type	Neutron Counts (counts > 6600 in boldface)	Neutron Count (maximum counts after pond filled)	Neutron Counts Relative to Pre-Test Values (% Difference)
Lithological Data Report - Feb. 1998	*Lithological Data Report - Feb. 1998*	*Data Report Section II.2*	*Data Report Section II.2*	*Data Report Section II.2*
		5463	6274	15
		4170	4330	4
		4804	4845	1
		5291	5303	0
		5662	5615	1
		6359	6643	4
		6290	6513	4
		5652	5770	2
		6046	6223	3
		6658	7110	7
		6332	8106	28
		5095	5323	4
		6376	7101	11
vesicular		4476	4607	3
vesicular		5090	5742	13
basalt		5077	5220	3
basalt		5024	6922	38
basalt		5664	5615	1
basalt		5045	5321	5
basalt		5231	5234	0
basalt	high angle	5107	5341	5
basalt		5434	5481	1
basalt		5370	5422	1
basalt		5869	5991	2
basalt		**6855**	6993	2
vesicular		5274	5712	8
basalt		4609	5429	18
basalt	low angle	4641	5080	9
basalt		5351	5509	3
basalt		5572	5930	6
basalt		5516	5782	5
basalt	high angle	5446	6700	23
basalt		5666	5974	5
basalt		6376	7135	12
basalt		5542	6300	14
rubble		5359	7907	48
		6488	12288	89
		5349	5938	11
basalt		5157	6005	16
basalt		5588	5971	7
basalt		**6775**	7194	6
basalt	high angle zone	**8566**	8860	3
basalt	mixed angle zone	**7880**	8062	2
basalt		5284	5868	11
basalt		5411	5468	1
basalt		5525	5612	2
vesicular		5480	5727	5
vesicular		5905	6023	2
		6828	7013	3
		7445	7810	5

Table A.5-4. Summary of Instrument Responses to Infiltration and Tracer Tests for Wells II-5 and S-1 to S-4

Well ID	Distance Down Borehole (m)	Vertical Depth from Top of Borehole (m)	Reference Depth (m) *highest pt. (1599.5) - elevation*	Elevation (m)	Easting (m)	Northing (m)	Inside or Outside of Infiltration Pond?
II-5	0.3	0.3	0.1	1599.4	62.4	62.9	inside
II-5	1.5	1.5	1.3	1598.2	62.4	62.9	inside
II-5	4.0	4.0	3.8	1595.7	62.4	62.9	inside
II-5	5.8	5.8	5.6	1593.9	62.4	62.9	inside
II-5	7.6	7.6	7.4	1592.1	62.4	62.9	inside
II-5	9.4	9.4	9.2	1590.3	62.4	62.9	inside
II-5	10.8	10.8	10.6	1588.9	62.4	62.9	inside
II-5	11.0	11.0	10.8	1588.7	62.4	62.9	inside
II-5	12.8	12.8	12.6	1586.9	62.4	62.9	inside
II-5	14.0	14.0	13.8	1585.7	62.4	62.9	inside
II-5	14.2	14.2	14.0	1585.5	62.4	62.9	inside
II-5	18.0	18.0	17.8	1581.7	62.4	62.9	inside
S-1	0.6	0.5	0.4	1599.1	62.1	64.6	inside
S-1	1.8	1.6	1.5	1598.0	61.8	64.1	inside
S-1	3.0	2.6	2.5	1597.0	61.5	63.6	inside
S-1	4.3	3.7	3.6	1595.9	61.2	63.1	inside
S-2	0.9	0.8	0.8	1598.7	63.0	65.7	inside
S-2	2.3	2.0	1.9	1597.6	62.6	65.2	inside
S-2	3.0	2.6	2.6	1596.9	62.4	64.9	inside
S-2	4.3	3.7	3.7	1595.8	62.0	64.4	inside
S-3	0.8	0.7	0.6	1598.9	64.4	67.8	inside
S-3	2.0	1.7	1.6	1597.9	64.0	67.3	inside
S-3	3.4	2.9	2.8	1596.7	63.6	66.7	inside
S-3	4.6	4.0	3.9	1595.6	63.3	66.2	inside
S-3	5.9	5.1	5.1	1594.4	62.9	65.7	inside
S-3	8.1	7.0	6.9	1592.6	62.3	64.8	inside
S-3	9.1	7.9	7.8	1591.7	62.0	64.4	inside
S-3	10.7	9.2	9.2	1590.3	61.5	63.7	inside
S-4	1.5	1.3	1.3	1598.2	66.1	71.1	outside
S-4	3.0	2.6	2.6	1596.9	65.7	70.5	outside
S-4	4.6	4.0	4.0	1595.5	65.3	69.8	outside
S-4	5.8	5.0	5.0	1594.5	65.0	69.3	outside
S-4	7.6	6.6	6.6	1592.9	64.5	68.5	inside
S-4	10.2	8.8	8.8	1590.7	63.8	67.4	inside
S-4	12.5	10.8	10.8	1588.7	63.3	66.5	inside
S-4	13.4	11.6	11.6	1587.9	63.0	66.1	inside
S-4	14.6	12.7	12.7	1586.8	62.7	65.5	inside

Table A.5-4. Summary of Instrument Responses to Infiltration and Tracer Tests for Wells II-5 and S-1 to S-4

		Before Infiltration	After Infiltration		
Rock Type	Fracture Type	Water Sample Collected?	Water Sample Collected?	Bromide (>100 mg/l) Detected?	Response from ER Probes?
			[1] sampled, but dry		
			wet before infil. test	after tracer added	
			dry before infil. test		
Lithological Data Report - Feb. 1998	*Lithological Data Report - Feb. 1998*	*Data Report Section II.3*	*Data Report Section II.3*	*Data Report Section II.4*	*Data Report Section II.4*
rubble					yes
basalt	low angle zone				no
vesicular					no
vesicular					no
basalt	high angle zone				no
basalt	mixed angle zone				no
vesicular					no
rubble					yes
rubble					no
vesicular					no
rubble					
rubble					yes
vesicular	high angle zone				yes
basalt	low angle				yes
vesicular	low angle zone				no
basalt	high angle zone				no
vesicular					no
basalt	low angle				no
basalt					no
basalt					no
vesicular	low angle	not sampled	yes	yes	yes
basalt	low angle				no
basalt	low angle				yes
vesicular					no
basalt					no
basalt					yes
vesicular	low angle zone				no
basalt					no
basalt					no
vesicular	low angle				no
vesicular	mixed angle zone				no
vesicular					no
basalt	low angle zone				no
basalt	low angle				no
vesicular	high angle zone				no
vesicular					no
vesicular	mixed angle zone				yes

Table A.5-5. Summary of Instrument Responses to Infiltration and Tracer Tests for Wells T-1, T-8 and T-10

Well ID	Vertical Depth from Top of Borehole (m)	Reference Depth (m) *highest pt. (1599.5) - elevation*	Elevation (m)	Easting (m)	Northing (m)	Inside or Outside of Infiltration Pond?
T-1	0.2	0.0	1599.5	57.3	63.0	outside/at edge
T-1	0.8	0.6	1598.9	57.3	63.0	outside/at edge
T-1	1.2	1.1	1598.4	57.3	63.0	outside/at edge
T-1	1.8	1.7	1597.8	57.3	63.0	outside/at edge
T-1	2.7	2.6	1596.9	57.3	63.0	outside/at edge
T-1	3.0	2.9	1596.6	57.3	63.0	outside/at edge
T-1	4.4	4.2	1595.3	57.3	63.0	outside/at edge
T-1	4.7	4.5	1595.0	57.3	63.0	outside/at edge
T-1	5.7	5.6	1593.9	57.3	63.0	outside/at edge
T-1	6.0	5.9	1593.6	57.3	63.0	outside/at edge
T-8A	0.7	0.6	1598.9	58.9	65.6	inside
T-8A	1.3	1.2	1598.3	58.9	65.6	inside
T-8A	1.7	1.6	1597.9	58.9	65.6	inside
T-8A	2.8	2.7	1596.8	58.9	65.6	inside
T-8A	2.9	2.8	1596.7	58.9	65.6	inside
T-8A	4.3	4.2	1595.3	58.9	65.6	inside
T-8A	4.6	4.5	1595.0	58.9	65.6	inside
T-8A	5.8	5.7	1593.8	58.9	65.6	inside
T-8A	6.1	6.0	1593.5	58.9	65.6	inside
T-8A	6.4	6.3	1593.2	58.9	65.6	inside
T-8A	6.5	6.4	1593.1	58.9	65.6	inside
T-10	0.3	0.1	1599.4	61.7	65.7	inside
T-10	0.6	0.4	1599.1	61.7	65.7	inside
T-10	1.5	1.3	1598.2	61.7	65.7	inside
T-10	1.9	1.8	1597.7	61.7	65.7	inside
T-10	2.8	2.7	1596.8	61.7	65.7	inside
T-10	3.0	2.8	1596.7	61.7	65.7	inside
T-10	3.1	3.0	1596.5	61.7	65.7	inside

Table A.5-5. Summary of Instrument Responses to Infiltration and Tracer Tests for Wells T-1, T-8 and T-10

	Before Infiltration	After Infiltration	
Rock Type	Neutron Counts (counts > 6600 in boldface)	Neutron Count (maximum counts after pond filled)	Neutron Counts Relative to Pre-Test Values (% Difference)
Lithological Data Report - Feb. 1998	*Data Report Section II.2*	*Data Report Section II.2*	*Data Report Section II.2*
basalt	3530	6650	88
vesicular - sparse	4823	5458	13
vesicular - sparse	5181	5943	15
vesicular - sparse	5627	5907	5
basalt	5546	5694	3
basalt	5285	5580	6
basalt	5505	5788	5
basalt	5829	5986	3
basalt	**6600**	6584	0
vesicular	5387	5719	6
vesicular	**7203**	8700	21
basalt	4920	5668	15
basalt	5061	5580	10
basalt	5818	6078	4
basalt	5865	6180	5
basalt	6203	6965	12
basalt	5908	8725	48
vesicular	6036	6345	5
vesicular	5618	5933	6
	5163	5418	5
	5141	5885	14
vesicular	3573	6240	75
vesicular	5347	8134	52
basalt	5445	18129	233
basalt	6298	13050	107
basalt	5703	19121	235
basalt	5354	17923	235
	6672	16936	154

Table A.5-6. Summary of Instrument Responses to Infiltration and Tracer Tests for Wells T-2 to T-5 and T-7 to T-9

Well ID	Vertical Depth from Top of Borehole (m)	Reference Depth (m) *highest pt. (1599.5) - elevation*	Elevation (m)	Easting (m)	Northing (m)	Inside or Outside of Infiltration Pond?	Rock Type	Fracture Type	Before Infi Water Sample Collected?
							Lithological Data Rpt. - Feb. 1998	*Lithological Data Rpt. - Feb. 1998*	*Data Rpt. Sect. II.3*
T-2	0.5	0.5	1599.0	67.0	64.5	outside/at edge	basalt		
T-2	0.6	0.6	1598.9	67.0	64.5	outside/at edge	vesicular		*sampled, but dry*
T-2	1.5	1.5	1598.0	67.0	64.5	outside/at edge	basalt		
T-2	1.8	1.8	1597.7	67.0	64.5	outside/at edge	basalt		*sampled, but dry*
T-2	3.0	3.0	1596.5	67.0	64.5	outside/at edge	basalt		*sampled, but dry*
T-2	3.0	3.0	1596.5	67.0	64.5	outside/at edge	basalt	low angle	
T-2	4.4	4.4	1595.1	67.0	64.5	outside/at edge	basalt		*sampled, but dry*
T-2	4.4	4.4	1595.1	67.0	64.5	outside/at edge	basalt		
T-2	5.5	5.5	1594.0	67.0	64.5	outside/at edge	basalt		
T-2	5.9	5.9	1593.6	67.0	64.5	outside/at edge	vesicular		
T-3	0.5	0.2	1599.3	63.3	69.2	outside/at edge	vesicular		
T-3	0.6	0.4	1599.1	63.3	69.2	outside/at edge	vesicular		*sampled, but dry*
T-3	1.8	1.6	1597.9	63.3	69.2	outside/at edge	vesicular		*sampled, but dry*
T-3	3.0	2.8	1596.7	63.3	69.2	outside/at edge	vesicular		*sampled, but dry*
T-3 (T-4?)	4.0	3.7	1595.8	63.3	69.2	outside/at edge	vesicular		
T-3	4.6	4.3	1595.2	63.3	69.2	outside/at edge	vesicular - sparse	high angle	*sampled, but dry*
T-3 (T-4?)	5.8	5.5	1594.0	63.3	69.2	outside/at edge	basalt		
T-3	6.1	5.8	1593.7	63.3	69.2	outside/at edge	vesicular		*sampled, but dry*
T-4	0.5	0.4	1599.1	63.1	58.2	outside/at edge	vesicular		
T-4	0.6	0.5	1599.0	63.1	58.2	outside/at edge	vesicular		*sampled, but dry*
T-4	1.5	1.5	1598.0	63.1	58.2	outside/at edge	basalt	low angle	
T-4	1.6	1.6	1597.9	63.1	58.2	outside/at edge	basalt		
T-4	1.7	1.6	1597.9	63.1	58.2	outside/at edge	basalt		
T-4	2.7	2.7	1596.8	63.1	58.2	outside/at edge	vesicular		yes
T-4	2.8	2.7	1596.8	63.1	58.2	outside/at edge	vesicular		
T-4	4.1	4.0	1595.5	63.1	58.2	outside/at edge	vesicular		
T-4	4.3	4.2	1595.3	63.1	58.2	outside/at edge	vesicular		yes
T-4	5.7	5.7	1593.8	63.1	58.2	outside/at edge	basalt		
T-4	5.8	5.7	1593.8	63.1	58.2	outside/at edge	vesicular		*sampled, but dry*
T-5	0.3	0.1	1599.4	62.1	63.4	inside	vesicular		*sampled, but dry*
T-5	1.5	1.3	1598.2	62.1	63.4	inside	vesicular		*sampled, but dry*
T-5	3.0	2.8	1596.7	62.1	63.4	inside	vesicular		*sampled, but dry*
T-7	0.5	0.3	1599.2	59.7	62.8	inside	vesicular		
T-7	0.6	0.5	1599.0	59.7	62.8	inside	vesicular		not sampled
T-7	1.8	1.7	1597.8	59.7	62.8	inside	basalt	low angle zone	*sampled, but dry*
T-7	3.0	2.9	1596.6	59.7	62.8	inside	basalt		
T-7	4.6	4.4	1595.1	59.7	62.8	inside	basalt		*sampled, but dry*
T-7	5.8	5.7	1593.8	59.7	62.8	inside	vesicular		*sampled, but dry*
T-8	0.3	0.1	1599.4	59.7	64.3	inside	basalt	mixed angle zone	
T-8	1.5	1.3	1598.2	59.7	64.3	inside	basalt	high angle	
T-8	2.7	2.5	1597.0	59.7	64.3	inside	basalt	low angle	
T-9	0.3	0.1	1599.4	60.2	66.4	inside	vesicular		not sampled
T-9	1.5	1.3	1598.2	60.2	66.4	inside	basalt	low angle	yes
T-9	3.0	2.9	1596.6	60.2	66.4	inside	basalt		*sampled, but dry*

Table A.5-6. Summary of Instrument Responses to Infiltration and Tracer Tests for Wells T-2 to T-5 and T-7 to T-9

tration	After Infiltration							
Pre-Test Pressure (m) at Shallow Tensio-meters	Water Sample Collected? wet before infil. test; dry before infil. test	Bromide (>100 mg/l) Detected? [1] sampled, but dry after tracer added	Maximum Pressure (m) at Shallow Tensio-meters	Characteristics of Pressure Response from Shallow Tensiometers	Saturation based on pressure response from shallow tensiometers: rate of initial increase	after initial increase	Response at Deep Tensio-meters?	Response from Deep TDR Sensors?
Data Rpt. Sect. II.1.1	*Data Rpt. Sect. II.3*	*Data Rpt. Sect. II.4*	*Data Rpt. Sect. II.1.1*	*Data Rpt. Sect. II.1.1*	*Data Rpt. Sect. II.1.1*	*Data Rpt. Sect. II.1.1*	*Data Rpt. Sect. II.1.2*	*Data Rpt. Sect. II.7.2*
								yes
-0.30	yes	yes	0.60	incr. from - to +	fast			
							no effect	yes
-0.55	yes	yes	1.15	incr. from - to +	fast			
0.5?	yes	*no*						
			0.25	*uncertain*	*none*			no
	sampled, but dry	*sampled, but dry*						
								no
							no effect	
								no
								yes
-1.60	yes	*no*	0.63	incr. from - to +	fast			
-1.01	*sampled, but dry*	*sampled, but dry*	0.15	incr. from - to +	slow	*decrease*		
0?	*sampled, but dry*	*sampled, but dry*	-0.40	*uncertain*	slow	*decrease*		
							no effect	
	sampled, but dry	*sampled, but dry*						
							no effect	
	sampled, but dry	*sampled, but dry*						no
								no
-1.25	yes	*no*	0.65	incr. from - to +	fast	*decrease*		
-0.80								
								yes
			0.70	incr. from - to +	fast	*decrease*		
<0	yes	yes	1.20	incr. from - to +	fast	*decrease*		
								no
								yes
	yes	yes						
								yes
	yes	yes						
-0.62	*sampled, but dry*	*sampled, but dry*	0.30	incr. from - to +	fast			*no?*
-0.60	*sampled, but dry*	*sampled, but dry*	-0.53	*little/no change*	*none*			*no?*
-0.52	*sampled, but dry*	*sampled, but dry*	-0.09	incr. from - to +	slow	*decrease*		*no?*
								yes
-1.50	yes	yes	0.93	incr. from - to +	fast			*is this 1.5'?*
-0.45	yes	*sampled, but dry* [1]	0.35	incr. from - to +	slow			
-0.45			-0.35	*little/no change*	*none*			
	yes	*sampled, but dry* [1]						
	sampled, but dry	*sampled, but dry*						
-0.30			0.80	incr. from - to +	fast			yes
-0.35			0.55	incr. from - to +	fast			no
0?			0.67	*uncertain*	fast			no
-0.75	yes	yes	0.57	incr. from - to +	fast			yes
-0.61	yes	yes	1.53	incr. from - to +	fast			yes
-0.05	yes	yes	1.24	incr. from - to +	fast			yes

List of Figure Captions

Figure I.2-1. Well layout
Figure I.3-1. Map of infiltration pond: column tops, soils, and well locations
Figure I.4-1. Scheme of installation of instrumentation in boreholes: (a) conventional in a soil profile, and (b) a new technology for fractured rocks con
Figure I.7.1-1. Design of shallow tensiometers
Figure I.7.1-2. Dimensions of ceramic cup used in shallow tensiometers
Figure I.7.1-3. Diagram of shallow tensiometer dimensions
Figure I.7.6-1. The electrode configuration of the miniature ER probe installed in boreholes
Figure I.7.6-2. Arrangement of the miniature ER probe located in a nylon bag prepacked with sand
Figure I.7.7-1. Water supply system design
Figure I.7.8-1. Well and infiltrometer layout at the Box Canyon site
Figure I.7.8-2. Design of infiltration system used to measure spatial variability in infiltration rate
Figure I.7.10-1 Measurement of dielectric value with TDR
Figure I.8-1. Diagram of DAS used for the infiltration experiment
Figure II.1.1-1. Time trend of water pressure in well T-2
Figure II.1.1-2. Time trend of water pressure in well T-3
Figure II.1.1-3. Time trend of water pressure in well T-4
Figure II.1.1-4. Time trend of water pressure in well T-5
Figure II.1.1-5. Time trend of water pressure in well T-6
Figure II.1.1-6. Time trend of water pressure in well T-7
Figure II.1.1-7. Time trend of water pressure in well T-8
Figure II.1.1-8. Time trend of water pressure in well T-9
Figure II.1.1-9. Barometric pressure
Figure II.1.2-1. Time trend of water pressure measurements using DTs in well I-1
Figure II.1.2-2. Time trend of water pressure measurements using DTs in well I-2
Figure II.1.2-3. Time trend of water pressure measurements using DTs in well I-3
Figure II.1.2-4. Time trend of water pressure measurements using DTs in well T-2
Figure II.1.2-5. Time trend of water pressure measurements using DTs in well T-3
Figure II.1.2-6. Time trend of water pressure measurements using DTs in well T-6

Figure II.1.2-7. Time trend of water pressure measurements using DTs in well E-1
Figure II.1.2-8. Time trend of water pressure measurements using DTs in well E-2
Figure II.1.2-9. Time trend of water pressure measurements using DTs in well E-3
Figure II.1.2-10. Time trend of water pressure measurements using DTs in well E-4
Figure II.2-1. Relative neutron counts over during the first 185 hours of the infiltration test in well T-1
Figure II.2-2. Relative neutron counts over during the first 174 hours of the infiltration test in well T-8a
Figure II.2-3. Relative neutron counts over during the first 175 hours of the infiltration test in well T-10. Significant increases were observed at all depths.
Figure II.2-4. Relative neutron counts over during the first 197 hours of the infiltration test in well R-1
Figure II.2-5. Relative neutron counts over during the first 148 hours of the infiltration test in well R-2
Figure II.2-6. Relative neutron counts over during the first 197 hours of the infiltration test in well R-3
Figure II.2-7. Relative neutron counts over during the first 175 hours of the infiltration test in well R-4
Figure II.2-8. Final relative neutron counts for wells T-1, T-8a, R-1, R-2, R-3, and R-4
Figure II.4-1. Electrical resistivity measurements for well II-5
Figure II.4-2. Electrical resistivity measurements for well S-1
Figure II.4-3. Electrical resistivity measurements for well S-2
Figure II.4-4. Electrical resistivity measurements for well S-3
Figure II.4-5. Electrical resistivity measurements for well S-4
Figure II.4-6. Tracer breakthrough at two sampling locations in well I-1
Figure II.4-7. Tracer breakthrough at two sampling locations in well I-2
Figure II.4-8. Tracer breakthrough at two sampling locations in well T-2
Figure II.5-1. Temperature within pond and ambient air
Figure II.5-2. Time trend of temperature in well I-3
Figure II.5-3. Time trend of temperature in well I-3
Figure II.5-4. Time trend of temperature in well E-1
Figure II.5-5. Time trend of temperature in well E-1
Figure II.5-6. Time trend of temperature in well E-2
Figure II.5-7. Time trend of temperature in well E-2
Figure II.5-8. Time trend of temperature in well E-3
Figure II.5-9. Time trend of temperature in well E-3
Figure II.5-10. Time trend of temperature in well E-4

Figure II.6-1. Time-trend of cumulative water flux during the infiltration test in the pond
Figure II.6-2. Water level in infiltrometers within the pond when water supply was terminated
Figure II.7.1-1. Dielectric values before the ponding event
Figure II.7.1-2. Dielectric values during the ponding event
Figure II.7.1-3. Dielectric values after the ponding event
Figure II.7.2-1. Water contents at well I-1 estimated using the borehole TDR probes.
Figure II.8-1. Groundwater levels in the monitoring wells during the infiltration test
Figure A.1.1-1. Calibration layout for pressure tansducers

List of Tables

Table I.2-1.	Well Information for Box Canyon Site
Table I.7.1-1.	Shallow Tensiometer Dimensions
Table I.7.1-2	Water Level Height within the Pond
Table I.8-1.	Box Canyon Infiltration Experiment 1996, Summary of Parameters Measured
Table I.9-1.	Summary of Instrumentation at the Box Canyon Site
Table II.1-1.	Summary of Tensiometer and Lysimeter Correlations
Table II.3-1.	Water Samples Collected at the Box Canyon Site
Table II.3-2.	Water Sample Data
Table II.3-3.	Summary of Water Sample Data
Table II.4-1.	Bromide Concentrations (mg/l) – 1996 Tracer Test
Table II.4-2.	Characteristics of Arrival of Bromide Tracer at Selected Wells – 1996 Tracer Test
Table II.6-1.	Flow Rate Calculated for Individual Infiltrometers and Entire Pond on September 2-4
Table II.7.1-1.	Time to Wetting and Drying Determined from TDR probes
Table II.7.2-1.	Depths where TDR probes Responded to the Infiltration Test
Table A.1.2-1.	Calibration Data for Transducers
Table A.2.1-1.	Slow Neutron Counts Under Various Conditions and Through Casings of Variable Composition or Thickness (50 mCi source)
Table A.2.2-1.	Summary of Materials Tested for Backfill Design
Table A.5-1.	Summary of Instrument Responses to Infiltration and Tracer Tests for Wells E-1 to E-4
Table A.5-2.	Summary of Instrument Responses to Infiltration and Tracer Tests for Wells I-1 to I-3
Table A.5-3.	Summary of Instrument Responses to Infiltration and Tracer Tests for Wells R-1 to R-4
Table A.5-4.	Summary of Instrument Responses to Infiltration and Tracer Tests for Wells II-5 and S-1 to S-4
Table A.5-5.	Summary of Instrument Responses to Infiltration and Tracer Tests for Wells T-1, T-8A, and T-10
Table A.5-6.	Summary of Instrument Responses to Infiltration and Tracer Tests for Wells T-2 to T-5 and T-7 to T-9

Ernest Orlando Lawrence Berkeley National Laboratory
One Cyclotron Road | Berkeley, California 94720

Prepared for the U.S. Department of Energy under Contract No. DE-AC03-76SF00098